Synthesis and Application of [2.2]Paracyclophanes as Organic Semiconductors and Functional Polymers

Zur Erlangung des akademischen Grades eines

DOKTORS DER NATURWISSENSCHAFTEN

(Dr. rer. nat.)

von der KIT-Fakultät für Chemie und Biowissenschaften
des Karlsruher Instituts für Technologie (KIT)

genehmigte

DISSERTATION

von

Henrik Tappert
M.Sc.

1. Referent: Prof. Dr. Stefan Bräse

2. Referent: Prof. Dr. Michael A. R. Meier

Tag der mündlichen Prüfung: 12.12.2024

Honesty Declaration

This work was carried out from March 15th, 2021, through October 30th, 2024, at the Institute of Organic Chemistry, Faculty of Chemistry and Biosciences at the Karlsruhe Institute of Technology (KIT) under the supervision of Prof. Dr. Stefan Bräse.

Hereby, I, Henrik Tappert, declare that I completed the work independently, without any improper help, and that all material published by others is cited properly. This thesis has not been submitted to any other university before.

Die vorliegende Arbeit wurde im Zeitraum vom 15. März 2021 bis 30. Oktober 2024 am Institut für Organische Chemie (IOC) der Fakultät für Chemie und Biowissenschaften am Karlsruher Institut für Technologie (KIT) unter der Leitung von Prof. Dr. Stefan Bräse angefertigt.

Hiermit versichere ich, Henrik Tappert, die vorliegende Arbeit selbstständig verfasst und keine anderen als die angegebenen Hilfsmittel verwendet, sowie Zitate kenntlich gemacht zu haben. Die Dissertation wurde bisher an keiner anderen Hochschule oder Universität eingereicht.

German Title of this Thesis

Synthese und Anwendung von [2.2]Paracyclophanen als organische Halbleiter und funktionale Polymere

Table of Contents

Abstract

This thesis explores the synthesis and application of [2.2]paracyclophanes (PCPs) as organic semiconductors and functional polymers. The increasing global demand for energy and the need for sustainable, green alternatives have driven advancements in material science. PCP's unique structural characteristics, including their rigid, through-space conjugated system, make them promising candidates for use in optoelectronic applications such as charge transport materials in perovskite solar cells or as thermally activated delayed fluorescence (TADF) emitters in organic light-emitting diodes (OLEDs).

During this work, 19 novel PCP-based organic semiconductors were synthesized and characterized, focusing on modular designs. These compounds were created using three different PCP stereoisomers, four different π-bridges (thiophene, thienothiophene, dibenzothiophene, and carbazole), and three spacer groups (vinyl, ethynyl, and phenyl). This variety enabled a comprehensive exploration of these building blocks' effects on synthesis and electronic properties. Of the synthesized materials, nine demonstrated promising characteristics for optoelectronic applications such as perovskite solar cells (PSCs), with ionization potentials (IPs) between 5.17 eV and 5.35 eV and band gaps between 2.38 eV and 3.00 eV, indicating their potential as tunable semiconductors.

The application of PCPs in polymers was also examined. Chiral vinyl-PCP was used as a monomer to create both chiral homopolymers and chiral copolymers with styrene, retaining chirality up to 98% styrene content. Additionally, the synthesis of vinyl-DMAC-TRZ and its copolymerization with chiral vinyl-PCP yielded chiral TADF emitter polymers capable of circularly polarized luminescence (CPL).

The concept of PCP-based semiconductors was also extended to PCP polymers, producing seven new semiconducting polymers *via* step-growth cross-coupling polymerization. These polymers, integrating thienothiophene or thiophene units together with PCP, had molecular weights (M_w) between 3.83 kDa and 24.3 kDa and dispersity values from 2 to 4. Of these, three polymers successfully formed thin-films with energy levels suitable for PSCs, showing IPs between 5.26–5.39 eV and band gaps of 2.40–2.55 eV.

These results contribute to developing new PCP-based organic electronics, potentially paving the way for new, efficient applications in advanced materials.

Inhaltliche Zusammenfassung

Diese Dissertation befasst sich mit der Synthese von [2.2]Paracyclophanen als organische Halbleiter und funktionale Polymere sowie deren Anwendung. Der zunehmende weltweite Energiebedarf und die Notwendigkeit nachhaltiger, umweltfreundlicher Alternativen haben Fortschritte in der Materialwissenschaft, insbesondere in den Bereichen Solarenergienutzung und organische Elektronik, vorangetrieben. Die einzigartigen strukturellen Eigenschaften von PCPs, einschließlich ihres starren, raumübergreifend-konjugierten Systems, machen sie zu vielversprechenden Kandidaten für den Einsatz in Ladungstransportmaterialien für beispielsweise Perowskit-Solarzellen und als TADF-Emitter in OLEDs.

Im Rahmen dieser Arbeit wurden 19 neue PCP-basierte organische Halbleiter synthetisiert und charakterisiert, wobei der Schwerpunkt auf einem modularen Design lag. Diese Verbindungen wurden unter Verwendung dreier verschiedener PCP-Stereoisomere, vier verschiedener π-Brücken (Thiophen, Thienothiophen, Dibenzothiophen und Carbazol) sowie dreier Spacer-Gruppen (Vinyl, Ethinyl und Phenyl) hergestellt. Diese Vielfalt ermöglichte eine umfassende Untersuchung der Auswirkungen dieser Bausteine auf die Synthese und die elektronischen Eigenschaften der Halbleiter. Von den synthetisierten Materialien zeigten neun vielversprechende Eigenschaften für Anwendungen in der Optoelektronik, wie etwa Perowskit-Solarzellen, mit Ionisationspotentialen zwischen 5,17 eV und 5,35 eV und Bandlücken zwischen 2,38 eV und 3,00 eV, was ihr Potenzial zum flexiblen Einsatz in Halbleitern aufzeigt.

Auch die Anwendung von PCP in Polymeren wurde untersucht. Chirales Vinyl-PCP wurde als Monomer verwendet, um sowohl chirale Homopolymere als auch chirale Copolymere mit Styrol herzustellen, wobei ein Erhalt der Chiralität bis zu einem Styrolgehalt von 98 % nachgewiesen werden konnte. Zusätzlich führte die Synthese von Vinyl-DMAC-TRZ und dessen Copolymerisation mit chiralem Vinyl-PCP zu chiralen TADF-Emitter-Polymeren, die zu zirkular-polarisierter Lumineszenz (CPL) fähig sind.

Das Konzept der PCP-basierten Halbleiter wurde auch auf PCP-Polymere ausgeweitet, was zur Herstellung von sieben neuen halbleitenden Polymeren durch Kreuzkupplungspolymerisationen führte. Diese Polymere, die Thienothiophen- oder Thiopheneinheiten sowie PCP integrieren, hatten Molekulargewichte (M_w) zwischen 3,83 kDa und 24,3 kDa und Dispersitätswerte von 2 bis 4. Von diesen bildeten drei Polymere erfolgreich Dünnschichten mit Energieniveaus, die für PSCs geeignet sind, mit IP zwischen 5,26–5,39 eV und Bandlücken von 2,40–2,55 eV.

Diese Ergebnisse tragen zur Entwicklung neuer PCP-basierter organischer Elektronik bei und könnten den Weg für neue, effiziente Anwendungen in fortschrittlichen Materialien ebnen.

1. Introduction

Many of the world's challenges result from the ever-increasing need for energy and the pressing issue of transitioning to green, renewable sources of this same energy. A growing world population, the climate crisis, and the dominion of a few states over vast percentages of fossil fuels that currently represent the major energy source—all challenges that the ubiquitous availability of cheap, green energy would greatly improve.

The global community currently aims to achieve a net zero for emitted carbon dioxide in 2050. The worldwide energy demand projections predict that an increase of around 179 EJ in renewable energy, aside from hydro and nuclear energy, is needed to achieve this (Figure 1).[1]

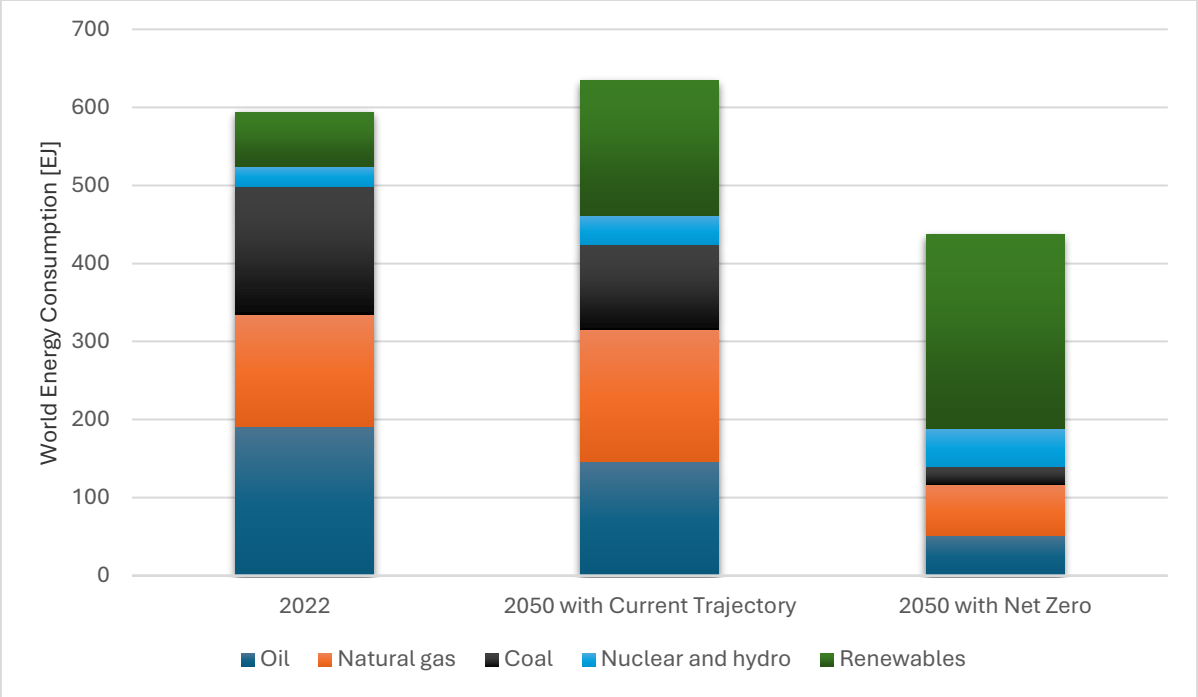

Figure 1: Current and projected world energy consumption by energy source reproduced from data of the BP energy outlook.[1]

This demonstrates the need for more and better methods to increase renewable energy, such as solar power and energy-efficient technologies for everyday use. The ongoing advancements in material science are largely driven by the demand for innovative compounds that address challenges in fields like organic electronics, solar energy harvesting, and semiconductor technologies. Among the diverse materials being explored, [2.2]paracyclophanes (PCPs) have emerged as intriguing candidates in multiple of those fields due to their unique molecular structure and versatile functionalization capabilities. Since their discovery, PCPs have garnered attention not only as chemical curiosities but also as valuable building blocks for advanced materials.

With regard to this background, this thesis focuses on the synthesis and application of [2.2]paracyclophanes as organic semiconductors and functional polymers. Recent developments in semiconductor technology have highlighted the need for materials that can efficiently transport charge, interact favorably with light, and maintain stability under operational conditions. With their rigid structure and conjugated system, PCP-based materials offer promising solutions in this regard, especially when fine-tuned.

This work aims to explore the potential of PCP-based materials further, building upon previous research that has shown their effectiveness in applications like charge transport layers for perovskite solar cells or TADF (thermally activated delayed fluorescence) emitters for organic light-emitting diodes (OLEDs). By investigating new variations in the PCP structure, such as stereoisomers, π-bridges, and the introduction of spacer groups, this thesis seeks to develop a comprehensive library of PCP-based semiconductors. This modular approach contributes to the goal of making it possible to predict and optimize the electronic properties of these materials, providing valuable insights into their structure-property relationships and paving the way for future innovations in organic electronics.

2. Theoretical Background

2.1. [2.2]Paracyclophanes

Since their discovery in 1949 by Brown and Farthing,[2] [2.2]paracyclophanes, a unique class of strained aromatic hydrocarbons, have made their way into a broad number of fields due to their unusual molecular structure and intriguing properties. Following the discovery and subsequent purposeful synthesis of the basic motif by Cram and Steinberg,[3] they have evolved from a chemical curiosity to a molecule of considerable importance in organic chemistry and material science.[4-6] Similarly, the production process evolved from yielding the compound as a side product during low-pressure pyrolysis of xylene to employing purposeful and efficient synthesis methods. For large-scale synthesis of unsubstituted PCP, a 1,5-Hofmann elimination is employed, which can, in turn, be functionalized further (Scheme 1a).[7] Another often-reported method for functionalized PCPs is the coupling of dibromomethyl benzenes and dithiamethyl benzenes, followed by extrusion of the sulfur under light (Scheme 1b).[8]

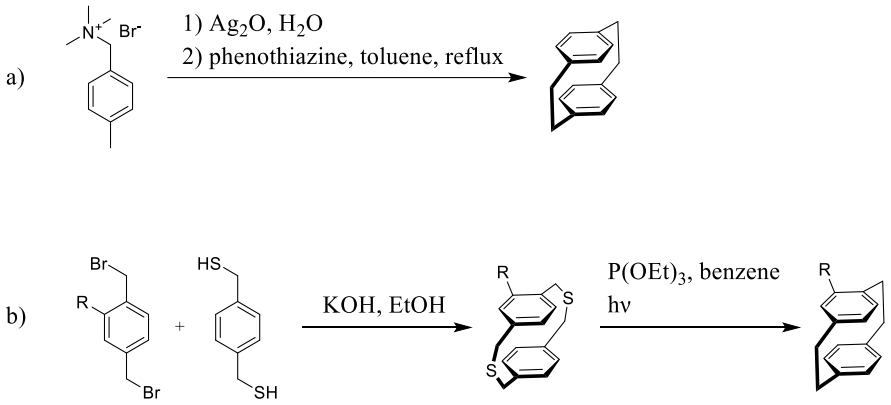

Scheme 1: Typical synthetic routes for PCPs. a) via *1,5-Hofmann elimination of quaternary ammonium salts. b)* via *synthesis of [3.3]dithiaparacyclophanes and extrusion of sulfur.*

The name [2.2]paracyclophane refers to the structure of two co-facially stacked benzene rings connected by two ethylene bridges at the *para* positions of both rings, forming a bicyclic structure (Figure 2).[9] Unlike other cyclophanes with longer bridging moieties, the short ethylene bridges (~2.78 Å)[10] rigidly lock the two aromatic rings in a fixed spatial arrangement, preventing their free rotation and causing the benzene rings to bend out of the plane. The two benzene rings are separated by only 3.09 Å at their farthest point,[10] a distance much shorter than in unstrained systems like graphite (3.4 Å).[11] This close proximity leads to significant transannular π–π interactions, which, in turn, affect the molecule's reactivity and optoelectronic properties.[12] These distinctive characteristics make [2.2]paracyclophane a valuable building block for developing various advanced materials.[13]

Figure 2: General structure of [2.2]paracyclophane and its 3D arrangement.[14]

The strain-induced interactions between the benzene rings result in high ring strain energy and a modified electronic structure, which can be observed in distinct changes of the UV-visible absorption spectra.[15-16] The strain also alters the reactivity of [2.2]paracyclophane, making it more susceptible to chemical reactions that are less favorable in unstrained aromatic systems, such as electrophilic substitution.[16]

In addition to these properties, [2.2]paracyclophane exhibits planar chirality when appropriately substituted because of the fixed spatial arrangement of the rings. To assign the absolute configuration of enantiopure [2.2]paracyclophanes, the Cahn-Ingold-Prelog (CIP) conventions, established in 1966, are employed (Figure 3).[17] Under these rules, the aromatic ring functionalized with the highest priority atoms or groups is considered the "chiral plane". The carbon atom of the ethylene bridge closest to the substituent on this plane is termed the "priority atom", while the second carbon, located outside the chiral plane, is the "pilot atom". The numbering of the carbon atoms starts from the pilot atom, and if the sequence from the priority atom circles clockwise, the molecule is assigned the R_p configuration; if counterclockwise, it is designated to S_p. These descriptors (where "p" indicates **p**lanar chirality) are now widely used to define the stereochemistry of [2.2]paracyclophanes.

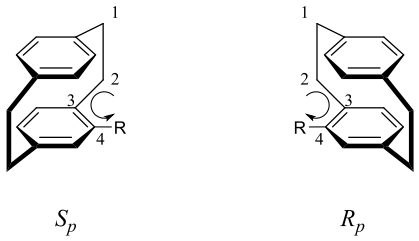

S_p R_p

Figure 3: CIP convention of numbering PCP atoms and assigning the stereodescriptor of their planar chirality.

Planar chirality is inherent to all monosubstituted paracyclophanes, as well as bifunctionalized *para*, pseudo-*ortho*, and pseudo-*meta* substituted derivates, while *ortho*, *meta*, pseudo-*geminal*, and pseudo-*para* derivatives are only chiral if the two substituents differ (Figure 4). The prefix "pseudo", often shortened to “ps”, refers to a substitution pattern across both rings rather than just one.

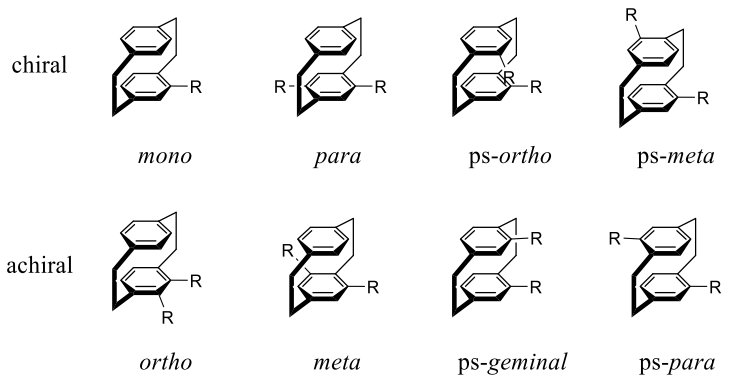

Figure 4: Substitution patterns of mono- and disubstituted [2.2]paracyclophane.

The inherent chirality of [2.2]paracyclophane makes it particularly valuable in asymmetric synthesis, where it can serve as a chiral catalyst or ligand.[18-19] Its chiral properties also enable applications in the development of organic chiral materials, including sensors and bio applications.[20-21] Beyond its chiral applications, [2.2]paracyclophane has demonstrated versatility in various achiral areas. It has been employed as a component in dyes,[22] TADF emitters,[23-24] and charge transport materials.[13] In materials science, it also serves as a precursor for synthesizing polymers, either retaining the intact [2.2]paracyclophane structure or as poly(*p*-xylylene), a highly resistant polymer with applications in coatings, dielectric materials, and protective films.[25-26] Likewise, this work aims to use PCPs in organic semiconductors and functional polymers.

2.2. Organic Semiconductors

Semiconductors play a crucial role in modern technology, forming the foundation of nearly all electronic devices we rely on today—from computers and smartphones to solar cells and light-emitting diodes (LEDs).[27-30] Their ability to control electrical conductivity makes them indispensable in circuits, where they act as the essential building blocks for transistors, diodes, and other components.[31-32] Traditionally, semiconductors are made from inorganic materials such as silicon or gallium arsenide, which have dominated the industry due to their reliability and well-understood properties.[33-34] However, as the demand for more versatile applications, flexible processing, and environmentally sustainable technologies grows, the spotlight has increasingly turned toward organic semiconductors (Figure 5).[35-36]

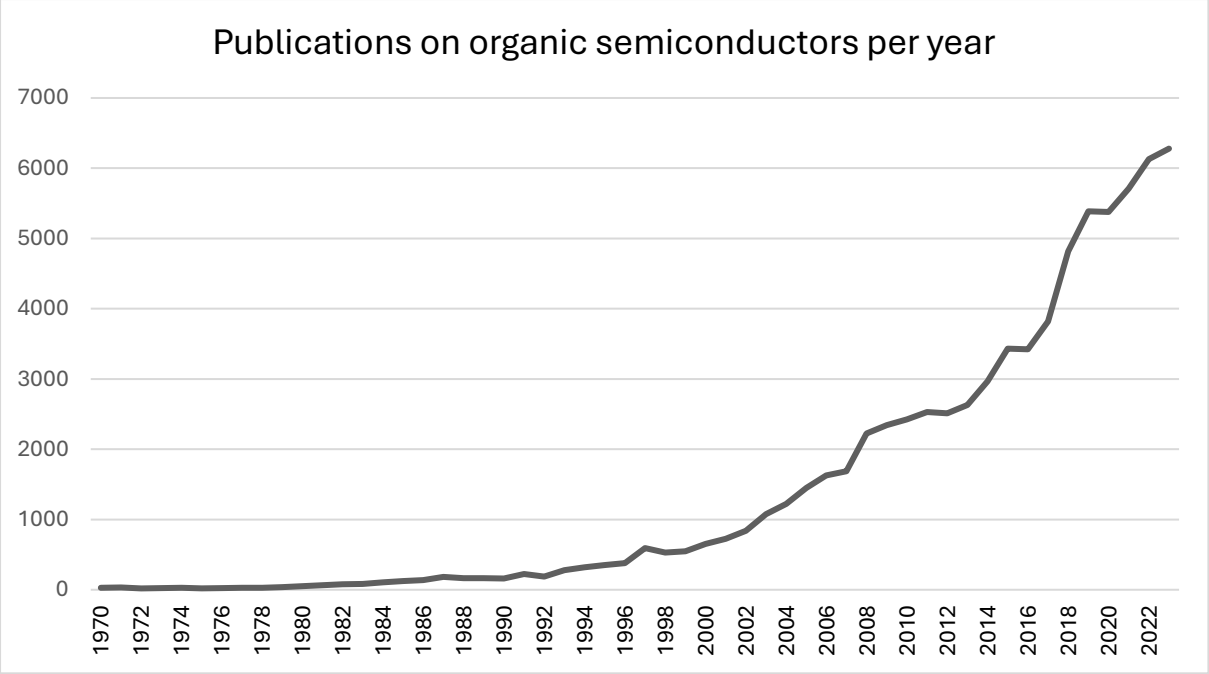

Figure 5: Publications on "organic semiconductor" from 1970 to 2023 according to Scopus.

Unlike their inorganic counterparts, organic semiconductors rely on the electronic properties of conjugated systems, where alternating single and double bonds allow for the delocalization of π-electrons.[37] This delocalization enables these materials to conduct electricity when doped or excited, similar to inorganic semiconductors and opens up the field of organic synthesis to meet the abovementioned demands.

Although earlier examples are known, the development of usable organic semiconductors can be traced back to the 1970s, especially to the Nobel Prize-winning work of Heeger, MacDiarmid, and Shirakawa, who discovered that polyacetylene could be made conductive by doping it with halogens or AsF_5.[38] This marked the beginning of organic electronics and sparked an interest in exploring other conjugated molecules with semiconducting properties. Since then, the field has evolved rapidly, developing a wide range of organic semiconductors with tunable electronic and optical properties.[39] Advances in molecular design have significantly improved the performance of organic semiconductors, making them viable alternatives to traditional inorganic semiconductors.[40]

The key to conductivity in any material lies in the behavior of electrons within its energy bands.[41] Semiconductors occupy a middle ground between insulators and conductors (Figure 6).

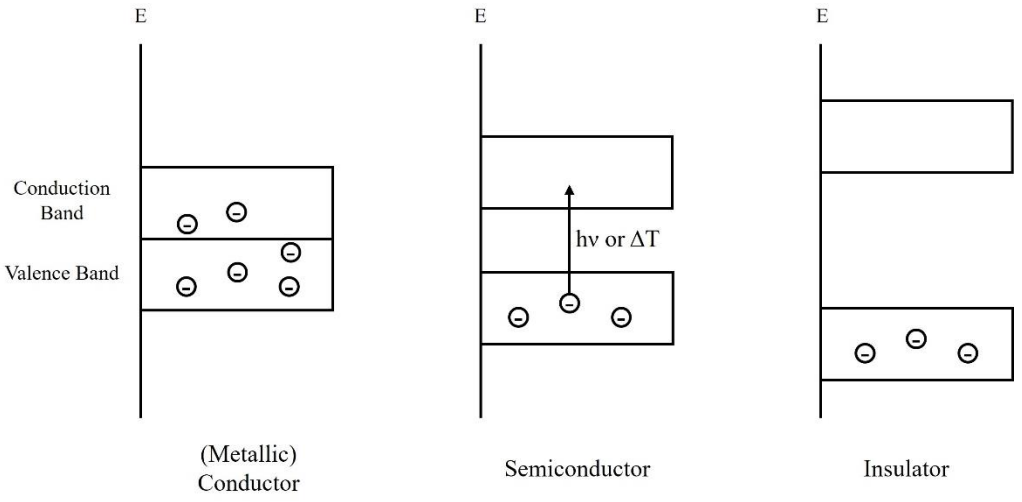

Figure 6: Band gaps in conductors, semiconductors, and isolators.

In conductors, the valence band (VB) and conduction band (CB) overlap, allowing free electron movement and, thus, high conductivity. In insulators, the gap between the valence and conduction band is too large for electrons to cross without an extreme energy input that is unavailable in any practical setting (typically >3.0 eV).[27] Semiconductors, however, only have a small band gap between the VB and CB, which can be overcome with external energy, such as ambient heat or light. When enough energy is provided, an electron can "jump" from the VB to the CB, resulting in a hole in the VB. Both the excited electron (negative charge) and the hole (positive charge) can contribute to the conductivity. The size of the band gap in semiconductors determines their electrical and optical properties, and it can be tuned depending on the material composition. Organic semiconductors operate on the same principles but rely on molecular orbitals instead of energy bands. Consequently, the highest occupied molecular orbital (HOMO) and the lowest unoccupied molecular orbital (LUMO) are roughly analogous to the valence and conduction bands in inorganic materials.[42]

Aside from that, organic semiconductors differ from most inorganic semiconductors in another fundamental way. Inorganic semiconductors typically form crystalline structures with a highly ordered atomic arrangement, leading to efficient charge transport and high carrier mobilities. Organic semiconductors, by contrast, consist of flexible, disordered molecular structures. This results in lower charge carrier mobility and less efficient charge transport. At first glance, what seems like an insurmountable disadvantage can be effectively compensated by the advantages those flexible organic structures offer. By eliminating the necessity for crystalline structures, the needed thickness is significantly reduced by approximately 1000 times (organic: 10-100 nm[43] vs. crystal: 1-100 µm[44]). The lower conductivity (organic: up to 10^2 $cm^2/(Vs)$[45] vs. inorganic: 10^4 $cm^2/(Vs)$[46]) is therefore

compensated by a shorter travel distance for the charges. Furthermore, there are several benefits in processing and field of application. The inherent flexibility enables the production of bendable, stretchable, and lightweight electronic devices—features that are difficult to achieve with rigid inorganic semiconductors. Furthermore, organic semiconductors can be solution-processed at room temperature, allowing for large-area fabrication techniques such as printing and roll-to-roll manufacturing. This, combined with a lower cost for organic materials compared to most inorganic elements, makes them potentially much less expensive. Lastly, the larger chemical space of organic semiconductors allows them to easily be modified in their electronic, optical, and mechanical properties. This enables tailored materials for specific applications where the common inorganic semiconductors cannot be used.[47]

As a result, several organic semiconductors have become well-known (Figure 7). To name a few: pentacene has been extensively used in organic thin-film transistors,[48-49] fullerenes (*e.g.*, phenyl-C61-butyric acid methyl ester (PCBM), commonly used as electron acceptors in organic solar cells,[50-51] or tetrathiafulvalene (TTF), an important material from the early development of organic semiconductors.[52-53] There are also known examples of PCPs (chapter 2.1).[54-56] Furthermore, many conductive polymers are well-used as semiconductors such as poly(3-hexylthiophene) (P3HT), a high-performance polymer used extensively in organic photovoltaics (OPVs) and organic field-effect transistors (OFETs),[57-58] or poly(*para*-phenylene vinylene) (PPV), one of the first conductive polymers to be studied and widely used in OLEDs.[59-60]

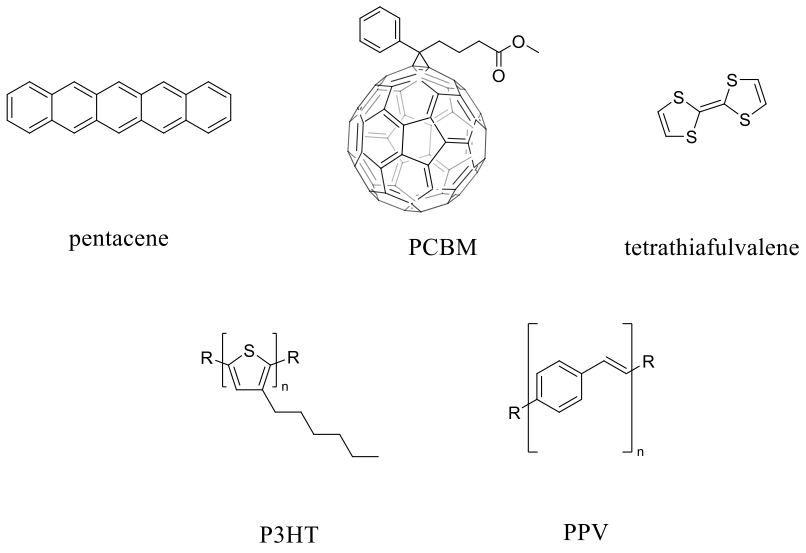

Figure 7: Typical examples of organic semiconductors, both monomeric (top) and polymeric (bottom).

Many more examples in interesting fields could be named, and still organic semiconductors advance, offering new opportunities in new areas. Their role in flexible, low-cost, and sustainable electronics will only grow further as research progresses. As the semiconductors synthesized in this work are intended to be used in solar cells, this field of application shall be explained in more detail.

2.3. Solar Cells and Charge Transport Materials

2.3.1. History and Theory behind Solar Cells

Solar cells are fundamental for transitioning to sustainable energy, offering a clean, renewable alternative to fossil fuels.[61] Achieving clean energy plays a vital role in solving many of the current worldwide problems, such as reducing greenhouse gas emissions and thus combating climate change and making energy more affordable and readily accessible to all without relying on a few resource-rich nations. Solar cells can be deployed in various settings, from large-scale solar farms to residential rooftops, providing flexibility in energy generation. This, in turn, creates economic opportunities through the growth of new and old industries. With continuous advancements in efficiency and cost reduction, solar cells are poised to become a cornerstone of the global energy system, helping to meet growing energy demands sustainably.[62]

The ability to harvest energy or electricity from sunlight is based on the photovoltaic effect, first described by A. E. Becquerel as early as 1839.[63] He observed electricity generation when metal electrodes made of platinum were submerged in a conductive solution and irradiated. In modern solar cells, this principle relies on semiconductors to convert sunlight into usable electrical energy. Figure 8 illustrates the basic process: sunlight excites electrons in a suitable semiconductor, leaving behind a hole (positive charge), leading to charge separation. In most cases, those charges would recombine through one of multiple possible processes *via* radiative relaxation, defects, or Auger recombination. Radiative recombination is the simplest and most common recombination for semiconductors. The excited electron loses the energy it absorbed from a photon by emitting a photon with a higher wavelength.[64-65] When the semiconductor contains defects, whether natural or artificial (dopants), the excited electron can first relax to the energy level of the defects inside the band gap and then relax further to recombine with the hole. The electron also can get excited again before it recombines.[66] In the case of the Auger recombination, the electron does not emit energy as a photon but passes the energy to another electron, which then carries coth of their energies, while the first recombines.[67]

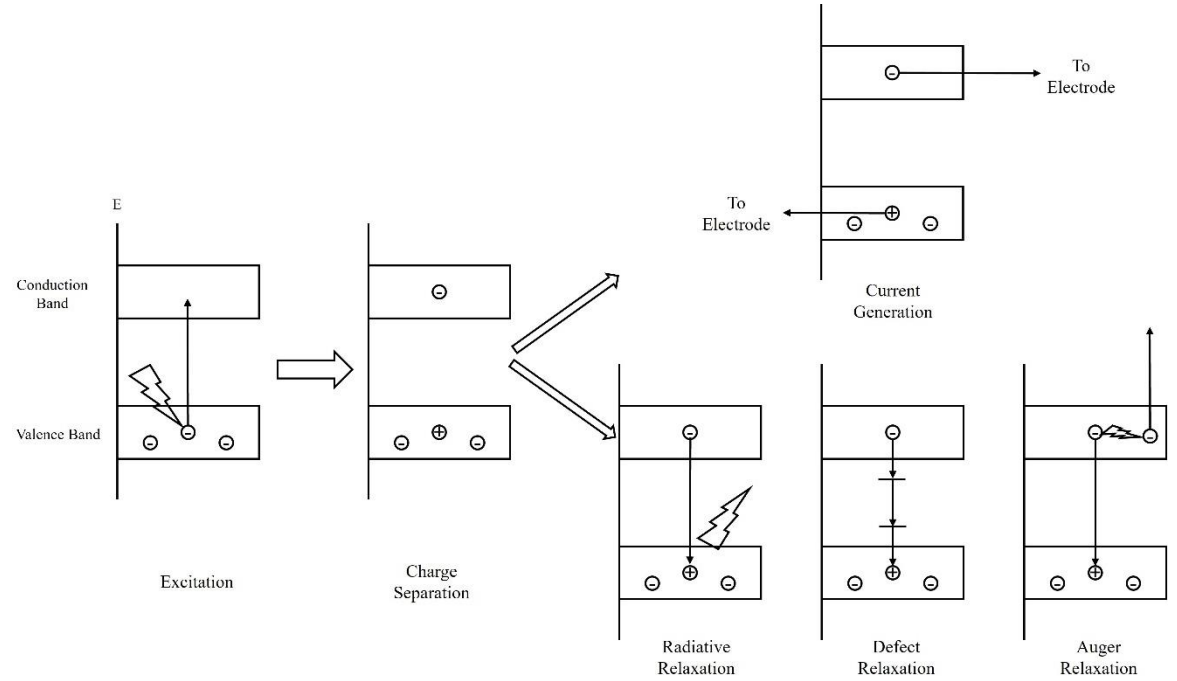

Figure 8: Processes in solar cells upon excitation by sunlight. The separate charges can be transported to electrodes to produce electricity (top) or recombine (bottom).

For the semiconductor material to avoid recombination efficiently and produce current instead, fast separation and transport of the charges are necessary. This can be achieved by adding two doped materials: one n-type (negative type), where an electron donor allows for easier travel of the electrons, and one p-type (positive type), where the holes travel, helped by an electron acceptor. This selective charge movement through the circuit generates electricity and allows energy to be harnessed effectively.

The ease of transport and the reduction of recombination are two of several factors that determine a solar cell's overall power conversion efficiency (PCE, η), which allows comparison of the usable energy per incoming (solar) energy. Efficiency is calculated as the ratio of the applied power (P_{in}, from the energy source) to the output power (P_{out}) (Equation (*1*).

$$\eta = \frac{P_{out}}{P_{in}} = \frac{FF * V_{OC} * I_{SC}}{P_{in}} \quad (1)$$

To get the P_{out}value for the solar cells the values for fill factor (FF), open circuit voltage (V_{OC}), and short circuit current (I_{SC}) are necessary. These values can be easily derived from the current-voltage curve (I-V curve) (Figure 9): The voltage at infinite resistance and, therefore, a current of zero is the V_{OC}, while the current at zero resistance and, thus, a voltage of zero is the I_{SC}. The fill factor is the ratio of the maximum power point (MPP), where current and voltage are equal, to the product of I_{SC} and V_{OC} (Equation (*2*).

$$FF = \frac{V_{MPP} I_{MPP}}{V_{OC} I_{SC}} \quad (2)$$

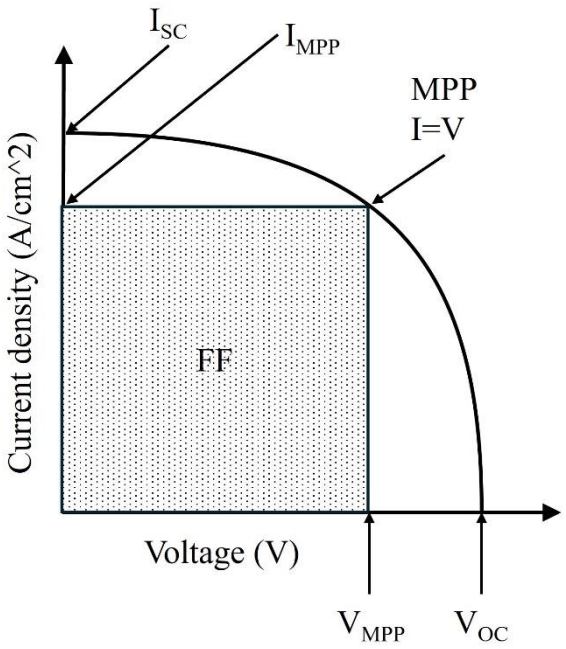

Figure 9: I-V diagram with important values for PCE calculation. Fill factor (FF), open circuit voltage (V_{OC}), short circuit current (I_{SC}), maximum power point (MPP), maximum power point current (I_{MMP}), and maximum power point voltage (V_{MPP}).

To compare the results of different solar cells, tests are conducted under standard conditions for P_{in}, set by the International Electrotechnical Commission at a temperature of 25 °C, a light spectrum of AM1.5G, and an irradiation power of 1000 Wm^{-2}, mimicking the average solar conditions of the USA on a clear day.

Since the first description of the photovoltaic effect, the concept of solar cells has come a long way. Early experiments included repetitions of Becquerel's first observation[63] with materials like selenium in the 1870s.[68] In 1954, Bell Laboratories developed the first commercial solar cell, utilizing the earlier described effect of doped semiconductors. Using monocrystalline silicon doped with gallium and lithium, they achieved an efficiency of 6% in controlled conditions.[69] This development was followed by increasing research, especially during the 1960s space race and the 1970s oil crisis, where solar energy's advantages became apparent, leading to investments in solar technology. By the 1990s, silicon solar cells with boron as a p-type dopant and phosphorus as an n-type dopant had become the most common type and achieved efficiencies of over 20%.[70] This type of crystalline solar cell is now known as the “first generation” of solar cells (Figure 10). Today, commercial silicon cells achieve as much as 25% efficiency,[71] with the maximum theoretical efficiency for single-junction cells, known as the Shockley-Queisser limit, being around 30%.[72] Most of the missing efficiency is due to losses from reflection and electrode blockage, which cannot be solved by optimizing the semiconductor. However, silicon-based solar cells face challenges due to the material’s indirect band gap. This requires a wafer thickness of approximately 100 µm to absorb sufficient sunlight. The need for high-purity silicon and the energy-intensive process to produce such wafers also increases costs significantly.[73]

This led to the introduction of thin-film solar cells in the 1960s and 1970s, using compounds like cadmium telluride (CdTe)[74] or copper-indium-gallium-diselenide (CIGS),[75] which allowed for thinner layers (1–2 μm). They became known as the second generation of solar cells. These heterojunction solar cells, often composed of materials from groups III and V of the periodic table, reduced the thickness needed for absorption, made the production process more efficient, and allowed for new applications such as bendable solar cells. Despite these advantages, the toxicity of certain materials and the scarcity of others limit their widespread use, especially outside specialized fields such as space engineering. Variations with more readily available materials, such as amorphous silicon, on the other hand, suffer from low efficiency of typically 10–18%.[76]

In the search for further alternatives, multiple new concepts emerged, which together became known as the third generation (Figure 10). In this group, there are organic solar cells (OSC),[77] as well as dye-sensitized (DSSC),[78] perovskite (PSC),[79] quantum dot,[80] and multi-junction solar cells.[81] Although materials that technically work as OSCs were known for quite some time, extremely low efficiencies let them drop out of focus in the early stages of development. The first OSC to achieve 1% was created by Tang *et al*. in 1986 by layering organic materials in a heterojunction structure.[82] In modern research, advances in OSC technology have pushed efficiencies to over 20%.[83] DSSCs use a dye sandwiched between electron- and hole-conducting layers to generate electricity, while perovskite and quantum dot solar cells do the same with their respective material.[84-85] They all offer benefits like low material costs, flexible applications, and low-temperature manufacturing processes but often suffer lower efficiencies than silicon solar cells.[76] Multi-junction cells, on the other hand, combine multiple stacked junctions to harvest a broader range of light or reabsorb radiative losses. This leads to far higher efficiencies of up to 47%, more than any single junction can achieve.[86] As a downside, they are highly complex and, therefore, expensive. Since their introduction, all fields have shown rapid improvement and are the target of much current research.

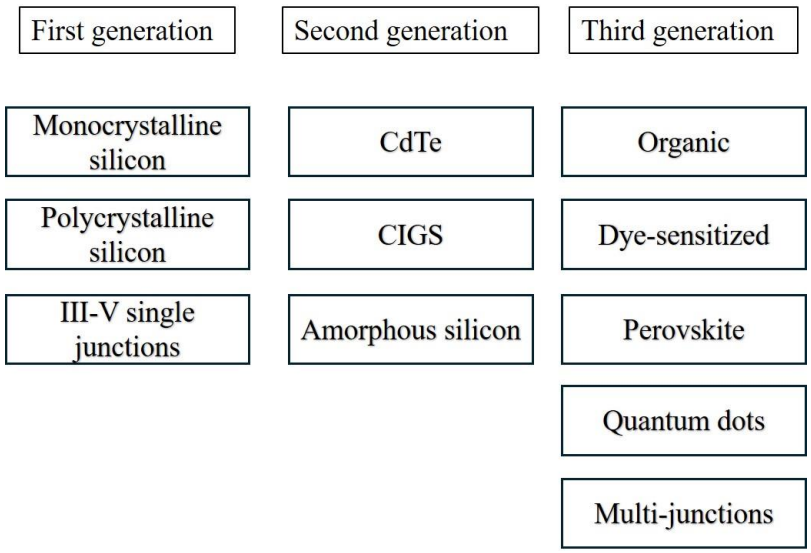

Figure 10: Overview of solar cell generations and their sub-categories.

The key role of semiconductors in solar cells cannot be overstated. They enable the controlled movement of electrons and holes, facilitate the photovoltaic effect, and maximize energy conversion from sunlight. Whether in silicon, thin-film, organic, or emerging technologies like perovskite solar cells, semiconductors are the backbone of modern solar energy systems, driving advancements in efficiency, cost, and scalability.

2.3.2. Solar Cell Architecture and Charge Transport Layers

The different categories of solar cells discussed in the previous chapter mostly depend on what material is used to generate the charge separation from light, which is the active layer of a solar cell. However, other layers are necessary to build a solar cell that generates a useful amount of energy. Even the simplest setup needs the active layer to be connected to two electrodes and a shell to protect it. On at least one side, the electrode must be transparent. For the shell, using glass is easy enough and indium tin oxide (ITO) provides all the necessary properties for the transparent electrode, making it the most used material for transparent electrodes. Additionally, to ensure the generated charges are transported to the respective electrode fast and without recombining, two additional transport layers can be included that take in one charge while blocking the other (Figure 11). Additional layers can be included at every junction to improve transport and reduce defects and are the topic of ongoing research.[87-90]

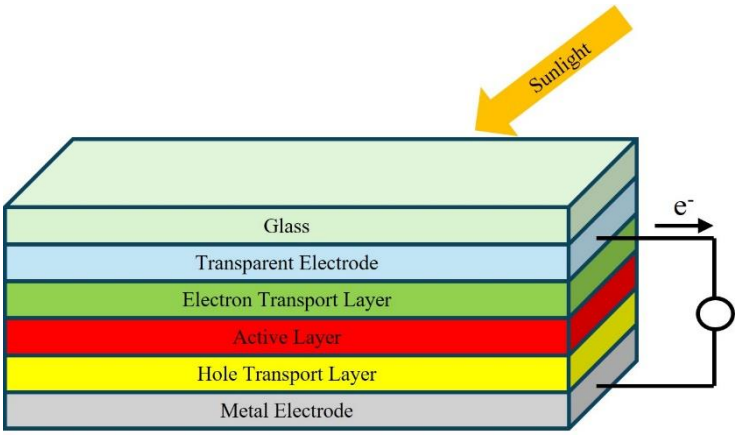

Figure 11: General device architecture of a simple solar cell.

The key requirement for transport layers is that their energy levels align with the active layer to enable selective charge transport. For the electron transport layer, this means having a conduction band slightly lower than that of the active layer, allowing electrons to move easily. The valence band must also be significantly lower to prevent electrons from returning to the active layer (Figure 11). The opposite applies to the hole transport layer: it requires a slightly higher valence band and a significantly higher conduction band. In perovskite solar cells, the band gap of transport materials typically ranges from at least 2.5 to 3.5 eV, with one energy level positioned as close to the active layer as possible.[91]

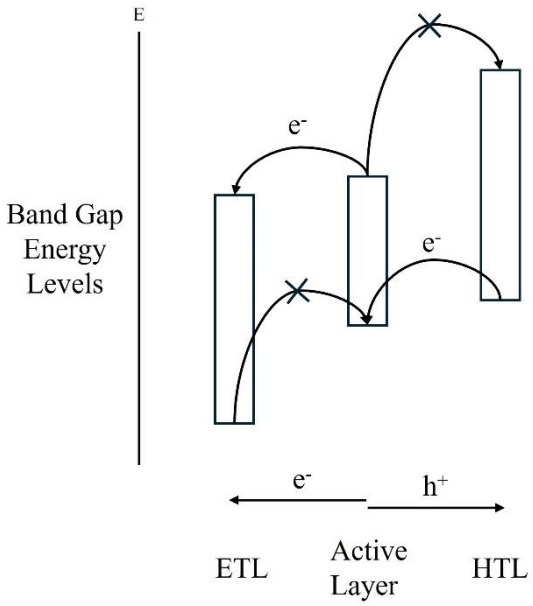

Figure 12: Energy levels of the transport layers that are necessary to allow one-directional electron travel only (electron transport layer, ETL), and therefore, the hole travels in the opposite direction (hole transport layer, HTL).

The transport layers can greatly improve the overall efficiency of a solar cell, and as such, they became a focus of research, especially for third-generation solar cells. The following section briefly overviews the most important transport material developments.

2.3.2.1. Electron Transport Materials (ETMs)

As discussed earlier, ETMs transport electrons from a device's active layer to the electrode while blocking holes, improving overall performance. They need high electron mobility, fitting energy levels for efficient electron injection, and sufficient stability. Metal salts like TiO_2 or ZnO are the most used materials for third-generation solar cells. Still, there are also common examples of organic molecules serving this function, such as fullerenes or bathophenanthroline (BPhen).

TiO_2, a widely used inorganic ETM in perovskite and dye-sensitized solar cells, offers the needed electronic properties: a good electron mobility, a conductive band at ca. -4.0 eV, depending on the phase, which is slightly lower than the most commonly used perovskite methylammonium lead iodide (MAPbI, -3.9 eV)[92] and therefore allows electrons to travel easy and a sufficiently wide band gap of about 3.2 eV, which blocks the holes from entering.[93] Furthermore, it shows great chemical stability, the cost and toxicity of TiO_2 are low, and it is readily available, making it useful for large-scale implementation. Much effort has been made to find the optimal doping, phase, and structuring of the TiO_2 to improve mobility and reduce defects. Doping can be efficiently done with for example, niobium,[94] nickel,[95] or rubidium,[96] while the structure can range from the plain crystal layers to mesoporous layers[97] to nanoparticles.[98] Improving from this, ZnO is known for its even lower cost, higher electron mobility, and an even larger band gap of 3.8 eV.[99] Additionally, it has a big transparency window throughout the visible spectrum, ensuring a high absorbance rate in the active layer, and it is easy to process *via* solution.[100] At the same time, most setups using ZnO are trailing behind appropriately doped and structured TiO_2 devices in efficiency and are still the topic of much research.[101]

For organic ETMs (Figure 13), BPhen is commonly used in OLEDs and organic solar cells. It offers good electron transport properties and can form stable interfaces.[102-103] Its conductive band is at -3.2 eV, and the band gap is 3.2 eV wide.[104] Additionally, the use of derivatives of BPhen was researched, and promising improvements have been shown.[105-106] Likewise, often used as organic ETMs are fullerenes, such as the classic C_{60}, a pure fullerene molecule that is an excellent electron acceptor in OPVs.[107] It has a high electron affinity and forms stable heterojunctions with various donor materials, ensuring efficient electron transport. Further derivatization, e.g., with arenes,[108] heteroarenes,[109] or aliphatic groups,[110] improved upon efficiency, processability, or device stability.[111] Of those, one fullerene derivate is especially often used: PCBM. This fullerene is one of the most popular ETMs for organic solar cells, often combined with other ETMs, due to its high electron mobility, ability to form favorable interfaces with other materials, and its stability in devices.[112-114]

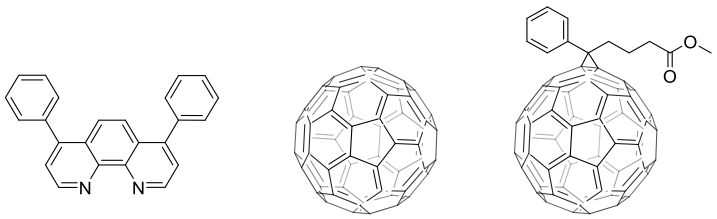

BPhen C_{60} PCBM

Figure 13: Examples of organic ETMs.

2.3.2.2. Hole Transport Materials (HTMs)

HTMs, like ETMs, are essential components in electronic devices, but their primary role is reversed. They transport holes from the active layer to the electrode while blocking electron transport. By enabling efficient hole movement, HTMs improve charge separation and reduce recombination losses. Similar to ETMs, these materials must be designed with high hole mobility, good energy alignment, and stability, and they are crucial for optimizing efficiency in current-generation solar cells. For inorganic HTMs, there is a plethora of metal salts possible, of which a few important examples will be mentioned here.

NiO is one of the most widely used inorganic HTMs in perovskite solar cells due to its valence band energy of -5.2 eV being close to that of common perovskites (~ -5.4 eV[92]) and a wide bandgap of 3.5 eV, as well as good stability.[115-117] It provides efficient hole extraction and is compatible with various solar cell architectures.[115] Another common oxide used as a buffer layer and HTM in organic and perovskite solar cells is MoO_3.[118-120] It enhances hole transport by adjusting the work function of electrodes and improving interface properties, leading to better performance. Finally, copper salts have many promising candidates such as CuI, CuSCN, and CuS. For CuI, the valence band energy is around -5.1 eV, and the conduction band lies at approximately -2.6 eV, giving it a band gap of ~2.5 eV. CuI is well-regarded for its p-type semiconducting properties and is often used as an HTM in photovoltaic devices when paired with perovskite materials.[121-123] The alignment of the valence band of CuI closely matches that of common perovskites, aiding in enhanced charge transfer at the interface. For CuSCN, the valence band energy is approximately -5.5 eV, while the conduction band energy is at -1.8 eV, resulting in a band gap of about 3.7 eV.[124-126] This wide band gap, the material's transparency, and excellent hole transport characteristics make CuSCN a highly effective HTM in perovskite solar cells. CuS, with a narrower band gap of around 2.0 eV, features a valence band at ~ -5.2 eV and a conduction band at ~ -3.2 eV.[127] CuS is primarily known for its p-type conductivity and use in photoelectrochemical and thermoelectric applications. While less commonly used as an HTM in perovskite solar cells than CuI or CuSCN, its properties allowed the use of its nanoparticles for applications requiring efficient charge transfer and absorption in the infrared spectrum.[128-129]

While those inorganic HTMs are interesting candidates that fulfill the wanted criteria, they cannot compare to the sheer mass of possible organic molecules. Again, only the most common materials will be discussed in the scope of this work. Many of the most frequently used molecules for organic HTMs come from the group of polymers (Figure 14). Polythiophene and its variations are among the oldest but still widely applied examples. This conjugated polymer becomes conductive when oxidized, with good hole mobility and stability.[130] The tunability of its electronic properties depends on dopant concentration, which makes it a versatile HTM. Still, generally, the LUMO and HOMO energies are around -1.6 eV and -5.8 eV giving a band gap of around 4.2 eV.[131] Also beneficial is the ease with which thiophen can be functionalized, giving rise to molecules such as poly(3-hexylthiophene) (P3HT) or poly[3-(4-carboxybutyl)thiophene-2,5-diyl] with comparable electronic properties but advantages such as better processability and morphology.[130, 132-133] Arguably, the most routinely employed organic polymer for hole transport is also a polythiophene derivate: poly(3,4-ethylenedioxythiophene) (PEDOT). With HOMO/LUMO energies at -5.3 eV and -2.2 eV,[134] this cheap polymer is widely used in organic solar cells and OLEDs due to its excellent conductivity, stability, and transparency.[135-136] Yet nearly all publications use it as a blend with other molecules due to its low solubility. This is most often polystyrene sulfonate (PSS), which allows solution processing from aqueous dispersions. Conversely, this method makes precise control over morphology difficult and can impair the stability of the neighboring layers if they are moisture-sensitive, like most perovskites.[137] To solve this, different blends can be utilized, such as lignosulfonate[138] or poly(bis(4-phenoxysulfonic acid)phosphazene).[139] Other works use PEDOT derivatives[140] or specialized fabrication methods like oxidative chemical vapor deposition[141-143] to circumvent the solubility problem. One last group of polymers worth mentioning is poly(bis-(4-phenyl)-(2,4,6-trimethylphenyl)-amine) (PTAA) and its modifications. PTAA is a high-performance HTM that offers ease of fabrication, transparency to visible light, mechanical flexibility, conductivity, and stability.[144-146] It has its frontier orbital energies at -5.2 eV and -1.7 eV and is widely used in perovskite and organic solar cells.[134]

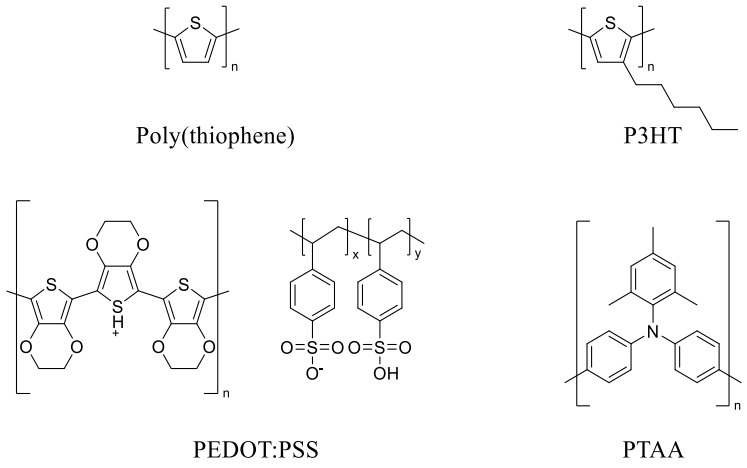

Figure 14: Examples of organic polymer HTMs.

On the forefront of small molecules, the undisputed gold standard, especially in perovskite solar cells, is 2,2',7,7'-tetrakis(*N,N*-di-*p*-methoxyphenylamine)-9,9'-spirobifluorene (spiro-OMeTAD, Figure 15). Spiro-OMeTAD is known for its excellent hole mobility, high efficiency, and compatibility with perovskite layers (HOMO/LUMO energies: -5.2 eV/-2.5 eV) achieving reliably high efficiencies with a benchmark PCE of 25.7%.[147-148] Despite its impressive efficiency, multiple properties still motivate researchers to replace spiro-OMeTAD. Most critical is the need for dopants to achieve these peak performances,[149] which impacts stability since they are typically hygroscopic and lead to ion migration and accumulation,[150-151] and a challenging synthesis, mainly due to the spiro connection.[152] Both lead to high production costs and lower appeal for long-term applications. Consequently, the search for better materials continues, including extensive variations of the spiro motif,[153-156] better processing of spiro-OMeTAD,[149] and completely new molecular motifs.[157-159]

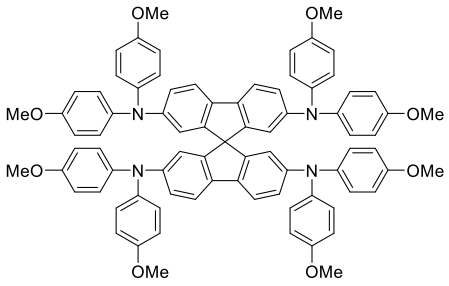

spiro-OMeTAD

Figure 15: The gold standard for perovskite solar cell HTMs: spiro-OMeTAD.

Given the topic of this thesis, the alternative motif that should be highlighted here is PCP-based materials. First tested for its charge transport properties by Park *et al.* in 2015 with tetra-triphenylamine-PCP,[160] it showed impressive efficiency, beating undoped spiro-OMeTAD with 17.6% compared to 15.4%. Later, Park *et al.* also tested tri- and disubstituted alternatives.[161] Otterbach and Schulz later explored this more in-depth with di- and tetrasubstituted thiophene-PCPs,[162-163] which this thesis aims to improve upon by exploring further interesting variations of this motif.

3. Library of PCP-based Organic Semiconductors

3.1. Motivation and Approach

The previous chapters, 2.2 and 2.3, highlighted the development and importance of solar cells and semiconductors. In the context of the KIT project, KeraSolar, new ferroelectric solar cells are developed and tested. By combining photovoltaics with ceramic materials research, it aims to use semiconducting oxide ceramics for charge carrier generation. Ferroelectric polarization in perovskite structures could help spatially separate charge carriers, reducing recombination and achieving high efficiency even with a large number of defects. With the changes in the active layer, especially changes in the energy levels, new materials for the surrounding charge transport layers become necessary. By setting up a modular library of molecules, it becomes possible to study the structure-property relation of the semiconductors and synthesize a matching molecule for every new material.

The [2.2]paracyclophane is a promising candidate as a base scaffold for the semiconductor library. Its many substitution patterns, the through-space conjugated system, and its properties, as discussed in chapter 2.1, make it an interesting target molecule with many possible variations. The proof that PCPs are promising as semiconductors was provided by Park *et al.* with a simple attachment of triphenylamine (TPA) donors to PCP, which gave good results with PCEs of up to 17.6% (Figure 16).[160-161] Otterbach expanded on this by adding thiophene and derivatives as π-bridges and exploring the effects on energy levels and efficiency as HTL in perovskite solar cells.[162-163] He further studied the impact of functionalization of triphenylamines and carbazole donors with methoxy and *tert*-butyl groups.[164]

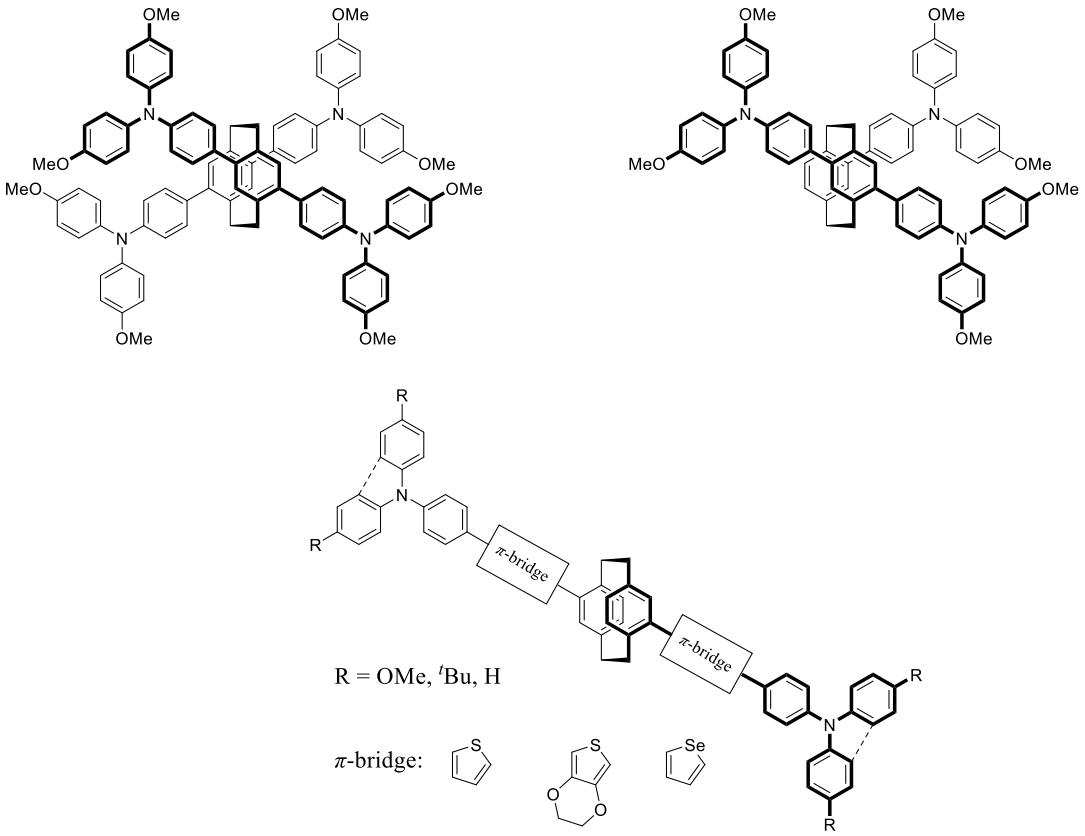

Figure 16: Examples of known PCP-based semiconductors by Park (top) and Otterbach (bottom).

This work focuses on the synthesis and analysis of new [2.2]paracyclophane-based semiconductors using new π-bridges. Thieno[3,2-b]thiophene, dibenzothiophene, and carbazole were employed, which all promise improvements in specific areas such as layer interactions, layer morphology, or solubility (Figure 17). As part of the combinatorial approach, different synthetical options will be explored to enable the desired flexibility, where every tested block can be easily combined with all others. Additionally, going from the *psp* isomer to other possible but more demanding stereoisomers of PCP gives the possibility to explore the isomeric effects on chemical, physical, and electronic properties. Furthermore, aside from monomeric semiconductors, polymeric materials with the same motifs were also tested.

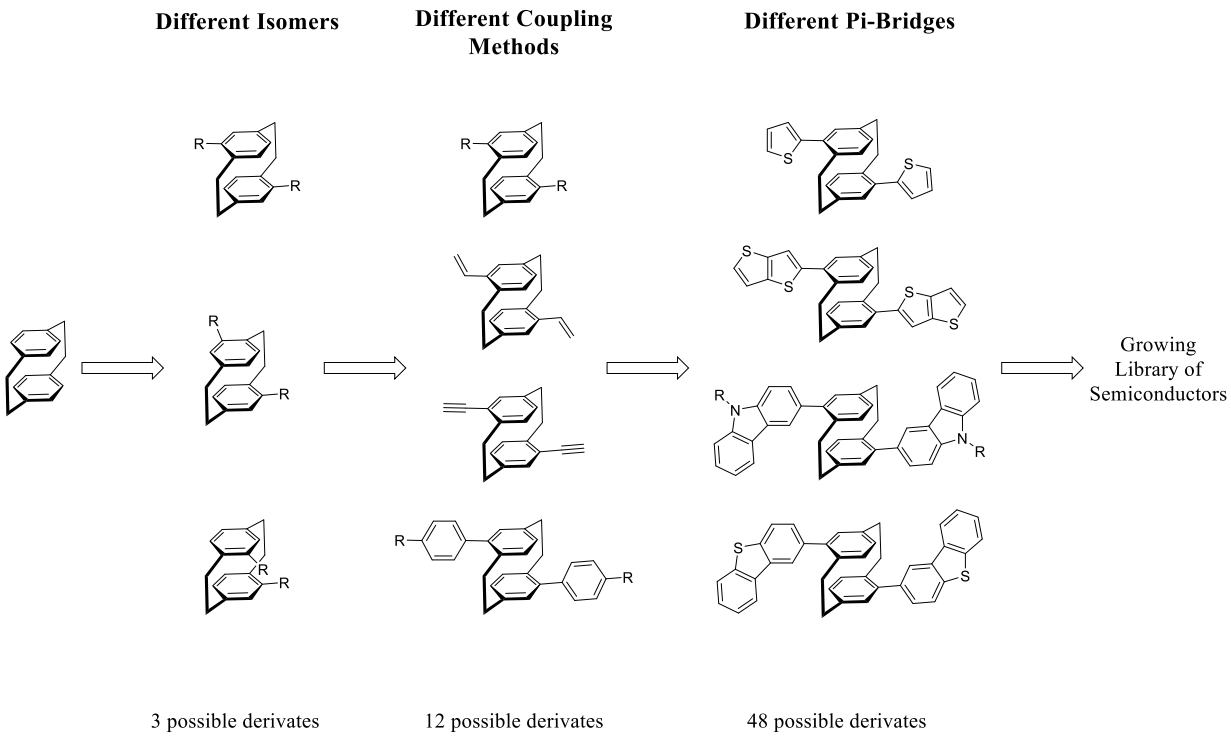

Figure 17: Overview of the combinatorial library with the chosen variations of regioisomers, coupling methods, and π-bridges.

3.2. Effects of Stereoisomers on Thiophene-based Semiconductors

The variation of the used PCP stereoisomers is a straightforward approach to start expanding the examples of PCP semiconductors discussed in the chapters above.[160-163] Those examples show good PCEs and have established synthetic routes, while the PCP as a core allows using these routes for many substitution patterns. The marked differences in 3D structure should lead to distinct differences in properties like solubility and layer morphology, which is important in processing and improving interactions with the surrounding layers in devices. At the same time, properties such as energy levels should not be influenced strongly, thus allowing implementation in the same devices.

Of the seven patterns for the disubstitution of PCP (see chapter 2.1) the ps-*para* is used most frequently. This is due to the accessibility of the *psp* halogenated isomer as a precursor. The dibromination to the *psp* isomer **1** is a one-step synthesis utilizing elemental bromine under iron catalysis and a subsequent crystallization (Scheme 2).[165] The ps-*meta* isomer **2** results from the same reaction but requires more purification effort. Multiple crystallization and washing steps are necessary to separate the less soluble *psp* isomer, often resulting in a lower yield. When focusing on optimizing the yield of the *psm* isomer, *psp* **1** and *psm* **2** could be synthesized for this work in 29% and 37% yield, respectively. Both can then be further isomerized to ps-*ortho* **3** and ps-*geminal* **4** at temperatures above 210 °C in triglyme. Both *psm* and *pso* are generally more soluble than *psp* because of their asymmetrical structure. The *Psg* isomer also shows improved solubility but tends to suffer from steric hindrances when attempted with sterically more demanding substituents. Substitutions on the same ring are less preferred in many reactions and thus typically involve multiple steps or a synthesis starting from substituted benzenes with low yields (see chapter 2.1). For this work, only *psp* (**1**), *psm* (**2**), and *pso* (**3**) derivatives were used to focus on the most promising candidates.

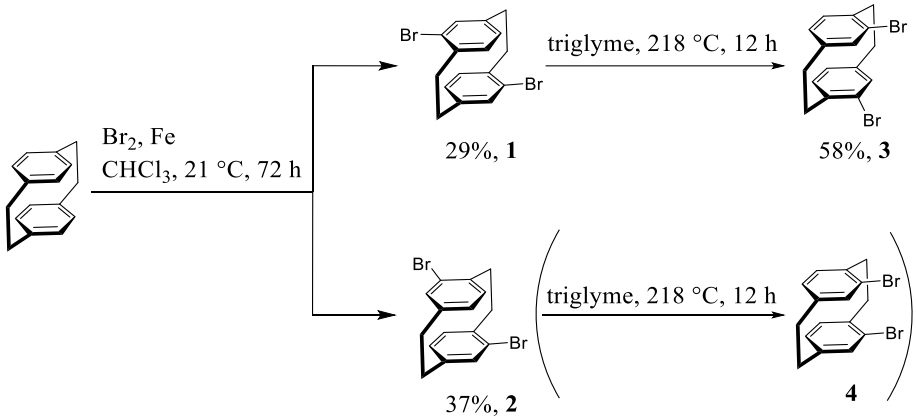

Scheme 2: Synthetic route for pseudo-dibrominated PCPs.

Based on the previously reported structure **5**, a set of semiconducting materials was prepared to directly compare the regioisomers **5**-**7** (Figure 18).[164]

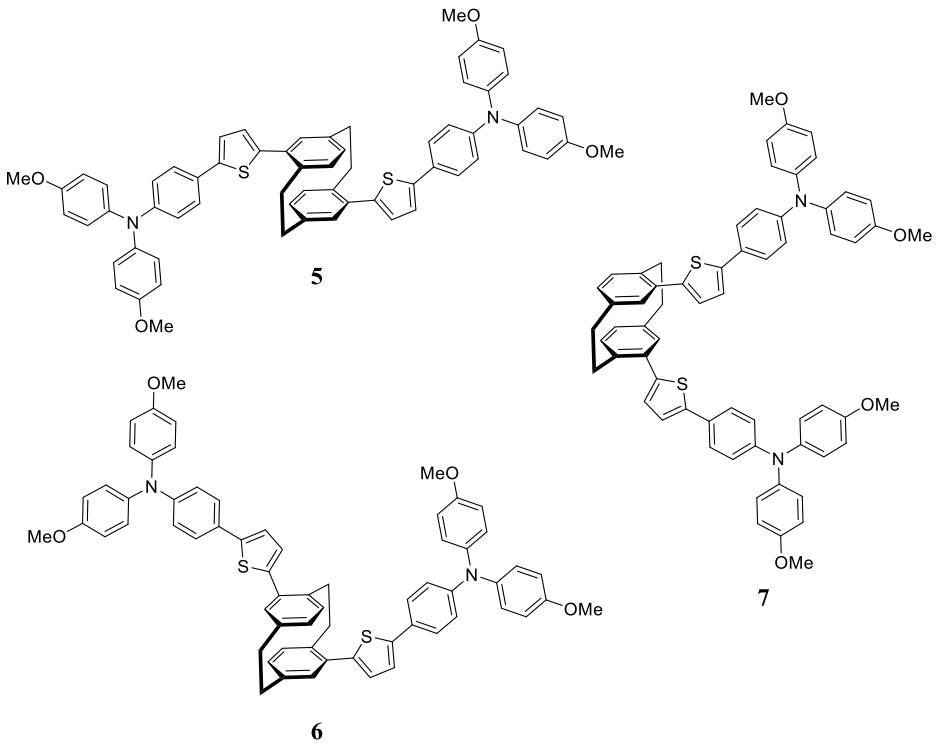

*Figure 18: Target molecules **5**-**7** for direct comparison of the effect of isomerization on semiconductor properties.*

Here, the semiconductor uses triphenylamine functionalized with methoxy groups as donor and thiophene as π-bridge. For the target molecules' synthesis, the donor was first synthesized, then the π-bridge was prepared for coupling, and lastly, they were combined (Scheme 3). Of all the available donors, the 4-methoxy substituted triphenylamine (OMe-TPA) was chosen as the standard for this work since it showed the best combination of efficiency and ease of synthesis in Otterbach's work.[164] Preparation of the donor follows a literature-known procedure using Ullmann condensation and yields 72% of the desired donor **8**.[166] The thiophene bridge was borylated to enable Suzuki coupling. This involved lithiation with *n*-Butyllithium (*n*-BuLi), followed by substitution with a pinacol boron ester, giving **9** in 72% yield.[167] Afterward, both were coupled in a standard Suzuki coupling procedure using $Pd(dppf)Cl_2$ and K_2CO_3 to yield 69% of **10**, for an overall yield of 50%.

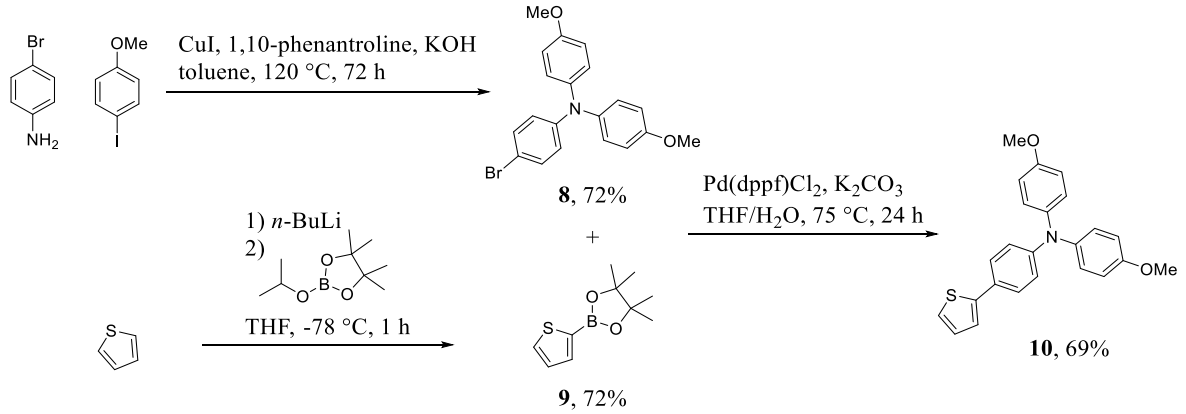

*Scheme 3: Preparation of donor **8** and bridge **9**, followed by Suzuki coupling to **10**.*

With molecule **10** prepared, synthesizing the target molecules **6** and **7** could be attempted (Scheme 4). For this, multiple coupling reactions can be considered. Still, a Negishi coupling with *in situ* synthesis of the metalated species worked best in Otterbach's tests with the *psp* derivate **5**.[164] It was, therefore, employed for the *psm* and *pso* isomers **6** and **7**. The donor was lithiated with *n*-BuLi and transmetalated with $ZnCl_2$ to produce the zinc organyl *in situ* and then combined with the brominated PCPs and the catalyst Pd-PEPPSI®-*i*Pr. The yield was lower than expected, given that even fourfold coupling yielded 64% in the source literature. The main reason for this and the 20%-point difference between *psm* and *pso* isomers is the difficult purification, often needing multiple chromatographies as well as washing and crystallization steps. Especially for the last method, the now improved solubility hinders good results. This must be addressed in future work if a practical application is to be attempted.

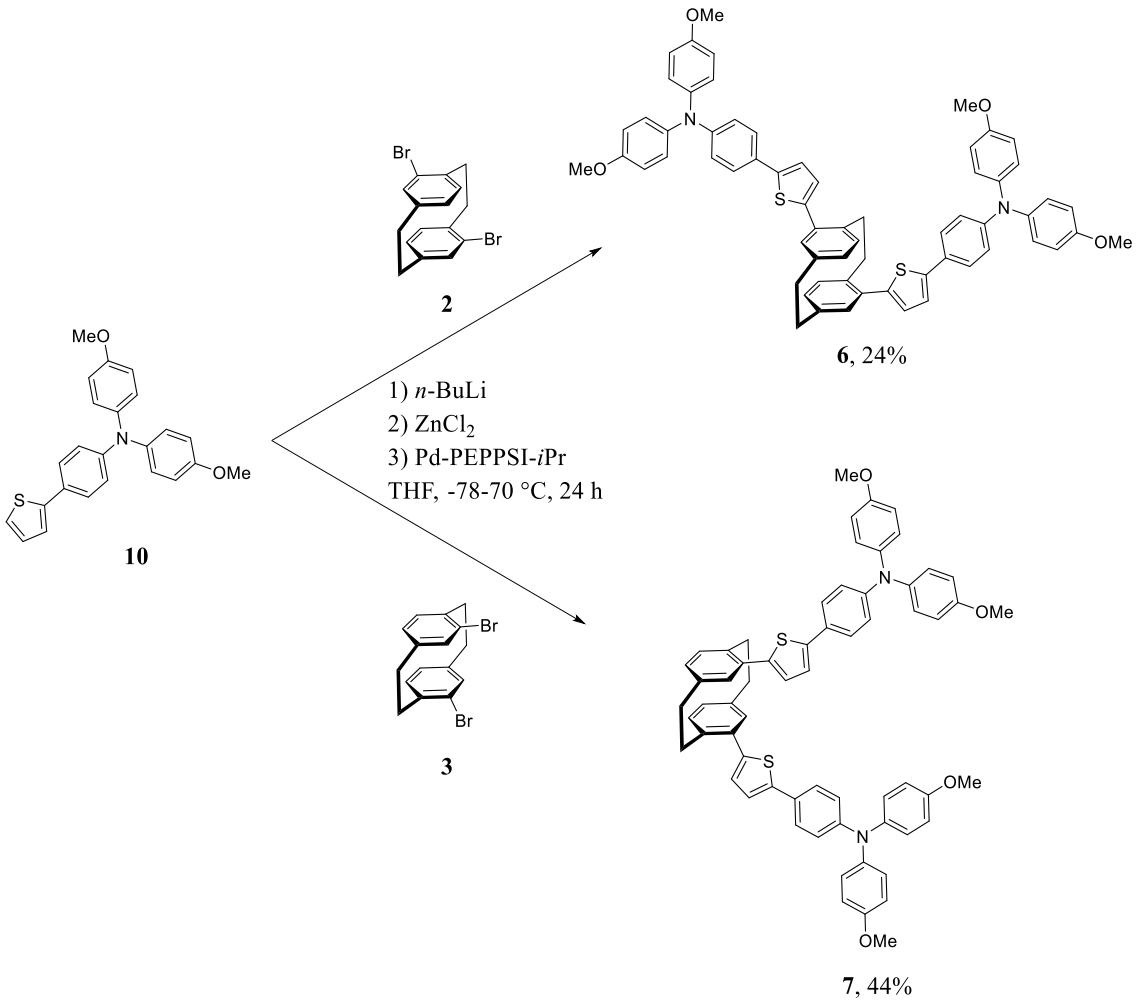

*Scheme 4: Synthesis of target molecules **6** and **7*** via *Negishi coupling.*

The Colsmann group tested the properties of the two newly synthesized target molecules **6** and **7** as thin-films. All results are summarized and discussed in chapter 3.5. To validate the effects of different isomers received for the thiophene-based target materials **5-7**, other π-bridged molecules will also be tested and discussed as different isomers in the following chapters.

3.3. Variation of π-Bridges

By far the most impactful variation of the target material attempted in this thesis, especially regarding electronic properties, is the selection of the π-bridge. Together with the donor, it is crucial for tuning the HOMO/LUMO levels, as well as improving interactions with surrounding layers in the device. Additionally, it can help improve physical properties like solubility, stacking, and stability.[168-170] Currently, all tested bridges for PCP-semiconductors are thiophene or closely related molecules like selenophene or ethylendioxythiophene.

For this thesis, three distinct heteroarenes were chosen, each with its possible benefits and challenges that will help better understand the chemistry of PCP-based semiconductors, thus further establishing the library of hole transport materials for KeraSolar. The tested bridges were thienothiophene, dibenzothiophene, and *N*-substituted carbazoles (Figure 19). Each will be discussed separately in the following section, while the benefits and drawbacks of each will be compared.

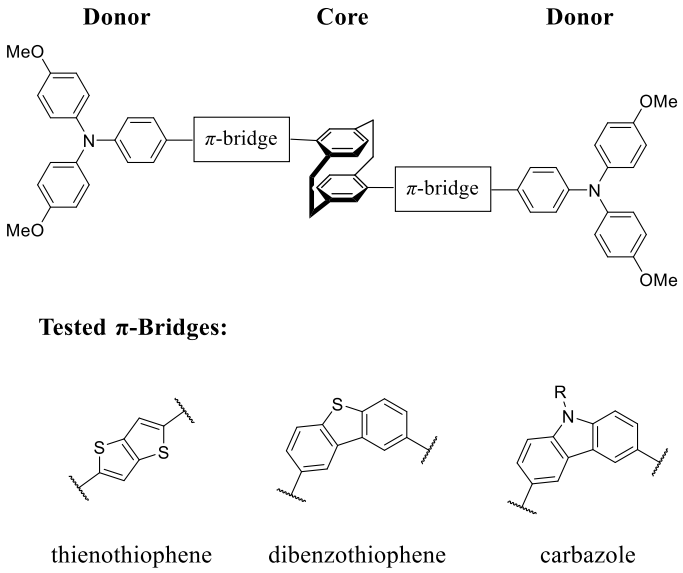

Figure 19: Selection of tested π-bridges.

3.3.1. Thienothiophenes

Thienothiophene, or more specifically thieno[3,2-*b*]thiophene, the commercially most available isomer, is chemically closely related to the known thiophene bridge and shows similar behavior in reactions. At the same time, it has a larger, linear π-system and, therefore, a stronger planar character in the final materials, which enables better stacking in solid films. It also has a higher sulfur content that is known to show beneficial interactions, especially with lead-based perovskites, thus improving the charge transfer.[171]

To synthesize thienothiophene-bridged PCP semiconductors, two different general approaches were tested: Starting with the PCP core and working from the inside out to the donor or starting with the donor and going outside-in to the core (Scheme 5).

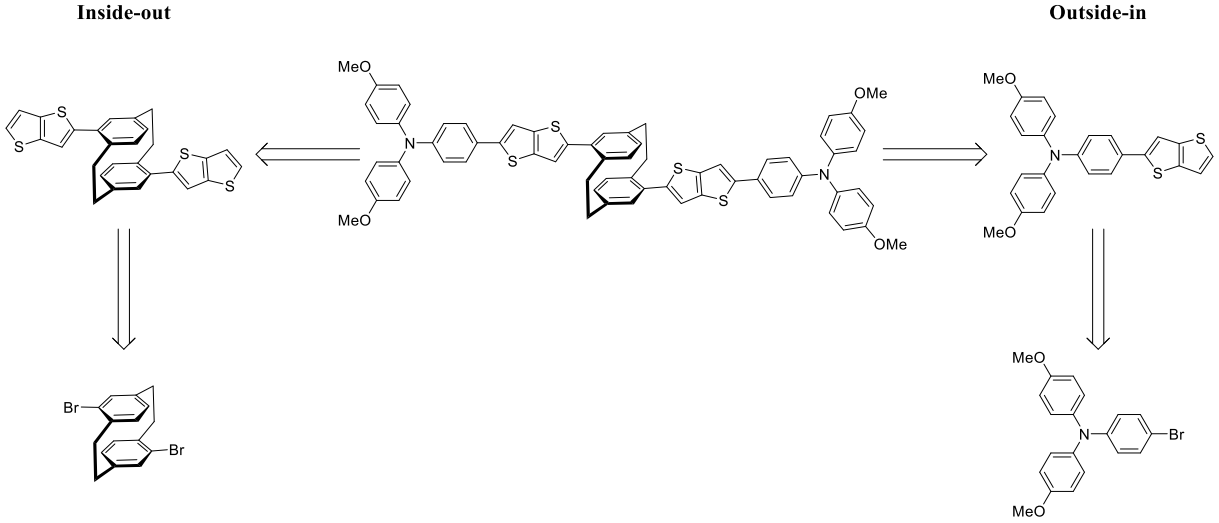

Scheme 5: Comparison of inside-out approach vs. outside-in approach.

The first step in an inside-out approach is coupling the thienothiophene with the halogenated PCP core. Possible options would be a cross-coupling reaction like a Suzuki coupling or a CH activation since thienothiophene possesses the same reactive CH bond in the 2-position as thiophenes (Scheme 6). CH activation has the advantage of not needing an additional functional group, saving a reaction step. Tests for the CH activation were conducted with conditions that worked well for thiophene (Table 1, entry 1),[164] ethylendioxythiophene (entry 2),[172] as well as thienothiophene itself with other arenes (entry 3)[173] and conditions that worked for PCP couplings with other arenes for the author (entry 4). None of them yielded the desired product in more than trace amounts and showed either no conversion or consumed the thienothiophene to produce side products only.

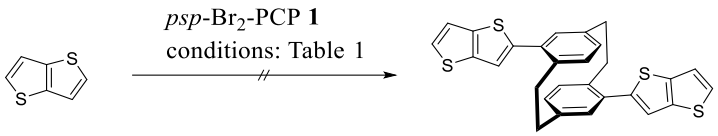

11

*Scheme 6: CH activation coupling of thienothiophene and PCP **1**.*

Table 1: Tested reaction conditions for CH activation coupling of PCP and thienothiophene. All reactions were run for 24 h and controlled by TLC.

Entry	Thienothiophene (equiv.)	Catalyst	Ligand	Additive	Temperature [°C]	Solvent
1	20.0	$Pd(OAc)_2$	$P(Ph)_3$	PivOH	100	DMF
2	2.00	$Pd(OAc)_2$	$P(m\text{-}Tol)_3$	Cs_2CO_3	110	toluene
3	2.00	$Pd(OAc)_2$		KOAc	120	DMAc
4	3.00	Pd_2dba_3	SPhos	NaO^tBu	140	xylene

This implies that PCP is significantly less prone to react in this setting than thienothiophene is to react in a side reaction. The main side reaction in this case is the homocoupling of thienothiophene. So instead, a Suzuki cross-coupling was tested. For this, the thienothiophene pinacol ester **12** was synthesized by lithiation, followed by borylation, with a yield of 79% (Scheme 7).

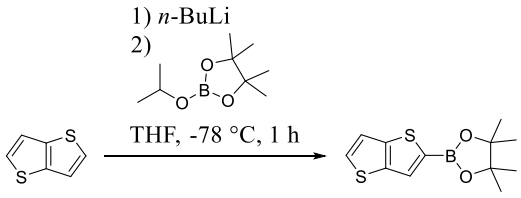

12, 79%

*Scheme 7: Synthesis of **10** by lithiation and substitution with isopropoxyboronic acid pinacol ester.*

The borylated thienothiophene was used in a standard Suzuki coupling using $Pd(dppf)Cl_2$ and potassium carbonate in a toluene/water mixture (Scheme 8). Again, no product formation was observed, and **12** was defunctionalized instead. The following efforts focused on the outside-in approach, as it showed slightly better results in literature with thiophene.[164]

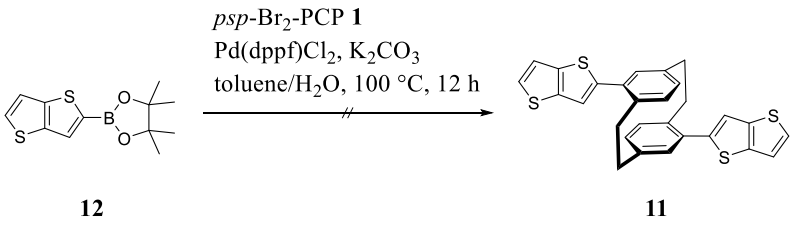

*Scheme 8: Tested Suzuki coupling to synthesize thienothiophene-PCP **11** from **12**.*

For the outside-in approach, the first step combines the π-bridge and the donor, in this case, the brominated OMe-TPA **8**. Multiple ways were tested for this: First, a CH activation like the one used in the inside-out approach, offering a direct route with few steps. Second, the Negishi coupling with *in situ* generation of the metalated species, as introduced in chapter 3.2, giving another direct route with a more activated coupling partner. And third, a Suzuki coupling that offers a more indirect route, where coupling partners have to be prepared first, but which is generally less susceptible to degradation in air and moisture.

CH activation, while generally working, needed high reaction times to achieve even moderate yields of 38%, and like the coupling to PCP, if less extreme, it suffered from side reactions (Scheme 9). While working faster, the Negishi coupling showed a similarly low yield of 33% but even more degradation of starting materials, likely because of the extreme sensitivity of the Negishi species (Scheme 9).

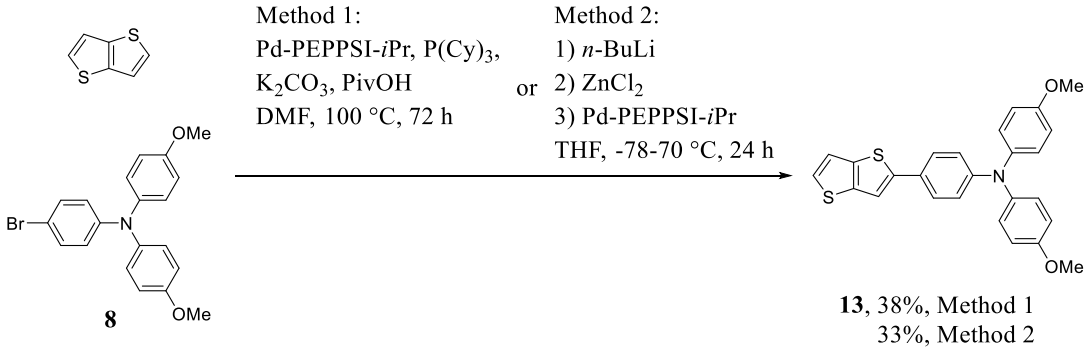

*Scheme 9: Direct route synthesis of thienothiophene-OMe-TPA **13*** via *CH activation (Method 1) or Negishi coupling (Method 2).*

The route of choice was, therefore, the Suzuki coupling. For this, a borylated species must be synthesized, either at the donor or the thienothiophene, with a halogen at the opposing moiety (Scheme 10).

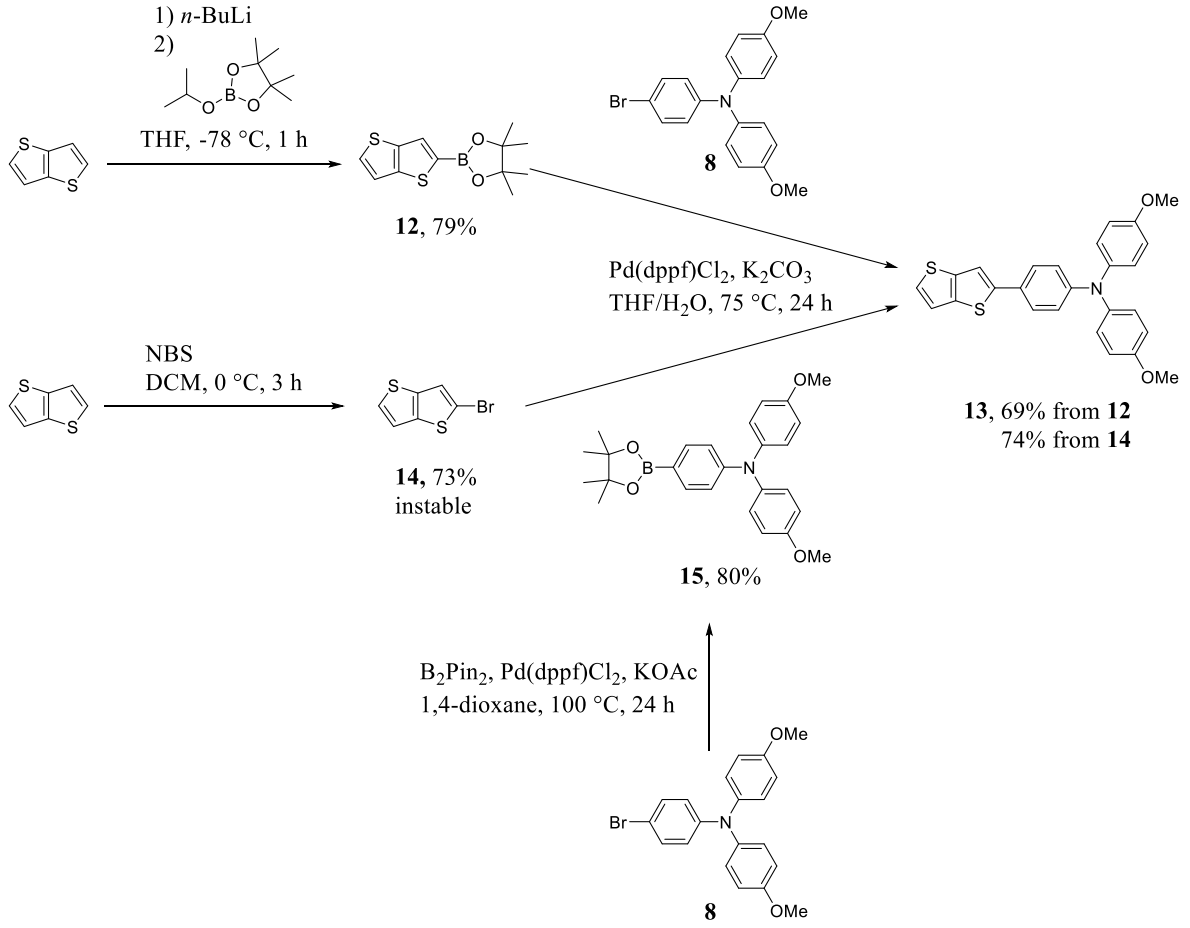

Scheme 10: Tested routes for Suzuki coupling to 13 starting from thienothiophene.

Both routes have nearly the same overall yield, 55% for borylated thienothiophene **12** and 54% for borylated donor **15**. The preparation of the borylated thienothiophene **12** has a higher yield (79%) compared to the combined preparation of **14** and **15** (73% + 80%) for the second route but a lower yield in the following coupling (69% vs. 74%).

Overall, the first route is preferable since it has one step less, and more importantly, its coupling partners **12** and **8** are stable, while **14** must be synthesized, purified, and used in a day or less to prevent spontaneous cleaving of the bromine, followed by polymerization. The resulting poly(thienothiophene) can be observed as a baseline spot in the thin layer chromatography (TLC) of the previously purified bromo-thienothiophene (**14**) and as a metallic green color appearing in the normally colorless **14**. Degradation in storage could be reduced by using diluted solutions and cooling at -20 °C, but this still impacted the isolated yields.

With the donor arm 1**3** in hand, coupling to target molecule **17** was attempted (Scheme 11). Again, CH activation did not result in the target molecule. It can be assumed that this is for the same reasons molecule **11** could not be realized: Side reactions like homocoupling were preferred to the desired coupling. Electrospray ionization mass spectrometry (ESI MS) confirmed the formation of homocoupling product, but no pure fraction could be separated.

For the next attempt, the borylated species **16** needed for Suzuki coupling had to be synthesized, which could be achieved with a 71% yield under the same conditions as for **12**. However, the following coupling step did not result in the desired product. What finally allowed for the successful synthesis and purification of **17** was the Negishi coupling that was also used in chapter 3.2 for the thiophenes. While it proved less effective in earlier steps due to its sensitivity, its high reactivity was necessary in this case and resulted in a yield of 27%.

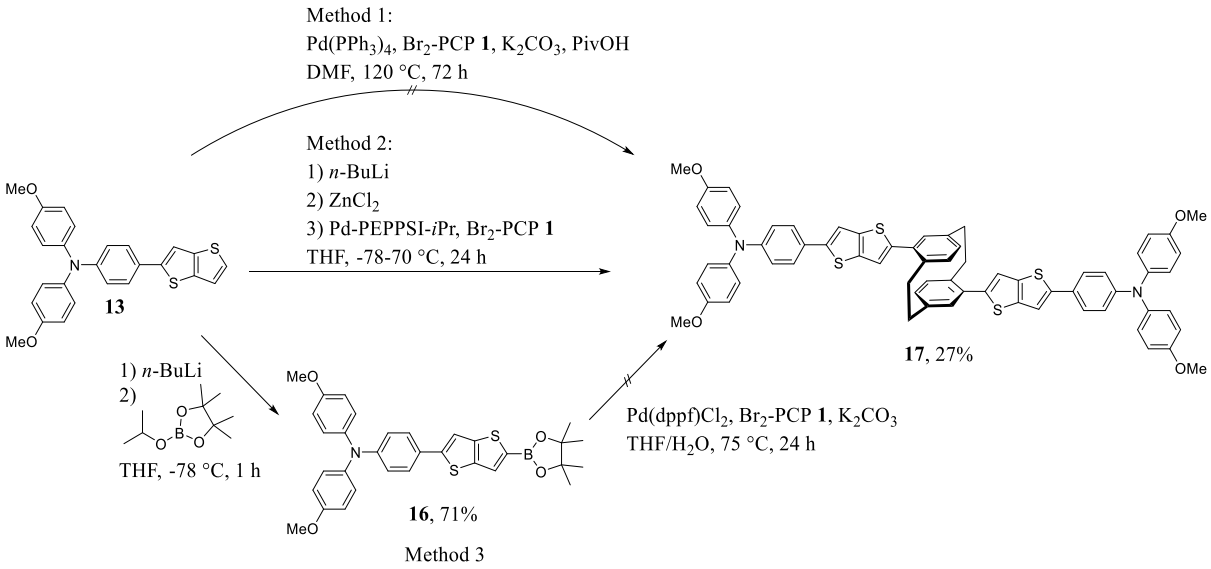

*Scheme 11: Attempted routes to synthesize target molecule **17** from **13*** via *CH activation (Method 1), Negishi coupling (Method 2), and Suzuki coupling (Method 3).*

After the successful synthesis of **17**, these conditions could be applied to other isomers. For this the *psp*-Br_2-PCP **1** was exchanged with *psm*- and *pso*-Br_2-PCP **2** and **3** (Scheme 12). The yield for the *pso* isomer, with 42%, was slightly higher than that of the *psm* isomer, similar to the results for thiophene derivates **6** and **7**. The trend for the yield roughly follows the solubility from *psp* over *psm* to *pso* but cannot be finally confirmed with the low number of examples. Further tests must prove that the trend holds true in the future and can try to optimize the yield overall.

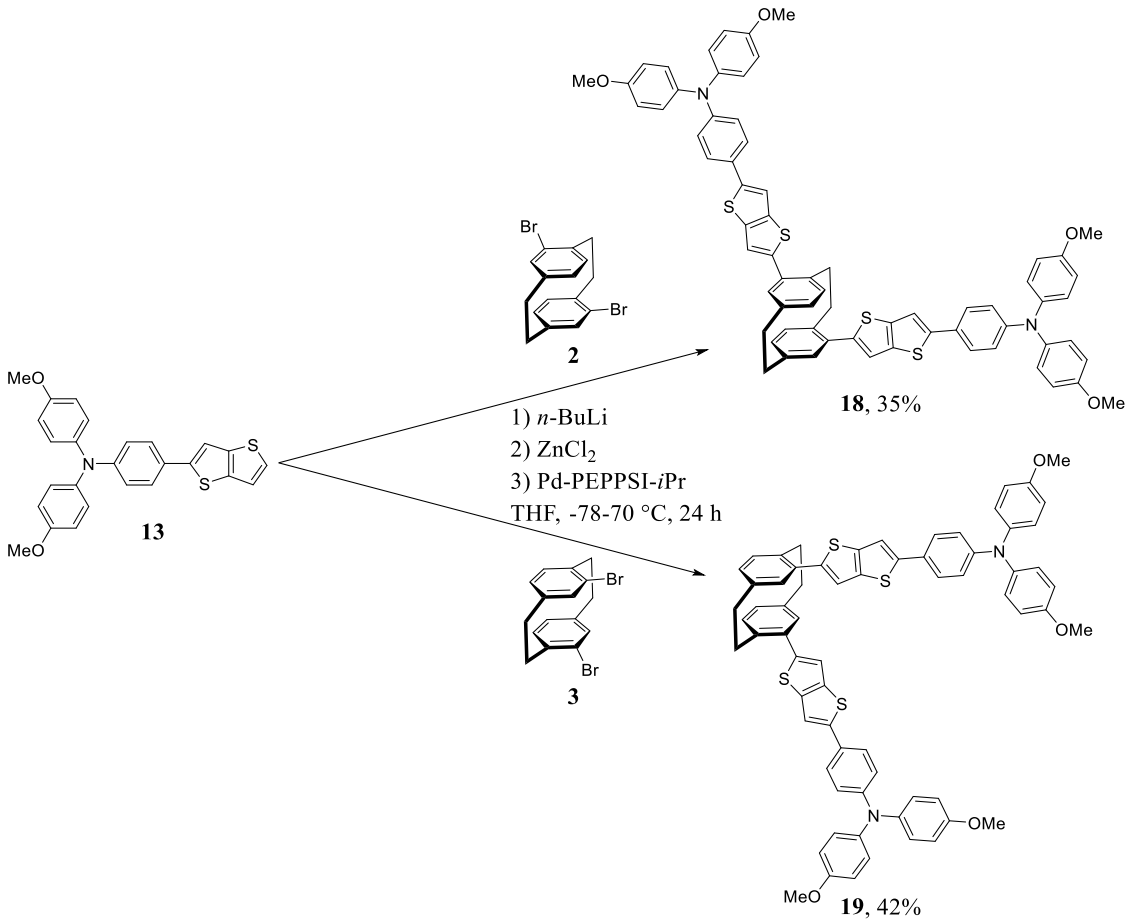

*Scheme 12: Synthesis of the isomers **18** and **19** from **13**.*

Summerized, the thienothiophene bridge was successfully synthesized and combined with three PCP isomers to yield three novel semiconductors. The Colsmann group tested the properties of the successfully synthesized target molecules as thin-films. All results are summarized and discussed in chapter 3.5.

3.3.2. Dibenzothiophenes

The second new π-bridge tested was the dibenzothiophene, in which thiophene is fused with a benzene ring on each side. This gives an even larger planar system than with thienothiophene, offering great conditions for stacking in films and, therefore, improved intermolecular conductivity in devices.[174-175] Additionally, the sulfur in dibenzothiophene is known to be easily oxidized to sulfoxide and sulfone, giving two more molecules to test for each synthesized target molecule. On the other hand, developing the synthetic routes from scratch is necessary: The reactivity is decidedly different than in thiophene or thienothiophene, not having the activated CH bond, thus being closer to an inactive benzene. For this reason, direct reactions like CH activation coupling or reactions with mild conditions are hardly possible. This is readily observable in the very first functionalization. A bromination of dibenzothiophene is impossible with *N*-bromosuccinimide (NBS) or similar soft methods. Even in a reaction with elemental bromine, reaction times of a week or even longer are necessary to give acceptable yields.[176] In the end, adding iron as a catalyst solved this problem and allowed for yields of 98% within 16 h.

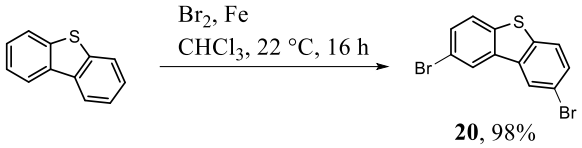

20, 98%

Scheme 13: Bromination of dibenzothiophene with elemental bromine under iron catalysis.

In turn, the need for those harsh methods gave rise to another challenge. A monobromination would ensure good selectivity and yield in the donor coupling. Still, it would be impossible to selectively brominate the dibenzothiophene a second time since the OMe-TPA donor would brominate first.[177] For a direct CH activation, the reactivity of dibenzothiophene and PCP is too low. Therefore, the dibrominated thiophene **20** was used directly, partially leading to over-functionalization upon coupling with the respective donor. Nevertheless, up to 53% yields could be achieved in the coupling. Noteworthy is also the low solubility of the synthesized dibenzothiophene, which necessitates large quantities of solvents for the reaction to work smoothly.

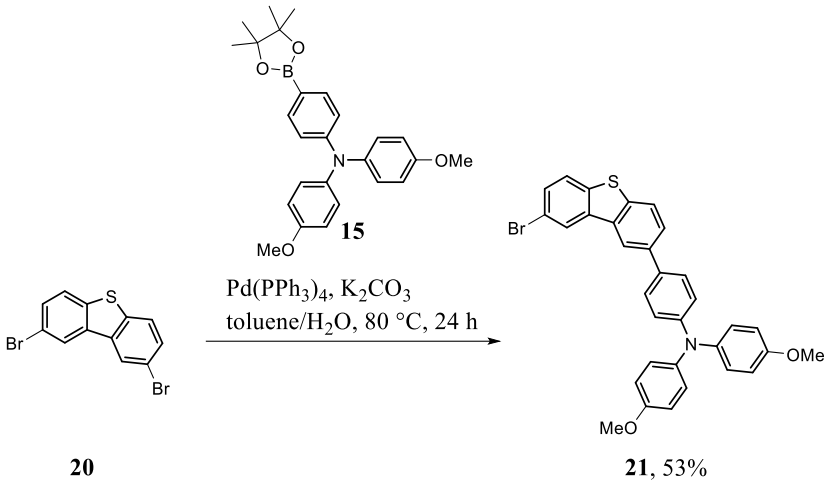

*Scheme 14: The synthesis of donor arm **21** from dibrominated dibenzothiophene **20**.*

Coupling the synthesized arm **21** with PCP was tested with the Negishi coupling that enabled the synthesis of thienothiophene derivates. Sadly, even the highly reactive Negishi reactant did not yield target molecule **22**. It is unclear if this is solely because of the low reactivity or because of solubility issues, which were also noticeable in the former reactions with dibenzothiophene but would be more pronounced with the larger system of **22**. The less aggressive coupling variations were not tested.

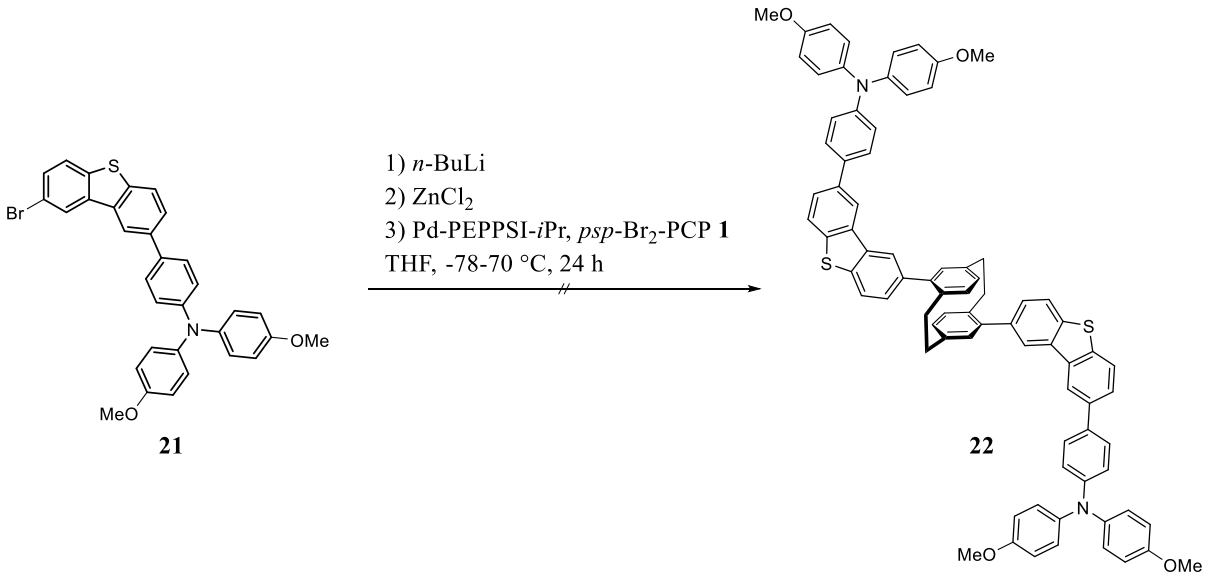

*Scheme 15: Tested Negishi coupling of **21** with PCP **1** to yield **22**.*

While solubility issues could at least partly be alleviated by switching to the more soluble *psm* and *pso* isomers, it is unlikely to have a strong enough effect to give usable yields. Therefore, another method must be found to couple dibenzothiophene and other similarly unreactive building blocks that may arise in the future. A possible strategy is to introduce small, conjugated groups that react well with either of the molecules between the unreactive bridge and the likewise unreactive PCP. Groups such as vinyl, alkyne, or phenyl are possible candidates for spacer groups, and will be discussed later in chapter 3.4.

3.3.3. Carbazoles

The last π-bridge tested for this thesis was the carbazole. Structurally close to dibenzothiophene, the switch in heteroatom significantly influences the molecule's properties and reactivity. While the loss of sulfur means abandoning the beneficial interactions with the perovskite layer, the nitrogen's free position allows for many further functionalizations. The newly introduced groups can bring benefits ranging from improving solubility or layer morphology to introducing additional donor groups and including groups with interactions tailored to the molecules of the surrounding layers, such as amines or phosphate esters (Figure 20).

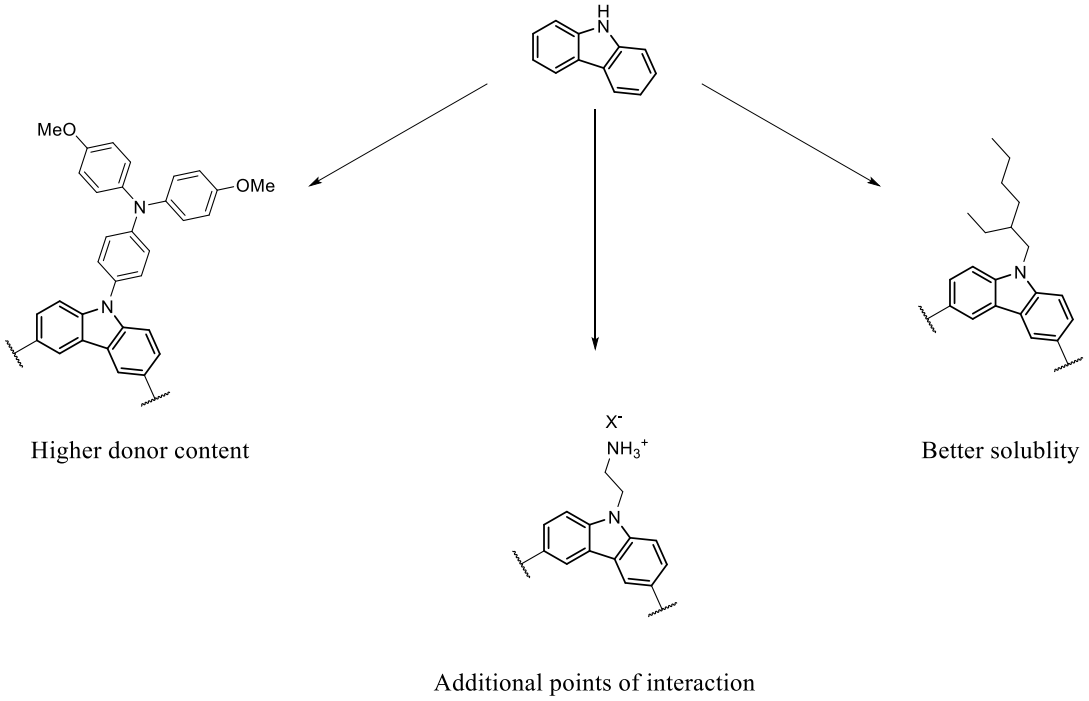

Figure 20: Examples of the introduction of functional groups at the N-*position of carbazole and their possible benefits.*

N-Functionalization can be done before or after introducing groups in *para* positions to facilitate further reactions like coupling. For this work, bromination was carried out first since mono- and dibromination could be easily done on a big scale with NBS at low temperatures, or the resulting carbazoles simply bought commercially (Scheme 16).

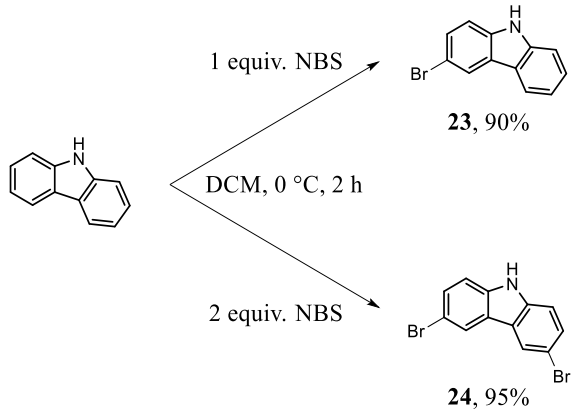

23, 90%

24, 95%

Scheme 16: Bromination of carbazole with NBS. Mono- vs. disubstitution is controlled by the equivalents of NBS.

Afterward, the *N*-functionalization can be done either by a base-promoted substitution reaction or Pd-catalyzed coupling. Substitution generally shows better acceptance of functional groups but is less reactive than Pd-catalyzed reactions.

The first tests were carried out with ethylhexane, a group commonly used to increase solubility, since the experiments with thienothiophene and especially dibenzothiophene showed that the bigger planar system decreased the solubility enough to create challenges in reaction and processing. The synthesis of the substituted carbazole **25** was easily achieved with a variation of the literature-known substitution procedure with ethylhexl bromide using KOH in dimethylformamide (DMF) with a yield of 98% (Scheme 17).[178] The effect of the attached ethylhexyl group was immediately obvious. The product was a honeylike oil instead of a solid like the starting material or the comparable dibenzothiophene **20**.

The following coupling with the donor was done under the same conditions as the comparable step for the dibenzothiophene **21**. Yet, while the coupling was successful and led to the desired monocoupling (with the expected disubstituted side product), ^{1}H nuclear magnetic resonance spectroscopy (NMR) showed a significantly lower proton count for the alkyl chain than anticipated.

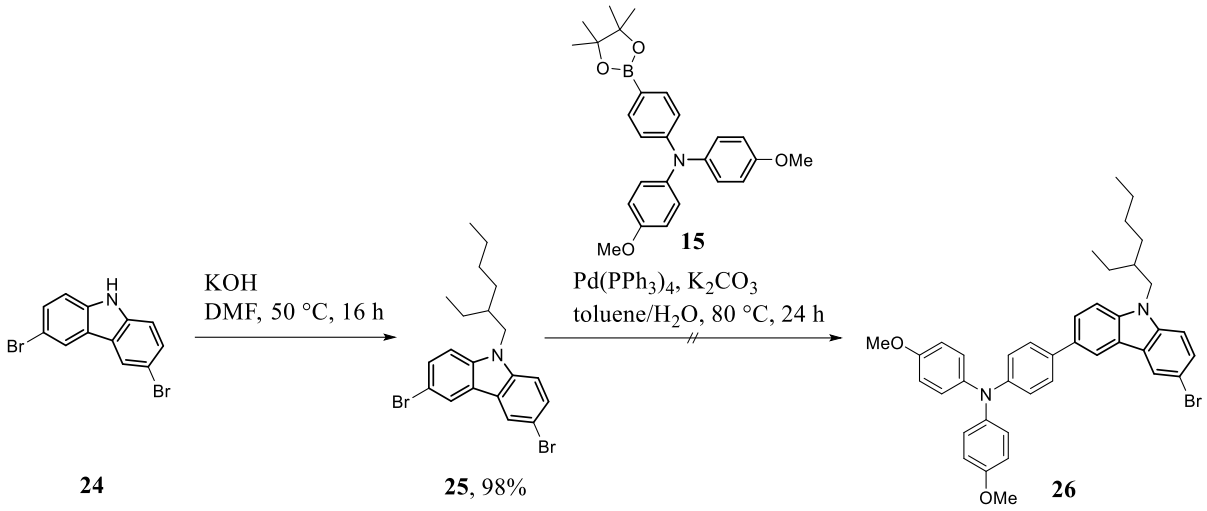

*Scheme 17: Functionalizing **24** with ethylhexyl bromide and subsequent coupling with the TPA donor.*

This was true for both mono- and disubstituted products as well as in reaction with other catalyst systems. This led to the conclusion that the alkyl is instable under the coupling conditions. Literature supports this with other examples, where *N*-substituted alkyls were cleaved with either heat or Pd-catalysis.[179-180]

Consequently, further attempts were restricted to aromatic moieties. While plenty of aromatic groups are known to improve solubility, this work focused on OMe-TPA, which can serve two roles at once: as a donor and, thanks to its methoxy groups and its twisted character, to improve solubility. Three possible routes were tested to functionalize the *N*-position with the OMe-TPA donor (Scheme 18). Adding the donor stepwise to the carbazole using commercially available building blocks, S_NAr reaction with the fluoro-substituted donor **27**, and an Ullmann condensation with the iodine-substituted donor **28**.

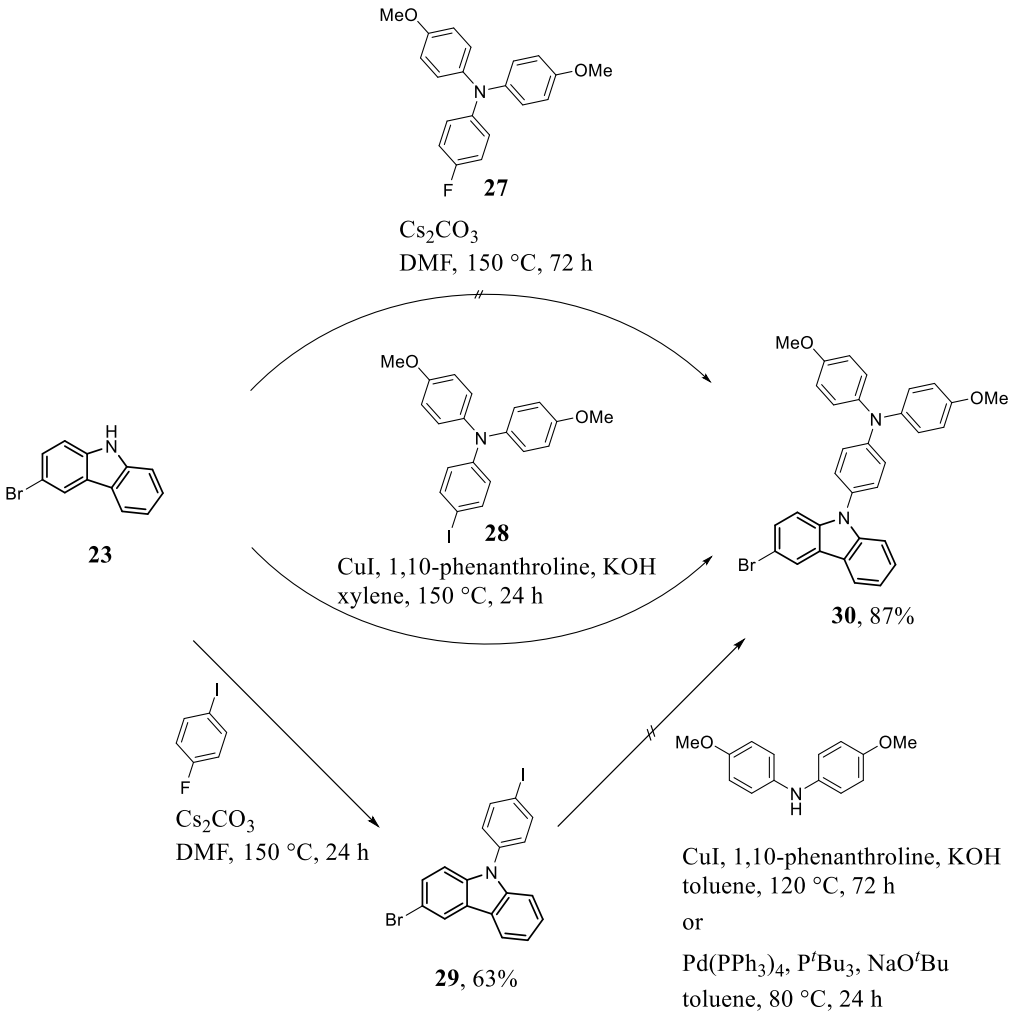

*Scheme 18: Three possible routes for synthesizing **30**: Top: S_NAr substitution with F-OMe-TPA (**27**). Middle: Ullmann condensation with I-OMe-TPA (**28**). Bottom: Two-step synthesis of TPA directly at the carbazole by S_NAr with 1-flouro-4-iodobenzene, followed by Hartwig-Buchwald or Ullmann condensation with bis(4-OMe-phenyl)amine.*

The first method uses the different reactivities of the halogenes fluorine, bromine, and iodine to allow stepwise reaction. First, commercially available 1-fluoro-4-iodobenzene reacts in an S_NAr selectively at the *F*-position, leaving the bromine and iodine. Then, the properties of iodine as a better leaving group can be used to react with bis(4-OMe-phenyl)amine in an Ullman condensation or a Hartwig-Buchwald coupling, leaving the bromine for further reactions. While the first step works as intended, giving **29** in 63% yield, the second does not yield the desired product. Due to time constraints, this route was not explored further within the scope of this work.

Instead, reactions of **23** with a completed donor moiety were tested. The desired donors **27** and **28** were successfully synthesized by Ullmann condensation (Scheme 19). Fluoro-substituted OMe-TPA **27** was realized in one step with a yield of 42%. At the same time, the iodo-substituted **28** needed an intermediate step with a 72% yield of the unfunctionalized **31**, followed by iodination with *N*-iodosuccinimide (NIS) to give 75% **28** (an overall yield of 54%).

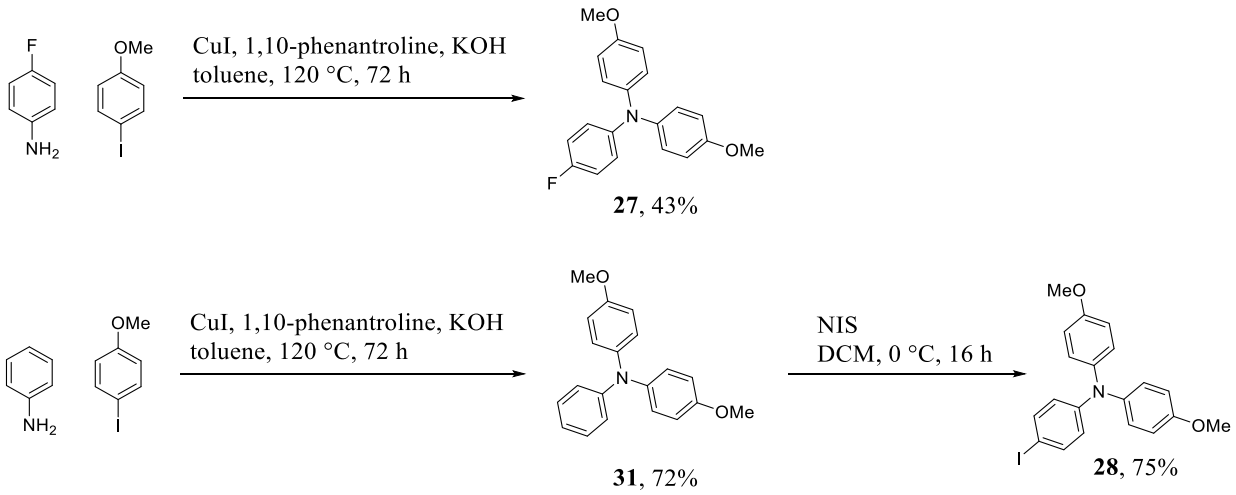

*Scheme 19: Synthesis of the donors **27** (top) and **28** (bottom) using Ullmann condensation.*

The S_NAr reaction using **27** under the same conditions that successfully synthesized **29** yielded no result (Scheme 18). The electronic situation in the fully built TPA does not allow the effective substitution possible with benzenes. On the other hand, **28** could be successfully reacted in an Ullmann condensation to give **30** with a yield of 87%.

After successfully *N*-functionalizing the carbazole, the donor was also attached to the *para* position of the carbazole, utilizing the bromine group of **30** for a Suzuki coupling with donor **15**. This yielded carbazole **32** with a 73% yield (Scheme 20).

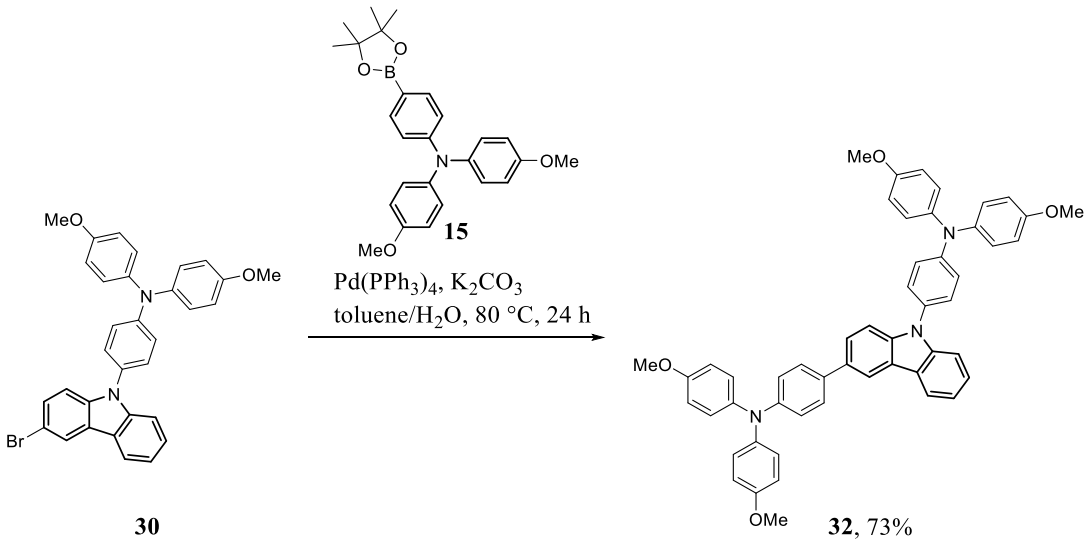

*Scheme 20: Suzuki coupling of carbazole **30** with TPA **15** to yield **32**.*

Parallel tests with the dibrominated carbazole, equivalent to the experiments with dibenzothiophene, gave good results for the Ullmann coupling (giving carbazole **33** in 97% yield) but resulted in selective disubstitution for the Suzuki coupling with 34% yield (Scheme 21). The resulting molecule **34** is also

predicted to show semiconducting properties and was, therefore, included in later tests but cannot be used for further reactions with PCP.

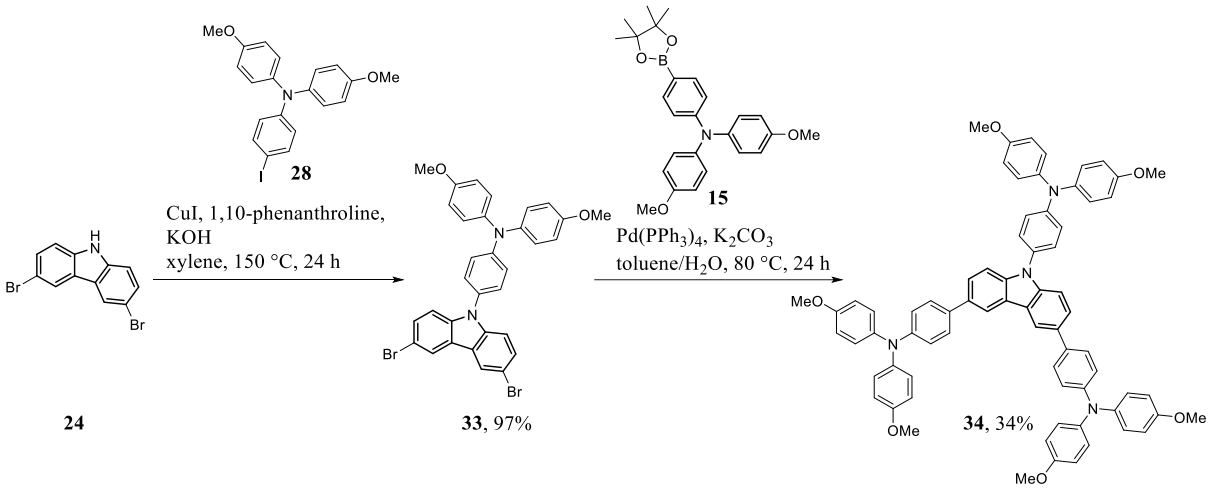

*Scheme 21: Synthesis and coupling of the dibrominated carbazole **33**, yielding dicoupled **34** selectively instead of a monocoupled product.*

The coupling of the one-armed carbazole **32** with PCP was done using the Negishi coupling established in the earlier tests with thienothiophene and dibenzothiophene. The coupling with the *psp* dibromo-PCP **1** yielded 40% of **35**, while the coupling with *psm* isomer **2** gave 22% of target molecule **36**.

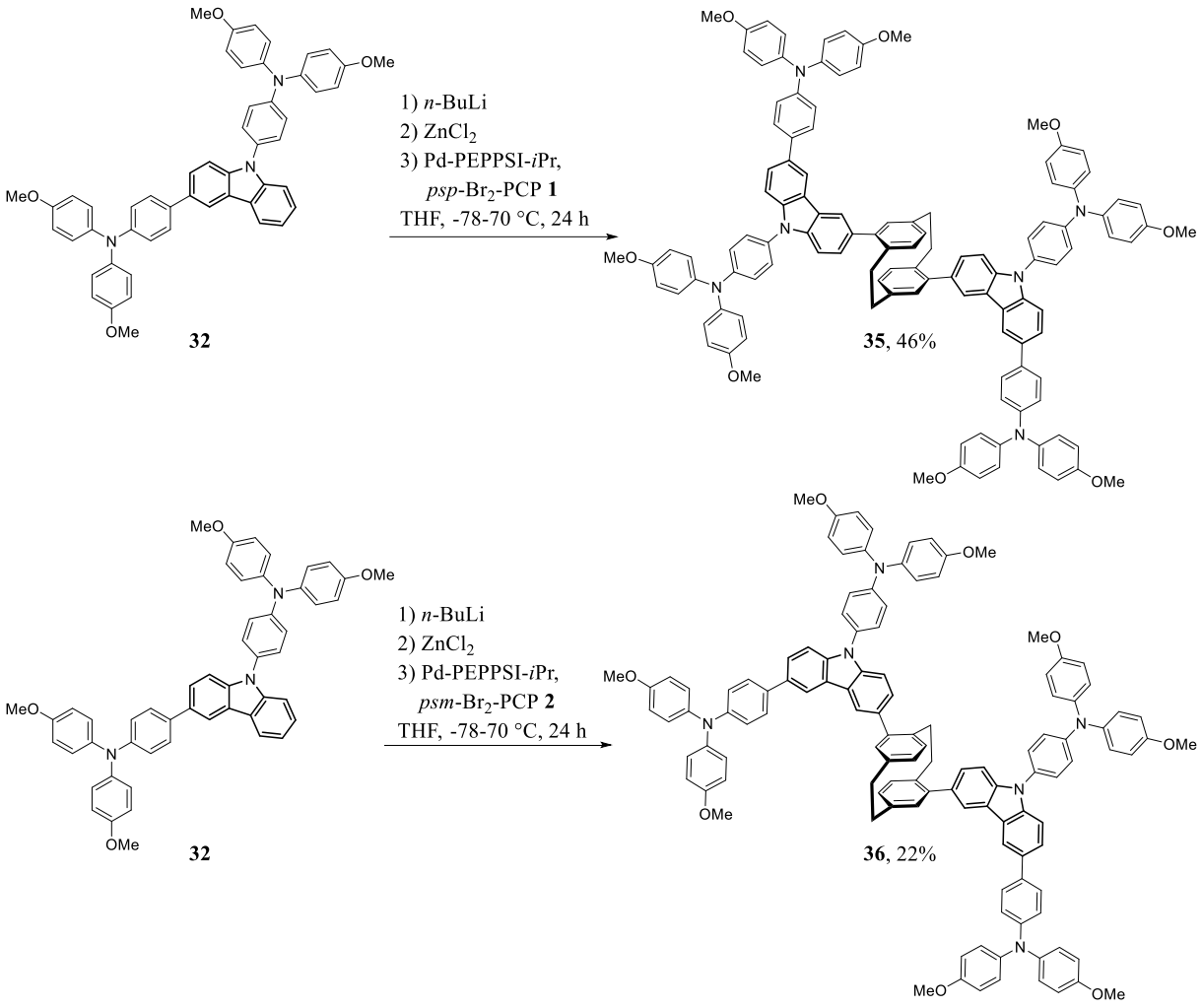

*Scheme 22: Negishi coupling of carbazole **32** with PCPs **1** and **2** to yield target molecules **35** and **36**.*

Overall, carbazole-bearing two donor moieties were successfully synthesized and used to produce three new semiconductors: **34**, **35**, and **36**. The Colsmann group tested the properties of the synthesized target molecules as thin-films. All results are summarized and discussed in chapter 3.5.

The last type of tested *N*-functionalization was aimed at interacting closely with perovskites. Both ammonium and phosphate esters are known to be closely bonded to the ionic structure of perovskite, possibly even being partly built into the lattice; ammonium as cation, the phosphate oxygen as anion.[181-184] This allows great interaction, thinner layers, and improved stability through surface modification.

To test the interactions, both groups were introduced with an ethyl spacer to carbazole without further modifications, giving the carbazoles **37** and **38**, both known to literature (Figure 21).[183, 185]

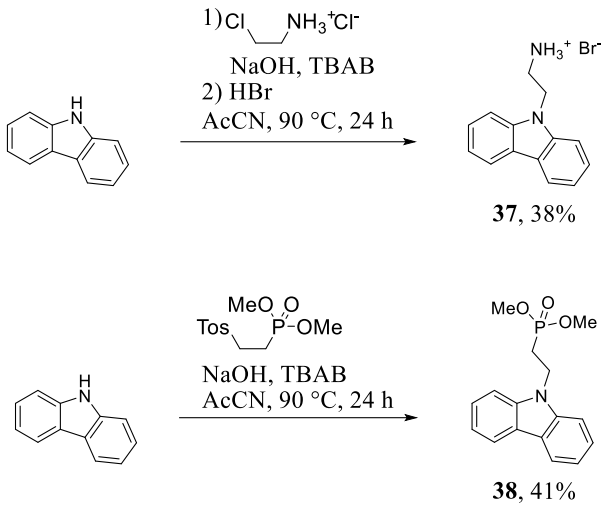

*Figure 21: Synthesis of literature-known carbazoles **37** and **38** for interaction tests with perovskites.*

Interaction tests were carried out by Alexander Deniz Schulz. Perovskite layers were spin-coated with the carbazoles and thoroughly heated. While slight differences in free energy and quantum yields were measurable, they were below 1% and not significant. The hypothesis that the deposited layers were too thick was tested by introducing a washing step with ethanol after heating to wash away excess carbazoles not directly bound to the perovskite. Despite the expected strong interaction between ammonium and phosphate groups and the perovskite, the results of those measurements indicated a complete loss of the carbazole layer. Comparative tests were conducted using *n*-butyl ammonium bromide to narrow the source of the less-than-optimal results. Here, significant formation of low dimensional structures on the perovskite surface was visible in X-ray diffraction (XRD), as well as an increase in quantum yield of 2.7% and free energy of 40 meV. This shows that the challenge arises not from the ammonium but from the carbazole. Further tests are needed to establish a working system that can be used for the planned PCP semiconductors but could not be realized in the scope of this work.

3.4. Introduction of Spacer-Groups

A common challenge in the previous chapters, especially with the dibenzothiophenes of chapter 3.3.2, is the need for highly reactive species to couple the desired building blocks to the PCP core. This is not only tedious and makes the reactions extremely sensitive, as well as making side reactions more likely, but it also completely exempts some less reactive molecules like dibenzothiophene from adding to the library of PCP-based semiconductors. Thus, a solution for this had to be developed. One way is the introduction of spacer groups between the PCP core and the π-bridge to offset low reactivity. This spacer group must have suitable reactivity to work with PCP, must be conjugated to ensure conductive properties, and, in the optimal case, must be small enough not to change the overall electronic properties, to allow still an easy mix-and-match of the components of the library.

As candidates for the spacer, three carbohydrate groups were chosen that reacted well with PCP in literature: the vinyl, the alkyne, and the phenyl group (Figure 22).[186-188] All three are small, conjugated, and lack functional groups that could involuntarily impact electronic properties. Also, they all allow for effective coupling by commonly used cross-coupling reactions.

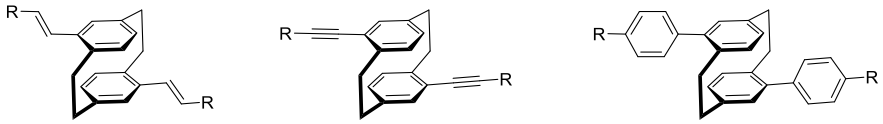

Figure 22: The chosen candidates for spacer groups attached to PCP to give the new core molecules divinyl-PCP, diethynyl-PCP, and diphenyl-PCP.

In the following, each group will be synthesized and coupled to the various π-bridges introduced in chapter 3.3 for the *psp* and *psm* isomers. Tests with the *pso* isomer could not be realized in the scope of this work but the remain an interesting option for future tests.

3.4.1. Vinyl-Spacer

The first group examined is the vinyl, famously the core of the Heck cross-couplings. It can be easily introduced to Br_2-PCP *via* Stille coupling with a vinyl stannane in a one-step reaction (Scheme 23). The *psp* isomer **39** was synthesized with an 80% yield, while the *psm* isomer **40** only yielded 52%. The difference is more likely due to chance variations in purification than in reactivity since the *psp* isomer was also observed to yield lower amounts of product in other iterations under the same conditions.

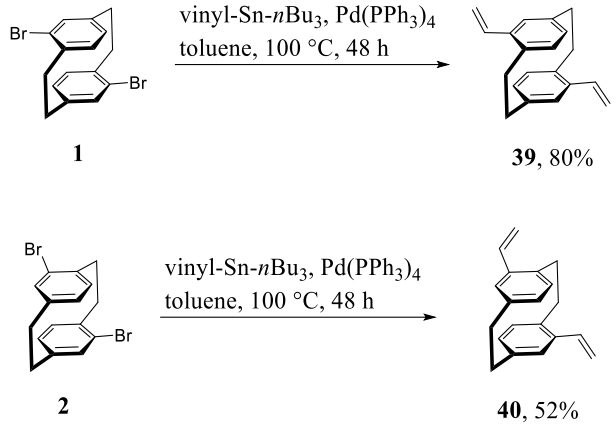

*Scheme 23: Synthesis of vinyl-PCPs **39** and **42** by Stille coupling.*

With the vinyl spacers attached to the PCP core, a Heck coupling to the various donor arms can be tested. First are the basic thiophenes to allow direct comparison to the target materials of chapter 3.2. The thiophene-TPA arm **10**, synthesized in chapter 3.2, was halogenated to enable the Heck coupling. This was achieved with NBS in DCM at low temperatures, giving **41** excellent yields of up to 98% (Scheme 24). **41** had to be purified and used quickly as the bromine is prone to spontaneously cleave, giving rise to dimerization as was already observed in thienothiophene in chapter 3.3.1. Its quick usage in a Heck reaction using palladium acetate, K_2CO_3, and *tert*-butyl ammonium bromide (TBAB) gave the *psp* target molecule **42** in a yield of up to 49% and the *psm* isomer **43** in up to 67% yield. When comparing the yields of this Heck coupling to reactions directly at the PCP core no extreme differences are noticeable. Some methods show lower yields, such as the Negishi coupling with 24–44%; others show similar yields, like the CH activation with 38–62%. While the conversions and yields of the semiconductors using the vinyl spacer were improved as intended, the purification process remained challenging. The instability of the brominated thiophene **41** led to a significant number of side products, and column chromatography was suffering from trailing, likely due to the amine groups and, for the *psp* isomer, also due to solubility issues. Crystallization, especially for the *psm* isomer, resulted in significant yield losses without noticeable improvements in purity. The estimates by ^{1}H NMR give 92% and 80% purity for *psp* and *psm*. This is sufficient for preliminary tests on film morphology and electronic properties but must be improved before tests with devices can begin.

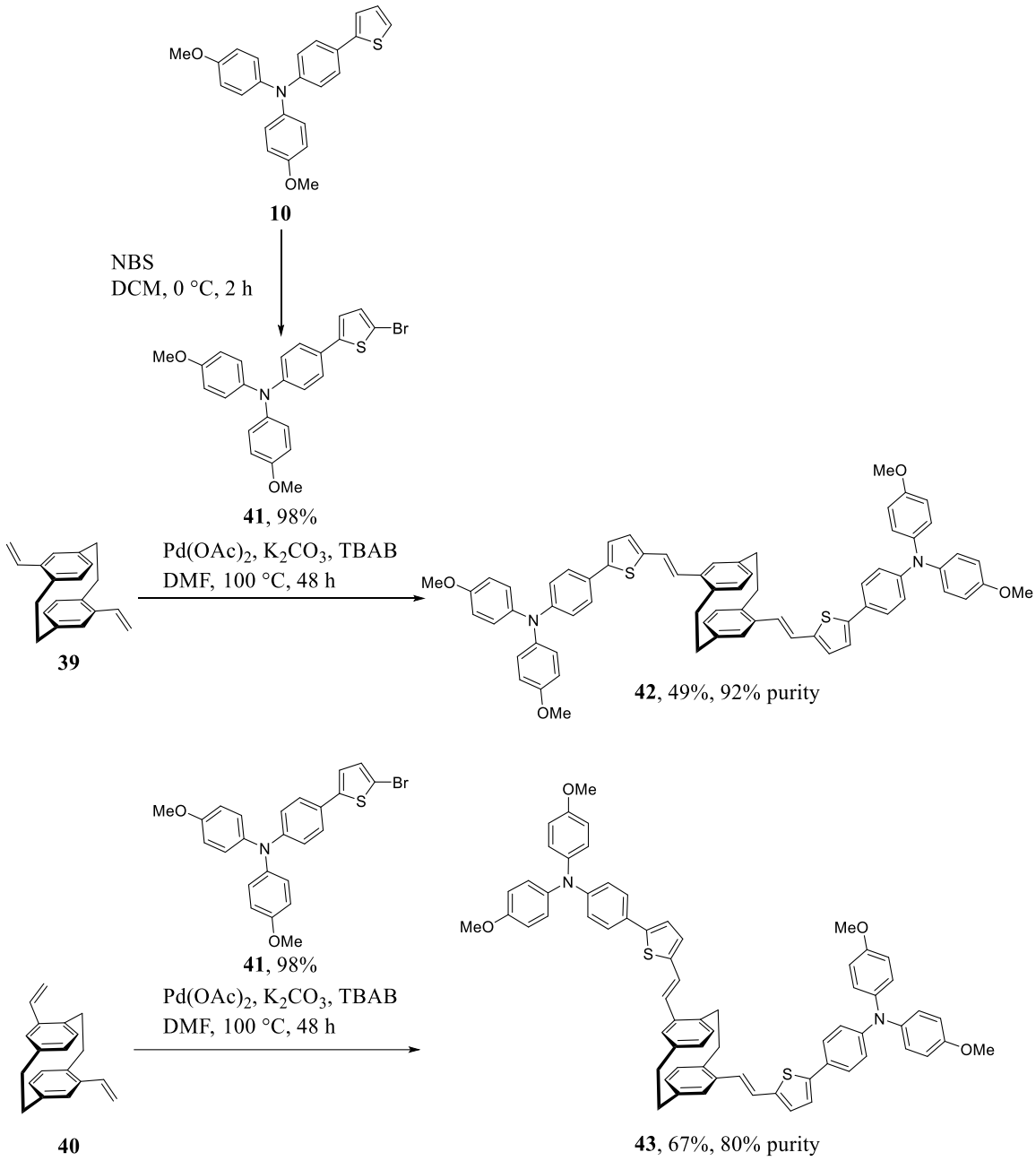

*Scheme 24: Synthesis of target molecules **42** and **43*** via *Heck coupling of OMe-TPA-thiophene **41** and vinyl-PCPs **39** and **40**.*

Similar results were achieved for thienothiophene. Again, the brominated species, in this case **44**, had to be used quickly in a Heck reaction using palladium acetate, K_2CO_3, and TBAB. While the *psp* target molecule **45** could not be isolated successfully, the *psm* isomer **46** was isolated in up to 24% yield (Scheme 25). Both reactions show low selectivity and produce multiple side products. The main side reactions, or in the case of the *psp* isomer even the main reaction, was a monocoupling instead of dicoupling, as well as homocoupling of the brominated thienothiophene-donor **44**. With this, the reactions with thienothiophene are less successful than for the thiophene derivates due to the fast decomposition and homocoupling of the brominated species. The challenges in purification were equivalent to the thiophene derivates. The estimates by ^{1}H NMR give values of 75% purity for

psm isomer **46**. Again, this is sufficient for preliminary tests on film morphology and electronic properties but must be improved before tests with devices can begin.

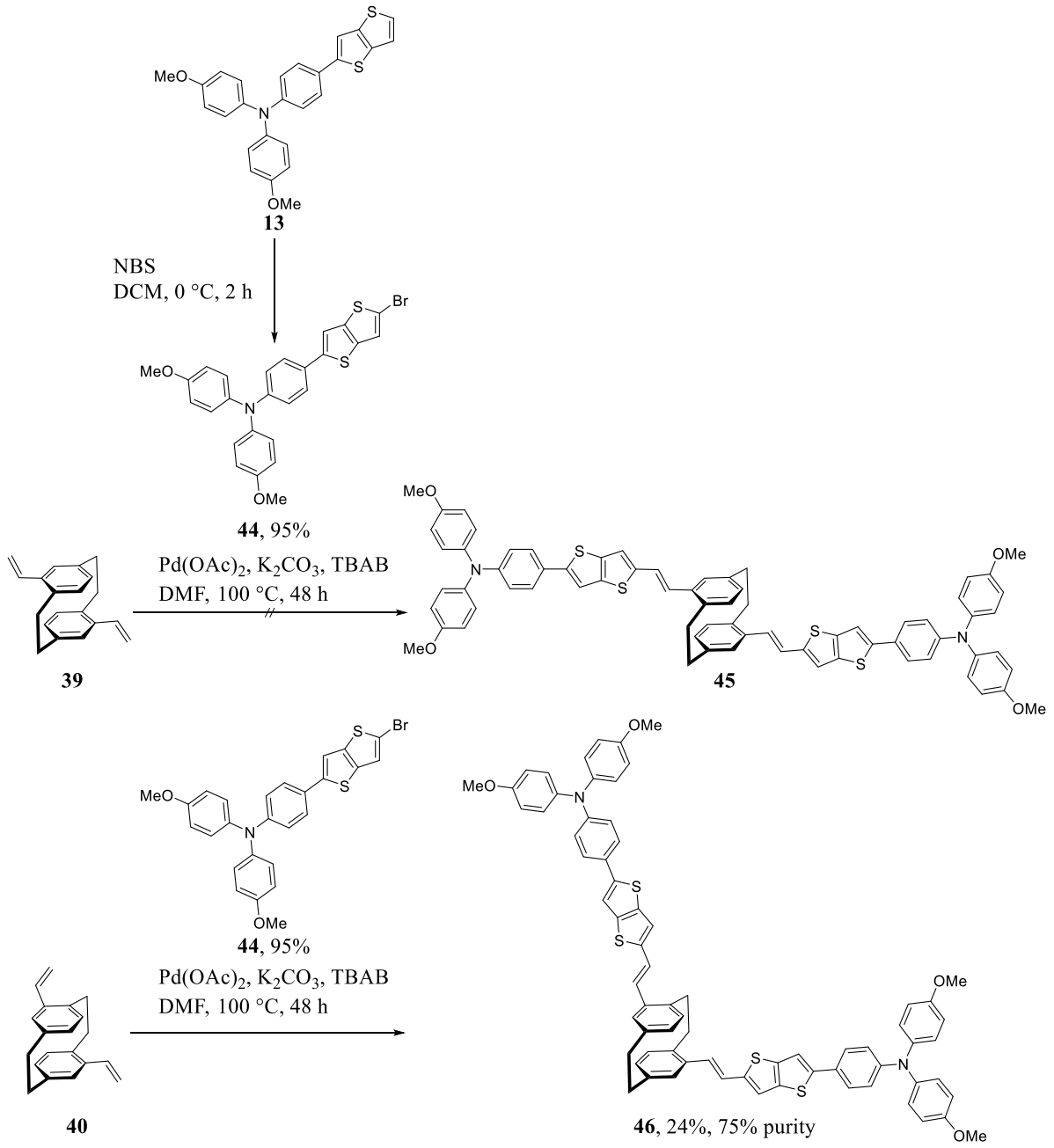

*Scheme 25: Synthesis of target molecules **45** and **46** via Heck coupling of thienothiophene-TPA **44** and vinyl-PCPs **39** and **40**.*

The most obvious beneficial effect from the vinyl spacer was observed when combined with dibenzothiophene. While no tested reaction type allowed its attachment to PCP directly, a Heck coupling to vinyl-PCP was successful, albeit needing a higher reaction temperature than thiophene and thienothiophene to show conversion (Scheme 26). At a yield of 52% for **47**, it shows surprisingly good results compared to thienothiophene and was easier to purify due to the lower number of side products, which strengthens the hypotheses that the instability of the bromine on the thiophene ring leads to the

loss in yield. The semiconductor **47**, while more successful in the synthesis, had very low solubility and did not form sufficient films for many tests of its electronic properties. The *psm* and *pso* isomers could improve on this but could not be realized in the scope of this work.

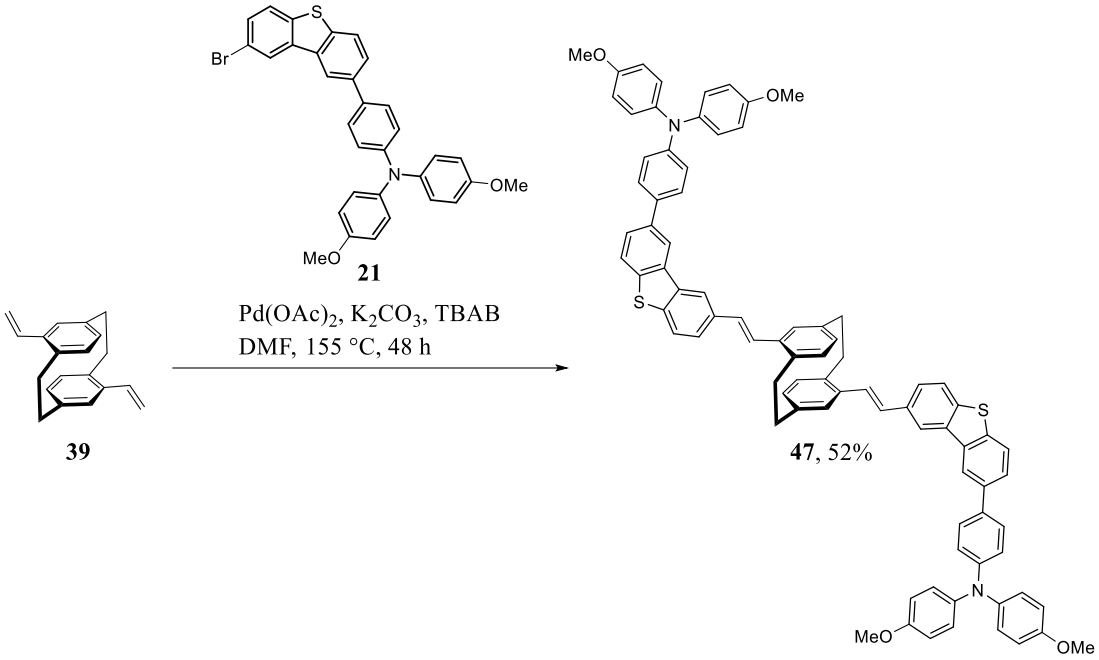

*Scheme 26: Heck coupling of vinyl-PCP **39** and dibenzothiophene-TPA **21** to give target material **47**.*

All in all, the introduction of vinyl as a spacer group allowed for the synthesis of four new PCP-based semiconductors: **42** and **43** using thiophene as π-bridge, **46** with thienotiophene, and **47** with the formerly unreactive dibenzothiophene. The properties of the synthesized target molecules were tested by the Colsmann group as thin-films. All results are summarized and discussed in chapter 3.5.

3.4.2. Alkyne-Spacer

The second tested group was the ethynyl group. Routinely used in the Sonogashira cross-coupling, it is similar in reactivity to the vinyl but results in more linear structures. This should affect reactivity through steric effects as well as the intermolecular interactions of the target molecules. The synthesis of the spacer group-bearing PCP is straightforward and utilizes the mentioned Sonogashira cross-coupling with trimethylsilyl (TMS) protected ethynyl to prevent polymerization (Scheme 27). This yields 81% of **48** from *psp*-Br_2-PCP **1** and 85% of **50** from the *psm* isomer **2**. Afterward, the TMS group can be cleaved with *tert*-butyl ammonium fluoride (TBAF), yielding the ethynyl-PCPs **49** and **51** in 65% and 68%, respectively. Overall, the yields are 55% and 58% for *psp* and *psm* isomer, respectively.

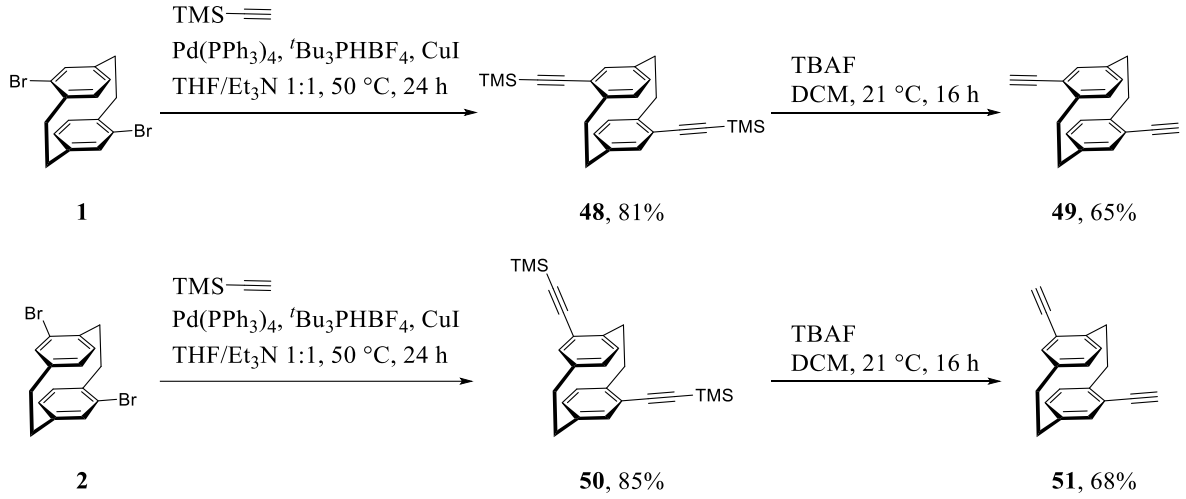

Scheme 27: Synthesis of psp- *and* psm-*ethynyl-PCP **49** and **53** by Sonogashira coupling followed by deprotection of the trimethylsilyl group.*

Equivalent to the experiments of chapter 3.4.1, the synthesized core molecules were coupled with the brominated OMe-TPA-thiophene **41**, now using Sonogashira coupling conditions instead of Heck. After 48 hours with $Pd(PPh_3)_2Cl_2$ and copper(I) iodide in THF/triethylamine at 70 °C the *psp* isomer **49** yielded 88% for target molecule **52**, and the *psm* isomer **51** gave 61% yield for **53** (Scheme 28). Those yields are higher than what was achieved in the Heck couplings, with 49%–67%. The reason for this could be the lower reaction temperature that potentially slowed down the degradation of the donor arm **41**. Still, purification remained challenging. While the *psp* isomer could successfully be purified, the estimates by ^{1}H NMR only give a value of 91% purity for *psm*.

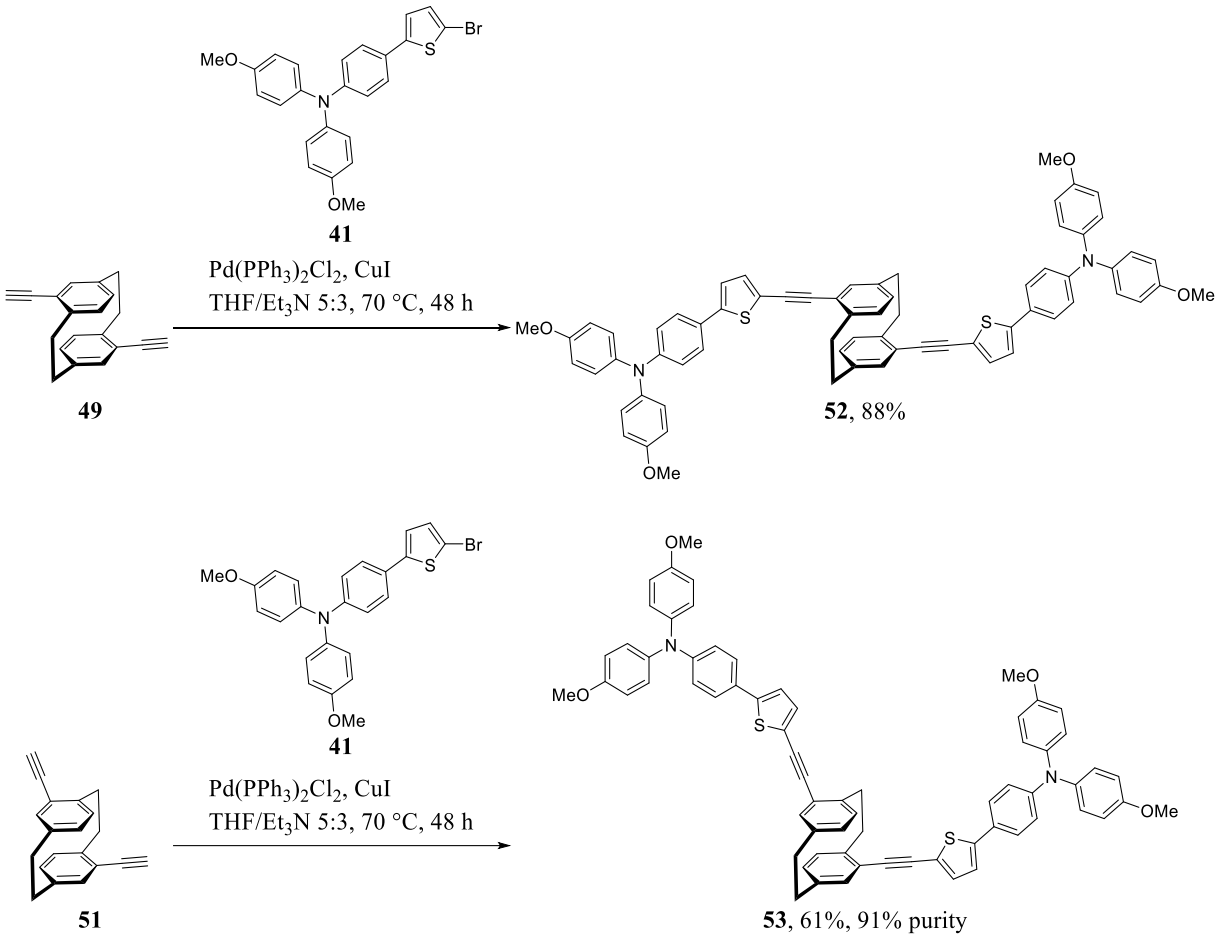

*Scheme 28: Sonogashira coupling to yield target molecules **52** and **53**.*

In parallel, the same reaction was tested with thienothiophene (Scheme 29). The same conditions yielded the *psp* isomer **54** with 41% and the *psm* isomer **55** with 29%. Again, the yields are slightly higher than in the Heck reaction, where only **24**–**31**% were achieved. As was observable in the Heck reactions, the yields for thienothiophene are lower than for thiophene, combined with only giving purities of 92% and 83% for *psp* and *psm*, respectively. Again, this indicates higher instability in the thienothiophene moiety than in thiophene.

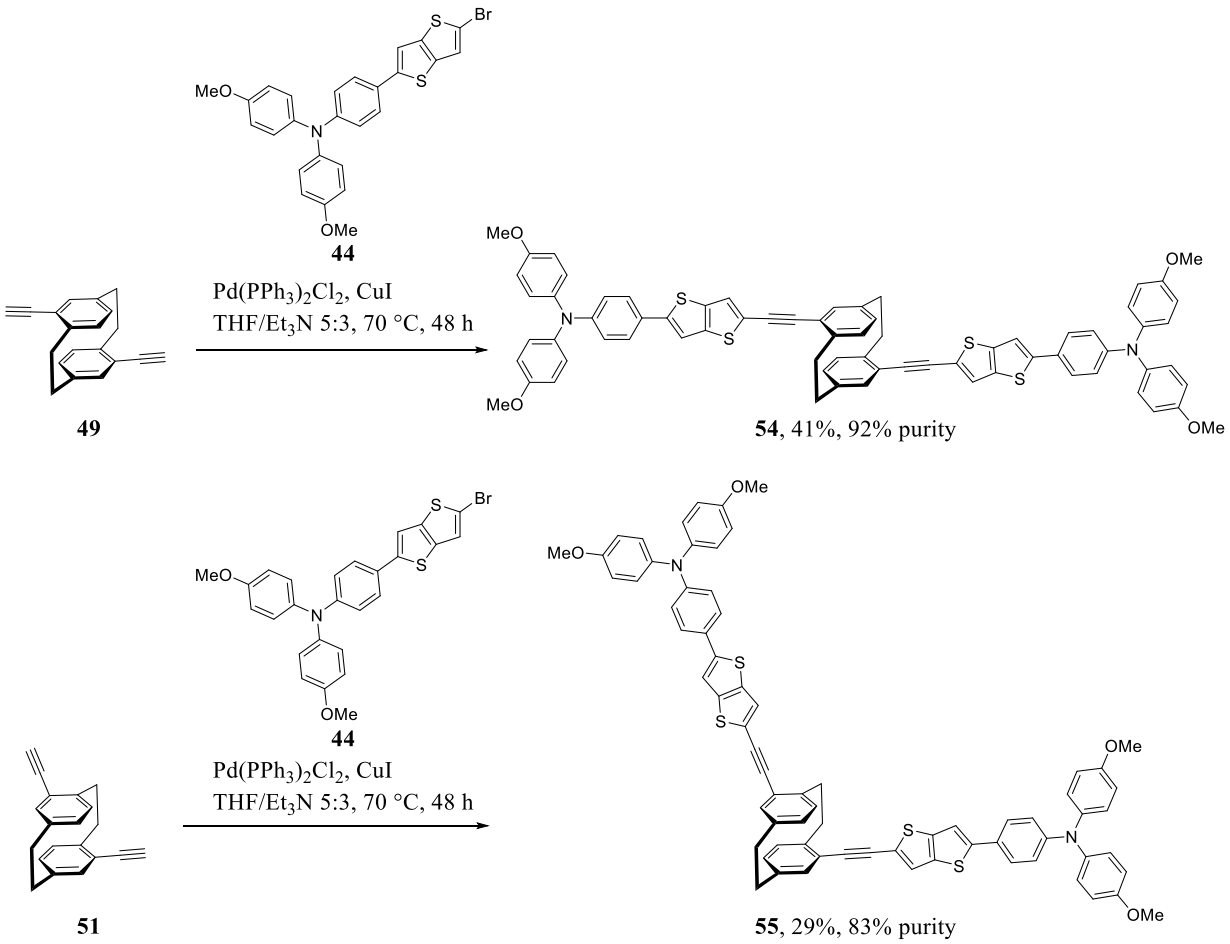

*Scheme 29: Sonogashira coupling to yield thienothiophene target molecules **54** and **55**.*

Summerized, the introduction of ethynyle as a spacer group allowed for the synthesis of the four new semiconductors: **52** and **53** using thiophene as π-bridge and **54** and **55** using thienothiophene. Overall, the synthesis using the alkyne produces higher yields and better purities than the use of the alkene in the former chapter. Still, using brominated thiophene-containing molecules remains challenging, even more so for thienothiophene. The properties of the synthesized target molecules were tested by the Colsmann group as thin-films. All results are summarized and discussed in chapter 3.5.

3.4.3. Phenyl-Spacer

The last spacer group tested in the frame of this work was the phenyl group. Bigger than the former two, it also contributes considerably more to the planarity and π-stacking of the target molecules. Other than the vinyl and ethynyl group, it does not lend itself directly to a coupling method and thus, must be sufficiently functionalized. A procedure by Hasegawa *et al*. gives a direct route to an iodo-functionalized phenyl PCP in two steps using first a Suzuki coupling with a TMS-phenyl boronic acid followed by substitution of the TMS group by an iodine with the help of the reactive iodine monochloride (Scheme 30).[186] The first step gives TMS-phenyl-PCPs **56** and **58** in 63% and 74% yield, respectively. The follow-up step gives the iodo-phenyl-PCPs **57** and **59** in 65% and 54% yield, resulting in 41% overall yield for the *psp* isomer and 40% for the *psm* isomer.

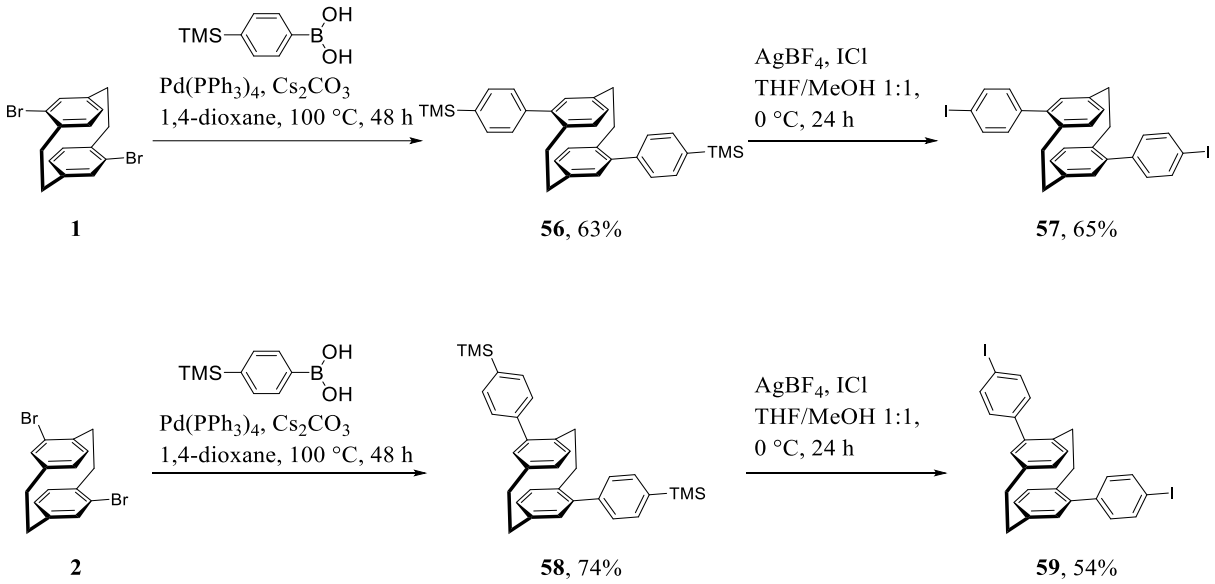

*Scheme 30: Synthesis of iodo-phenyl-PCPs **57** and **59** in two steps: Suzuki coupling, followed by substitution with ICl.*

Both phenyl-substituted core molecules were tested in a cross-coupling with thiophene-donor arm **10** in a Negishi coupling (Scheme 31). The target molecules **60** and **61** could be synthesized using the established conditions in 33% and 45% yield, respectively. This is close to the values achieved for Negishi coupling directly to the PCP core with 22–44%. Further tests with other coupling methods are needed to determine if this comparable reactivity is true across the board or only in the case of the highly reactive but sensitive Negishi coupling.

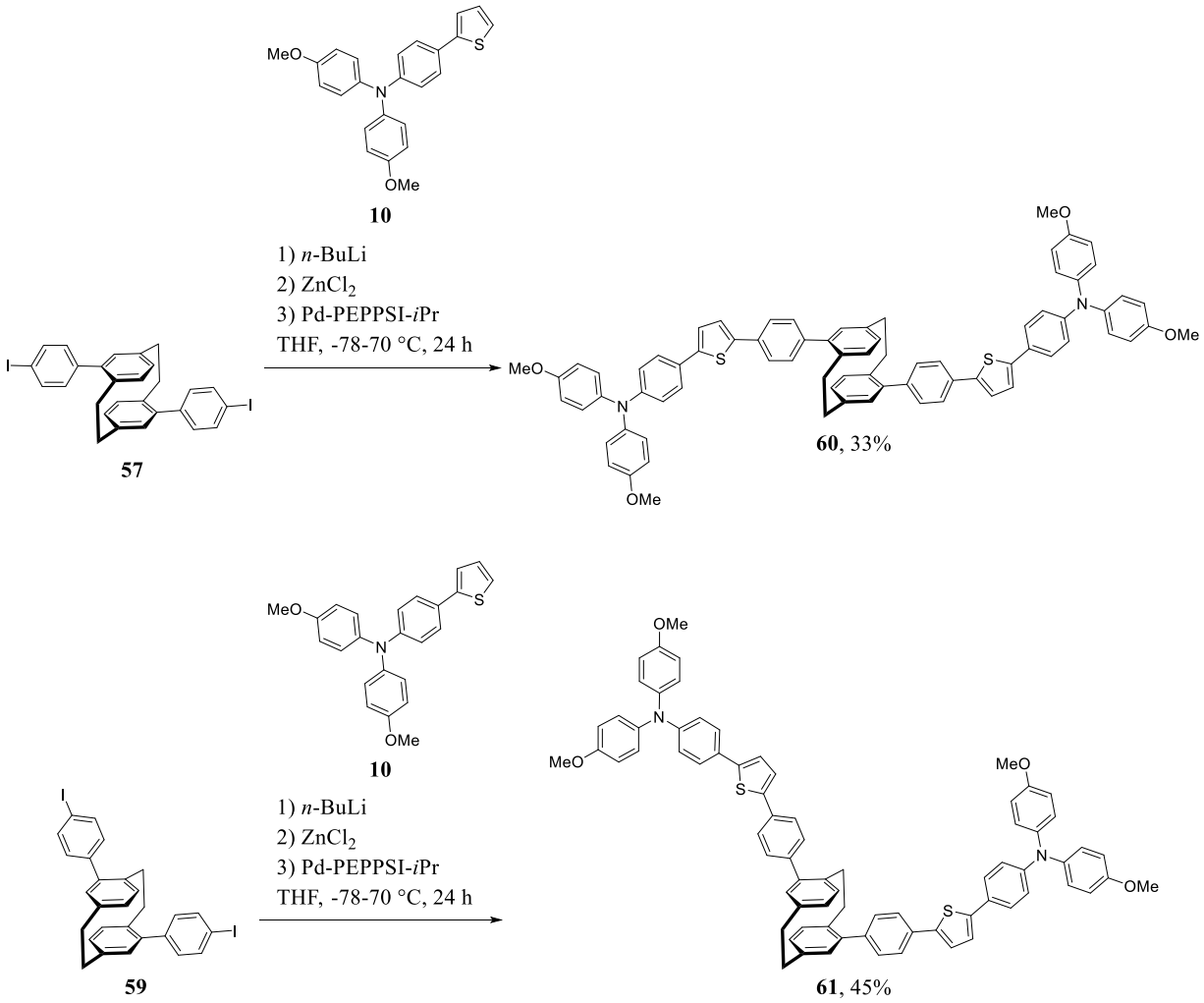

*Scheme 31: Negishi coupling of the phenyl-PCPs **57** and **59** with thiophene-TPA **10** to yield target molecules **60** and **61**.*

Notable with the phenyl spacer is also a decrease in solubility compared to the vinyl- and alkyne-bearing molecules. In the case of the *psp* isomer **61**, the solubility is too low to give reasonably well-resolved NMR spectra. Thus, no estimates on purity can be given. In contrast, pure *psm* isomer could be successfully characterized.

As in former chapters, the tests were also carried out with thienothiophene-TPA **13** in parallel (Scheme 32). Here similar results to the thiophene could be observed. With 52% for **62** and 26% for **63**, the yields are close in range but inversed for the *psp* and *psm* isomers. This allows for multiple conclusions to be drawn. First, the variations in yield are more likely due to the sensitivity of the Negishi reactant, which impacts the reproducibility of the results, than it is to any isomeric effects. Secondly, it reinforces that differences in yield in the earlier chapters, 3.4.1 and 3.4.2, resulted from the brominated thiophene being more stable than the brominated thienothiophene derivates since the effect could not be observed here.

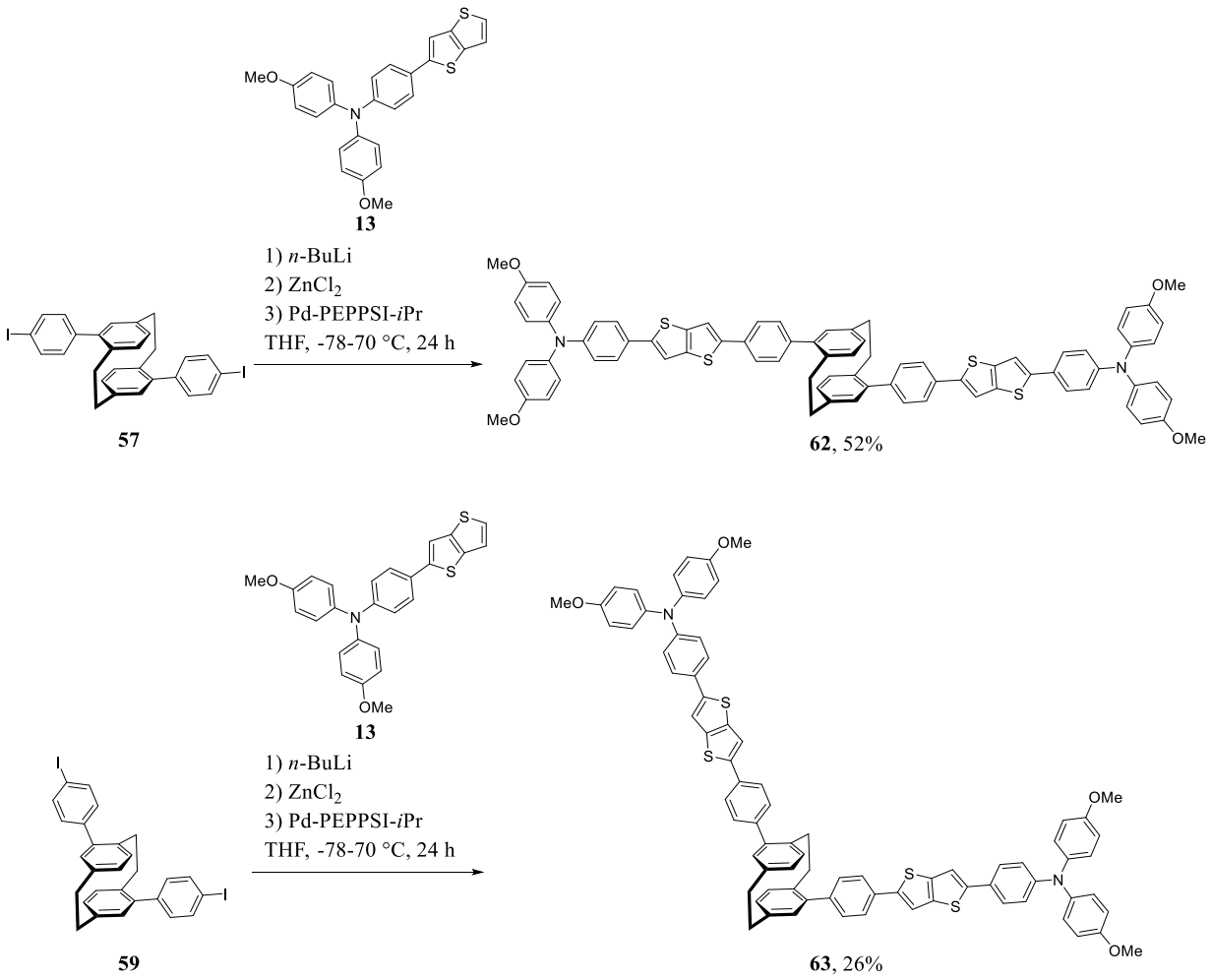

*Scheme 32: Negishi coupling of the phenyl-PCPs **57** and **59** with OMe-TPA-thienothiophene **13** to yield target molecules **62** and **63**.*

Overall, four new semiconductors were synthesized, two using thiophene as π-bridge (**60** and **61**), two using thienothiophene (**62** and **63**). Compared to the synthesis in the former two chapters utilizing vinyl and ethynyl as spacer groups, the purification was easier and overall, more successful. On the other hand, the challenges of the *in situ* Negishi coupling discussed in chapters 3.2 and 3.3.1 remain. Additionally, the added planarity of the phenyl group poses new challenges regarding solubility. Therefore, the introduction of the solubility-improving groups of the carbazoles discussed in chapter 3.3.3 is of great interest for future tests. The properties of the synthesized target molecules were tested by the Colsmann group as thin-films. All results are summarized and discussed in chapter 3.5.

3.5. Optoelectronic Measurements

All target molecules successfully synthesized in the above chapters were given to Holger Röhm and Tilman Bohnert of the Colsmann group for film morphology tests and tests on their electronic properties.

Of the 19 target molecules successfully synthesized, nine showed sufficient film formation when spin-coated from chlorobenzene and could be directly used for further tests of their electronic properties. The other molecules need additional tests regarding their solubility in other suitable solvents or have to be processed differently. This could not be implemented in the time frame of this work. An overview of the successfully tested molecules and their structure is given in Table 2.

Table 2: Overview of the synthesized semiconductors that gave sufficient films when spin-coated from chlorobenzene.

Sample	Structure	Sample	Structure
7	*pso*-(TPA-T)PCP	**52**	*psp*-(TPA-T)alkyne-PCP
17	*psp*-(TPA-TT)PCP	**54**	*psp*-(TPA-TT)alkyne-PCP
18	*psm*-(TPA-TT)PCP	**60**	*psp*-(TPA-T)phenylene-PCP
19	*pso*-(TPA-TT)PCP	**61**	*psm*-(TPA-T)phenylene-PCP
34	$(TPA)_3$-carbazole		

Thin-films were spin-coated at 2000 rpm over the span of 30 s using 30 µL of a saturated solution in chlorobenzene (Figure 23). The best film formation was observed for **7** and **34** giving smooth films with low artifact formation. **17**, **19**, **52**, **54**, and **60** formed even films but showed clear artifacts. **18** and **61** only barely formed measurable films. While for **18** and **61** measurements could be done, the results have to be taken as preliminary until better films can be tested.

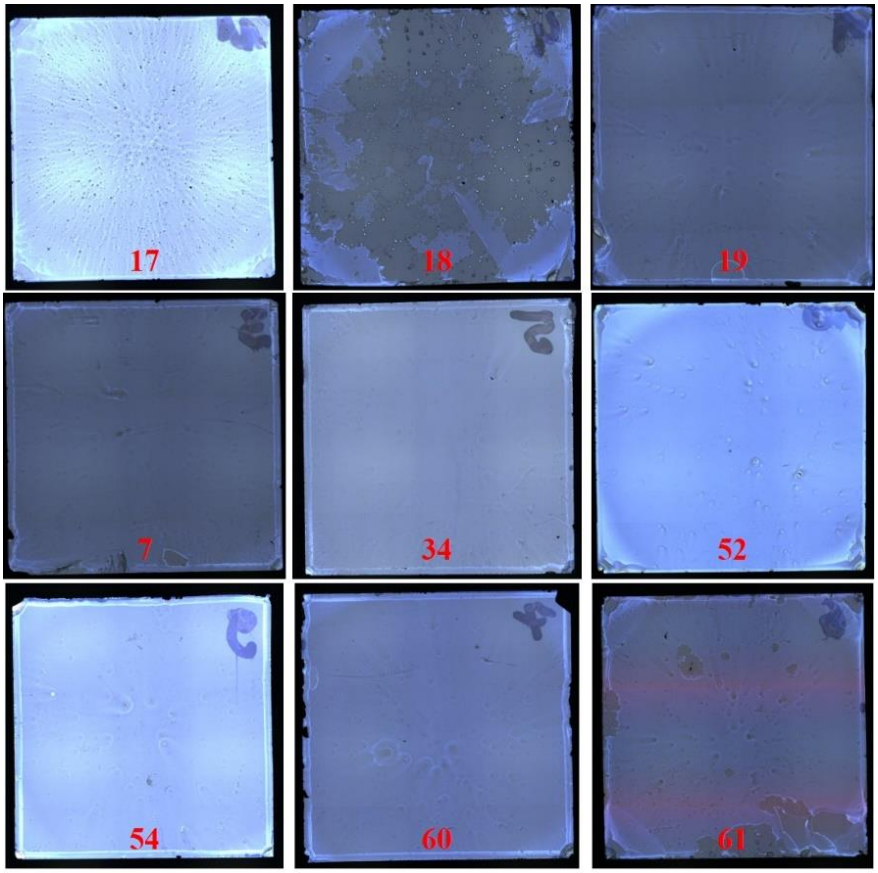

Figure 23: Thin-films of all nine molecules that form measurable films.

The first analytic applied was UV-Vis spectroscopy of the produced films (Figure 24). This gives a good first impression of the electronic effects the introduced variations have on the semiconductors. Regarding the used π-bridge, the observation that can be made, is that exchanging thiophene (T) for thienothiophene (TT) only has a small effect on the curve form and absorption maxima λ_{max}, with the thienothiophenes **17**–**19** being slightly red-shifted from the 385 nm of **7** to 396–402 nm (Table 3). On the other hand, the introduction of carbazole blue-shifts the maximum significantly to 341 nm for **34**, an effect that is also observable when using carbazole moities as donor.[164] Further tests with the semiconductors using both carbazole and PCP (**35** and **36**) have to be done to narrow down the effect of the carbazole alone. The effects of the PCP isomer used was as expected small. For thienothiophene all three synthesized isomers were in the range of 396–402 nm.

The effects of the spacer groups on the λ_{max} were a red-shift for both alkynyl and phenyl spacers. For thienothiophene, the additional alkynes red-shifted the λ_{max} slightly from 402 nm to 417 nm. For thiophene the shift was unexpectedly significant from 385 nm to 431 nm. The inclusion of phenylenes into the thiophene-bearing semiconductors red-shifted λ_{max} from 385 nm to 400–403 nm, again with only small changes between isomers. The effect of the vinyl group could not be estimated in the scope of this work since none of the synthesized molecules formed sufficient films.

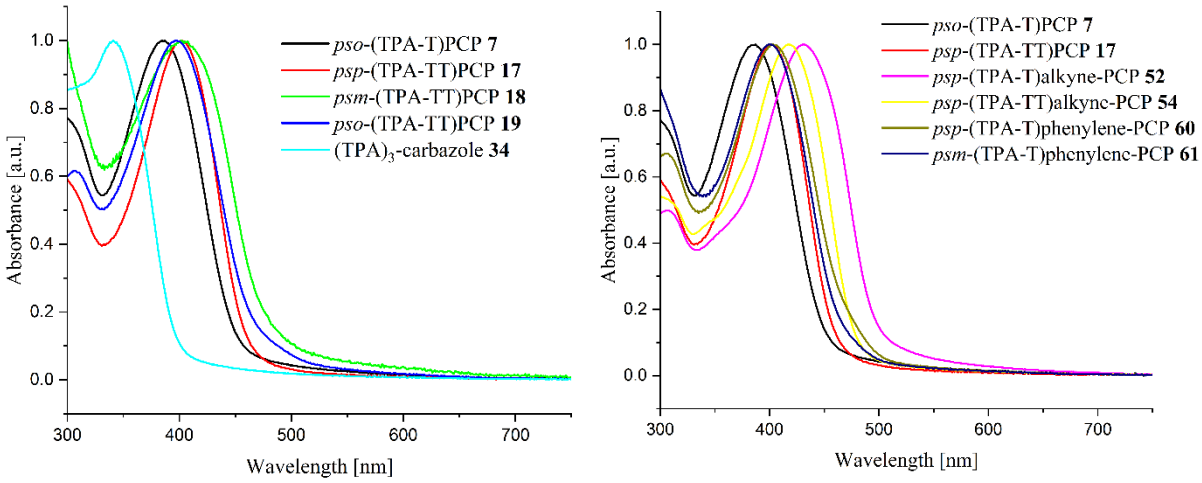

Figure 24: UV-Vis spectra for synthesized semiconductors bearing different π-bridges (left) or spacer groups (right).

The received values for λ_{max} of the highest-wavelength maximum could be used to calculate the optical band gap ΔE_{opt} using equation (3) (Table 3).[189]

$$\Delta E_{opt} = \frac{hc}{\lambda_{max}} = \frac{1024}{\lambda_{max}} \quad (3)$$

All tested semiconductors have sufficiently large band gaps to act as hole transport materials, blocking electrons from entering. The values range from 2.38 eV for **52** up to 3.00 eV for **34**.

Table 3: Overview of λ_{max} and ΔE_{opt} values resulting from UV-Vis absorption spectroscopy.

Sample	Structure	λ_{max} [nm]	ΔE_{opt} [eV]
7	*pso*-(TPA-T)PCP	385	2.66
17	*psp*-(TPA-TT)PCP	402	2.55
18	*psm*-(TPA-TT)PCP	402	2.55
19	*pso*-(TPA-TT)PCP	396	2.59
34	$(TPA)_3$-carbazole	341	3.00
52	*psp*-(TPA-T)alkyne-PCP	431	2.38
54	*psp*-(TPA-TT)alkyne-PCP	417	2.46
60	*psp*-(TPA-T)phenylene-PCP	400	2.56
61	*psm*-(TPA-T)phenylene-PCP	403	2.54

Photoemission spectroscopy in air (PESA) was also measured (Figure 25). This allows to calculate the work function of the films which equals the ionization potential (IP) of the semiconductors. If Koopmans' theorem is applied, this can also be assumed to equal the HOMO energy level of the molecules (Table 4).[190] The derived values of this approximation are expected to follow the same trend

but may vary quantitatively. Together with the band gap derived from UV-Vis this allows also the calculation of the LUMO energy.

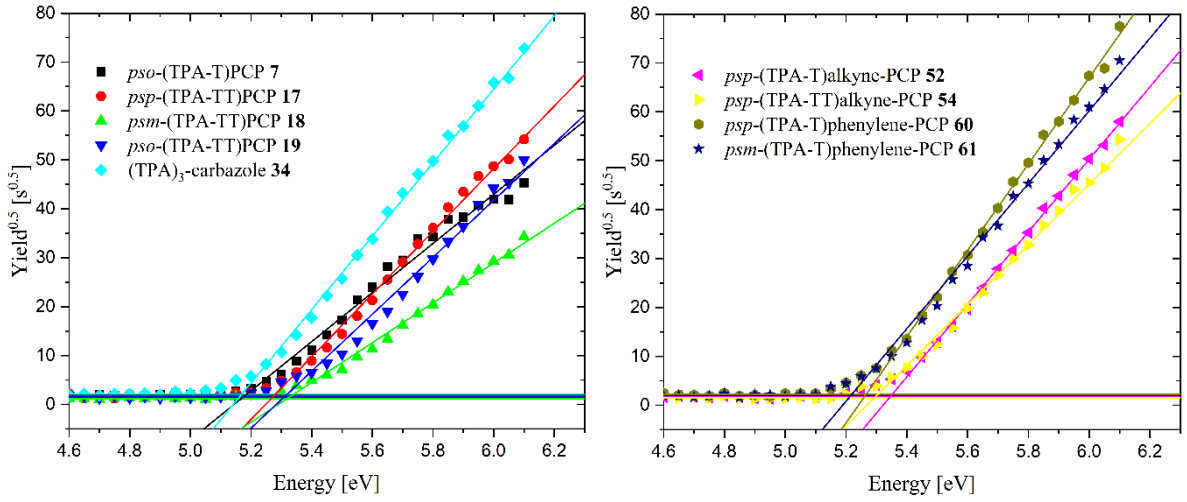

Figure 25: PESA measurements for synthesized semiconductors bearing different π-bridges (left) and spacer groups (right).

For all measured semiconductors the IP values are in the range of 5.17–5.35 eV and, therefore, show good energy alignment with common perovskites such as MAPbI (~5.4 eV) to act as hole transport materials. The lowest value was measured for the carbazole derivate and the highest for molecule **52** based on thiophene with an alkyne spacer. The trend follows roughly the results from UV-Vis with the red-shifted molecules showing higher ionization potentials.

Table 4: Overview of the ionization potentials (IP) resulting from the PESA measurements and LUMO levels derived from this using the optical band gap.

Sample	Structure	IP_{PESA} (~HOMO) [eV]	LUMO [eV]
7	*pso*-(TPA-T)PCP	5.19	2.53
17	*psp*-(TPA-TT)PCP	5.27	2.72
18	*psm*-(TPA-TT)PCP	5.32	2.77
19	*pso*-(TPA-TT)PCP	5.31	2.72
34	$(TPA)_3$-carbazole	5.17	2.17
52	*psp*-(TPA-T)alkyne-PCP	5.35	2.97
54	*psp*-(TPA-TT)alkyne-PCP	5.29	2.83
60	*psp*-(TPA-T)phenylene-PCP	5.26	2.70
61	*psm*-(TPA-T)phenylene-PCP	5.21	2.67

Summerized, all tested semiconductors show good energy alignment with perovskites and a sufficiently big bang gap to make them attractive candidates for hole transport materials in PSCs. Further efforts have to be invested to produce thin-films from the remaining ten semiconductors. Furthermore, the implementation in complete solar cells has to be attempted to test their conductivity and overall PCE.

4. PCP-Polymers as Functional Materials

Since their discovery in 1949,[2] PCP and its derivatives have been used successfully in many fields, as discussed in chapter 2.1. While PCP derivates are mostly used as monomers, as in the previous chapters, there are many polymers based on them (Figure 26). Some utilize the strained PCP structure in polymerizations to open the PCP ring, giving rise to parylenes in chemical vapor deposition, which can be used to coat surfaces.[191] Also possible are ring-opening metathesis polymerizations (ROMP) that yield poly(phenylvinylene)s, a semiconducting polymer often seen in organic electronics.[192] Others build macroscopic structures using the rigid paracyclophane to control the emerging angles or to include novel properties.[26, 193-194]

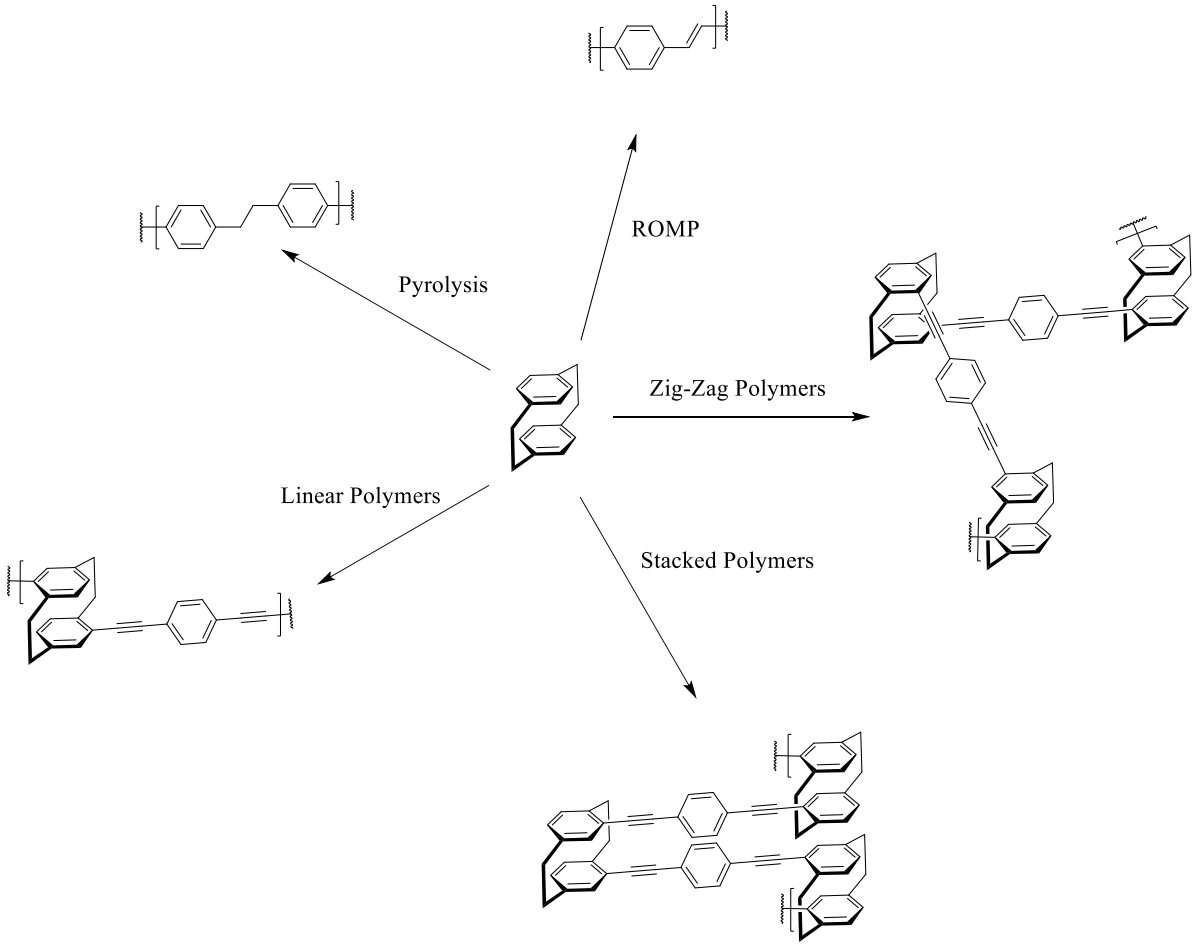

Figure 26: Excerpt of literature-known polymeric structures using paracyclophane as a starting point.

These examples provide a good idea of what is possible by using macroscopic PCP structures, but there are still many unexplored ways and PCP derivates that can be tested. Especially interesting is the option to use chiral PCPs as a side chain, creating chiral polymers. Some of the known, but for PCP unused, ways of (chiral) polymerization were published as part of this thesis in the non-peer-reviewed paper "Molecular Structuring of Novel Chiral Polymers *via* Cyclophane-based Monomer Design Strategies" (Figure 27).[195]

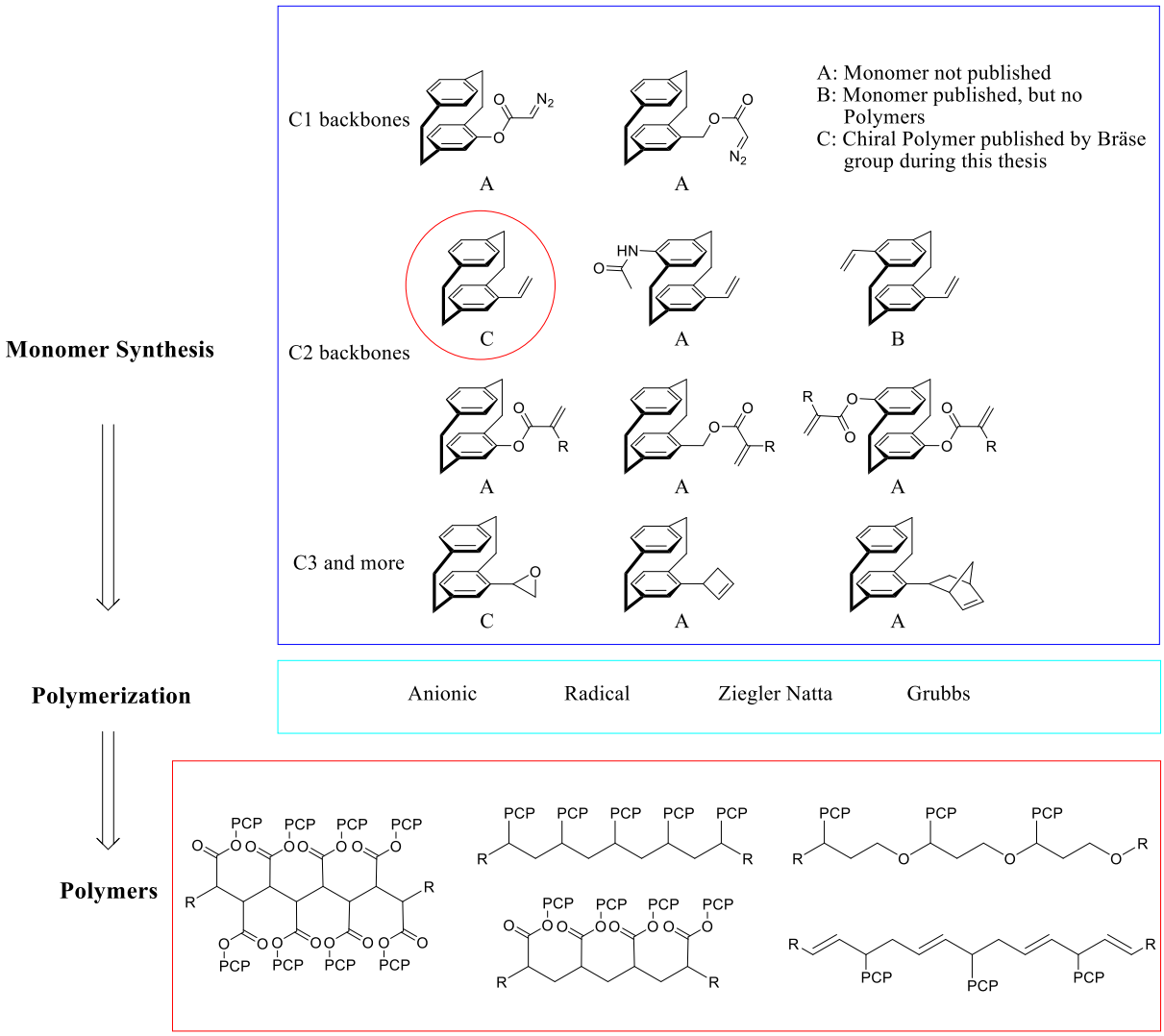

Figure 27: A small excerpt of possible polymerizations using various PCP monomers to create (chiral) polymers with PCP in the side chains.

Of those examples, the following chapters focus on polymers based on chiral vinyl-PCP, which allows for a simple methodology for both polymerization and synthesis of the chiral precursor. It also incorporates the semiconductors of the former chapters into a polymeric backbone. The following chapters discuss the synthetic route from monomer to functional material and their application results.

4.1. Chiral PCP-Polymers and their Application in CP-TADF Emitters

The first step towards chiral polymers utilizing the intrinsic planar chirality of PCP is the synthesis of a chiral monomer, namely R_p- and S_p-vinyl[2.2]paracyclophane (**67**). Christoph Zippel of the Bräse group developed a convenient synthetic route to achieve both enantiomers.[196] This was accomplished through a kinetic resolution, usable on a gram scale, without chiral chromatography. A three- to four-step synthesis (Scheme 33) yields the R_p enantiomer at 13% and the S_p enantiomer at 22% (using *R*-RUCY-XylBINAP, *S*-RUCY-XylBINAP will yield the reverse enantiomers), resulting in a combined 35% overall yield starting from PCP.

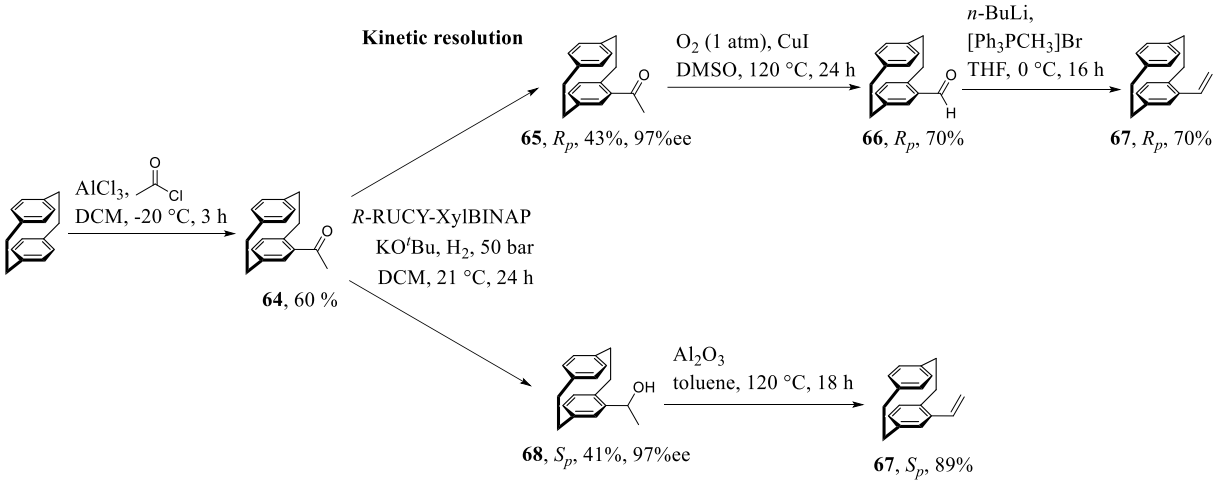

Scheme 33: Synthesis of R_p- *and* S_p-*vinyl[2.2]paracyclophane (**67**)* via *kinetic resolution using* R-*RUCY-XylBINAP.*

With the chiral PCP monomer prepared, the next step was the polymerization to yield chiral polymers (Scheme 34). Several methods are available for vinyl polymerization, with the most basic being radical, anionic, and cationic approaches.

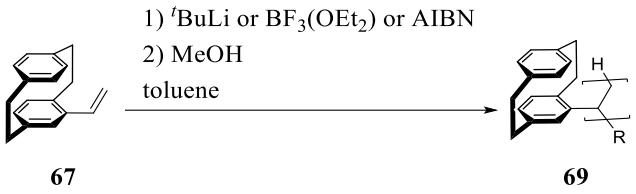

*Scheme 34: Homopolymerization of chiral vinyl-PCP to poly-vinyl-PCP (**69**) using anionic, cationic, and radical methods. All polymerizations were stopped by adding methanol after a set time.*

These methods were initially applied to racemic vinyl-PCP in 1994 by Iwatsuki *et al.*,[197] who demonstrated that all three techniques were viable, with radical polymerization yielding the highest molecular weight and anionic polymerization achieving the highest conversion. Similar results were observed in experiments for this thesis with the chiral variant (Table 5). Anionic polymerization using *tert*-butyllithium (^{t}BuLi) achieved up to 93% conversion and produced a product mass near the expected decamer. Since Iwatsuki's study didn't specify the type of BuLi used, *n*- and *sec*-BuLi were also tested,

which provided comparable but slightly lower conversion rates. Cationic polymerization with boron trifluoride etherate produced outcomes consistent with Iwatsuki's findings, showing lower conversion (68%) and significantly lower molecular masses than could be normally anticipated. Radical polymerization using azobisisobutyronitrile (AIBN) resulted in slow and incomplete conversion, even after extending the reaction time by 24 hours. Only 18% conversion was achieved overall (4–9% when stopped after 24 hours), though the number average molecular weight (M_n) was similar to that of anionic polymerization. Using dibenzoyl peroxide as the initiator produced equivalent results.

All findings suggest that vinyl-PCP has lower reactivity than styrene, which is further supported by its stability over several months without refrigeration or protection from light, which would not be possible for styrene. This lower reactivity may be attributed to the bulkier structure of PCP, which likely creates steric hindrance during polymerization. Similar conclusions were drawn by Iwatsuki and in a work on similar polymethylene-PCP.[198]

Attempts to achieve higher molecular masses by reducing initiator concentrations in radical and anionic polymerizations proved difficult. In both cases, the resulting polymers were insoluble in common organic solvents (toluene, THF, DCM, dimethylacetamide, hexafluoroisopropanol, EtOAc, acetone, MeCN, alcohols, and alkanes), suggesting that the soluble monomer had reacted, but preventing molecular weight analysis. Future work could explore using functional groups such as alkyl chains on the PCP to improve solubility and potentially enable the production of high-mass poly-PCP monomers.

*Table 5: Overview of conditions and results for the homopolymerization of chiral vinyl-PCP **67**. M_n = number average molecular weight; M_w = weight average molecular weight; D = dispersity.*

Enantiomer	Conditions	M_n [kDa]	M_w [kDa]	D	Conversion [%]
S_p	10 mol% ^{t}BuLi, toluene, 0 °C, 24 h	1.78	2.03	1.14	93
R_p	10 mol% ^{t}BuLi, toluene, 0 °C, 24 h	1.01	3.25	3.21	92
S_p	1 mol% ^{t}BuLi, toluene, 0 °C, 24 h	N/A	N/A	N/A	97[1]
S_p	10 mol% BF_3OEt_2, toluene, 0 °C, 24 h	0.58	0.79	1.36	68
S_p	10 mol% AIBN, toluene, 60 °C, 24 h	1.66	1.89	1.14	4
R_p	10 mol% AIBN, toluene, 60 °C, 24 h	0.78	1.38	1.77	9
S_p	2 x 10 mol% AIBN, toluene, 60 °C, 48 h	1.72	2.74	1.60	18
S_p	1 mol% AIBN, bulk, 60 °C, 24 h	N/A	N/A	N/A	34[1]

[1] Conversion for insoluble polymers was calculated by the dividing mass of the resulting solid after washing steps by the mass of used monomers. Because of limited analytics, no statement about purity can be made.

To address solubility issues, increase molecular weight using the given monomer, and to demonstrate the retention of chiral properties when combined with achiral monomers for broader application potential, copolymerization with styrene was conducted at varying ratios (Scheme 35). Radical polymerization was selected due to its ease of use and more reliable outcomes despite achieving lower conversion rates than the anionic method, which is highly sensitive to trace amounts of oxygen or moisture.

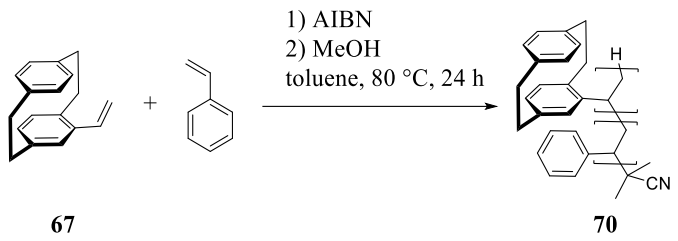

67 **70**

*Scheme 35: Radical copolymerization of vinyl-PCP **69** and styrene in ratios of 1:1, 1:10, 1:20, and 1:50 using AIBN to yield poly(vinyl[2.2]paracyclophane-co-styrene) (**70**).*

For copolymerization, PCP:styrene ratios of 1:1, 1:10, 1:20, and 1:50 were tested, progressively increasing the proportion of styrene until chiral properties were no longer detectable in optical rotation measurements (Table 6). As anticipated, adding styrene significantly improved polymerization efficiency, raising conversions to 37–85%, compared to a maximum of 18% for pure vinyl-PCP. Furthermore, M_n values increased to 2.56–6.02 kDa, with M_w reaching up to 13.9 kDa. ^{1}H NMR analysis confirmed that the composition of the copolymers closely matched the monomer ratios used, suggesting that styrene and vinyl-PCP were consumed at similar rates. This supports the hypothesis that the low reactivity observed in vinyl-PCP homopolymerization is due to steric hindrance rather than a fundamental issue with the vinyl group's reactivity.

In addition to improved molecular weights, the solubility of the copolymers in organic solvents was greatly enhanced compared to the homopolymer. For instance, in THF, solubility increased from less than 1 g/L for poly(vinyl[2.2]paracyclophane) (**69**) with an M_n of approximately 1.8 kDa to over 20 g/L for poly(vinyl[2.2]paracyclophane-co-styrene) (**70**) with an M_n of 4.8 kDa and a PCP ratio of 1:1.4. The specific rotation of the copolymers decreased as expected with increasing amounts of achiral monomer, but due to the high initial optical rotation of the monomer at ±248 (deg·mL)/(g·dm) (for comparison: fructose = ±92.4 (deg·mL)/(g·dm)[199]; progesterone = 182 (deg·mL)/(g·dm)[200]; cholesterol = –37.5 (deg·mL)/(g·dm)[201]), even polymers with lower PCP content exhibited optical rotation values potentially suitable for chiral applications.

Table 6: Overview of results for copolymerizing S_p*-vinyl-PCP (**67**) and styrene in varying ratios with 2 mol% AIBN after 24 h at 80 °C.* M_n *= number average molecular weight;* M_w *= weight average molecular weight, D = dispersity.*

Ratio Vinyl-PCP:styrene used	**Ratio Vinyl-PCP:styrene in polymer[1]**	**M_n [kDa][2]**	**M_w [kDa][2]**	**D[2]**	**Conversion [%]**	**Specific Rotation α_D^{20} [(deg*mL)/(g*dm)]** Comparison: S_p-vinyl monomer +284
1:1	1:1.4	4.79	10.5	2.18	37	102.1
1:10	1:9.6	2.56	13.9	5.44	66	51.9
1:25	1:28.3	4.68	10.6	2.27	57	14.6
1:50	1:45.1	6.02	13.7	2.28	85	7.9

[1] Determined by ^{1}H NMR.

[2] Determined by gel permeation chromatography (GPC).

Following the promising results, which demonstrated that the polymers retained their chiral properties even with significant amounts of non-chiral copolymer, the next step was to explore further applications. To achieve this, chiral vinyl-PCP was combined with a TADF emitter to create a CP-TADF (circularly polarized TADF) system, which holds potential in fields such as sensing and optics.[202] Integrating a TADF and a non-TADF moiety offers several advantages. Firstly, the non-TADF component can act as a host material, preventing self-quenching of the emitter units by physically separating them. This function typically requires an additional material, such as mCP (1,3-bis(N-carbazolyl)benzene) or DPEPO (bis[2-(diphenylphosphino)phenyl] ether oxide), when constructing a device based on small organic molecules, but now can be incorporated directly into the emitter polymer.[203] Secondly, the planar chirality of the PCP unit can influence the entire emitter polymer, enabling CP-TADF emission without needing a chiral center in the TADF-emissive molecule itself.[204-205]

For copolymerization with vinyl-PCP, a polymerizable group was needed, preferably another vinyl group to ensure a similar polymerization rate. To achieve this, the well-known TADF emitter 9,10-dihydro-9,9-dimethyl-10-(4-(4,6-diphenyl-1,3,5-triazin-2-yl)phenyl)acridine DMAC-TRZ (**71**) was functionalized in a straightforward two-step synthesis, yielding 48% overall. First, selective monobromination was performed at the *para* position of the DMAC moiety using *N*-bromosuccinimide at low temperature, giving 93% yield, followed by a Stille coupling with tributyl-vinyl-stannane yielding 52% (Scheme 36). This method can theoretically be applied to a wide range of common TADF emitters, as the only requirement is a position suitable for halogenation.

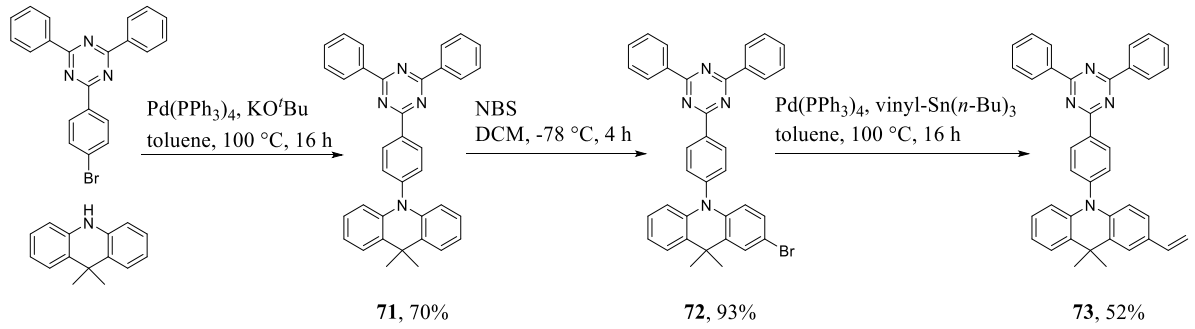

*Scheme 36: Synthesis of vinyl-DMAC-TRZ (**73**) in three steps, starting from DMAC and Br-TRZ-*

Radical initiation with AIBN was selected for copolymerization, as the more reactive ^{t}BuLi could potentially attack other positions within the TADF emitter (Scheme 37). Based on previous tests with styrene, it has been shown that even small fractions of PCP can impart chirality. However, to effectively express the influence of the host material, a higher proportion of PCP is necessary since typical doping concentrations for host materials are in the low single digits. To account for this, PCP:emitter ratios of 10:1, 20:1, 50:1, and 100:1 were tested.

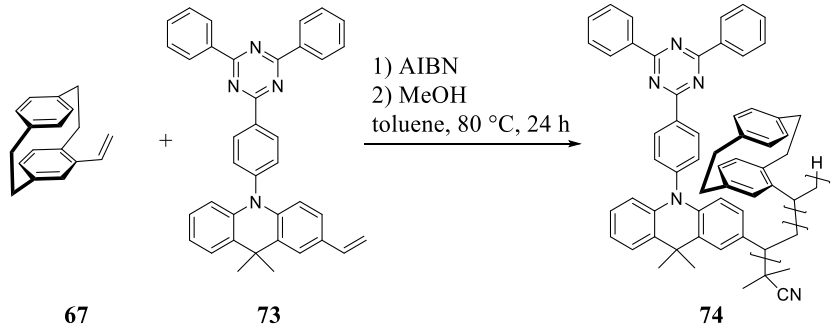

*Scheme 37: Radical copolymerization of vinyl-PCP (**67**) and vinyl-DMAC-TRZ (**73**) using AIBN yields poly(vinyl[2.2]paracyclophane-co-vinyl-DMAC-TRZ) (**74**).*

For comparison, vinyl-DMAC-TRZ (**73**) was also homopolymerized (Scheme 38).

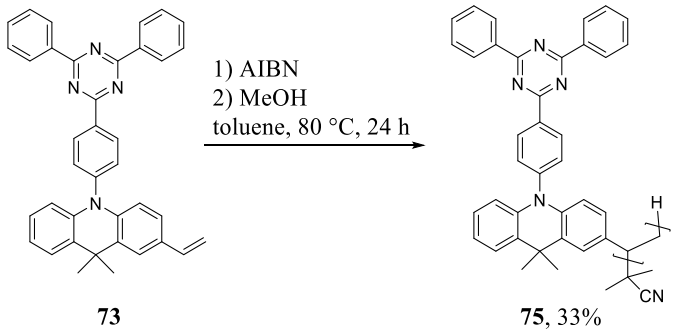

*Scheme 38: Radical homopolymerization of vinyl-DMAC-TRZ (**73**) using AIBN yields poly(vinyl-DMAC-TRZ) (**75**).*

The radical polymerization in this setup showed lower conversion rates and broader molecular weight dispersities (Table 7), likely due to the small scale of the reaction and solubility issues, similar to those observed in the homopolymerization of vinyl-PCP. Additionally, the TADF emitter monomer appeared to be preferentially incorporated compared to vinyl-PCP, leading to 3–6 times more TADF emitter units in the polymers than initially aimed for. As previously discussed, the bulkiness of the PCP likely hinders the continuous incorporation of vinyl-PCP, a limitation not shared by the more planar DMAC-TRZ moiety, resulting in higher emitter content in the polymer. With increasing PCP content, the molecular weights achieved approached those observed for pure poly(vinyl-PCP), with the 50:1 and 100:1 ratios falling into the same range. The 20:1 ratio appeared as a slight outlier but remained within the expected range of variation, given the simplicity of the experimental setup. Although not yet optimized, these results demonstrate the approach's feasibility and can be further refined with more advanced and specialized setups in future studies.

*Table 7: Overview of results for the copolymerization of vinyl-PCP (**67**) and vinyl-DMAC-TRZ (**73**) in varying ratios with 2 mol% AIBN after 24 h at 80 °C. M_n = number average molecular weight; M_w = weight average molecular weight, D = dispersity.*

Sample	Ratio Vinyl-PCP:TADF in polymer[1]	M_n [kDa][2]	M_w [kDa][2]	D[2]	Conversion [%]
Poly-(vinyl-DMAC-TRZ) (**75**)	0:1	1.46	2.71	1.86	33
Vinyl-PCP:TADF 10:1 R_p	3.6:1	1.17	6.57	5.63	20
Vinyl-PCP:TADF 20:1 R_p	6.8:1	2.43	15.7	6.46	32
Vinyl-PCP:TADF 50:1 R_p	10.6:1	0.89	3.98	4.47	30
Vinyl-PCP:TADF 100:1 R_p	17.9:1	0.51	1.96	3.85	23
Vinyl-PCP:TADF 20:1 S_p	5.8:1	0.73	2.19	2.99	56
Vinyl-PCP:TADF 50:1 S_p	14.5:1	0.76	2.27	3.00	28

[1] Determined by ^{1}H NMR.

[2] Determined by GPC.

Emma Puttock and Sebastian Ortiz measured the resulting copolymers for their photoluminescence (PL) and TADF properties, paying particular attention to the effects of increasing PCP content as a built-in host material.

When excited at 370 nm under nitrogen, higher concentrations of PCP led to a noticeable blue shift in the emission wavelength, from 526 nm for the pure poly(vinyl-DMAC-TRZ) (**75**) to 510 nm for the polymer with a 50:1 PCP emitter ratio (Figure 28 + Table 8). This results from the host function of the PCP, spacing the emitter moieties and stopping concentration quenching. The polymer with a 100:1 ratio showed a slight deviation, emitting at 513 nm, likely due to aggregation of the increasingly insoluble polymers in the film. This was also evidenced by precipitation from solutions and the hazy quality of the drop-cast sample. This trend was mirrored in the photoluminescence quantum yield

(PLQY) results. The PLQY increased consistently from 26.8% for the pure TADF polymer under nitrogen to 47.2% for the polymer with a 50:1 ratio. However, for the 100:1 ratio polymer, the PLQY dropped to 38.0%, possibly again due to aggregation effects or because of the continued dilution of the emitter moieties.

*Table 8: Results of PL measurements for poly(vinyl-DMAC-TRZ) (**75**) and the varying ratios of copolymer* R_p*-poly(vinyl-PCP-co-vinyl-DMAC-TRZ) (**74**).*

Sample	**λ_{max} (nm) at 370 nm excitation**	**PLQY in air (%)**	**PLQY in N_2 (%)**	**Prompt Emission (ns)**	**Delayed Emission (µs)**
Poly-(vinyl-DMAC-TRZ) (**75**)	526	23.8	26.8	14	0.70
Vinyl-PCP:TADF 10:1 R_p	525	27.3	29.1	15	0.87
Vinyl-PCP:TADF 20:1 R_p	513	40.9	40.8	17	1.20
Vinyl-PCP:TADF 50:1 R_p	510	45.6	47.2	17	1.01
Vinyl-PCP:TADF 100:1 R_p	513	37.0	38.0	16	0.43

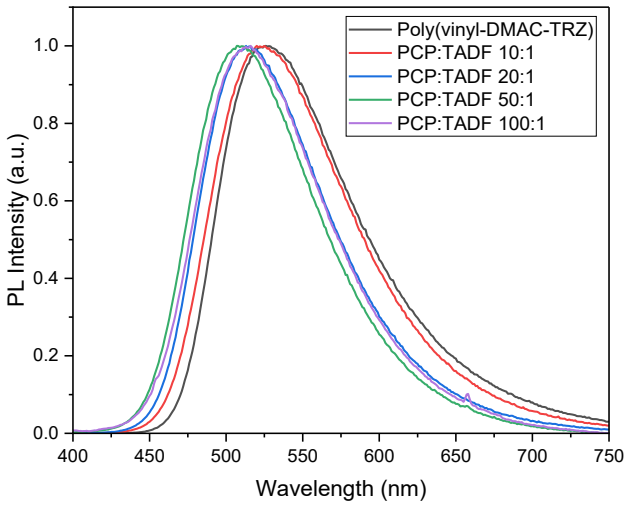

*Figure 28: Photoluminescence spectra for poly(vinyl-PCP-co-vinyl-DMAC-TRZ) (**74**) and poly(vinyl-DMAC-TRZ) (**75**) upon excitation at 370 nm.*

Lifetimes of emission were measured to confirm that the observed luminescence originated from TADF. Time-correlated single photon counting (TCSPC) measurements revealed both prompt decays (14-17 ns) and delayed decays ranging from 0.43 µs for the 100:1 polymer to 1.20 µs for the 20:1 polymer (Figure 29, Table 8).

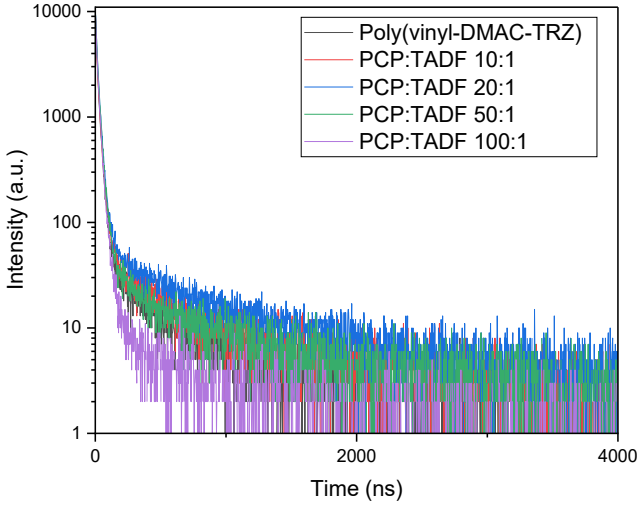

Figure 29: Lifetimes of TADF-polymers measured by TCSPC.

In addition to their TADF properties, the polymers' chirality suggested their potential as circularly polarized luminescence (CPL) emitters. The 20:1 and 50:1 polymers, which showed the most promising TADF performance, were selected for chiroptical property measurements, specifically circular dichroism (CD) and CPL. The CD spectra (Figure 30) displayed distinct mirror-image Cotton effects at 240 and 267 nm, confirming the polymers' chiral nature. Experimental CPL measurements verified activity for the 20:1 polymer (Figure 31, left), showing a roughly mirror-image relationship for enantiomers with similar molecular weights, though with low dissymmetry factors (2×10^{-4} and -1×10^{-4}) and some noise in the signals. The 50:1 polymer also exhibited CPL but a much lower signal-to-noise ratio (Figure 31, right). To date, only a few chiral TADF polymers have been successfully synthesized.

Novel approaches are needed to improve CPL activity, and the current work introduces a new method towards this goal. The next step will involve optimizing strategies to enhance CPL efficiency.

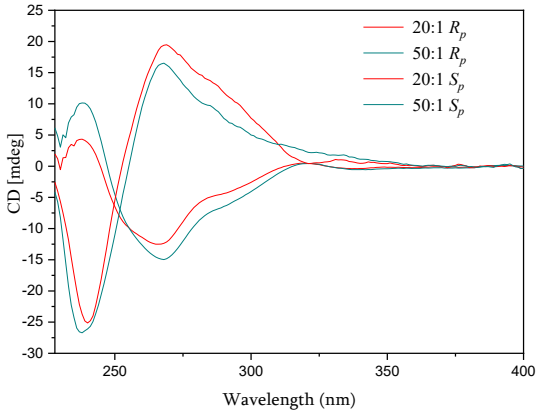

*Figure 30: CD spectra of the 20:1 and 50:1 polymers measured in DCM at a molarity of 5*10^{-6} M.*

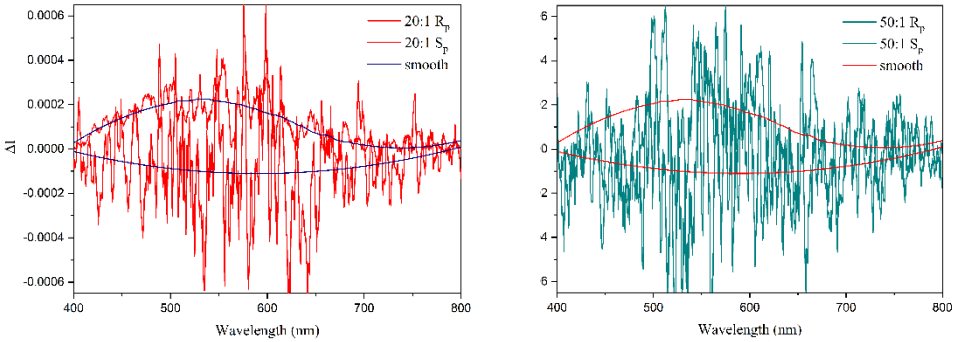

*Figure 31: CPL measurements in DCM with excitation at 320 nm for poly(vinyl-PCP-co-vinyl-DMAC-TRZ) (**74**) with 20:1 (left) and 50:1 (right) PCP:emitter ratio.*

These findings demonstrate that chiral vinyl-PCP monomers can effectively produce a CPL emitter from an achiral TADF emitter. Coupled with the promising TADF and photoluminescence properties, chiral PCP polymers represent a viable option for future applications in functional materials that integrate both chiral and optoelectronic characteristics. Future tests could also combine the benefits of the two copolymers used in this chapter and combine styrene, vinyl-PCP, and TADF emitter in a single polymer.

4.2. PCP-Polymers as Semiconductors

After using PCP monomers as semiconductors in chapter 3 and PCP polymers as functional material in chapter 4.1, it is a logical next step to combine the two and try for polymeric semiconductors based on PCP. Opposed to the TADF materials of chapter 4.1, the semiconductors don't benefit from chiral properties. Therefore, the simpler synthesis of vinyl-PCPs from chapter 3.4.1 can be used. Furthermore, the approach with PCP as a side chain on an alkyl backbone has shown severe back draws in low solubility and reactivity due to steric hindrance in the previous chapter. Those are estimated to only increase with the larger semiconducting side chains. Consequently, a strategy to build the backbone from the PCP and donor moieties seems more promising (Figure 32). It circumvents the steric hindrance and provides the additional benefit of a combined conjugated system that is less reliant on through-space conduction.[206]

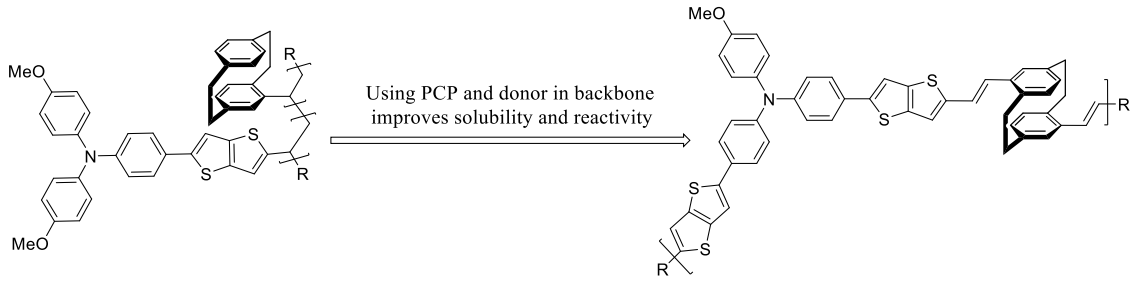

Figure 32: Example of changing from a side chain approach (left) to a backbone approach (right).

Without the need for chiral properties, utilizing the other tested cross-coupling methods from chapter 3 in cross-coupling polymerizations with minor changes to the used building blocks is also easily possible. Now, both used starting materials for the coupling reaction must be difunctionalized to facilitate the continuous reaction. The PCP core molecule is already difunctionalized, and the donor needs only a small alteration (Scheme 39).

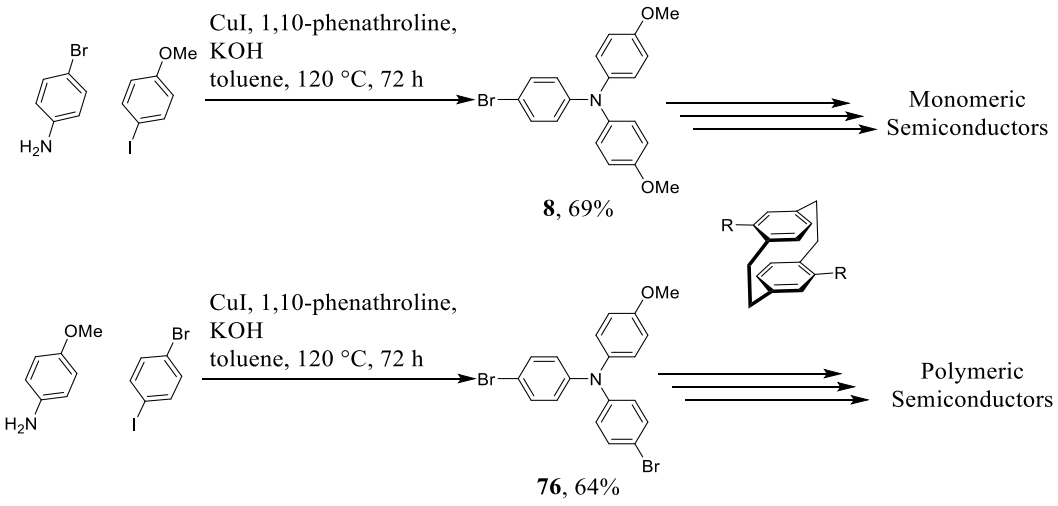

Scheme 39: Comparison of donor synthesis for the monomeric semiconductors of chapter 3 and the polymers of this chapter.

The synthesis of the TPA **76**, wearing two bromines, yields 64% and is only slightly less effective than that of the TPA **8**, which has only one bromine (69%). Donor **76** could then be combined with the π-bridges thiophene and thienothiophene using their borylated derivatives **9** and **12** in a Suzuki coupling to yield the two-armed molecules **77** and **79** in 69% and 67% yield for thiophene and thienothiophene respectively (Scheme 40). In both cases, this was followed up by bromination with NBS to use them in cross-couplings with the vinyl- and ethynyl-substituted PCPs. In agreement with the results for the one-armed molecules of chapter 3, the brominations work with excellent yields of 83% and 93% for thiophene and thienothiophene and result in the instable intermediates **78** and **80**.

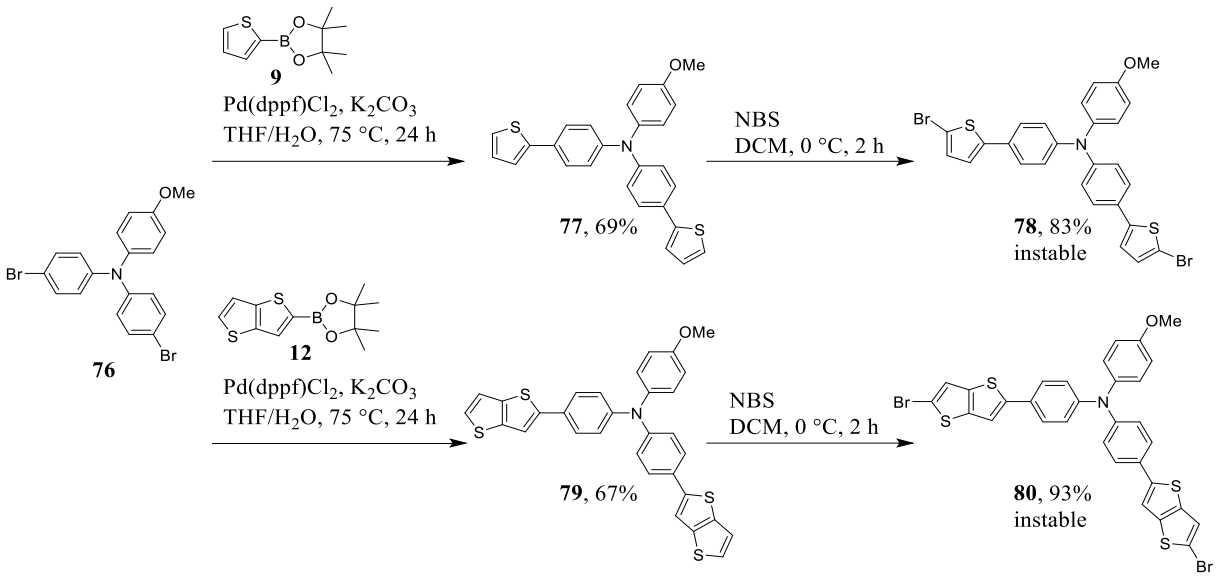

Scheme 40: Synthesis of the difunctionalized donor moieties containing thienothiophene (top) and thiophene (bottom).

In this case, the tendency for spontaneous coupling can also be used to produce a novel semiconducting polymer from **79** or **80** that does not include PCP (Scheme 41). While the brominated species **80** can undergo this reaction spontaneously, the reaction speed is low, as is the synthetic control. From a synthetical point of view, using **79** in a planned CH activation is more sensible and gives the polymer **81** in 32% yield. The isolated polymer has an M_n of 1.42 kDa, an M_w of 5.15 kDa, and a dispersity of 3.63 (Overview Table 9). Polymer **81** delivers a good comparison for the effects the inclusion of PCP into the polymers can have.

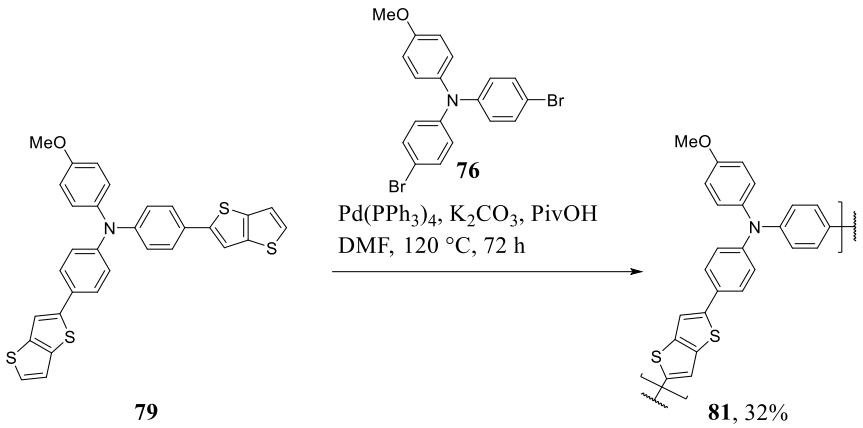

*Scheme 41: Polymerization of the two-armed thienothiophene in a CH activation polymerization to yield the polymer **81**.*

For the PCP-polymers, cross-coupling polymerization of the brominated thiophene- and thienothiophene-TPAs **78** and **80** with the vinyl- and ethynyl-substituted PCPs **39**, **40**, **49**, and **51** were carried out. The results of the application will be compared for all polymeric semiconductors at the end of the chapter. The more robust Heck and Sonogashira cross-coupling polymerizations should deliver larger and more monodisperse polymers than the direct Negishi coupling would provide. While tests with the Negishi coupling could still deliver interesting insights, they could not be realized in the time frame of this thesis.

The first tests were carried out with the thienothiophene derivate **80** and vinyl-PCPs **39** and **40** (Scheme 42). The *psp*-connected polymer **82** was isolated in 27% yield with an M_n of 1.54 kDa, an M_w of 4.05 kDa, and a dispersity of 2.63. The *psm* isomer **83** delivered similar results with a yield of 30%, an M_n of 1.65 kDa, an M_w of 3.83 kDa, and a dispersity of 2.32 (Overview Table 9). Compared to the polymers of chapter 4.1, the molecular weights are higher, but the dispersity is significantly broader. This results from the switch in polymerization technique from a chain-growth polymerization to a step-growth polymerization. This allows high-weight polymers in a short time but also makes the effects of low conversion on the dispersity much more pronounced. For the first tests and conclusions on the usability of the polymers, the molecular weights and dispersities play only a minor role. Still, future tests on the most promising candidates must consider their effects.

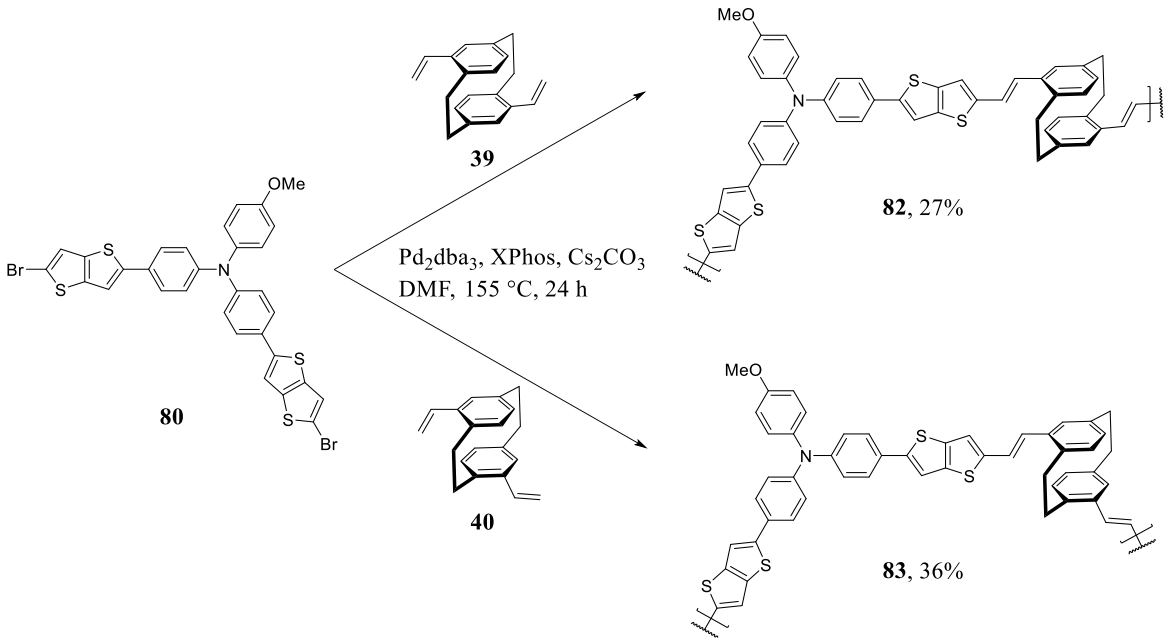

*Scheme 42: Heck cross-coupling polymerization to yield target polymers **82** and **83**.*

The next reactions combined the thienothiophene with the ethynyl-PCPs **49** and **51** in a Sonogashira coupling (Scheme 43). As was already observed in the small molecule equivalents, the yields were slightly higher than in the Heck reactions, giving 27% for the *psp* isomer **84** and 36% for the *psm* isomer **85**. Additionally, the molecular weights are drastically higher, with 5.67 kDa M_n, 24.3 kDa M_w, and a dispersity of 4.28 for *psp* polymer **84** and with 3.63 kDa M_n, 8.07 kDa M_w and a dispersity of 2.22 for *psm* polymer **85** (Overview Table 9).

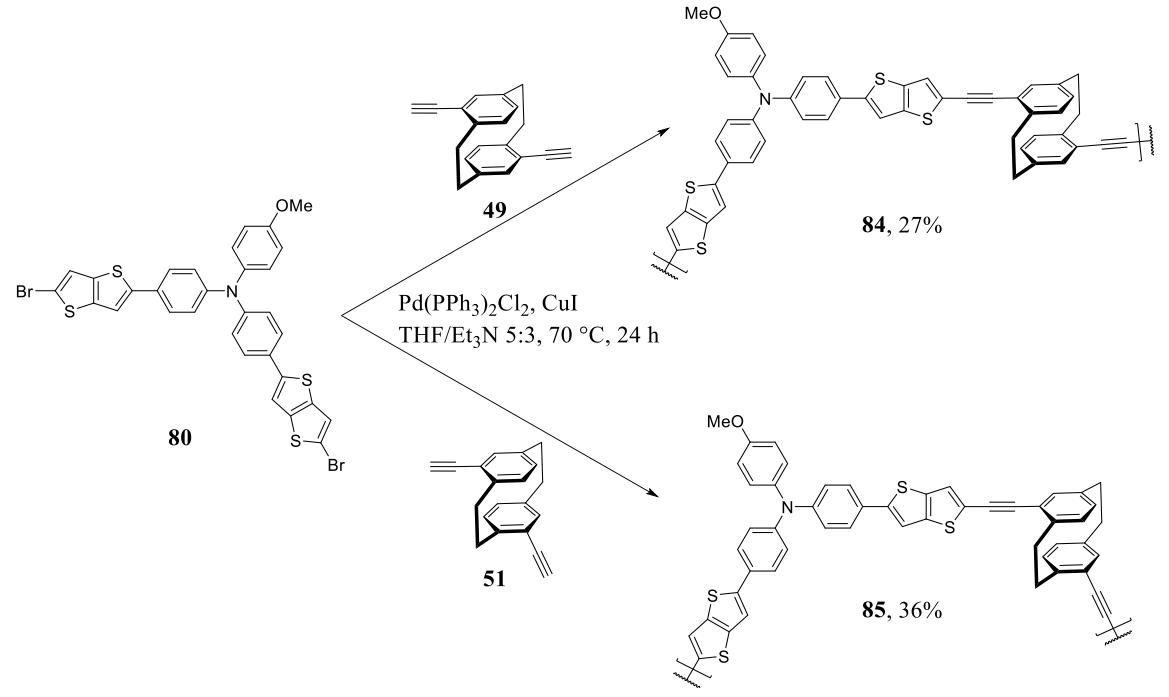

*Scheme 43: Sonogashira cross-coupling polymerization to yield target polymers **84** and **85**.*

Lastly, both Heck and Sonogashira coupling were carried out with the thiophene π-bridge and the *psm* isomers of vinyl- and ethynyl-PCP (Scheme 44). As was observed in the monomeric semiconductors, the results for thiophene are slightly better than for thienothiophene. The yields rise to 32% for **86** in the Heck coupling and 43% for **87** in the Sonogashira coupling. The results for the molecular weight of the alkyne polymer **87** are similar to the results with thienothiophene polymer **85**, giving 3.93 kDa M_n, 12.7 kDa M_w, and a dispersity of 3.24. The results of the Heck coupling to **86** are around three times higher than the respective results with the corresponding thienothiophene polymer **83** with 3.76 kDa M_n, 12.8 kDa M_w, and a dispersity of 4.21. This might be an outlier based on the exponential chain growth in step-growth polymerizations, but further tests are necessary to confirm this.

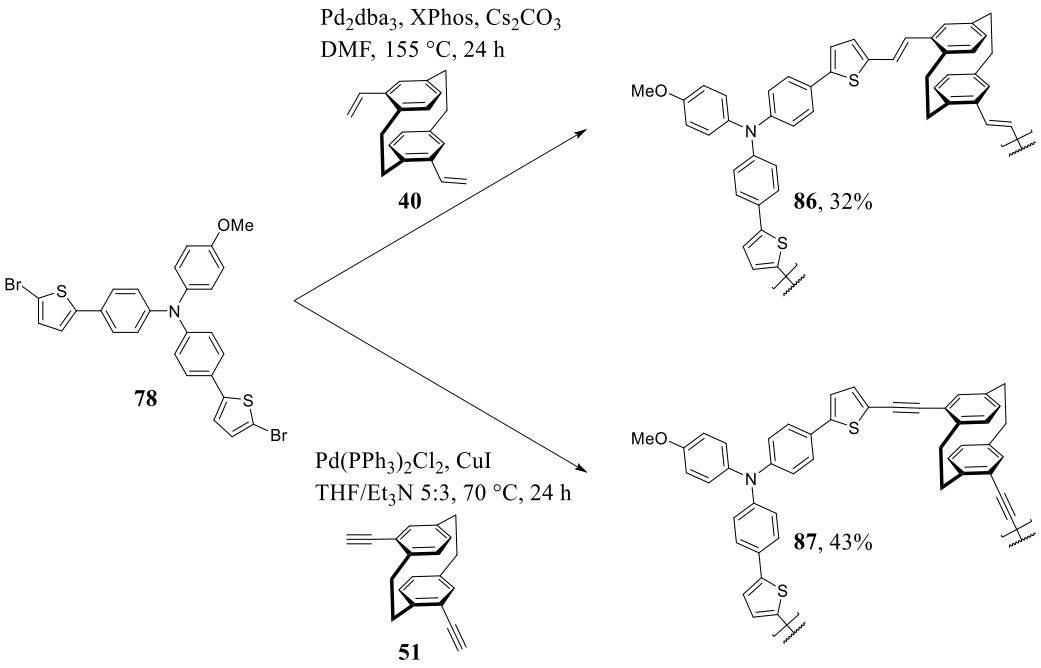

*Scheme 44: Heck and Sonogashira cross-coupling polymerization to yield target polymers **86** and **87**, respectively.*

Table 9: Overview of results for the synthesis of semiconducting polymers.

Sample	M_n [kDa][1]	M_w [kDa][1]	D[1]	Conversion [%]
81 (thienothiophene, CH activation)	1.42	5.15	3.63	32
82 (thienothiophene, *psp*-PCP, Heck)	1.54	4.05	2.63	27
83 (thienothiophene, *psm*-PCP, Heck)	1.65	3.83	2.32	30
84 (thienothiophene, *psp*-PCP, Sonogashira)	5.67	24.3	4.28	27
85 (thienothiophene, *psm*-PCP, Sonogashira)	3.63	8.07	2.22	36
86 (thiophene, *psm*-PCP, Heck)	3.76	15.8	4.21	32
87 (thiophene, *psm*-PCP, Sonogashira)	3.93	12.7	3.24	43

[1] Determined by GPC.

All seven semiconductor polymers were given to Holger Röhm and Tilman Bohnert of the Colsmann group for tests on electronic properties and film morphology. Of the seven polymers that were successfully synthesized, three showed sufficient film formation when spin-coated from chlorobenzene and could be directly used for further tests of their electronic properties (Figure 33). The other molecules need additional tests regarding their solubility in other suitable solvents or have to be processed differently. Thin-films were spin-coated at 2000 rpm over the span of 30 s using 30 µL of a saturated solution in chlorobenzene. The three polymers **85**–**87** formed even films, but **85** and **86** showed clear formation of artifacts. The better solubility of the thiophene compared to thienothiophene as well as *psm* isomers compared to *psp* isomers can be seen in these results.

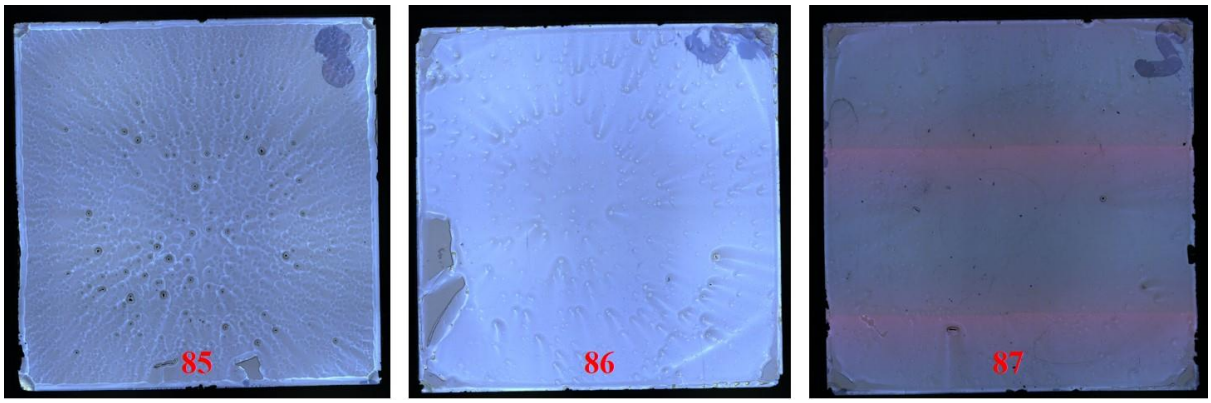

Figure 33: Thin-films of the three polymers that form measurable films

In UV-Vis absorption spectroscopy all three polymers showed clearly broadened absorption bands compared to the monomeric semiconductors (Figure 34). While the highest-wavelenght maxima λ_{max} stayed in the same region of 401–427 nm (417–431 nm for comparable monomeric molecules, chapter 3.5), the bands now reach much farther into the blue-shifted region.

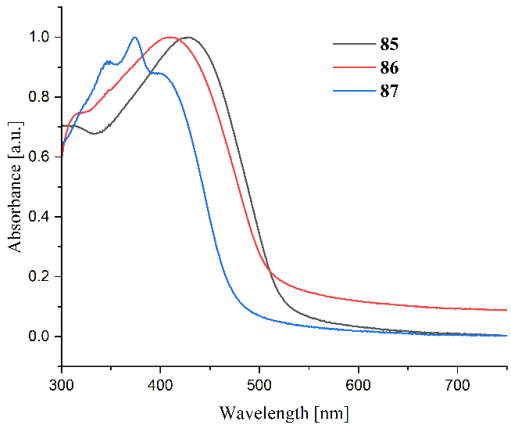

*Figure 34:UV-Vis spectra for thin-films of polymers **85**–**87**.*

Again, using equation 3 from chapter 3.5, the values for λ_{max} allow for the calculation of the optical band gap. The band gap of all three semiconductors is similar to each other as well as to the related monomers, ranging between 2.40 eV fo **85** up to 2.55 eV for **87**. This is large enough to ensure selective charge transport in solar cells.

Table 10: Summary of λ_{max} and band gap ΔE_{opt} as received from UV-Vis.

Sample	λ_{max} [nm]	ΔE_{opt} [eV]
85 (thienothiophene, *psm*-PCP, Sonogashira)	427	2.40
86 (thiophene, *psm*-PCP, Heck)	410	2.50
87 (thiophene, *psm*-PCP, Sonogashira)	401	2.55

Next were PESA tests to get the ionization potential which, with Koopmans' theorem applied, equals the HOMO energy level of the molecules (Figure 35, Table 11).[190] Together with the optical band gap this also allows calculation of the LUMO energy.

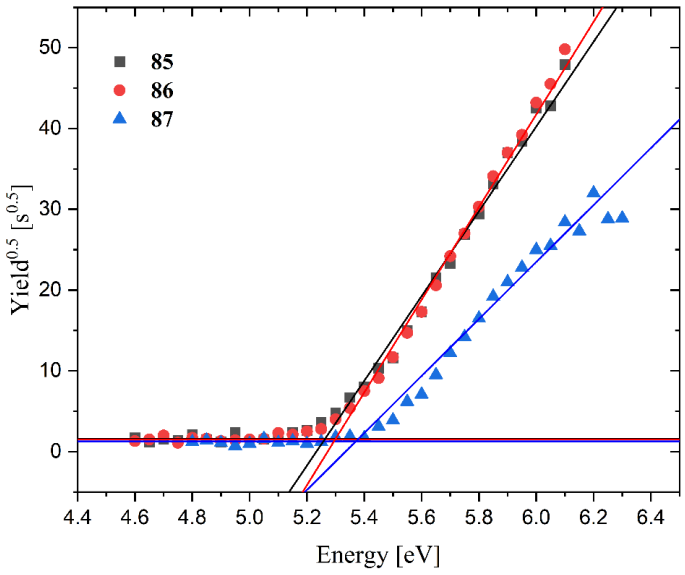

*Figure 35: PESA measurements of the three polymers **85**–**87**.*

Here as well, the values for the tested semiconductor polymers do not vary to much ranging from 5.26 to 5.39 eV. Given the structural similarity this was to be expected. Further test with, for example, carbazole containing polymers or polymer **81**, which lacks the PCP, have to be conducted to explore variations that influence the energy levels more strongly.

Table 11: Summary of the ionization potential (IP) and the approximated HOMO and LUMO energies.

Sample	IP_{PESA} (~HOMO) [eV]	LUMO [eV]
85 (thienothiophene, *psm*-PCP, Sonogashira)	5.26	2.86
86 (thiophene, *psm*-PCP, Heck)	5.29	2.79
87 (thiophene, *psm*-PCP, Sonogashira)	5.39	2.84

Summarized, seven new polymeric semiconductors were synthesized: four based on thienothiophene and PCP, two based on thiophene and PCP, and one thiophene-based polymer without PCP. The molecular weight ranges from 1.42 kDa to 24.3 kDa on average, with rather broad dispersity of 2–4. Of those, three polymers formed sufficient films to conduct optoelectronic mesaurements. All three yielded similar values and have energy levels appropriate for use in common PSCs. Future focus should be polymers with a narrower dispersity and polymers with other monomers, especially those that promise solubility improvements as well as finding improved ways to form thin-films.

5. Conclusion and Outlook

During the course of this work, it was possible to successfully synthesize and characterize a library of 19 novel PCP-based organic semiconductors, focusing on modular designs. This involved the use of different stereoisomers of PCP, the four π-bridges thiophene, thieneothiophene, dibenzothiophene, and carbazole, as well as the three spacer groups vinyl, ethynyl, and phenyl. This allowed to explore the effects and effectiveness of those building blocks in various synthetic approaches. Of the synthesized materials nine demonstrated promising characteristics for use in optoelectronic applications such as perovskite solar cells, based on their suitability for thin-film formation and electronic properties. They exhibite IPs between 5.17 eV and 5.35 eV as well as band gaps between 2.38 eV and 3.00 eV. These findings highlight the potential of PCP-based materials as highly tunable semiconductors.

Furthermore, the application of PCP in polymers was explored. The use of chiral vinyl-PCP as monomer allowed for the synthesis of chiral homopolymers as well as chiral copolymers with styrene retaining their chirality up to 98% styrene content. Lastly the synthesis of vinyl-DMAC-TRZ and its copolymerization with the chiral vinyl-PCP gave rise to chiral TADF emitter polymers that demonstrated CPL.

It was also possible to combine the concepts of the PCP-based semiconductors with the field of PCP-polymers to give rise to seven new semiconducting polymers utilizing step-growth cross-coupling polymerization integrating thienothiophene- or thiophene-based units as well as PCPs. The molecular weights M_w of these polymers varied from 3.83 kDa to 24.3 kDa with dispersity values ranging from 2 to 4. Of these polymers, three were successfully processed to thin-films and show energy levels appropriate for application in PSCs with IPs between 5.26–5.39 eV and band gaps of 2.40–2.55 eV.

Building on the insights gained, future research can focus on several avenues to optimize the functionality and applicability of PCP-based functional materials. Improving the solubility and film-forming properties of PCP-based molecules is a clear priority since they greatly impact the effectiveness of the achived molecules. Future work could explore alternative building blocks or side-chain modifications that offer better solubility. For the polymers a better control over molecular weight and dispersity is also of great interest. This should help to achieve more uniform thin-films essential for device fabrication. As with all synthetic work, addressing synthesis efficiency and reaction scalability will be essential for future practical applications. Further optimization of coupling reactions, as well as completely new approaches to circumvent instable intermediates, could improve yields and minimize side reactions. Last but not least, the insights achieved for PCPs, could be extended by exploring alternative cores like porphyrins. Preliminary tests show promising results for the application of the phenyl and ethynyl spacers giving rise to four-armed semiconductors.

Overall, this thesis underscores the versatility and potential of PCP-based materials in organic electronics. Future research, as outlined, holds promise for advancing the applicability of these molecules, ultimately supporting broader implementation in advanced materials.

6. Experimental Section

6.1. General Remarks

The following supporting information covers detailed material on the conducted experiments and their results, including the characterization of the obtained compounds. The data that support this study's findings are available in the repository Chemotion (https://www.chemotion-repository.net/).

6.1.1. Materials and Methods

The starting materials, solvents, and reagents were purchased from abcr (Karlsruhe, Germany), Acros (Geel, Belgium), Bernd Kraft (Duisburg, Germany), arbosynth (Redcar, United Kingdom), ChemPUR (Karlsruhe, Germany), Honeywell (Offenbach, Germany), Merck (Darmstadt, Germany), Sigma Aldrich (St. Louis, MO, US), TCI (Tokyo, Japan), and Thermo Fisher Scientific (Waltham, MA, US) and used without further purification unless stated otherwise.

Solvents of technical quality were purified by distillation or with the solvent purification system MB SPS5 (acetonitrile, dichloromethane (DCM), diethyl ether, tetrahydrofuran (THF), toluene) from MBraun (Garching, Germany). Solvents of p.a. quality were purchased from Acros (Geel, Belgium), Fisher Scientific (Waltham, MA, US), Sigma Aldrich (St. Louis, MO, US), Roth (Karlsruhe, Germany), or Riedel-de Haën (Seelze, Germany) and were used without further purification. Spectroscopic grade toluene was purchased from VWR (Darmstadt, Germany) and used without further purification.

Oxygen-free solvents were obtained by freeze-pump-thaw (three cycles) technique.

Air- and moisture-sensitive reactions were carried out under an argon atmosphere in oven-dried glassware using standard Schlenk techniques.

Liquids were added with a stainless-steel cannula, and solids were added in powdered shape.

Reactions at low temperatures were cooled using flat dewars produced by Isotherm (Karlsruhe, Germany) with water/ice or isopropanol/dry ice mixtures.

Solvents were evaporated under reduced pressure at 45 °C using a rotary evaporator. For solvent mixtures, each solvent was measured volumetrically.

Flash column chromatography was performed using Merck (Darmstadt, Germany) silica 60 (0.040 × 0.063 mm, 230–400 mesh ASTM) and quartz sand (glowed and purified with hydrochloric acid).

All reactions were monitored by thin-layer chromatography using silica-coated aluminum plates (Merck (Darmstadt, Germany), silica 60, F254). UV-active compounds were detected with a UV lamp at 254 nm and 366 nm excitation.

6.1.2. Devices

Melting Point (M.p.)

Melting points were detected on an OptiMelt MPA100 device from the Stanford Research System (Sunnyvale, CA, US).

Optical Rotation

Optical rotation was measured with a Perkin Elmer (Rodgau, Germany) 241 Polarimeter using a 100 mm glass cell, a suitable solvent at the sodium-D-lines (589.0 and 589.6 nm), and a constant temperature of 20 °C.

Nuclear Magnetic Resonance Spectroscopy (NMR)

NMR spectra were recorded on a Bruker (Karlsruhe, Germany) Avance 400 NMR instrument at 400 MHz for ^{1}H NMR and 101 MHz for ^{13}C NMR.

The NMR spectra were recorded at room temperature in deuterated solvents acquired from Eurisotop (Saint-Aubin, France). The chemical shift δ is displayed in parts per million (ppm), and the references used were the ^{1}H and ^{13}C peaks of the solvents themselves as follows:

d_1-chloroform ($CDCl_3$): 7.26 ppm for ^{1}H and 77.16 ppm for ^{13}C

d_2-dichloromethane (CD_2Cl_2): 5.32 ppm for ^{1}H and 53.84 ppm for ^{13}C

d_8-tetrahydrofuran (THF): 3.58 ppm for ^{1}H and 67.57 ppm for ^{13}C

For the characterization of centrosymmetric signals, the signal's median point was chosen for multiplets in the signal range. The following abbreviations were used to describe the proton splitting pattern: d = doublet, t = triplet, m = multiplet, dd = doublet of a doublet, ddd = doublet of a doublet of a doublet, and dt = doublet of a triplet, etc. Absolute values of the coupling constants "J" are given in Hertz [Hz] in absolute value and decreasing order. Signals of the ^{13}C spectrum were assigned by distortionless enhancement by polarization transfer (DEPT) spectra DEPT90 and DEPT135 or phase-edited heteronuclear single quantum coherence (HSQC). They were specified in the following way: + = primary or tertiary carbon atoms (positive phase), − = secondary carbon atoms (negative phase), and C_q = quaternary carbon atoms (no signal).

Infrared Spectroscopy (IR)

The infrared spectra were recorded with a Bruker Alpha P instrument. All samples were measured by attenuated total reflection (ATR). The positions of the absorption bands are given in wavenumbers $\tilde{\nu}$ in cm^{-1} and were measured in the range from 3600 cm^{-1} to 500 cm^{-1}. Characterization of the absorption bands was performed in dependence of the ab-sorption strength with the following abbreviations: vs

(very strong, 0–9%), s (strong, 10–39%), m (medium, 40–69%), w (weak, 70–89%), and vw (very weak, 90–100%).

Mass Spectrometry (MS)

Electron ionization (EI) and fast atom bombardment (FAB) experiments were conducted using a Finnigan, MAT 95 (70 eV) instrument, with 3-nitrobenzyl alcohol (3-NBA) as the matrix and reference for high resolution. For the interpretation of the spectra, molecular peaks $[M]^+$, peaks of protonated molecules $[M+H]^+$, and characteristic fragment peaks are indicated with their mass-to-charge ratio (m/z) and their intensity in percent, relative to the base peak (100%), is given.

ESI experiments were recorded on a Q-Exactive (Orbitrap) mass spectrometer (Thermo Fisher Scientific, San Jose, CA, USA) equipped with a HESI II probe to record high resolution. The tolerated error is ±5 ppm of the molecular mass. The spectra were interpreted by molecular peaks $[M]^+$, peaks of protonated molecules $[M+H]^+$, and characteristic fragment peaks and indicated with their mass-to-charge ratio (*m/z*).

Gel Permeation Chromatography (GPC)

For GPC measurements, a PSS SECcurity2 GPC-System with Agilent infinity 1260 II hardware was used. The device uses a refractive index detector and runs on THF as a polar phase with a flow rate of 1 mL/min at 30 °C. The used column system consists of a PSS SDV analytical column (3 µm, 300×8.0 mm^2, 1000 Å) with a PSS SDV analytical pre-column (3 µm, 50×8.0 mm^2). Poly(methyl methacrylate) with masses ranging from 102 to 62000 Da were used for calibration.

Optical Spectroscopy

The PL spectra were recorded using an Edinburgh Instruments FS5 spectrofluorometer, exciting at 370 nm. Neat film PLQYs were measured in an integrating sphere with ex-citation from a xenon lamp (370 nm). Samples were excited with a pulsed LED (340 nm, pulse width: 1 ns) for the transient photoluminescence measurements. Neat films were fabricated by drop-casting toluene solutions of the compounds (100 µl, 2 mg ml^{-1}) onto quartz substrates and then annealed at 50 °C for 15 minutes.

UV-vis absorption spectra were recorded on an Analytik Jena SPECORD 50 Plus. Before the measurement, the samples were dissolved in tetrahydrofuran and filled in glass cuvettes with a layer thickness of 0.1 cm.

Electronic Circular Dichroism (ECD) and Circularly Polarized Luminescence (CPL)

CD spectra of polymers were measured in dichloromethane solutions with a Jasco J-815 instrument. CPL measurements were performed using a home-built CPL spectrofluoropolarimeter (constructed with the help of the JASCO Company). The samples were excited using a 90° geometry with a 150 W LS

Xenon ozone-free lamp. The samples were measured at ca. 5×10^{-6} M in DCM. The samples were excited at 320 nm, and 5-9 scan accumulations were used.

Film Morphology

For the photography of spin-coated films on glass a Zeiss Smartzoom 5 digital microscope was used.

Photoelectron Spectroscopy in Air (PESA)

Measurements of thin-film IPs were carried out with a Riken Keiki AC-2E photoelectron spectrometer. The samples were measured at a UV intensity of 5 nW. The photoelectron yields were corrected for the quantity of light and fitted with a power number of 0.5 to obtain the IPs.

6.2. Synthetic Procedures

Molecule **37** was synthesized, replicating the procedures of Zhou *et al*.[183] Molecule **38** was synthesized replicating the procedures of Tang *et al*. [185] The molecules **64-68** were synthesized, replicating the procedures of Zippel *et al*.[196] All analytics matched the literature.

6.2.1. Procedures Chapter 3 "Library of PCP-based Organic Semiconductors"

4,16-Dibromo[2.2]paracyclophane (**1**), **4,15-Dibromo[2.2]paracyclophane** (**2**)

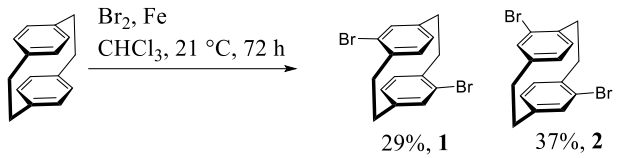

Bromine (46.0 g, 14.8 mL, 288 mmol, 3.00 equiv.) was diluted with chloroform (30 mL). [2.2]Paracyclophane (20.0 g, 96.0 mmol, 1.00 equiv.) was dissolved in chloroform (150 mL) with iron shavings (617 mg, 11.0 mmol, 0.0500 equiv.), and the bromine solution was added dropwise and stirred for 30 min. The solution was then stirred for 72 h. Sodium sulfite (300 mL, sat. aq. solution) was added and stirred until the organic layer turned colorless. The solution was filtered, and the residual solid was washed with cHex (2 x 100 mL) and Et_2O (2 x 100 mL). The solid (impure 4,16-dibromobromo[2.2]paracyclophane) was kept for later while the organic phase was evaporated. The residual solid from the organic phase was washed with Et_2O (2 x 100 mL), then it was recrystallized three times from cyclohexane to separate 4,16-dibromobromo[2.2]paracyclophane (solid) and 4,15-dibromo[2.2]paracyclophane (solution). The solution was evaporated to yield 4,15-dibromo[2.2]paracyclophane (13.7 g, 35.7 mmol, 37% yield) as a colorless solid. The solid was combined with the impure 4,16-dibromobromo[2.2]paracyclophane and recrystallized from hot toluene to yield pure 4,16-dibromobromo[2.2]paracyclophane (10.0 g, 27.4 mmol, 29% yield) as colorless crystals.

R_f = 4,16-Br_2-PCP = 0.48; 4,15-Br_2-PCP = 0.48 (pentane/DCM = 10:1).

4,16-Br_2-PCP:

M.p.: 245 °C

^{1}H NMR (400 MHz, Chloroform-d [7.26 ppm], ppm) δ = 7.14 (dd, *J* = 7.9 Hz, *J* = 1.8 Hz, 2H, CH_{Ar}), 6.51 (d, *J* = 1.8 Hz, 2H, CH_{Ar}), 6.44 (d, *J* = 7.8 Hz, 2H, CH_{Ar}), 3.50 (ddd, *J* = 13.0 Hz, *J* = 10.4 Hz, *J* = 2.3 Hz, 2H, PCP-CH_2), 3.16 (ddd, *J* = 12.6 Hz, *J* = 10.3 Hz, *J* = 4.9 Hz, 2H, PCP-CH_2), 2.95 (ddd, *J* = 12.7 Hz, *J* = 10.7 Hz, *J* = 2.3 Hz, 2H, PCP-CH_2), 2.85 (ddd, *J* = 13.2 Hz, *J* = 10.7 Hz, *J* = 4.9 Hz, 2H, PCP-CH_2);

^{13}C NMR (100 MHz, Chloroform-d [77.16 ppm], ppm) δ = 141.2 (C_q, 2C, C_{Ar}), 138.5 (C_q, 2C, C_{Ar}), 137.3 (+, CH, 2C, *C*H$_{Ar}$), 134.1 (+, CH, 2C, *C*H$_{Ar}$), 128.3 (+, CH, 2C, *C*H$_{Ar}$), 126.8 (C_q, 2C, C_{Ar}), 35.4 (–, CH_2, 2C, PCP-*C*H$_2$), 32.9 (–, CH_2, 2C, PCP-*C*H$_2$);

MS (EI, 70 eV, 120 °C), m/z (%): 364/366/368 (9/21/9) $[M]^+$, 184 (91), 182 (100), 103 (40), 77 (42). HRMS–EI (m/z): $[M]^+$ calcd for 365.9436; found 365.9438;

IR (ATR, ṽ) = 2962 (w), 2934 (m), 2890 (w), 2850 (w), 1584 (m), 1536 (m), 1473 (m), 1449 (m), 1432 (m), 1390 (vs), 1347 (w), 1313 (w), 1286 (w), 1241 (w), 1187 (m), 1157 (w), 1105 (w), 1030 (vs), 948 (w), 899 (vs), 887 (s), 856 (vs), 830 (vs), 771 (m), 730 (w), 705 (vs), 698 (vs), 669 (vs), 647 (vs), 598 (w), 578 (w), 555 (w), 523 (vs), 465 (vs), 438 (w), 431 (w), 392 (s), 380 (m) cm^{-1}.

4,15-Br$_2$-PCP:

M.p.: 125 °C

^{1}H NMR (400 MHz, Chloroform-d [7.26 ppm], ppm) δ = 7.21–7.14 (m, 2H, C*H*$_{Ar}$), 6.59–6.55 (m, 2H, C*H*$_{Ar}$), 6.51–6.43 (m, 2H, C*H*$_{Ar}$), 3.37–3.28 (m, 2H, PCP-CH_2), 3.07 (m, 4H, PCP-CH_2), 2.95–2.84 (m, 2H, PCP-CH_2);

^{13}C NMR (100 MHz, Chloroform-d [77.16 ppm], ppm) δ = 141.1 (C_q, 2C, C_{Ar}), 139.0 (C_q, 2C, C_{Ar}), 136.8 (+, CH, 2C, *C*H$_{Ar}$), 130.9 (+, CH, 2C, *C*H$_{Ar}$), 130.2 (+, CH, 2C, *C*H$_{Ar}$), 127.6 (C_q, 2C, C_{Ar}), 34.6 (–, CH_2, 2C, PCP-*C*H$_2$), 33.5 (–, CH_2, 2C, PCP-*C*H$_2$);

MS (FAB, 3-NBA), m/z (%): 364/366/368 (17/34/17) $[M]^+$, 154 (100), 138 (32), 137 (52), 136 (67). HRMS (FAB, matrix NBA): m/z = calcd for $C_{16}H_{14}{}^{79}Br^{81}Br$ $[M]^+$: 365.9436; found 365.9435;

IR (ATR, ṽ) = 3037 (w), 2952 (w), 2928 (s), 2888 (w), 2850 (w), 1584 (m), 1538 (w), 1476 (s), 1449 (m), 1431 (m), 1391 (s), 1354 (w), 1317 (w), 1269 (w), 1237 (w), 1203 (w), 1186 (w), 1162 (w), 1047 (w), 1030 (vs), 956 (w), 904 (vs), 863 (m), 840 (vs), 807 (m), 790 (m), 756 (w), 705 (vs), 684 (s), 671 (m), 662 (s), 649 (vs), 596 (w), 585 (w), 518 (vs), 476 (vs), 436 (w), 414 (w), 397 (w) cm^{-1}.

Additional information on chemical synthesis is available *via* the Chemotion repository:

https://doi.org/10.14272/reaction/SA-FUHFF-UHFFFADPSC-YLZWSUSKID-UHFFFADPSC-NUHFF-NUHFF-NUHFF-ZZZ.2

Additional information on the analysis of the target compound is available *via* the Chemotion repository:

https://doi.org/10.14272/QDMAXRJHDMKTQH-UHFFFAOYSA-N.9

https://doi.org/10.14272/YTVHCBMSDDDSSN-UHFFFAOYSA-N.3

4,12-Dibromo[2.2]paracyclophane (3)

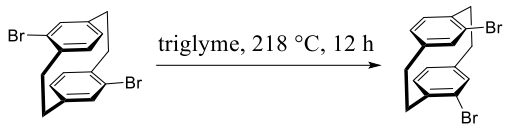

58%, **3**

A mixture of 4,16-dibromo[2.2]paracyclophane (15.0 g, 41.0 mmol, 1.00 equiv.) and triglyme (70 mL) was refluxed at 220 °C for 4 h. After cooling to 22 °C; the reaction mixture was cooled in an ice bath. The formed precipitate (4,16-dibromoparacyclophane) was filtered off, washed with 10 mL of Et_2O, and heated again in triglyme (40 mL). After repeating the cycle two more times in decreasing amounts of solvent (20 mL and 10 mL of triglyme, respectively), the filtrates were combined, and 60% aq. EtOH (300 mL) was added dropwise under vigorous stirring over 3 h. The precipitate was filtered off, washed once with 70% aq EtOH, and dried on air to yield the pure 4,12-dibromo[2.2]paracyclophane (9.25 g, 23.8 mmol, 58% yield) as a colorless solid.

R_f = 0.48 (pentane/DCM 10:1).

M.p.: 180-190 °C

^{1}H NMR (400 MHz, Chloroform-d [7.26 ppm], ppm) δ = 7.19 (d, *J* = 1.7 Hz, 2H, CH_{Ar}), 6.55 (d, *J* = 7.8 Hz, 2H, CH_{Ar}), 6.52 (dd, *J* = 7.8 Hz, *J* = 1.7 Hz, 2H, CH_{Ar}), 3.45 (ddd, *J* = 13.3 Hz, *J* = 9.5 Hz, *J* = 2.2 Hz, 2H, PCP-CH_2), 3.12–2.98 (m, 4H, PCP-CH_2), 2.81 (ddd, *J* = 13.3 Hz, *J* = 10.1 Hz, *J* = 6.9 Hz, 2H, PCP-CH_2);

^{13}C NMR (100 MHz, Chloroform-d [77.16 ppm], ppm) δ = 141.3 (C_q, 2C), 138.7 (C_q, 2C), 135.0 (+, CH, 2C), 132.7 (+, CH, 2C), 131.6 (+, CH, 2C), 126.6 (C_q, 2C), 35.8 (–, CH_2, 2C), 32.5 (–, CH_2, 2C);

MS (FAB, 3-NBA), m/z (%): 366/368/364 (31/16/16) $[M]^+$, 184 (23), 182 (25), 155 (27), 154 (100), 138 (40), 137 (70), 136 (80). HRMS (FAB, matrix NBA): m/z = calcd for $C_{16}H_{14}{}^{79}Br^{81}Br$ $[M]^+$: 365.9436; found 365.9438;

IR (ATR, $\tilde{\nu}$) = 2961 (w), 2931 (s), 2888 (w), 2850 (m), 1584 (m), 1536 (m), 1473 (m), 1449 (m), 1432 (m), 1390 (vs), 1313 (w), 1286 (w), 1273 (w), 1239 (w), 1200 (w), 1186 (m), 1157 (w), 1135 (w), 1105 (m), 1030 (vs), 959 (w), 948 (w), 899 (vs), 887 (s), 856 (vs), 829 (vs), 816 (s), 785 (m), 771 (m), 705 (vs), 669 (vs), 647 (vs), 598 (w), 523 (vs), 476 (m), 465 (vs), 431 (w), 419 (w), 394 (m), 375 (w) cm^{-1}.

Additional information on chemical synthesis is available *via* the Chemotion repository:

https://doi.org/10.14272/reaction/SA-FUHFF-UHFFFADPSC-QDMAXRJHDM-UHFFFADPSC-NUHFF-NUHFF-NUHFF-ZZZ.4

Additional information on the analysis of the target compound is available *via* the Chemotion repository:

https://doi.org/10.14272/QDMAXRJHDMKTQH-UHFFFAOYSA-N.10

4,15-(Bis(thiophene-5,2-diyl-*N,N*-bis(4-methoxyphenyl)aniline)[2.2]paracyclophane (6)

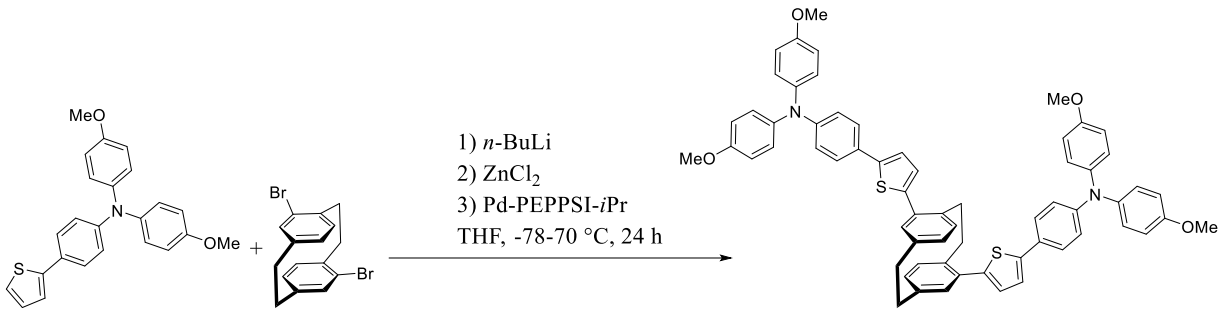

6, 24%

Preparation of Negishi reactant:

Bis(4-methoxyphenyl)-[4-(2-thienyl)phenyl]amine (116 mg, 300 µmol, 2.20 equiv.) was added to a crimp cap vial and flushed with Ar three times. 5 mL of dry THF was added, and the mixture was cooled to -78 °C. *n*-Butyllithium solution (22.7 mg, 142 µL, 355 µmol, 2.50M in hexane, 2.60 equiv.) was added dropwise, and the reaction mixture was allowed to warm to 22 °C. After stirring for 30 min, the reaction mixture was cooled to 0 °C, and zinc chloride solution (55.8 mg, 410 µL, 410 µmol, 1.00M in THF, 3.00 equiv.) was added. The reaction was stirred for 15 min at 0 °C and then warmed to 22 °C.

Negishi coupling:

4,15-Dibromo[2.2]paracyclophane (50.0 mg, 137 µmol, 1.00 equiv.) and PEPPSI-IPr catalyst (9.31 mg, 13.7 µmol, 0.100 equiv.) were added to a crimp cap vial and flushed with Ar three times. 5 mL of dry THF and zinc chloride solution (55.8 mg, 410 µL, 410 µmol, 1.00M in THF, 3.00 equiv.) was added. After dissolving, the Negishi reactant was added *via* syringe, and the reaction mixture was heated to 70 °C. After three days, the reaction was allowed to cool to 22 °C, and the solvent was removed under reduced pressure. Column chromatography on silica using cHex/DCM 1:0 to 1:2 as eluent yielded 4,15-(bis(thiophene-5,2-diyl-*N,N*-bis(4-methoxyphenyl)aniline)[2.2]paracyclophane (32.6 mg, 33.3 µmol, 24% yield) as a yellow solid.

R_f = 0.38 (cHex/DCM 2:1).

M.p.: 117 °C

^{1}H NMR (400 MHz, Dichloromethane-d_2 [5.32 ppm], ppm) δ = 7.51–7.43 (m, 4H), 7.24–7.19 (m, 2H), 7.12–7.05 (m, 10H), 6.95–6.91 (m, 4H), 6.89–6.84 (m, 10H), 6.68 (d, *J* = 1.9 Hz, 2H), 6.55 (dd, *J* = 7.8

Hz, *J* = 1.9 Hz, 2H), 3.80 (s, 12H, OMe-CH_3), 3.67–3.60 (m, 2H, PCP-CH_2), 3.20–3.11 (m, 2H, PCP-CH_2), 3.06–2.99 (m, 2H, PCP-CH_2), 2.71–2.64 (m, 2H, PCP-CH_2);

^{13}C NMR (100 MHz, Dichloromethane-d_2 [53.84 ppm], ppm) δ = 156.2 (C_q, 4C), 148.4 (C_q, 2C), 144.3 (C_q, 2C), 142.1 (C_q, 2C), 140.6 (C_q, 4C), 140.1 (C_q, 2C), 137.4 (C_q, 2C), 135.4 (C_q, 2C), 132.6 (+, CH, 2C), 132.5 (+, CH, 2C), 131.2 (+, CH, 2C), 126.8 (+, CH, 2C), 126.7 (+, CH, 8C), 126.4 (C_q, 2C), 126.1 (+, CH, 4C), 122.2 (+, CH, 2C), 120.3 (+, CH, 4C), 114.7 (+, CH, 8C), 55.4 (+, CH_3, 4C, OMe-CH_3), 34.8 (–, CH_2, 2C, PCP-CH_2), 33.8 (–, CH_2, 2C, PCP-CH_2);

MS (ESI), m/z (%): 978 (9) $[M]^+$, 490 (46), 489 (100), 163 (55). HRMS (ESI): m/z = calcd for $C_{64}H_{54}N_2O_4{}^{32}S_2$ $[M]^+$: 978.3525; found 978.3515;

IR (ATR, $\tilde{\nu}$) = 2941 (w), 2929 (w), 2897 (w), 2833 (w), 1601 (w), 1588 (w), 1500 (vs), 1483 (vs), 1456 (s), 1439 (s), 1408 (w), 1278 (m), 1235 (vs), 1191 (s), 1177 (s), 1164 (s), 1103 (m), 1031 (vs), 952 (w), 899 (w), 875 (w), 824 (vs), 798 (vs), 727 (s), 700 (m), 657 (w), 633 (w), 595 (m), 575 (s), 524 (s), 487 (m), 446 (w), 426 (m), 399 (m), 388 (w) cm^{-1}.

Additional information on chemical synthesis is available *via* the Chemotion repository:

https://doi.org/10.14272/reaction/SA-FUHFF-UHFFFADPSC-QJUGOXCZRN-UHFFFADPSC-NUHFF-NUHFF-NUHFF-ZZZ

Additional information on the analysis of the target compound is available *via* the Chemotion repository:

https://doi.org/10.14272/QJUGOXCZRNWVMY-UHFFFAOYSA-N.1

4,12-(Bis(thiophene-5,2-diyl-*N,N*-bis(4-methoxyphenyl)aniline)[2.2]paracyclophane (7)

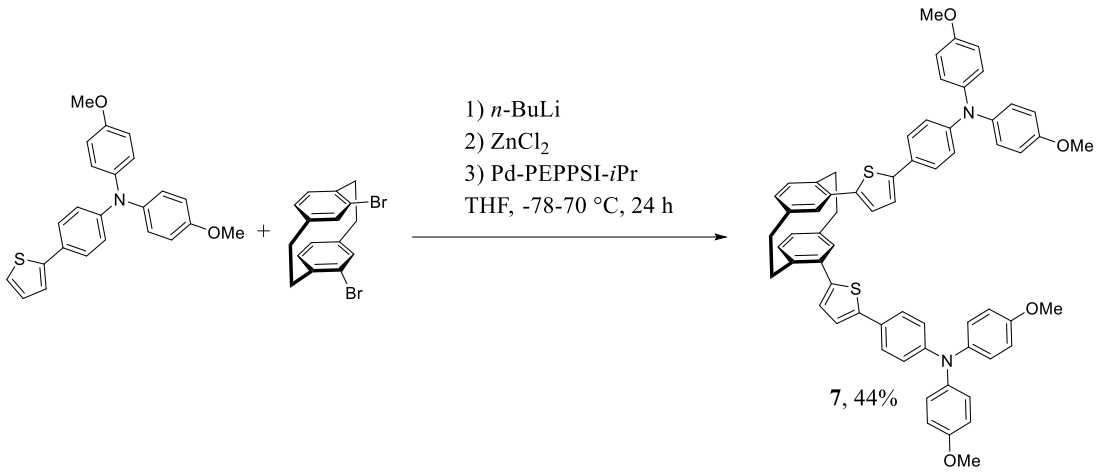

Preparation of Negishi reactant:

Bis(4-methoxyphenyl)-[4-(2-thienyl)phenyl]amine (116 mg, 300 µmol, 2.20 equiv.) was added to a crimp cap vial and flushed with Ar three times. 5 mL of dry THF was added, and the mixture was cooled to -78 °C. *n*-Butyllithium solution (22.7 mg, 142 µL, 355 µmol, 2.50M in hexane, 2.60 equiv.) was added dropwise, and the reaction mixture was allowed to warm to 22 °C. After stirring for 30 min, the reaction mixture was cooled to 0 °C, and zinc chloride solution (55.8 mg, 410 µL, 410 µmol, 1.00M in THF, 3.00 equiv.) was added. The reaction was stirred for 15 min at 0 °C and then warmed to 22 °C.

Negishi coupling:

4,12-Dibromo[2.2]paracyclophane (50.0 mg, 137 µmol, 1.00 equiv.) and PEPPSI-IPr catalyst (9.31 mg, 13.7 µmol, 0.100 equiv.) were added to a crimp cap vial and flushed with Ar three times. 5 mL of dry THF and zinc chloride solution (55.8 mg, 410 µL, 410 µmol, 1.00M in THF, 3.00 equiv.) was added. After dissolving, the Negishi reactant was added *via* syringe, and the reaction mixture was heated to 70 °C. After three days, the reaction was allowed to cool to 22 °C, and the solvent was removed under reduced pressure. Column chromatography on silica using cHex/DCM 1:0 to 1:2 as eluent yielded 4,12-(bis(thiophene-5,2-diyl-*N,N*-bis(4-methoxyphenyl)aniline)[2.2]paracyclophane (58.9 mg, 60.1 µmol, 44% yield) as a yellow solid.

R_f = 0.38 (cHex/DCM 2:1).

M.p.: 79 °C

^{1}H NMR (400 MHz, Chloroform-d [7.26 ppm], ppm) δ = 7.47–7.43 (m, 4H), 7.20 (d, *J* = 3.7 Hz, 2H), 7.10–7.02 (m, 10H), 6.93–6.91 (m, 4H), 6.88–6.81 (m, 10H), 6.66 (d, *J* = 7.8 Hz, 2H), 6.58 (dd, *J* = 7.3 Hz, *J* = 1.4 Hz, 2H), 3.92–3.83 (m, 2H, PCP-CH_2), 3.80 (s, 12H, OMe-CH_3), 3.14–3.06 (m, 2H, PCP-CH_2), 2.96–2.88 (m, 4H, PCP-CH_2);

^{13}C NMR (100 MHz, Chloroform-d [77.16 ppm], ppm) δ = 155.9 (C_q, 4C), 148.1 (C_q, 2C), 144.3 (C_q, 2C), 141.8 (C_q, 2C), 140.8 (C_q, 2C), 139.9 (C_q, 4C), 136.6 (C_q, 4C), 135.8 (+, CH, 4C), 134.3 (C_q, 2C), 131.9 (+, CH, 4C), 130.1 (+, CH, 2C), 126.8 (+, CH, 2C), 126.6 (+, CH, 8C), 126.3 (+, CH, 2C), 122.2 (+, CH, 2C), 121.0 (+, CH, 2C), 114.9 (+, CH, 8C), 55.5 (+, CH_3, 4C, OMe-CH_3), 35.3 (–, CH_2, 2C, PCP-CH_2), 33.9 (–, CH_2, 2C, PCP-CH_2);

MS (ESI), m/z (%): 978 (18) $[M]^+$, 490 (44), 489 (61), 432 (29), 431 (100). HRMS (ESI): m/z = calcd for $C_{64}H_{54}N_2O_4{}^{32}S_2$ $[M]^+$: 978.3525; found 978.3514;

IR (ATR, ṽ) = 3036 (w), 2997 (w), 2922 (m), 2849 (w), 2833 (w), 2793 (w), 1601 (w), 1587 (w), 1500 (vs), 1482 (s), 1459 (s), 1451 (s), 1439 (s), 1401 (w), 1317 (m), 1281 (m), 1265 (m), 1235 (vs), 1191 (s), 1177 (s), 1164 (s), 1105 (m), 1033 (vs), 952 (w), 901 (w), 860 (w), 824 (vs), 798 (vs), 781 (m), 721 (s), 703 (m), 681 (w), 653 (w), 640 (w), 633 (w), 596 (m), 575 (s), 524 (s), 493 (m), 482 (m), 446 (w), 429 (w), 421 (w), 409 (w), 390 (w) cm^{-1}.

Additional information on chemical synthesis is available *via* the Chemotion repository:

https://doi.org/10.14272/reaction/SA-FUHFF-UHFFFADPSC-BHWXSUYBQO-UHFFFADPSC-NUHFF-NUHFF-NUHFF-ZZZ.1

Additional information on the analysis of the target compound is available *via* the Chemotion repository:

https://doi.org/10.14272/BHWXSUYBQOTELE-UHFFFAOYSA-N.2

(4-Bromophenyl)-bis(4-methoxyphenyl)amine (8)

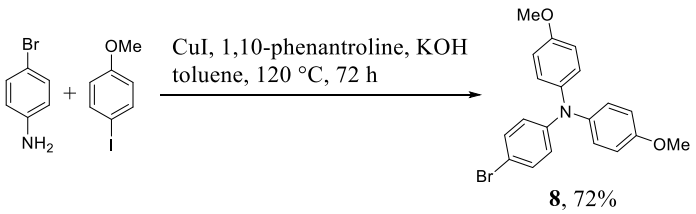

8, 72%

A solution of 4-bromoaniline (5.00 g, 29.1 mmol, 1.00 equiv.), 1-iodo-4-methoxybenzene (15.0 g, 63.9 mmol, 2.20 equiv.), copper(I) iodide (554 mg, 2.91 mmol, 0.100 equiv.), 1,10-phenanthroline (524 mg, 2.91 mmol, 0.100 equiv.), and potassium hydroxide (13.0 g, 233 mmol, 8.00 equiv.) in 150 mL of toluene was fitted with a Dean-Stark trap and reflux condenser. The solution was stirred at 120 °C for 3 days. The solvent was evaporated, and the crude product was purified by flash column chromatography on silica using cHex/EtOAc 20:1 as eluent to yield (4-bromophenyl)-bis(4-methoxyphenyl)amine (8.01 g, 20.9 mmol, 69% yield) as an off-white solid.

R_f = 0.35 (cHex/EtOAc 10:1).

M.p.: 98 °C

^{1}H NMR (400 MHz, Chloroform-d [7.26 ppm], ppm) δ = 7.25–7.21 (m, 2H, CH_{Ar}), 7.05–7.00 (m, 4H, CH_{Ar}), 6.83–6.81 (m, 4H, CH_{Ar}), 6.80–6.78 (m, 2H, CH_{Ar}), 3.80 (s, 6H, OCH_3);

^{13}C NMR (100 MHz, Chloroform-d [77.16 ppm], ppm) δ = 156.0 (C_q, 2C, C_{Ar}), 147.9 (C_q, C_{Ar}), 140.6 (C_q, 2C, C_{Ar}), 131.8 (+, CH, 2C, CH_{Ar}), 126.6 (+, CH, 4C, CH_{Ar}), 122.0 (+, CH, 2C, CH_{Ar}), 114.8 (+, CH, 4C, CH_{Ar}), 112.4 (C_q, C_{Ar}), 55.5 (+, CH_3, 2C, OCH_3);

MS (FAB, 3-NBA), m/z (%): 383/385 (57/57) $[M]^+$, 368/370 (26/26) $[M\text{-}CH_3]^+$, 231 (28), 181 (97), 131 (100). HRMS (FAB, matrix NBA): m/z = calcd for $C_{20}H_{18}{}^{79}BrNO_2$ $[M]^+$: 383.0521; found 383.0520;

IR (ATR, $\tilde{\nu}$) = 3036 (w), 2995 (w), 2952 (w), 2931 (w), 2904 (w), 2832 (w), 1604 (vw), 1585 (w), 1500 (vs), 1483 (vs), 1462 (vs), 1452 (s), 1436 (s), 1402 (w), 1315 (w), 1298 (w), 1283 (s), 1271 (s), 1237 (vs), 1188 (m), 1176 (vs), 1162 (s), 1118 (m), 1101 (s), 1072 (m), 1027 (vs), 1003 (s), 952 (w), 941 (w), 916 (w), 830 (s), 820 (vs), 800 (vs), 778 (s), 728 (m), 710 (w), 696 (s), 635 (w), 601 (w), 572 (vs), 535 (s), 523 (s), 507 (s), 493 (s), 460 (w), 438 (m), 418 (m), 412 (m) cm^{-1}.

Additional information on chemical synthesis is available *via* the Chemotion repository:

https://doi.org/10.14272/reaction/SA-FUHFF-UHFFFADPSC-XXCDCFFPMM-UHFFFADPSC-NUHFF-NUHFF-NUHFF-ZZZ.1

Additional information on the analysis of the target compound is available *via* the Chemotion repository:

https://doi.org/10.14272/XXCDCFFPMMCPEE-UHFFFAOYSA-N.2

4,4,5,5-Tetramethyl-2-(2-thienyl)-1,3,2-dioxaborolane (9)

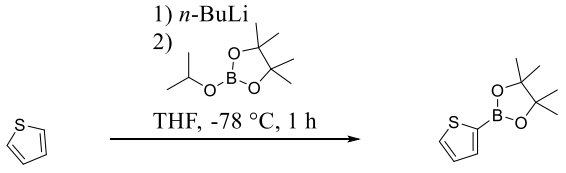

9, 72%

n-Butyllithium solution (419 mg, 2.61 mL, 6.54 mmol, 2.50M in hexane, 1.10 equiv.) was added dropwise to a solution of thiophene (500 mg, 472 µL, 5.94 mmol, 1.00 equiv.) in 15 mL of dry THF at −78 °C. The solution was stirred for 30 min while warming to 20 °C. After cooling to −78 °C again, 2-isopropoxy-4,4,5,5-tetramethyl-1,3,2-dioxaborolane (1.66 g, 1.82 mL, 8.91 mmol, 1.50 equiv.) was added and the reaction mixture was stirred for 30 min while warming to 20 °C. After evaporating the

solvent under reduced pressure, the crude mixture was purified *via* filter column chromatography on silica gel using cHex/EtOAc 4:1 as eluent to yield 4,4,5,5-tetramethyl-2-thiophen-2-yl-1,3,2-dioxaborolane (893 mg, 4.25 mmol, 72% yield) as an off-white solid.

R_f = 0.73 (cHex/EtOAc 4:1).

M.p.: 66 °C

^{1}H NMR (400 MHz, Chloroform-d [7.26 ppm], ppm) δ = 7.67–7.63 (m, 2H), 7.20 (dd, *J* = 4.7 Hz, *J* = 3.4 Hz, 1H), 1.36 (s, 12H, pinacol-CH_3);

^{13}C NMR (100 MHz, Chloroform-d [77.16 ppm], ppm) δ = 137.2 (CH), 132.4 (CH), 128.2 (CH), 84.1 (C_q, 2C, pinacol-C), 24.8 (+, CH_3, 4C, pinacol-CH_3). Missing signal (C_q, 1C, C_{Ar}-B) was not observed due to broadening;

^{11}B NMR (128 MHz, ppm) δ = 28.8 (s, 1B);

MS (EI, 70 eV, 20 °C), m/z (%): 210 (79) $[M]^+$, 195 (57), 124 (94), 111 (100), 110 (43). HRMS (EI): m/z = calcd for $C_{10}H_{15}O_2{}^{11}B^{32}S$ $[M]^+$: 210.0880; found 210.0879;

IR (ATR, $\tilde{\nu}$) = 2997 (w), 2978 (w), 2928 (w), 1519 (vs), 1482 (w), 1468 (w), 1422 (vs), 1360 (vs), 1329 (vs), 1295 (vs), 1266 (s), 1208 (m), 1166 (m), 1135 (vs), 1112 (m), 1078 (m), 1055 (vs), 1017 (vs), 1000 (m), 956 (m), 928 (w), 914 (w), 849 (vs), 826 (m), 778 (m), 754 (w), 722 (vs), 687 (s), 664 (vs), 630 (w), 577 (w), 550 (w), 541 (w), 518 (w), 507 (w), 490 (w), 473 (vw), 455 (vw), 429 (w), 408 (w), 397 (w) cm^{-1}.

Additional information on chemical synthesis is available *via* the Chemotion repository:

https://doi.org/10.14272/reaction/SA-FUHFF-UHFFFADPSC-FFZHICFAHS-UHFFFADPSC-NUHFF-NUHFF-NUHFF-ZZZ.2

Additional information on the analysis of the target compound is available *via* the Chemotion repository:

https://doi.org/10.14272/FFZHICFAHSDFKZ-UHFFFAOYSA-N.3

***N,N*-Bis(4-methoxyphenyl)-4-(2-thienyl)aniline (10)**

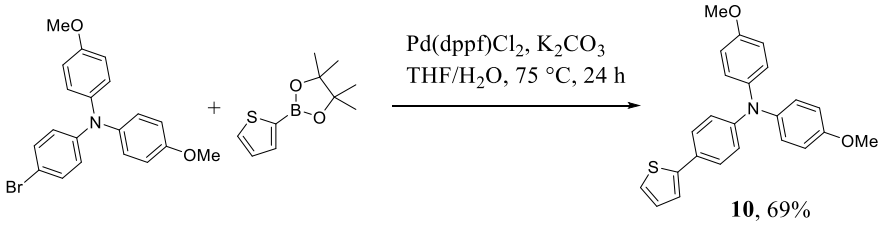

4,4,5,5-Tetramethyl-2-thiophen-2-yl-1,3,2-dioxaborolane (902 mg, 4.29 mmol, 1.10 equiv.), *N*-(4-bromophenyl)-4-methoxy-N-(4-methoxyphenyl)aniline (1.50 g, 3.90 mmol, 1.00 equiv.), Pd(dppf)Cl_2 (286 mg, 390 µmol, 0.100 equiv.), and K_2CO_3 (2.16 g, 15.6 mmol, 4.00 equiv.) were added in 5 mL of water and 20 mL of THF under argon. After purging with argon for 10 min, the mixture was stirred at 75 °C for 24 h. After evaporation of the solvent, the obtained crude product was purified *via* column chromatography on silica using pentane/DCM 2:1 as eluent to yield *N,N*-bis(4-methoxyphenyl)-4-(2-thienyl)aniline (1.04 g, 2.69 mmol, 69% yield) as a yellow solid.

R_f = 0.53 (pentane/DCM 1:1).

M.p.: 115 °C

^{1}H NMR (400 MHz, THF-d_8 [3.58 ppm], ppm) δ = 7.42–7.38 (m, 2H, CH_{Ar}), 7.23 (dd, *J* = 5.1 Hz, *J* = 1.1 Hz, 1H, CH_{Ar}), 7.21 (dd, *J* = 3.6 Hz, *J* = 1.2 Hz, 1H, CH_{Ar}), 7.07–6.96 (m, 5H, CH_{Ar}), 6.89–6.78 (m, 6H, CH_{Ar}), 3.74 (s, 6H, OMe-CH_3);

^{13}C NMR (100 MHz, THF-d_8 [67.57 ppm], ppm) δ = 154.5 (C_q, 2C), 146.4 (C_q), 142.5 (C_q), 138.7 (C_q, 2C), 125.7 (+, CH), 124.7 (C_q), 124.6 (+, CH, 4C), 124.3 (+, CH, 2C), 121.3 (+, CH), 119.6 (+, CH), 118.5 (+, CH, 2C), 112.6 (+, CH, 4C), 52.7 (+, CH_3, 2C, OMe-CH_3);

MS (FAB, 3-NBA), m/z (%): 387 (100) $[M]^+$, 154 (24). HRMS (FAB, matrix NBA): m/z = calcd for $C_{24}H_{21}O_2N^{32}S$ $[M]^+$: 387.1288; found 387.1286;

IR (ATR, $\tilde{\nu}$) = 3106 (w), 3068 (w), 3037 (w), 3004 (w), 2946 (w), 2924 (w), 2901 (w), 2832 (w), 1601 (m), 1534 (w), 1493 (vs), 1456 (s), 1434 (s), 1320 (m), 1296 (s), 1288 (m), 1265 (m), 1235 (vs), 1191 (s), 1180 (vs), 1162 (vs), 1102 (s), 1082 (w), 1033 (vs), 1009 (m), 956 (w), 911 (w), 846 (w), 824 (vs), 813 (vs), 781 (s), 745 (w), 735 (m), 718 (m), 696 (vs), 642 (m), 632 (m), 595 (s), 571 (vs), 527 (vs), 497 (m), 487 (m), 472 (s), 448 (m), 431 (m), 408 (m), 384 (m) cm^{-1}.

Additional information on chemical synthesis is available *via* the Chemotion repository:

https://doi.org/10.14272/reaction/SA-FUHFF-UHFFFADPSC-XYJCIDLTSV-UHFFFADPSC-NUHFF-NUHFF-NUHFF-ZZZ.1

Additional information on the analysis of the target compound is available *via* the Chemotion repository:

https://doi.org/10.14272/XYJCIDLTSVUDLE-UHFFFAOYSA-N.2

4,4,5,5-Tetramethyl-2-(thieno[3,2-b]thiophen-2-yl)-1,3,2-dioxaborolane (**12**)

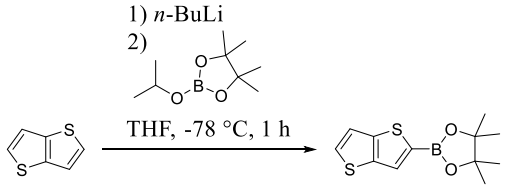

12, 79%

n-Butyllithium solution (251 mg, 1.57 mL, 3.92 mmol, 2.50M in hexane, 1.10 equiv.) was added dropwise to a solution of thieno[3,2-b]thiophene (500 mg, 3.57 mmol, 1.00 equiv.) in 15 mL of dry THF at −78 °C. The solution was stirred for 30 min while warming to 20 °C. After cooling to −78 °C, 2-isopropoxy-4,4,5,5-tetramethyl-1,3,2-dioxaborolane (995 mg, 1.09 mL, 5.35 mmol, 1.50 equiv.) was added and the reaction mixture was stirred for 30 min while warming to 20 °C. After evaporating the solvent under reduced pressure, the crude mixture was purified *via* filter column chromatography on silica using cHex/EtOAc 4:1 to yield 4,4,5,5-tetramethyl-2-(thieno[3,2-b]thiophen-2-yl)-1,3,2-dioxaborolane (750 mg, 2.82 mmol, 79% yield) as an off-white solid

R_f = 0.74 (cHex/EtOAc 4:1).

M.p.: 67 °C

^{1}H NMR (400 MHz, Dichloromethane-d_2 [5.32 ppm], ppm) δ = 7.73 (s, 1H), 7.52 (d, *J* = 5.2 Hz, 1H), 7.29 (d, *J* = 5.2 Hz, 1H), 1.35 (s, 12H, pinacol-CH_3);

^{13}C NMR (100 MHz, Dichloromethane-d_2 [53.84 ppm], ppm) δ = 145.4 (C_q), 140.8 (C_q), 130.2 (+, CH), 128.7 (+, CH), 119.4 (+, CH), 84.3 (C_q, 2C, pinacol-C), 24.6 (+, CH_3, 4C, pinacol-CH_3). Missing signal (C_q, 1C, C_{Ar}-B) was not observed due to broadening;

^{11}B NMR (128 MHz, ppm) δ = 29.1 (s, 1B);

MS (FAB, 3-NBA), m/z (%): 266 (100) $[M]^+$. HRMS (FAB, matrix NBA): m/z = calcd for $C_{12}H_{15}O_2{}^{11}B^{32}S$ $[M]^+$: 266.0601; found 266.0603;

IR (ATR, ṽ) = 3102 (vw), 3085 (vw), 2973 (m), 2929 (w), 2860 (vw), 1504 (vs), 1460 (s), 1380 (s), 1370 (s), 1353 (vs), 1326 (vs), 1289 (s), 1262 (vs), 1214 (m), 1191 (m), 1163 (m), 1136 (vs), 1108 (s), 1017 (vs), 999 (m), 956 (s), 924 (w), 905 (s), 882 (w), 849 (vs), 826 (s), 789 (w), 771 (m), 754 (w), 722

(vs), 684 (s), 662 (vs), 640 (vs), 578 (s), 521 (w), 499 (w), 466 (w), 453 (w), 433 (m), 399 (w), 381 (m) cm^{-1}.

Additional information on chemical synthesis is available *via* the Chemotion repository:

https://doi.org/10.14272/reaction/SA-FUHFF-UHFFFADPSC-ZOGRODFFPR-UHFFFADPSC-NUHFF-NUHFF-NUHFF-ZZZ

Additional information on the analysis of the target compound is available *via* the Chemotion repository:

https://doi.org/10.14272/ZOGRODFFPRPMDQ-UHFFFAOYSA-N.1

4-Methoxy-*N*-(4-methoxyphenyl)-*N*-(4-(thieno[3,2-b]thiophen-2-yl)phenyl)aniline (13)

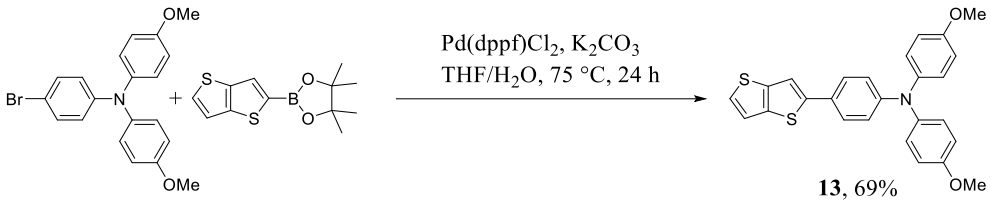

4,4,5,5-Tetramethyl-2-thieno[3,2-b]thiophen-5-yl-1,3,2-dioxaborolane (1.90 g, 7.16 mmol, 1.10 equiv.), *N*-(4-bromophenyl)-4-methoxy-*N*-(4-methoxyphenyl)aniline (2.50 g, 6.51 mmol, 1.00 equiv.), $Pd(dppf)Cl_2$ (476 mg, 651 µmol, 0.100 equiv.), and K_2CO_3 (3.60 g, 26.0 mmol, 4.00 equiv.) were added with 10 mL of water and 40 mL of THF under argon. The solution was purged with argon for 10 min and stirred at 75 °C for 24 h. After evaporating the solvent under reduced pressure, the obtained crude product was purified *via* column chromatography on silica using pentane/DCM 3:1 as an eluent to yield 4-methoxy-*N*-(4-methoxyphenyl)-*N*-(4-(thieno[3,2-b]thiophen-2-yl)phenyl)aniline (1.98 g, 4.47 mmol, 69% yield) as a yellow solid.

R_f = 0.48 (pentane/DCM 1:1).

M.p.: 144 °C

^{1}H NMR (500 MHz, THF-d_8 [3.58 ppm], ppm) δ = 7.46 (d, *J* = 0.7 Hz, 1H, CH_{Ar}), 7.44–7.42 (m, 2H, CH_{Ar}), 7.39 (d, *J* = 5.2 Hz, 1H, CH_{Ar}), 7.24 (dd, *J* = 5.3 Hz, *J* = 0.7 Hz, 1H, CH_{Ar}), 7.07–7.01 (m, 4H, CH_{Ar}), 6.90–6.87 (m, 2H, CH_{Ar}), 6.87–6.83 (m, 4H, CH_{Ar}), 3.75 (s, 6H, OMe-CH_3);

^{13}C NMR (125 MHz, THF-d_8 [67.57 ppm], ppm) δ = 156.5 (C_q, 2C), 148.7 (C_q), 146.4 (C_q), 140.5 (C_q, 2C), 140.2 (C_q), 137.5 (C_q), 126.7 (C_q), 126.6 (+, CH, 4C), 126.0 (+, CH, 3C), 120.1 (+, CH, 2C), 119.3 (+, CH), 114.5 (+, CH, 4C), 113.7 (+, CH), 54.6 (+, CH_3, 2C, OMe-CH_3);

MS (FAB, 3-NBA), m/z (%): 443 (100) $[M]^+$, 306 (29), 305 (88). HRMS (FAB, matrix NBA): m/z = calcd for $C_{26}H_{21}O_2N^{32}S_2$ $[M]^+$: 443.1008; found 443.1009;

IR (ATR, $\tilde{\nu}$) = 3081 (vw), 3071 (vw), 3055 (vw), 3037 (vw), 2973 (w), 2949 (w), 2931 (w), 2904 (w), 2833 (w), 1599 (w), 1500 (vs), 1489 (vs), 1459 (s), 1439 (s), 1388 (w), 1364 (w), 1319 (m), 1285 (m), 1265 (m), 1235 (vs), 1162 (vs), 1102 (m), 1033 (vs), 967 (w), 931 (w), 912 (w), 892 (s), 844 (m), 826 (vs), 781 (m), 766 (s), 749 (m), 722 (m), 696 (s), 653 (w), 633 (w), 606 (w), 574 (vs), 521 (s), 486 (m), 470 (m), 418 (w), 409 (w), 395 (w), 387 (w) cm^{-1}.

Additional information on chemical synthesis is available *via* the Chemotion repository:

https://doi.org/10.14272/reaction/SA-FUHFF-UHFFFADPSC-VGZXOQHDXU-UHFFFADPSC-NUHFF-NUHFF-NUHFF-ZZZ

Additional information on the analysis of the target compound is available *via* the Chemotion repository:

https://doi.org/10.14272/VGZXOQHDXUTYOF-UHFFFAOYSA-N.1

5-Bromothieno[3,2-b]thiophene (14)

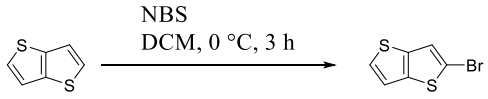

14, 73%
instable

Thieno[3,2-b]thiophene (500 mg, 3.57 mmol, 1.00 equiv.) was dissolved in 12.5 mL of DMF at 0 °C. *N*-Bromosuccinimide (666 mg, 3.74 mmol, 1.05 equiv.) was added portionwise, stirring the reaction mixture for 3 h. 100 mL of water was added, and the mixture was extracted thrice with 20 mL of Et_2O. The organic phase was washed four times with 50 mL water, dried, and concentrated in vacuum. Flash column chromatography on silica gel using pentane as eluent afforded 5-bromothieno[3,2-b]thiophene (569 mg, 2.60 mmol, 73% yield) as a colorless solid.

The product is instable and must be used immediately.

R_f = 0.70 (pentane).

^{1}H NMR (400 MHz, Chloroform-d [7.26 ppm], ppm) δ = 7.40 (d, J = 5.3 Hz, 1H), 7.27 (s, 1H), 7.17 (d, J = 5.5 Hz, 1H).

Bis(4-methoxyphenyl)-[4-(4,4,5,5-tetramethyl-1,3,2-dioxaborolan-2-yl)phenyl]amine (15)

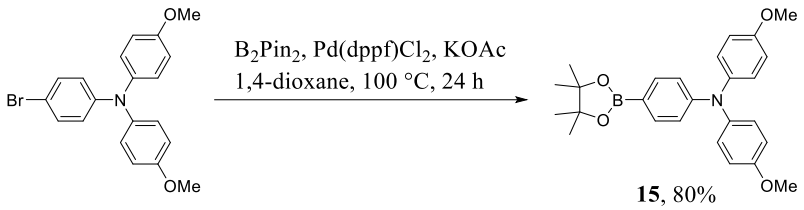

15, 80%

(4-Bromophenyl)-bis(4-methoxyphenyl)amine (1.00 g, 2.60 mmol, 1.00 equiv.), 4,4,5,5-tetramethyl-2-(4,4,5,5-tetramethyl-1,3,2-dioxaborolan-2-yl)-1,3,2-dioxaborolane (991 mg, 3.90 mmol, 1.50 equiv.), potassium acetate (766 mg, 7.81 mmol, 3.00 equiv.) and $Pd(dppf)Cl_2$ (190 mg, 260 µmol, 0.100 equiv.) were dissolved in 15 mL of 1,4-dioxane under argon atmosphere. The reaction mixture was stirred under reflux at 100 °C for 24 h. The mixture was filtered, diluted with 50 mL of EtOAc, and washed with 3 x 100 mL of water. The organic layer was dried over Na_2SO_4, and the solvent evaporated in vacuo. After column chromatography on silica using cHex/EtOAc 10:1 as eluent and evaporation of the solvent, the product was washed with 5 mL of heptane and dried under vacuum to yield bis(4-methoxyphenyl)-[4-(4,4,5,5-tetramethyl-1,3,2-dioxaborolan-2-yl)phenyl]amine (898 mg, 2.08 mmol, 80% yield) as an off-white solid.

R_f = 0.20 (cHex/EtOAc 10:1).

M.p.: 119 °C

^{1}H NMR (400 MHz, Chloroform-d [7.26 ppm], ppm) δ = 7.63–7.59 (m, 2H, CH_{Ar}), 7.09–7.04 (m, 4H, CH_{Ar}), 6.91–6.85 (m, 2H, CH_{Ar}), 6.85–6.81 (m, 4H, CH_{Ar}), 3.80 (s, 6H, OCH_3), 1.33 (s, 12H, pinacol-CH_3);

^{13}C NMR (100 MHz, Chloroform-d [77.16 ppm], ppm) δ = 156.2 (bs, C_q, 2C, C_{Ar}), 151.3 (C_q, C_{Ar}), 140.4 (bs, C_q, 2C, C_{Ar}), 135.8 (+, CH, 2C, CH_{Ar}), 127.1 (+, CH, 4C, CH_{Ar}), 118.6 (+, CH, 2C, CH_{Ar}), 114.7 (+, CH, 4C, CH_{Ar}), 83.4 (C_q, 2C, pinacol-C_q), 55.5 (+, CH_3, 2C, OCH_3), 24.9 (+, CH_3, 4C, pinacol-CH_3). Missing signals: a C_q (1C) signal missing due to coupling with B;

^{11}B NMR (400 MHz, Chloroform-d, ppm) δ = 30.7 (bs, 1B);

MS (FAB, 3-NBA), m/z (%): 431 (100) $[M]^+$, 430 (25). HRMS (FAB, matrix NBA): m/z = calcd for $C_{26}H_{30}O_4N^{11}B$ $[M]^+$: 431.2262; found 431.2264;

IR (ATR, ṽ) = 3055 (vw), 2997 (w), 2979 (w), 2969 (w), 2959 (w), 2932 (w), 2910 (w), 2836 (w), 1611 (m), 1596 (s), 1557 (vw), 1503 (vs), 1462 (m), 1439 (w), 1421 (w), 1395 (m), 1360 (vs), 1327 (vs), 1316 (vs), 1285 (vs), 1242 (vs), 1232 (vs), 1197 (s), 1179 (m), 1166 (s), 1142 (vs), 1106 (s), 1092 (vs), 1031 (vs), 1011 (m), 960 (m), 916 (w), 860 (s), 841 (m), 830 (vs), 816 (s), 798 (w), 779 (m), 734 (m),

717 (w), 684 (w), 676 (w), 657 (vs), 646 (m), 595 (m), 578 (vs), 547 (s), 531 (m), 524 (m), 476 (w), 446 (w), 433 (w), 402 (w), 398 (w), 387 (w), 375 (w) cm^{-1}.

Additional information on chemical synthesis is available *via* the Chemotion repository:

https://doi.org/10.14272/reaction/SA-FUHFF-UHFFFADPSC-MARLZALFJN-UHFFFADPSC-NUHFF-NUHFF-NUHFF-ZZZ.1

Additional information on the analysis of the target compound is available *via* the Chemotion repository:

https://doi.org/10.14272/MARLZALFJNQDEJ-UHFFFAOYSA-N.2

4-Methoxy-*N*-(4-methoxyphenyl)-*N*-(4-(5-(4,4,5,5-tetramethyl-1,3,2-dioxaborolan-2-yl)thieno[3,2-b]thiophen-2-yl)phenyl)aniline (16)

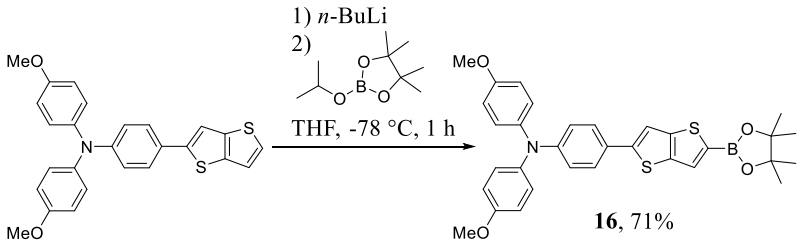

n-Butyllithium solution (15.9 mg, 99.2 µL, 248 µmol, 2.50M in hexane, 1.10 equiv.) was added dropwise to a solution of 4-methoxy-*N*-(4-methoxyphenyl)-*N*-(4-(thieno[3,2-b]thiophen-2-yl)phenyl)aniline (100 mg, 225 µmol, 1.00 equiv.) in 4 mL of dry THF at −78 °C. The solution was stirred for 30 min at room temperature. After cooling to −78 °C, 2-isopropoxy-4,4,5,5-tetramethyl-1,3,2-dioxaborolane (83.9 mg, 92.0 µL, 451 µmol, 2.00 equiv) was added and the reaction mixture was stirred for 60 min at room temperature. After evaporating the solvent under reduced pressure, the crude mixture was purified *via* filter column chromatography on silica using cHex/EtOAc 20:1 to 5:1 as eluent to yield 4-methoxy-*N*-(4-methoxyphenyl)-*N*-(4-(5-(4,4,5,5-tetramethyl-1,3,2-dioxaborolan-2-yl)thieno[3,2-b]thiophen-2-yl)phenyl)aniline (91.6 mg, 161 µmol, 71% yield) as yellow solid.

R_f = 0.40 (cHex/EtOAc 10:1).

M.p.: 102 °C

^{1}H NMR (400 MHz, Dichloromethane-d_2 [5.32 ppm], ppm) δ = 7.67 (d, *J* = 0.7 Hz, 1H), 7.44 (d, *J* = 8.8 Hz, 2H), 7.38 (d, *J* = 0.7 Hz, 1H), 7.09–7.07 (m, 4H), 6.91–6.88 (m, 2H), 6.87–6.84 (m, 4H), 3.79 (s, 6H, OMe-CH_3), 1.35 (s, 12H, pinacol-CH_3);

^{13}C NMR (100 MHz, Dichloromethane-d_2 [53.84 ppm], ppm) δ = 156.4 (C_q, 2C), 149.4 (C_q), 149.0 (C_q), 146.3 (C_q), 140.3 (C_q, 2C), 138.8 (C_q), 129.0 (+, CH), 127.0 (+, CH, 4C), 126.4 (+, CH, 2C), 126.1 (C_q), 119.8 (+, CH, 2C), 114.7 (+, CH, 4C), 113.6 (+, CH), 84.3 (C_q, 2C, pinacol-C_q), 55.4 (+, CH_3, 2C, OMe-CH_3), 24.6 (+, CH_3, 4C, pinacol-CH_3). Missing signal (C_q, 1C, C_q-B) not observed due to broadening;

^{11}B NMR (128 MHz, ppm) δ = 29.9 (1B);

MS (ESI), m/z (%): 568/569 (9/50), 282 (31), 280 (100), 221 (26). HRMS (ESI): m/z = calcd for $C_{32}H_{32}{}^{11}BNO_4S_2$ $[M]^+$: 569.1866; found 569.1861;

IR (ATR, ṽ) = 2973 (vw), 2924 (w), 2830 (vw), 1601 (w), 1497 (vs), 1462 (w), 1441 (w), 1417 (w), 1387 (w), 1364 (vs), 1320 (s), 1281 (m), 1264 (s), 1238 (vs), 1194 (w), 1177 (m), 1166 (m), 1137 (vs), 1105 (m), 1031 (s), 966 (w), 952 (w), 881 (vw), 850 (w), 826 (s), 812 (m), 781 (w), 721 (w), 701 (w), 684 (w), 663 (m), 630 (w), 591 (w), 577 (m), 562 (w), 518 (w), 484 (w), 446 (vw), 402 (vw) cm^{-1}.

Additional information on chemical synthesis is available *via* the Chemotion repository:

https://doi.org/10.14272/reaction/SA-FUHFF-UHFFFADPSC-CYZUSUQDZX-UHFFFADPSC-NUHFF-NUHFF-NUHFF-ZZZ

Additional information on the analysis of the target compound is available *via* the Chemotion repository:

https://doi.org/10.14272/CYZUSUQDZXLTMI-UHFFFAOYSA-N.1

4,16-(Bis(thieno[3,2-b]thiophene-5,2-diyl-*N*,*N*-bis(4-methoxyphenyl)aniline)[2.2]paracyclophane (17)

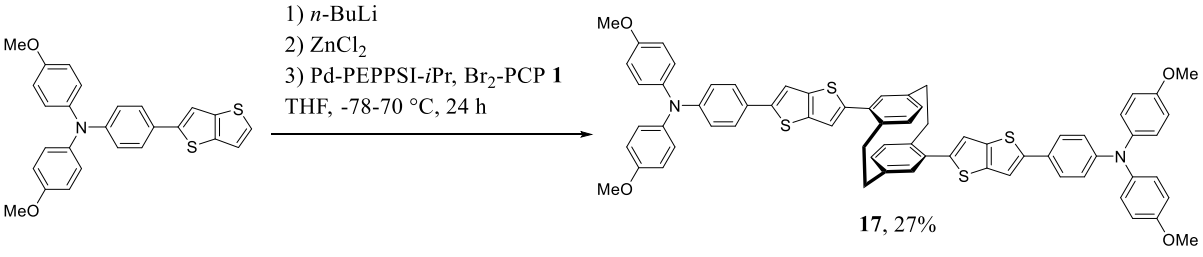

Preparation of Negishi reactant:

4-Methoxy-*N*-(4-methoxyphenyl)-*N*-(4-(thieno[3,2-b]thiophen-2-yl)phenyl)aniline (127 mg, 287 µmol, 2.10 equiv.) was added to a crimp cap vial and flushed with Ar three times. 5 mL of dry THF was added, and the mixture was cooled to -78 °C. *n*-Butyllithium solution (22.7 mg, 142 µL, 355 µmol, 2.50M in hexane, 2.60 equiv.) was added dropwise, and the reaction mixture was allowed to warm to 22 °C. After stirring for 30 min, the reaction mixture was cooled to 0 °C, and a zinc chloride solution

(55.8 mg, 410 µL, 410 µmol, 1.00M in THF, 3.00 equiv.) was added. The reaction was stirred for 15 min at 0 °C and then warmed to 22 °C.

Negishi coupling:

4,16-Dibromo[2.2]paracyclophane (50.0 mg, 137 µmol, 1.00 equiv.) and PEPPSI-IPr catalyst (9.31 mg, 13.7 µmol, 0.100 equiv.) were added to a crimp cap vial and flushed with Ar three times. 5 mL of dry THF and zinc chloride solution (55.8 mg, 410 µL, 410 µmol, 1.00M in THF, 3.00 equiv.) were added. After dissolving, the Negishi reactant was added *via* syringe, and the reaction mixture was heated to 70 °C. After three days, the reaction was allowed to cool to 22 °C, and the solvent was removed under reduced pressure. Column chromatography on silica using cHex/DCM 1:0 to 1:2 as eluent to yield 4,16-(bis(thieno[3,2-b]thiophene-5,2-diyl-*N,N*-bis(4-methoxyphenyl)aniline)[2.2]paracyclophane (40.7 mg, 37.3 µmol, 27% yield) as a yellow solid.

Due to the low solubility of the target molecule, no ^{13}C or 2D NMR could be recorded.

R_f = 0.35 (cHex/DCM 2:1).

M.p.: 301 °C

^1H NMR (400 MHz, Dichloromethane-d_2 [5.32 ppm], ppm) δ = 7.49–7.24 (m, 8H), 7.16–7.03 (m, 8H), 6.93–6.79 (m, 14H), 6.72–6.62 (m, 4H), 3.83–3.75 (m, 14H, OMe-CH_3 + PCP-CH_2), 3.11–2.98 (m, 2H, PCP-CH_2), 2.97–2.72 (m, 4H, PCP-CH_2);

MS (ESI), m/z (%): 1090 (1) $[M]^+$, 545 (34), 282 (63), 279 (27), 221 (94), 145 (72), 122 (29), 105 (34), 102 (41), 100 (100). HRMS (ESI): m/z = calcd for $C_{68}H_{54}N_2O_4S_4$ $[M]^+$: 1090.2967; found 1090.2919;

IR (ATR, $\tilde{\nu}$) = 3075 (w), 3034 (w), 3003 (w), 2962 (w), 2928 (w), 2897 (w), 2854 (w), 2830 (w), 1602 (w), 1587 (w), 1524 (w), 1500 (vs), 1477 (s), 1460 (s), 1436 (m), 1402 (w), 1320 (w), 1300 (w), 1281 (m), 1266 (m), 1239 (vs), 1193 (m), 1177 (m), 1108 (m), 1033 (s), 999 (w), 963 (w), 955 (w), 941 (w), 911 (w), 874 (w), 830 (s), 817 (vs), 783 (w), 731 (w), 720 (m), 701 (m), 670 (w), 660 (w), 637 (w), 632 (w), 616 (w), 592 (w), 575 (s), 554 (w), 526 (m), 510 (m), 487 (m), 470 (w), 463 (w), 453 (w), 439 (w), 424 (w), 405 (m), 391 (w) cm^{-1}.

Additional information on chemical synthesis is available *via* the Chemotion repository:

https://doi.org/10.14272/reaction/SA-FUHFF-UHFFFADPSC-NEAOJNOLOV-UHFFFADPSC-NUHFF-NUHFF-NUHFF-ZZZ.1

Additional information on the analysis of the target compound is available *via* the Chemotion repository:

https://doi.org/10.14272/NEAOJNOLOVRNDM-UHFFFAOYSA-N.2

4,15-(Bis(thieno[3,2-b]thiophene-5,2-diyl-*N*,*N*-bis(4-methoxyphenyl)aniline)[2.2]paracyclophane (18)

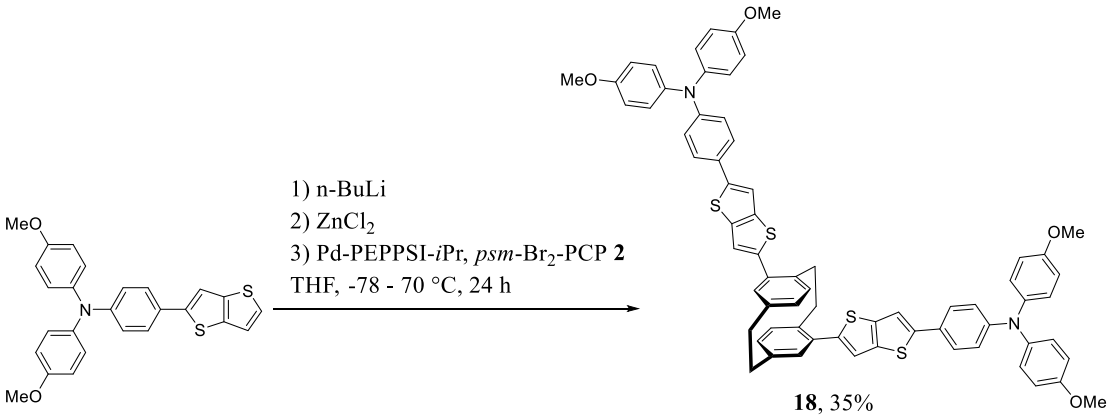

Preparation of Negishi reactant:

4-Methoxy-*N*-(4-methoxyphenyl)-*N*-(4-(thieno[3,2-b]thiophen-2-yl)phenyl)aniline (133 mg, 300 µmol, 2.20 equiv.) was added to a crimp cap vial and flushed with Ar three times. 5 mL of dry THF was added, and the mixture was cooled to -78 °C. *n*-Butyllithium solution (22.7 mg, 142 µL, 355 µmol, 2.50M in hexane, 2.60 equiv.) was added dropwise, and the reaction mixture was allowed to warm to 22 °C. After stirring for 30 min, the reaction mixture was cooled to 0 °C, and a zinc chloride solution (55.8 mg, 410 µL, 410 µmol, 1.00M in THF, 3.00 equiv.) was added. The reaction was stirred for 15 min at 0 °C and then warmed to 22 °C.

Negishi coupling:

4,15-Dibromo[2.2]paracyclophane (50.0 mg, 137 µmol, 1.00 equiv.) and PEPPSI-IPr catalyst (9.31 mg, 13.7 µmol, 0.100 equiv.) were added to a crimp cap vial and flushed with Ar three times. 5 mL of dry THF was added, and zinc chloride solution (55.8 mg, 410 µL, 410 µmol, 1.00M in THF, 3.00 equiv.) was added. After dissolving, the Negishi reactant was added *via* syringe, and the reaction mixture was heated to 70 °C. After three days, the reaction was allowed to cool to 22 °C, and the solvent was removed under reduced pressure. Column chromatography on silica using cHex/DCM 1:0- to 1:2 as eluent was performed to yield 4,15-(bis(thieno[3,2-b]thiophene-5,2-diyl-*N,N*-bis(4-methoxyphenyl)aniline)[2.2]paracyclophane (51.5 mg, 47.2 µmol, 35% yield) as a yellow solid.

R_f = 0.35 (cHex/DCM 2:1).

M.p.: 157 °C

^{1}H NMR (400 MHz, Dichloromethane-d_2 [5.32 ppm], ppm) δ = 7.49–7.45 (m, 4H), 7.42 (s, 2H), 7.29 (d, *J* = 0.6 Hz, 2H), 7.12–7.07 (m, 8H), 6.97–6.89 (m, 6H), 6.89–6.85 (m, 8H), 6.73 (d, *J* = 1.9 Hz, 2H), 6.66–6.57 (m, 2H), 3.79 (s, 12H, OMe-CH_3), 3.68–3.61 (m, 2H, PCP-CH_2), 3.23–3.16 (m, 2H, PCP-CH_2), 3.10–3.03 (m, 2H, PCP-CH_2), 2.79–2.68 (m, 2H, PCP-CH_2);

^{13}C NMR (100 MHz, Dichloromethane-d_2 [53.84 ppm], ppm) δ = 156.3 (C_q, 4C), 148.7 (C_q, 2C), 146.0 (C_q, 2C), 144.9 (C_q, 2C), 140.4 (C_q, 4C), 140.3 (C_q, 2C), 140.1 (C_q, 2C), 138.0 (C_q, 2C), 137.6 (C_q, 2C), 135.7 (C_q, 2C), 132.7 (+, CH, 2C), 132.7 (+, CH, 2C), 131.6 (+, CH, 2C), 126.9 (+, CH, 8C), 126.4 (C_q, 4C), 126.3 (+, CH, 2C), 120.0 (+, CH, 4C), 118.2 (+, CH, 2C), 114.7 (+, CH, 8C), 113.8 (+, CH, 2C), 55.4 (+, CH_3, 4C, OMe-CH_3), 34.8 (–, CH_2, 2C, PCP-CH_2), 33.8 (–, CH_2, 2C, PCP-CH_2);

MS (ESI), m/z (%): 1090 (5) $[M]^+$, 546 (71), 545 (100). HRMS (ESI): m/z = calcd for $C_{68}H_{54}N_2O_4S_4$ $[M]^+$: 1090.2967; found 1090.2964;

IR (ATR, $\tilde{\nu}$) = 3034 (w), 2993 (w), 2924 (w), 2902 (w), 2850 (w), 2830 (w), 1599 (m), 1500 (vs), 1483 (vs), 1462 (s), 1438 (s), 1402 (w), 1317 (m), 1282 (m), 1235 (vs), 1193 (s), 1174 (s), 1164 (s), 1103 (m), 1031 (vs), 967 (w), 950 (w), 909 (w), 875 (w), 822 (vs), 807 (vs), 779 (s), 721 (s), 701 (m), 653 (m), 640 (w), 630 (m), 611 (w), 589 (m), 575 (s), 520 (s), 479 (s), 432 (m), 425 (m), 407 (m), 397 (m), 384 (w) cm^{-1}.

Additional information on chemical synthesis is available *via* the Chemotion repository:

https://doi.org/10.14272/reaction/SA-FUHFF-UHFFFADPSC-OCUZMRQSGF-UHFFFADPSC-NUHFF-NUHFF-NUHFF-ZZZ

Additional information on the analysis of the target compound is available *via* the Chemotion repository:

https://doi.org/10.14272/OCUZMRQSGFRVGU-UHFFFAOYSA-N.1

4,12-(Bis(thieno[3,2-b]thiophene-5,2-diyl-*N*,*N*-bis(4-methoxyphenyl)aniline)[2.2]paracyclophane (19)

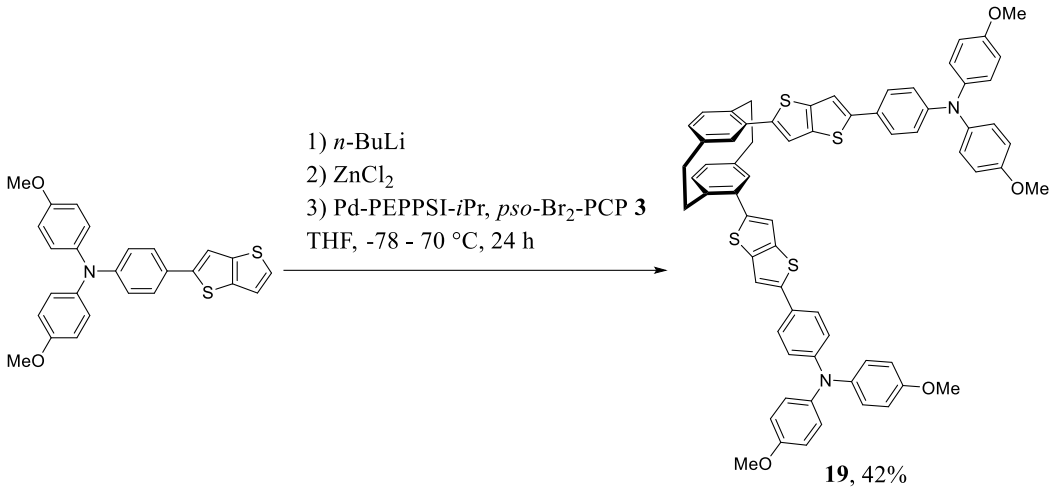

Preparation of Negishi reactant:

4-Methoxy-*N*-(4-methoxyphenyl)-*N*-(4-(thieno[3,2-b]thiophen-2-yl)phenyl)aniline (133 mg, 300 µmol, 2.20 equiv.) was added to a crimp cap vial and flushed with Ar three times. 5 mL of dry THF was added, and the mixture was cooled to -78 °C. *n*-Butyllithium solution (22.7 mg, 142 µL, 355 µmol, 2.50M in hexane, 2.60 equiv.) was added dropwise, and the reaction mixture was allowed to warm to 22 °C. After stirring for 30 min, the reaction mixture was cooled to 0 °C, and a zinc chloride solution (55.8 mg, 410 µL, 410 µmol, 1.00M in THF, 3.00 equiv.) was added. The reaction was stirred for 15 min at 0 °C and then warmed to 22 °C.

Negishi coupling:

5,11-Dibromo[2.2]paracyclophane (50.0 mg, 137 µmol, 1.00 equiv.) and PEPPSI-IPr catalyst (9.31 mg, 13.7 µmol, 0.100 equiv.) were added to a crimp cap vial and flushed with Ar three times. 5 mL of dry THF and zinc chloride solution (55.8 mg, 410 µL, 410 µmol, 1.00M in THF, 3.00 equiv.) were added. After dissolving, the Negishi reactant was added *via* syringe, and the reaction mixture was heated to 70 °C. After three days, the reaction was allowed to cool to 22 °C, and the solvent was removed under reduced pressure. Column chromatography on silica using cHex/DCM 1:0 to 1:2 as eluent was performed to yield 4,12-(bis(thieno[3,2-b]thiophene-5,2-diyl-*N,N*-bis(4-methoxyphenyl)aniline)[2.2]paracyclophane (63.5 mg, 58.2 µmol, 43% yield) as a yellow solid.

R_f = 0.35 (cHex/DCM 2:1).

M.p.: 166 °C

^{1}H NMR (400 MHz, Chloroform-d [7.26 ppm], ppm) δ = 7.48–7.44 (m, 4H), 7.40 (s, 2H), 7.26 (d, *J* = 3.7 Hz, 2H), 7.13–7.08 (m, 8H), 6.97–6.92 (m, 4H), 6.90–6.83 (m, 10H), 6.70 (d, *J* = 7.8 Hz, 2H), 6.64–6.61 (m, 2H), 3.94–3.87 (m, 2H, PCP-CH_2), 3.81 (s, 12H, OMe-CH_3), 3.16–3.09 (m, 2H, PCP-CH_2), 2.98–2.83 (m, 4H, PCP-CH_2);

^{13}C NMR (100 MHz, Chloroform-d [77.16 ppm], ppm) δ = 156.1 (C_q, 4C), 148.5 (C_q, 2C), 146.0 (C_q, 2C), 144.3 (C_q, 2C), 140.6 (C_q, 4C), 140.1 (C_q, 2C), 140.0 (C_q, 2C), 138.0 (C_q, 2C), 137.0 (C_q, 2C), 136.0 (+, CH, 2C), 134.5 (C_q, 2C), 132.2 (+, CH, 2C), 130.4 (+, CH, 2C), 126.8 (+, CH, 8C), 126.6 (C_q, 2C), 126.5 (+, CH, 4C), 120.4 (+, CH, 4C), 118.0 (+, CH, 2C), 114.8 (+, CH, 8C), 114.0 (+, CH, 2C), 55.5 (+, CH_3, 4C), 35.5 (–, CH_2, 2C), 33.9 (–, CH_2, 2C);

MS (ESI), m/z (%): 1090 (18) $[M]^+$, 746 (35), 681 (46), 546 (75), 545 (100), 123 (32). HRMS (ESI): m/z = calcd for $C_{68}H_{54}N_2O_4S_4$ $[M]^+$: 1090.2964; found 1090.2958;

IR (ATR, $\tilde{\nu}$) = 3037 (w), 2922 (m), 2849 (w), 2833 (w), 2795 (w), 1599 (w), 1524 (w), 1502 (vs), 1485 (s), 1460 (s), 1451 (m), 1439 (m), 1401 (w), 1317 (m), 1283 (m), 1266 (m), 1237 (vs), 1193 (m), 1176 (s), 1166 (s), 1103 (m), 1033 (s), 967 (w), 952 (w), 905 (w), 875 (w), 823 (vs), 781 (m), 721 (m), 701 (w), 684 (w), 671 (w), 650 (w), 630 (w), 591 (m), 577 (s), 523 (m), 510 (m), 489 (w), 459 (w), 448 (w), 425 (w), 409 (w), 388 (w) cm^{-1}.

Additional information on chemical synthesis is available *via* the Chemotion repository:

https://doi.org/10.14272/reaction/SA-FUHFF-UHFFFADPSC-NEAOJNOLOV-UHFFFADPSC-NUHFF-NUHFF-NUHFF-ZZZ

Additional information on the analysis of the target compound is available *via* the Chemotion repository:

https://doi.org/10.14272/NEAOJNOLOVRNDM-UHFFFAOYSA-N.1

2,8-Dibromodibenzothiophene (**20**)

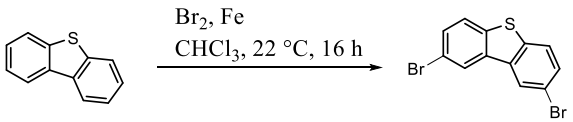

20, 98%

Dibenzothiophene (3.00 g, 16.3 mmol, 1.00 equiv.) was dissolved in 200 mL of chloroform, and iron shavings (45.5 mg, 814 µmol, 0.0500 equiv.) were added. Bromine (5.46 g, 1.75 mL, 34.2 mmol, 2.10 equiv.) was added dropwise at 23 °C, and the mixture was stirred for 16 h. Upon completion, the reaction mixture was quenched with 200 mL of saturated $NaSO_{3(aq.)}$, washed with 3 x 200 mL of $K_2CO_{3(aq.)}$, and the collected aqueous phases were extracted with 100 mL of chloroform. After

evaporating the solvent of the combined organic phases, the crude product was purified by column chromatography on silica by using pentane as the eluent to give 2,8-dibromodibenzothiophene (5.48 g, 16.0 mmol, 98% yield) as a colorless solid.

R_f = 0.48 (pentane).

M.p.: 213 °C

^{1}H NMR (400 MHz, Chloroform-d [7.26 ppm], ppm) δ = 8.22 (d, *J* = 1.9 Hz, 2H), 7.70 (d, *J* = 8.4 Hz, 2H), 7.57 (dd, *J* = 8.5 Hz, *J* = 1.9 Hz, 2H);

^{13}C NMR (100 MHz, Chloroform-d [77.16 ppm], ppm) δ = 138.6 (C_q, 2C), 136.2 (C_q, 2C), 130.3 (+, CH, 2C), 124.7 (+, CH, 2C), 124.2 (+, CH, 2C), 118.6 (C_q, 2C);

MS (ESI), m/z (%): 340/342/344 (1/2/1) $[M]^+$, 223 (37), 221 (49), 194 (29). HRMS (ESI): m/z = calcd for $C_{12}H_6{}^{32}S^{79}Br^{81}Br$ $[M]^+$: 341.8536; found 341.8530;

IR (ATR, ṽ) = 1877 (w), 1737 (w), 1598 (w), 1574 (w), 1541 (w), 1459 (w), 1445 (w), 1411 (s), 1381 (w), 1282 (w), 1167 (w), 1146 (w), 1075 (m), 1060 (m), 1014 (m), 938 (w), 858 (s), 834 (m), 799 (vs), 727 (w), 630 (w), 567 (w), 537 (w), 516 (vs), 446 (w), 415 (s) cm^{-1}.

Additional information on chemical synthesis is available *via* the Chemotion repository:

https://doi.org/10.14272/reaction/SA-FUHFF-UHFFFADPSC-WNEXSUAHKV-UHFFFADPSC-NUHFF-NUHFF-NUHFF-ZZZ.1

Additional information on the analysis of the target compound is available *via* the Chemotion repository:

https://doi.org/10.14272/WNEXSUAHKVAPFK-UHFFFAOYSA-N.2

4-(8-bromodibenzothiophen-2-yl)-*N,N*-bis(4-methoxyphenyl)aniline (21)

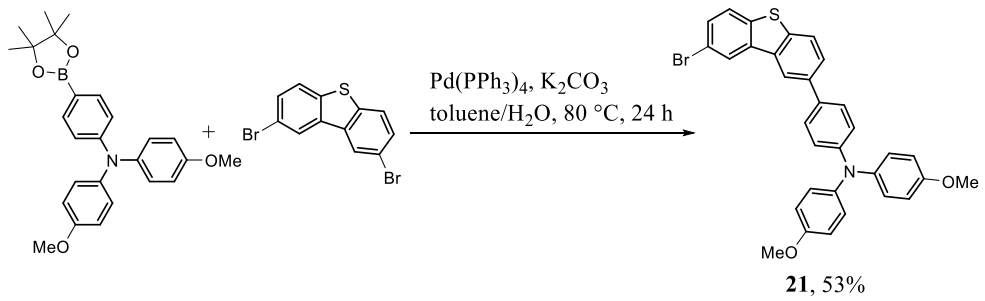

21, 53%

2,8-Dibromodibenzothiophene (100 mg, 292 µmol, 1.00 equiv.), *N,N*-bis(4-methoxyphenyl)-4-(4,4,5,5-tetramethyl-1,3,2-dioxaborolan-2-yl)aniline (126 mg, 292 µmol, 1.00 equiv.),

tetrakis(triphenylphosphine)palladium(0) (33.8 mg, 29.2 µmol, 0.100 equiv.), and dipotassium carbonate (162 mg, 1.17 mmol, 4.00 equiv.) were added together with 0.1 mL of water and 1 mL of toluene in a flask under argon. The mixture was purged with argon for 10 min. The mixture was stirred at 80 °C for 24 h. After washing with 25 mL water, extracting with 10 mL of DCM and drying over Na_2SO_4, the obtained crude product was purified *via* chromatography on silica gel using pentane/DCM 3:1 to 1:1 to yield 4-(8-bromodibenzothiophen-2-yl)-*N,N*-bis(4-methoxyphenyl)aniline (89.9 mg, 154 µmol, 53% yield) as a yellow solid.

R_f = 0.66 (pentane/DCM 1:2).

M.p.: 164 °C

^{1}H NMR (400 MHz, Chloroform-d [7.26 ppm], ppm) δ = 8.31–8.28 (m, 1H), 8.25–8.24 (m, 1H), 7.90–7.83 (m, 1H), 7.74–7.59 (m, 2H), 7.58–7.44 (m, 3H), 7.14–7.10 (m, 4H), 7.07–7.03 (m, 2H), 6.89–6.85 (m, 4H), 3.82 (s, 6H);

^{13}C NMR (100 MHz, Chloroform-d [77.16 ppm], ppm) δ = 156.0 (C_q, 2C), 148.3 (C_q), 140.9 (C_q, 2C), 138.6 (C_q), 138.2 (C_q), 138.0 (C_q), 137.4 (C_q), 135.0 (C_q), 132.6 (C_q), 129.6 (+, CH), 127.8 (+, CH, 2C), 126.7 (+, CH, 4C), 126.4 (+, CH), 124.6 (+, CH), 124.2 (+, CH), 123.0 (+, CH), 120.8 (+, CH, 2C), 119.4 (+, CH), 118.4 (C_q), 114.8 (+, CH, 4C), 55.5 (+, CH_3, 2C);

MS (ESI), m/z (%): 565/567 (66/69), 536 (12), 488 (35), 487 (100), 381 (67), 305 (28). HRMS (ESI): m/z = calcd for $C_{32}H_{24}{}^{79}BrNO_2S$ $[M]^+$: 565.0711; found 565.0699;

IR (ATR, ṽ) = 3036 (vw), 2997 (vw), 2949 (w), 2925 (w), 2868 (vw), 2849 (w), 2833 (w), 1601 (w), 1502 (vs), 1462 (vs), 1439 (m), 1392 (w), 1358 (vw), 1319 (m), 1278 (m), 1259 (m), 1237 (vs), 1194 (m), 1179 (m), 1166 (m), 1147 (w), 1105 (w), 1082 (w), 1072 (w), 1034 (s), 1007 (w), 960 (vw), 952 (vw), 907 (m), 884 (w), 868 (w), 850 (w), 827 (s), 809 (s), 781 (w), 764 (w), 730 (vs), 640 (w), 608 (w), 577 (m), 544 (w), 524 (w), 492 (vw), 482 (vw), 452 (vw), 435 (vw), 419 (w), 385 (vw) cm^{-1}.

Additional information on chemical synthesis is available *via* the Chemotion repository:

https://doi.org/10.14272/reaction/SA-FUHFF-UHFFFADPSC-NBMBLWBOEU-UHFFFADPSC-NUHFF-NUHFF-NUHFF-ZZZ

Additional information on the analysis of the target compound is available *via* the Chemotion repository:

https://doi.org/10.14272/NBMBLWBOEUGTIB-UHFFFAOYSA-N.1

3-Bromo-9*H*-carbazole (23)

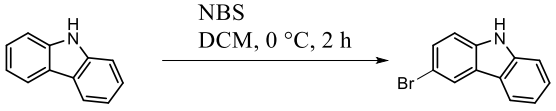

23, 90%

A round-bottom flask was charged with 9*H*-carbazole (4.50 g, 26.9 mmol, 1.00 equiv.), *N*-bromosuccinimide (5.27 g, 29.6 mmol, 1.10 equiv.) and 100 mL of DCM. The mixture was stirred at 22 °C for 4 h. The mixture was diluted with 100 mL water, and the aqueous layer was extracted with 3 x 50 mL of DCM. The combined organic phases were dried over Na_2SO_4 and concentrated under vacuum. The residue was purified by column chromatography on silica using hexane as eluent to obtain 3-bromo-9*H*-carbazole (5.95 g, 24.2 mmol, 90% yield) as a colorless solid.

R_f = 0.38 (pentane/DCM 10:1).

M.p.: 198 °C

^{1}H NMR (400 MHz, Chloroform-d [7.26 ppm], ppm) δ = 8.19 (d, *J* = 1.9 Hz, 1H), 8.07 (bs, 1H, NH), 8.03 (dt, *J* = 7.8 Hz, *J* = 0.9 Hz, 1H), 7.50 (dd, *J* = 8.6 Hz, *J* = 2.0 Hz, 1H), 7.45–7.42 (m, 2H), 7.31 (d, *J* = 8.5 Hz, 1H), 7.27–7.23 (m, 1H);

^{13}C NMR (100 MHz, Chloroform-d [77.16 ppm], ppm) δ = 139.8 (C_q), 138.1 (C_q), 128.5 (+, CH), 126.6 (+, CH), 125.2 (C_q), 123.1 (+, CH), 122.4 (C_q), 120.5 (+, CH), 119.9 (+, CH), 112.2 (C_q), 112.0 (+, CH), 110.8 (+, CH);

MS (ESI), m/z (%): 246/248 (100/97) $[M+H]^+$, 221 (38). HRMS (ESI): m/z = calcd for $C_{12}H_8{}^{79}BrN$ $[M]^+$: 244.9840; found 244.9834;

IR (ATR, $\tilde{\nu}$) = 3401 (vs), 3055 (w), 1928 (w), 1894 (w), 1883 (w), 1861 (w), 1820 (w), 1810 (w), 1776 (w), 1752 (w), 1731 (w), 1713 (w), 1694 (w), 1683 (w), 1662 (w), 1621 (w), 1598 (w), 1572 (w), 1564 (w), 1538 (w), 1466 (m), 1442 (s), 1436 (vs), 1397 (w), 1380 (w), 1330 (m), 1313 (w), 1288 (w), 1269 (m), 1237 (m), 1220 (m), 1200 (m), 1176 (w), 1142 (w), 1133 (w), 1108 (w), 1054 (m), 1017 (w), 1003 (w), 926 (m), 878 (s), 853 (w), 843 (w), 809 (vs), 766 (w), 755 (m), 744 (vs), 722 (vs), 677 (m), 582 (m), 568 (vs), 465 (s), 446 (vs), 428 (vs), 416 (vs) cm^{-1}.

Additional information on chemical synthesis is available *via* the Chemotion repository:

https://doi.org/10.14272/reaction/SA-FUHFF-UHFFFADPSC-LTBWKAYPXI-UHFFFADPSC-NUHFF-NUHFF-NUHFF-ZZZ

Additional information on the analysis of the target compound is available *via* the Chemotion repository:

https://doi.org/10.14272/LTBWKAYPXIIVPC-UHFFFAOYSA-N.1

3,6-Dibromo-9*H*-carbazole (**24**)

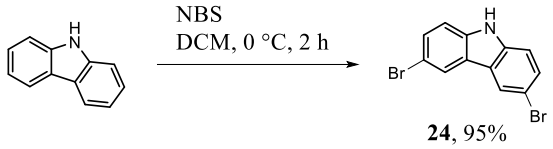

24, 95%

A round-bottom flask was charged with 9*H*-carbazole (3.00 g, 17.9 mmol, 1.00 equiv.), *N*-bromosuccinimide (6.71 g, 37.7 mmol, 2.10 equiv.) and 65 mL of DCM. The mixture was stirred at 22 °C for 4 h. The mixture was diluted with 60 mL water, and the aqueous layer was extracted with 3 x 30 mL DCM. The combined organic phases were dried over Na_2SO_4 and concentrated under vacuum. The residue was purified by column chromatography on silica using hexane as eluent to obtain 3,6-dibromo-9*H*-carbazole (5.53 g, 17.0 mmol, 95% yield) as a colorless solid.

R_f = 0.38 (pentane/DCM 10:1).

M.p.: 205 °C

^{1}H NMR (400 MHz, Chloroform-d [7.26 ppm], ppm) δ = 8.13 (d, *J* = 1.9 Hz, 2H), 8.11 (br.s, 1H, NH), 7.51 (dd, *J* = 8.6 Hz, *J* = 1.9 Hz, 2H), 7.31 (d, *J* = 8.5 Hz, 2H);

^{13}C NMR (100 MHz, Chloroform-d [77.16 ppm], ppm) δ = 138.4 (C_q, 2C), 129.3 (+, CH, 2C), 124.1 (C_q, 2C), 123.3 (+, CH, 2C), 112.7 (C_q, 2C), 112.2 (+, CH, 2C);

MS (ESI), m/z (%): 323/325/327 (12/24/11) $[M]^+$, 282 (38), 274 (100), 257 (29). HRMS (ESI): m/z = calcd for $C_{12}H_7{}^{79}Br^{81}BrN$ $[M]^+$: 324.8925; found 324.8908;

IR (ATR, $\tilde{\nu}$) = 3420 (m), 1868 (w), 1841 (w), 1823 (w), 1807 (w), 1782 (w), 1766 (w), 1734 (w), 1713 (w), 1694 (w), 1681 (w), 1621 (w), 1609 (w), 1598 (w), 1581 (w), 1562 (w), 1472 (m), 1465 (m), 1431 (s), 1378 (w), 1368 (w), 1322 (w), 1285 (m), 1239 (m), 1210 (w), 1188 (w), 1143 (w), 1126 (m), 1052 (m), 1014 (w), 935 (w), 895 (m), 866 (s), 800 (vs), 724 (w), 686 (w), 637 (m), 562 (vs), 439 (w), 412 (vs) cm^{-1}.

Additional information on chemical synthesis is available *via* the Chemotion repository:

https://doi.org/10.14272/reaction/SA-FUHFF-UHFFFADPSC-FIHILUSWIS-UHFFFADPSC-NUHFF-NUHFF-NUHFF-ZZZ.2

Additional information on the analysis of the target compound is available *via* the Chemotion repository:

https://doi.org/10.14272/FIHILUSWISKVSR-UHFFFAOYSA-N.4

3,6-Dibromo-9-(2-ethylhexyl)carbazole (25)

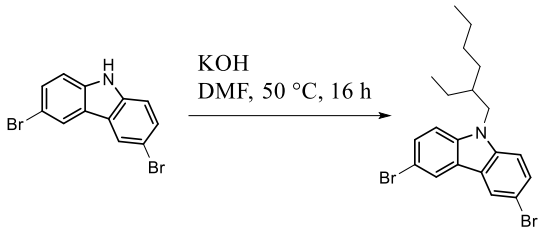

25, 98%

A mixture of 3,6-dibromo-9*H*-carbazole (1.00 g, 3.08 mmol, 1.00 equiv.), 3-(bromomethyl)heptane (688 mg, 634 µL, 3.38 mmol, 1.10 equiv.), and potassium hydroxide (259 mg, 4.62 mmol, 1.50 equiv.) in 40 mL of DMF was heated to 50 °C for 16 h. After removing the solvent in vacuo, the crude solid was extracted with 50 mL of EtOAc and washed with 3 x 150 mL water. Column chromatography on silica using pentane as eluent yielded 3,6-dibromo-9-(2-ethylhexyl)carbazole (1.20 g, 2.75 mmol, 89% yield) as a colorless oil.

R_f = 0.20 (pentane).

^{1}H NMR (400 MHz, Dichloromethane-d_2 [5.32 ppm], ppm) δ = 8.16 (d, *J* = 1.9 Hz, 2H, CH_{Ar}), 7.56 (dd, *J* = 8.7 Hz, *J* = 2.0 Hz, 2H, CH_{Ar}), 7.31 (d, *J* = 8.7 Hz, 2H, CH_{Ar}), 4.12 (dd, *J* = 7.6 Hz, *J* = 1.2 Hz, 2H, N-CH_2), 2.05–1.96 (m, 1H, alkyl-CH), 1.42–1.19 (m, 8H, alkyl-CH_2), 0.90 (t, *J* = 7.4 Hz, 3H, alkyl-CH_3), 0.84 (t, *J* = 7.1 Hz, 3H, alkyl-CH_3);

^{13}C NMR (100 MHz, Dichloromethane-d_2 [53.84 ppm], ppm) δ = 139.9 (C_q, 2C), 128.9 (+, CH, 2C), 123.3 (C_q, 2C), 123.0 (+, CH, 2C), 111.7 (C_q, 2C), 110.9 (+, CH, 2C), 47.6 (–, CH_2, N-CH_2), 39.3 (+, CH, alkyl-CH), 30.9 (–, CH_2), 28.7 (–, CH_2), 24.3 (–, CH_2), 23.0 (–, CH_2), 13.7 (+, CH_3), 10.6 (+, CH_3);

MS (ESI), m/z (%): 482/484/486 (37/87/58) $[M+H+2Na]^+$, 448/450/452 (49/100/47) $[M+NH_3]^+$, 436/438/440 (36/33/60) $[M+H]^+$, 435/437/439 (5/10/7) $[M]^+$. HRMS (ESI): m/z = calcd for $C_{20}H_{24}{}^{79}Br^{81}BrN$ $[M+H]^+$: 438.0255; found 438.0247;

IR (ATR, $\tilde{\nu}$) = 2956 (m), 2925 (m), 2871 (w), 2856 (w), 1849 (vw), 1720 (w), 1622 (w), 1591 (w), 1567 (w), 1470 (vs), 1436 (vs), 1378 (m), 1343 (m), 1317 (m), 1286 (vs), 1244 (w), 1217 (m), 1204 (m), 1147 (m), 1058 (s), 1017 (s), 965 (w), 931 (w), 905 (w), 864 (s), 832 (s), 795 (vs), 737 (w), 724 (w), 683 (w), 643 (s), 611 (w), 585 (w), 564 (s), 548 (w), 530 (w), 494 (m), 452 (w), 436 (w), 421 (m), 394 (w), 378 (w) cm^{-1}.

Additional information on chemical synthesis is available *via* the Chemotion repository:

https://doi.org/10.14272/reaction/SA-FUHFF-UHFFFADPSC-ZDFZWZGIGK-UHFFFADPSC-NUHFF-NUHFF-NUHFF-ZZZ

Additional information on the analysis of the target compound is available *via* the Chemotion repository:

https://doi.org/10.14272/ZDFZWZGIGKUBRA-UHFFFAOYSA-N.1

_N_-(4-fluorophenyl)-4-methoxy-_N_-(4-methoxyphenyl)aniline (27)

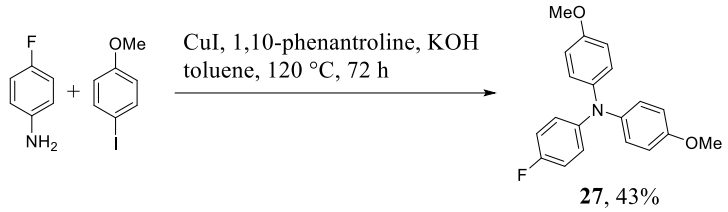

27, 43%

To 30 mL of toluene in a round-bottom flask fitted with a Dean-Stark trap and reflux condenser, was added 4-fluoroaniline (1.00 g, 853 µL, 8.82 mmol, 1.00 equiv.), 1-iodo-4-methoxybenzene (4.13 g, 17.6 mmol, 2.00 equiv.), copper(I) iodide (168 mg, 882 µmol, 0.100 equiv.), 1,10-phenanthroline (159 mg, 882 µmol, 0.100 equiv.), and potassium hydroxide (1.98 g, 35.3 mmol, 4.00 equiv). The resulting solution was stirred at 120 °C for 3 d. Purification by column chromatography on silica using cHex/EtOAc 20:1 as eluent yielded *N*-(4-fluorophenyl)-4-methoxy-*N*-(4-methoxyphenyl)aniline (1.24 g, 3.83 mmol, 43% yield) as a yellow solid.

R_f = 0.61 (cHex/EtOAc 10:1).

M.p.: 101 °C

^{1}H NMR (400 MHz, Chloroform-d [7.26 ppm], ppm) δ = 7.01–6.97 (m, 4H), 6.95–6.86 (m, 4H), 6.83–6.79 (m, 4H), 3.79 (s, 6H);

^{13}C NMR (100 MHz, Chloroform-d [77.16 ppm], ppm) δ = 157.9 (d, J = 240.5 Hz, C_q), 155.5 (C_q, 2C), 144.9 (d, J = 2.5 Hz, C_q), 141.5 (C_q, 2C), 125.6 (+, CH, 4C), 123.4 (d, J = 7.6 Hz, CH, 2C), 115.7 (d, J = 22.4 Hz, CH, 2C), 114.6 (+, CH, 4C), 55.5 (+, CH_3, 2C);

^{19}F NMR (376 MHz, ppm) δ = -122.51 (1F);

MS (ESI), m/z (%): 324 (100) $[M+H]^+$, 323 (85) $[M]^+$. HRMS (ESI): m/z = calcd for $C_{20}H_{18}FNO_2$ $[M]^+$: 323.1322; found 323.1313;

IR (ATR, ṽ) = 3067 (vw), 3041 (vw), 2997 (w), 2949 (w), 2929 (w), 2908 (w), 2849 (w), 2833 (w), 1874 (vw), 1731 (vw), 1606 (vw), 1588 (w), 1497 (vs), 1462 (s), 1441 (m), 1401 (w), 1378 (vw), 1315 (w), 1285 (m), 1264 (m), 1238 (vs), 1217 (vs), 1179 (s), 1154 (w), 1103 (w), 1061 (w), 1034 (s), 999

(w), 950 (vw), 914 (w), 875 (vw), 826 (vs), 788 (w), 781 (w), 764 (w), 721 (w), 636 (vw), 628 (vw), 574 (m), 516 (w), 487 (vw), 416 (vw) cm^{-1}.

Additional information on chemical synthesis is available *via* the Chemotion repository:

https://doi.org/10.14272/reaction/SA-FUHFF-UHFFFADPSC-WFRXNFYMSQ-UHFFFADPSC-NUHFF-NUHFF-NUHFF-ZZZ

Additional information on the analysis of the target compound is available *via* the Chemotion repository:

https://doi.org/10.14272/WFRXNFYMSQQOHC-UHFFFAOYSA-N.1

(4-Iodophenyl)-bis(4-methoxyphenyl)amine (28)

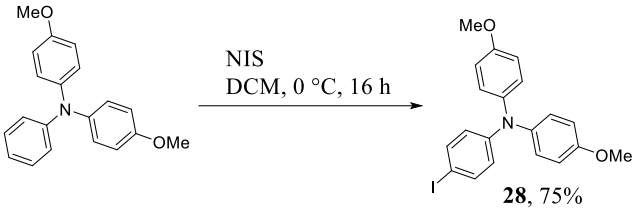

28, 75%

N-Iodosuccinimide (3.08 g, 13.7 mmol, 1.10 equiv.) was added to a solution of 4-methoxy-*N*-(4-methoxyphenyl)-*N*-phenylaniline (3.80 g, 12.4 mmol, 1.00 equiv.) in 100 mL of DMF, after being stirred at 21 °C for 16 h, brine (500 mL) was added. The reaction mixture was extracted with 3 x 50 mL EtOAc, dried over Na_2SO_4, and concentrated under reduced pressure. The residue was purified by column chromatography on silica using cHex/EtOAc 50:1 as eluent to obtain (4-iodophenyl)-bis(4-methoxyphenyl)amine (4.19 g, 9.72 mmol, 78% yield) as a yellow solid.

R_f = 0.45 (cHex/EtOAc 10:1).

M.p.: 109 °C

^{1}H NMR (400 MHz, Chloroform-d [7.26 ppm], ppm) δ = 7.44–7.39 (m, 2H), 7.07–6.97 (m, 4H), 6.88–6.78 (m, 4H), 6.71–6.66 (m, 2H), 3.78 (s, 6H, OMe-CH_3);

^{13}C NMR (100 MHz, Chloroform-d [77.16 ppm], ppm) δ = 156.1 (C_q, 2C), 148.6 (C_q), 140.4 (C_q, 2C), 137.7 (+, CH, 2C), 126.7 (+, CH, 4C), 122.3 (+, CH, 2C), 114.8 (+, CH, 4C), 82.0 (C_q), 55.5 (+, CH_3, 2C, OMe-CH_3);

MS (EI, 70 eV, 100 °C), m/z (%): 431 (100) $[M]^+$, 416 (42). HRMS (EI): m/z = calcd for $C_{20}H_{18}O_2N^{127}I$ $[M]^+$: 431.0377; found 431.0375;

IR (ATR, $\tilde{\nu}$) = 3034 (w), 2993 (w), 2951 (m), 2929 (m), 2902 (w), 2830 (m), 2038 (w), 1895 (w), 1871 (w), 1737 (w), 1606 (w), 1581 (m), 1499 (vs), 1482 (vs), 1460 (vs), 1452 (vs), 1436 (s), 1400 (m), 1316 (s), 1298 (w), 1283 (s), 1269 (s), 1237 (vs), 1190 (s), 1174 (vs), 1162 (vs), 1116 (s), 1101 (vs), 1061 (m), 1027 (vs), 1000 (vs), 950 (m), 939 (m), 916 (m), 895 (m), 830 (vs), 816 (vs), 800 (vs), 778 (s), 725 (s), 710 (m), 698 (s), 687 (s), 635 (m), 599 (s), 572 (vs), 533 (vs), 523 (vs), 506 (vs), 490 (s), 456 (m), 438 (m), 418 (m), 407 (s), 385 (m) cm^{-1}.

Additional information on chemical synthesis is available *via* the Chemotion repository:

https://doi.org/10.14272/reaction/SA-FUHFF-UHFFFADPSC-VGQDQJMYUY-UHFFFADPSC-NUHFF-NUHFF-NUHFF-ZZZ

Additional information on the analysis of the target compound is available *via* the Chemotion repository:

https://doi.org/10.14272/VGQDQJMYUYSINZ-UHFFFAOYSA-N.1

3-Bromo-9-(4-iodophenyl)carbazole (**29**)

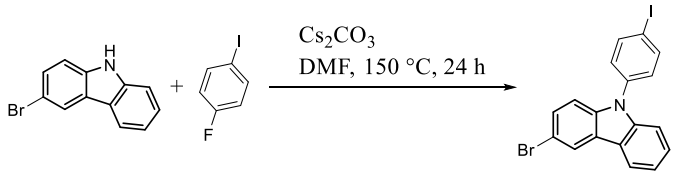

29, 63%

A mixture of 3-bromo-9*H*-carbazole (100 mg, 406 µmol, 1.00 equiv.), 1-fluoro-4-iodo-benzene (361 mg, 187 µL, 1.63 mmol, 4.00 equiv.), and dicesium carbonate (530 mg, 1.63 mmol, 4.00 equiv.) in 2 mL of DMF was heated to 150 °C for 16 h. The mixture was poured into 50 mL water and extracted with 3 x 10 mL of DCM. Column chromatography on silica gel using pentane/DCM 30:1 as eluent yielded 3-bromo-9-(4-iodophenyl)carbazole (114 mg, 254 µmol, 63% yield) as a colorless solid.

R_f = 0.63 (pentane/DCM 5:1).

M.p.: 162 °C

^{1}H NMR (400 MHz, Chloroform-d [7.26 ppm], ppm) δ = 8.24 (d, *J* = 1.9 Hz, 1H), 8.08 (dt, *J* = 7.8 Hz, *J* = 1.0 Hz, 1H), 7.96–7.90 (m, 2H), 7.49 (dd, *J* = 8.7 Hz, *J* = 2.0 Hz, 1H), 7.44 (ddd, *J* = 8.3 Hz, *J* = 7.0 Hz, *J* = 1.2 Hz, 1H), 7.36 (dt, *J* = 8.3 Hz, *J* = 1.0 Hz, 1H), 7.33–7.27 (m, 3H), 7.25 (d, *J* = 8.7 Hz, 1H);

^{13}C NMR (100 MHz, Chloroform-d [77.16 ppm], ppm) δ = 140.9 (C_q), 139.2 (+, CH, 2C), 137.0 (C_q), 128.9 (+, CH, 2C), 128.8 (+, CH), 126.8 (+, CH), 125.3 (C_q), 123.2 (+, CH), 122.4 (C_q), 120.7 (+, CH), 120.6 (+, CH), 113.0 (C_q), 111.1 (+, CH), 109.8 (+, CH), 92.5 (C_q), 77.2 (C_q);

MS (ESI), m/z (%): 448/450 (100/99) $[M+H]^+$, 441 (35), 419 (61). HRMS (ESI): m/z = calcd for $C_{18}H_{12}{}^{79}BrIN$ $[M+H]^+$: 447.9198; found 447.9187;

IR (ATR, $\tilde{\nu}$) = 3053 (w), 3043 (w), 2921 (w), 1584 (w), 1492 (vs), 1482 (m), 1466 (s), 1441 (vs), 1424 (m), 1397 (m), 1363 (m), 1340 (w), 1326 (m), 1312 (m), 1266 (s), 1231 (vs), 1180 (m), 1166 (m), 1147 (w), 1128 (m), 1099 (m), 1055 (m), 1023 (m), 1006 (s), 963 (w), 950 (w), 935 (m), 915 (m), 874 (m), 820 (vs), 799 (vs), 786 (vs), 762 (s), 742 (vs), 720 (vs), 707 (s), 671 (s), 642 (m), 625 (m), 618 (m), 578 (m), 557 (vs), 496 (vs), 462 (s), 416 (vs), 407 (s), 387 (m) cm^{-1}.

Additional information on chemical synthesis is available *via* the Chemotion repository:

https://doi.org/10.14272/reaction/SA-FUHFF-UHFFFADPSC-BTENQKLMZI-UHFFFADPSC-NUHFF-NUHFF-NUHFF-ZZZ

Additional information on the analysis of the target compound is available *via* the Chemotion repository:

https://doi.org/10.14272/BTENQKLMZIAXHX-UHFFFAOYSA-N.1

4-(3-Bromo-9*H*-carbazol-9-yl)-*N*,*N*-bis(4-methoxyphenyl)aniline (30)

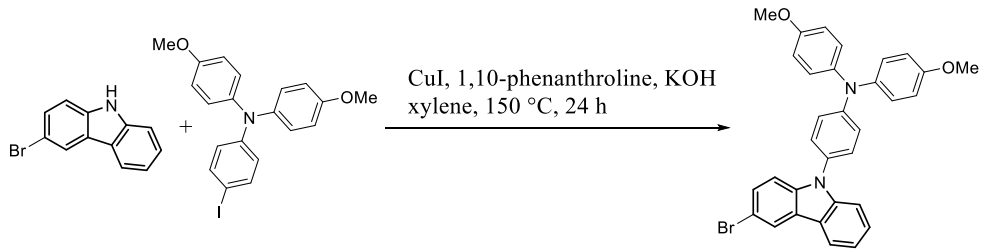

30, 87%

3-Bromo-9*H*-carbazole (250 mg, 1.02 mmol, 1.00 equiv.), (4-iodophenyl)-bis(4-methoxyphenyl)amine (526 mg, 1.22 mmol, 1.20 equiv.), copper(I) iodide (19.3 mg, 102 µmol, 0.100 equiv.), 1,10-phenanthroline (18.3 mg, 102 µmol, 0.100 equiv.), and potassium hydroxide (228 mg, 4.06 mmol, 4.00 equiv.) were added in 10 mL of dry *o*-xylene under argon. The resulting solution was stirred at 150 °C for 24 h. After purification by column chromatography on silica using pentane/DCM 4:1 as eluent, 4-(3-bromo-9*H*-carbazol-9-yl)-*N,N*-bis(4-methoxyphenyl)aniline (483 mg, 862 µmol, 85% yield) was received as an orange solid.

R_f = 0.59 (pentane/DCM 2:1).

M.p.: 72 °C

^{1}H NMR (400 MHz, Dichloromethane-d_2 [5.32 ppm], ppm) δ = 8.25 (d, *J* = 2.0 Hz, 1H), 8.10 (dt, *J* = 7.8 Hz, *J* = 1.0 Hz, 1H), 7.49 (dd, *J* = 8.7 Hz, *J* = 2.0 Hz, 1H), 7.46–7.38 (m, 2H), 7.33–7.24 (m, 4H), 7.22–7.15 (m, 4H), 7.08–7.01 (m, 2H), 6.94–6.82 (m, 4H), 3.82 (s, 6H, OMe-CH_3);

^{13}C NMR (100 MHz, Dichloromethane-d_2 [53.84 ppm], ppm) δ = 156.5 (C_q, 2C), 148.6 (C_q), 141.7 (C_q), 140.4 (C_q, 2C), 140.0 (C_q), 128.6 (C_q), 128.3 (+, CH), 127.5 (+, CH, 2C), 127.1 (+, CH, 4C), 126.5 (+, CH), 124.8 (C_q), 122.8 (+, CH), 121.9 (C_q), 120.3 (+, CH), 120.3 (+, CH, 2C), 120.0 (+, CH), 114.8 (+, CH, 4C), 112.1 (+, CH), 111.4 (+, CH), 110.1 (+, CH), 55.5 (+, CH_3, 2C, OMe-CH_3);

MS (ESI), m/z (%): 548/550 (58/54) $[M]^+$, 431 (100), 305 (94), 295 (27). HRMS (ESI): m/z = calcd for $C_{32}H_{25}{}^{79}BrN_2O_2$ $[M]^+$: 548.1100; found 548.1089;

IR (ATR, $\tilde{\nu}$) = 3038 (w), 2996 (w), 2924 (w), 2905 (w), 2846 (w), 2832 (w), 2791 (w), 1618 (vw), 1601 (w), 1500 (vs), 1466 (s), 1441 (s), 1315 (m), 1283 (m), 1268 (s), 1234 (vs), 1179 (s), 1166 (m), 1129 (w), 1105 (m), 1054 (w), 1033 (s), 1009 (m), 938 (w), 911 (w), 871 (w), 826 (vs), 799 (s), 765 (w), 744 (s), 720 (m), 676 (w), 663 (w), 647 (w), 632 (w), 619 (w), 598 (w), 575 (s), 562 (m), 531 (m), 520 (m), 496 (w), 489 (w), 463 (m), 446 (w), 441 (w), 419 (m), 392 (w) cm^{-1}.

Additional information on chemical synthesis is available *via* the Chemotion repository:

https://doi.org/10.14272/reaction/SA-FUHFF-UHFFFADPSC-NLVVMBWXRF-UHFFFADPSC-NUHFF-NUHFF-NUHFF-ZZZ

Additional information on the analysis of the target compound is available *via* the Chemotion repository:

https://doi.org/10.14272/NLVVMBWXRFXGHP-UHFFFAOYSA-N.1

Bis(4-methoxyphenyl)-phenyl-amine (31)

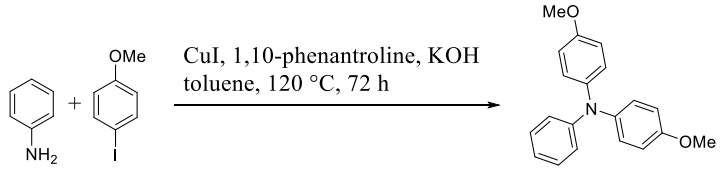

31, 72%

To 20 mL of toluene in a round-bottom flask fitted with a Dean-Stark trap and reflux condenser were added aniline (500 mg, 490 µL, 5.37 mmol, 1.00 equiv.), 1-iodo-4-methoxy-benzene (2.76 g, 11.8 mmol, 2.20 equiv.), copper(I) iodide (102 mg, 537 µmol, 0.100 equiv.), 1,10-phenanthroline (96.8 mg, 537 µmol, 0.100 equiv.), and potassium hydroxide (1.20 g, 21.5 mmol, 4.00 equiv.). The

resulting solution was stirred at 120 °C for 3 days. The solvent was evaporated, and the mixture was purified by column chromatography using cHex/EtOAc 20:1 as an eluent to yield bis(4-methoxyphenyl)-phenyl-amine (1.18 g, 3.80 mmol, 71% yield) as a yellow solid.

R_f = 0.38 (cHex/EtOAc 10:1).

M.p.: 98 °C

^{1}H NMR (400 MHz, Chloroform-d [7.26 ppm], ppm) δ = 7.22–7.13 (m, 2H), 7.09–7.01 (m, 4H), 6.94 (dt, *J* = 7.0 Hz, *J* = 1.2 Hz, *J* = 1.2 Hz, 2H), 6.87 (t, *J* = 7.3 Hz, *J* = 7.3 Hz, 1H), 6.84–6.80 (m, 4H), 3.79 (s, 6H, OMe-CH_3);

^{13}C NMR (100 MHz, Chloroform-d [77.16 ppm], ppm) δ = 155.7 (C_q, 2C), 148.8 (C_q), 141.2 (C_q, 2C), 128.9 (+, CH, 2C), 126.4 (+, CH, 4C), 120.9 (+, CH, 2C), 120.6 (+, CH), 114.7 (+, CH, 4C), 55.5 (+, CH_3, 2C);

MS (FAB, 3-NBA), m/z (%): 305 (100) $[M]^+$. HRMS (FAB, matrix NBA): m/z = calcd for $C_{20}H_{19}O_2N_1$ $[M]^+$: 305.1410; found 305.1410;

IR (ATR, ṽ) = 3077 (w), 3063 (w), 3034 (w), 3012 (w), 2953 (w), 2928 (w), 2912 (w), 2874 (w), 2853 (w), 2836 (w), 1591 (m), 1502 (vs), 1485 (vs), 1466 (vs), 1460 (vs), 1439 (vs), 1422 (m), 1319 (m), 1289 (vs), 1278 (s), 1269 (m), 1238 (vs), 1179 (vs), 1166 (vs), 1108 (s), 1084 (m), 1030 (vs), 990 (m), 959 (m), 939 (w), 911 (m), 894 (w), 830 (vs), 813 (vs), 782 (m), 756 (vs), 728 (vs), 715 (s), 700 (vs), 669 (w), 642 (w), 632 (w), 618 (w), 588 (vs), 574 (vs), 531 (s), 520 (vs), 514 (vs), 482 (s), 435 (m), 414 (m), 388 (m), 375 (w) cm^{-1}.

Additional information on chemical synthesis is available *via* the Chemotion repository:

https://doi.org/10.14272/reaction/SA-FUHFF-UHFFFADPSC-ZJPTYHDCQP-UHFFFADPSC-NUHFF-NUHFF-NUHFF-ZZZ

Additional information on the analysis of the target compound is available *via* the Chemotion repository:

https://doi.org/10.14272/ZJPTYHDCQPDNBH-UHFFFAOYSA-N.1

4,4'-(9*H*-carbazole-3,9-diyl)bis(*N*,*N*-bis(4-methoxyphenyl)aniline) (32)

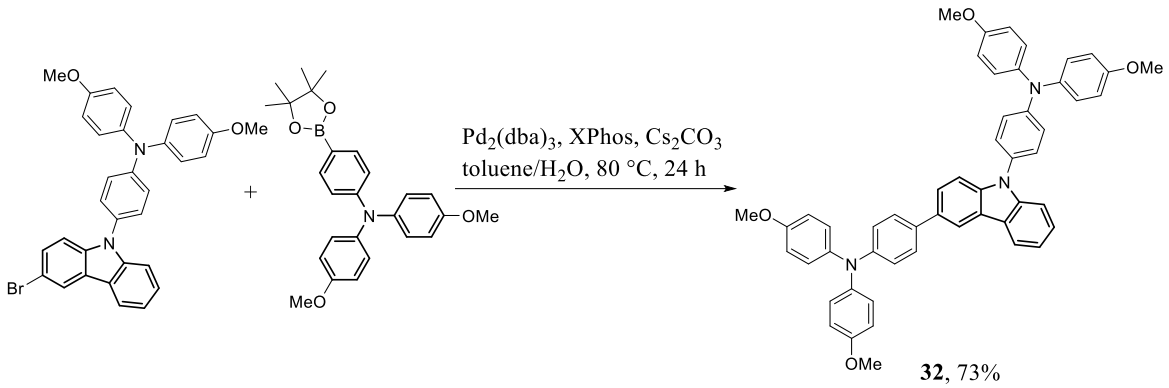

32, 73%

4-(3-Bromo-9*H*-carbazol-9-yl)-*N,N*-bis(4-methoxyphenyl)aniline (250 mg, 455 µmol, 1.00 equiv.), *N,N*-bis(4-methoxyphenyl)-4-(4,4,5,5-tetramethyl-1,3,2-dioxaborolan-2-yl)aniline (275 mg, 637 µmol, 1.40 equiv.), tris(dibenzylidenaceton)dipalladium(0) (20.8 mg, 22.7 µmol, 0.0500 equiv.), XPhos (21.7 mg, 45.5 µmol, 0.100 equiv.), dicesium carbonate (593 mg, 1.82 mmol, 4.00 equiv.) were added together with 0.75 mL of water, and 7.5 mL of THF in a vial under argon. The mixture was purged with argon for 10 min. Afterwards, the mixture was stirred at 75 °C for 48 h. The obtained crude product was purified *via* column chromatography on silica gel using cHex/EtOAc 5:1 as eluent to yield 4,4'-(9*H*-carbazole-3,9-diyl)bis(*N,N*-bis(4-methoxyphenyl)aniline) (258 mg, 330 µmol, 72% yield) as an orange solid.

R_f = 0.37 (cHex/EtOAc 5:1).

M.p.: 113 °C

^{1}H NMR (400 MHz, Dichloromethane-d_2 [5.32 ppm], ppm) δ = 8.30–8.29 (m, 1H), 8.15 (d, *J* = 7.8 Hz, 1H), 7.63–7.60 (m, 1H), 7.56–7.52 (m, 2H), 7.44–7.40 (m, 3H), 7.33–7.30 (m, 2H), 7.25 (dt, *J* = 8.0 Hz, *J* = 4.1 Hz, 1H), 7.18–7.14 (m, 4H), 7.10–7.05 (m, 6H), 7.00 (d, *J* = 8.2 Hz, 2H), 6.91–6.83 (m, 8H), 3.80 (s, 6H, OMe-CH_3), 3.78 (s, 6H, OMe-CH_3);

^{13}C NMR (100 MHz, Dichloromethane-d_2 [53.84 ppm], ppm) δ = 156.4 (C_q, 4C), 148.3 (C_q, 2C), 141.7 (C_q, 2C), 140.6 (C_q, 4C), 140.4 (C_q), 129.2 (C_q, 2C), 127.5 (+, CH, 4C), 127.1 (+, CH), 127.0 (+, CH, 4C), 126.4 (+, CH, 2C), 125.9 (+, CH), 124.8 (+, CH), 123.5 (C_q), 123.1 (C_q), 121.1 (+, CH, 2C), 120.4 (+, CH, 2C), 120.2 (+, CH), 119.6 (+, CH), 117.8 (+, CH, 2C), 114.8 (+, CH, 4C), 114.6 (+, CH, 4C), 110.0 (+, CH), 109.9 (+, CH), 55.5 (+, CH_3, 2C), 55.4 (+, CH_3, 2C);

MS (ESI), m/z (%): 773 (100) $[M]^+$, 609 (31), 608 (72). HRMS (ESI): m/z = calcd for $C_{52}H_{43}N_3O_4$ $[M]^+$: 773.3254; found 773.3224;

IR (ATR, ṽ) = 3037 (w), 2996 (w), 2948 (w), 2925 (w), 2904 (w), 2873 (w), 2849 (w), 2832 (w), 2792 (w), 1602 (w), 1500 (vs), 1473 (s), 1455 (vs), 1439 (s), 1315 (m), 1278 (m), 1232 (vs), 1177 (s), 1166

(s), 1103 (m), 1031 (vs), 911 (w), 885 (w), 824 (vs), 805 (vs), 781 (m), 768 (m), 745 (s), 731 (m), 722 (s), 703 (m), 667 (w), 639 (w), 635 (w), 620 (w), 601 (m), 574 (s), 520 (s), 494 (m), 486 (m), 469 (m), 453 (m), 422 (m), 418 (m), 398 (m), 391 (m), 377 (w) cm^{-1}.

Additional information on chemical synthesis is available *via* the Chemotion repository:

https://doi.org/10.14272/reaction/SA-FUHFF-UHFFFADPSC-VSJDGYHWIN-UHFFFADPSC-NUHFF-NUHFF-NUHFF-ZZZ

Additional information on the analysis of the target compound is available *via* the Chemotion repository:

https://doi.org/10.14272/VSJDGYHWINPRKI-UHFFFAOYSA-N.1

4-(3,6-Dibromo-9*H*-carbazol-9-yl)-*N*,*N*-bis(4-methoxyphenyl)aniline (33)

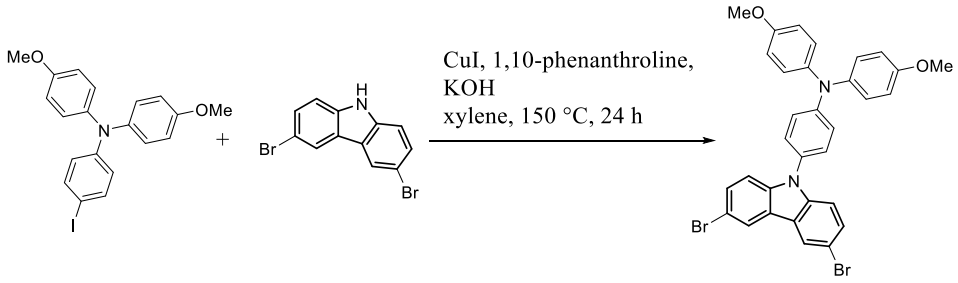

33, 97%

3,6-Dibromo-9*H*-carbazole (1.50 g, 4.62 mmol, 1.00 equiv.), (4-iodophenyl)-bis(4-methoxyphenyl)amine (2.39 g, 5.54 mmol, 1.20 equiv.), copper(I) iodide (87.9 mg, 462 µmol, 0.100 equiv.), 1,10-phenanthroline (83.2 mg, 462 µmol, 0.100 equiv.), and potassium hydroxide (1.04 g, 18.5 mmol, 4.00 equiv.) were added together in 60 mL of *o*-xylene under argon. The resulting solution was stirred at 150 °C for 24 h. Purification was done by column chromatography on silica using pentane/DCM 4:1 as eluent to yield 4-(3,6-dibromo-9*H*-carbazol-9-yl)-*N*,*N*-bis(4-methoxyphenyl)aniline (2.83 g, 4.50 mmol, 97% yield) as an orange solid.

R_f = 0.51 (pentane/DCM 1:1).

M.p.: 209 °C

^{1}H NMR (400 MHz, Dichloromethane-d_2 [5.32 ppm], ppm) δ = 8.19 (d, *J* = 1.9 Hz, 2H), 7.51 (dd, *J* = 8.7 Hz, *J* = 2.0 Hz, 2H), 7.26–7.18 (m, 8H), 7.08 (d, *J* = 8.5 Hz, 2H), 6.97–6.90 (m, 4H), 3.85 (s, 6H);

^{13}C NMR (100 MHz, Dichloromethane-d_2 [53.84 ppm], ppm) δ = 156.6 (C_q, 2C), 148.8 (C_q, 2C), 148.7 (C_q), 140.3 (C_q, 2C), 129.2 (+, CH, 2C), 129.1 (+, CH, 2C), 128.0 (C_q), 127.5 (+, CH, 2C), 127.2 (+,

CH, 2C), 123.6 (C_q, 2C), 123.0 (+, CH, 2C), 120.1 (+, CH, 2C), 114.8 (+, CH, 2C), 112.5 (+, CH, 2C), 111.7 (+, CH, 2C), 111.6 (C_q, 2C), 55.5 (+, CH_3, 2C);

MS (FAB, 3-NBA), m/z (%): 626/628/630 (4/9/4) $[M]^+$, 155 (30), 154 (100), 138 (39), 137 (68), 136 (86), 107 (31). HRMS (FAB, matrix NBA): m/z = calcd for $C_{32}H_{24}O_2N_2{}^{79}Br^{81}Br$ $[M]^+$: 628.0179; found 628.0179;

IR (ATR, $\tilde{\nu}$) = 3064 (w), 3040 (w), 3012 (w), 2941 (w), 2927 (w), 2901 (w), 2851 (w), 2832 (w), 1500 (vs), 1459 (vs), 1429 (s), 1316 (m), 1281 (s), 1269 (m), 1230 (vs), 1193 (s), 1179 (vs), 1167 (s), 1125 (m), 1106 (s), 1057 (m), 1027 (vs), 953 (w), 948 (w), 935 (m), 912 (w), 888 (w), 880 (m), 829 (vs), 810 (vs), 800 (vs), 779 (s), 759 (m), 715 (s), 671 (m), 633 (m), 599 (m), 579 (vs), 565 (vs), 524 (vs), 494 (m), 469 (w), 459 (w), 448 (w), 418 (s), 382 (w) cm^{-1}.

Additional information on chemical synthesis is available *via* the Chemotion repository:

https://doi.org/10.14272/reaction/SA-FUHFF-UHFFFADPSC-KXIRHZUWUI-UHFFFADPSC-NUHFF-NUHFF-NUHFF-ZZZ

Additional information on the analysis of the target compound is available *via* the Chemotion repository:

https://doi.org/10.14272/KXIRHZUWUICFMQ-UHFFFAOYSA-N.1

4,4',4''-(9*H*-Carbazole-3,6,9-triyl)tris(*N*,*N*-bis(4-methoxyphenyl)aniline) (34)

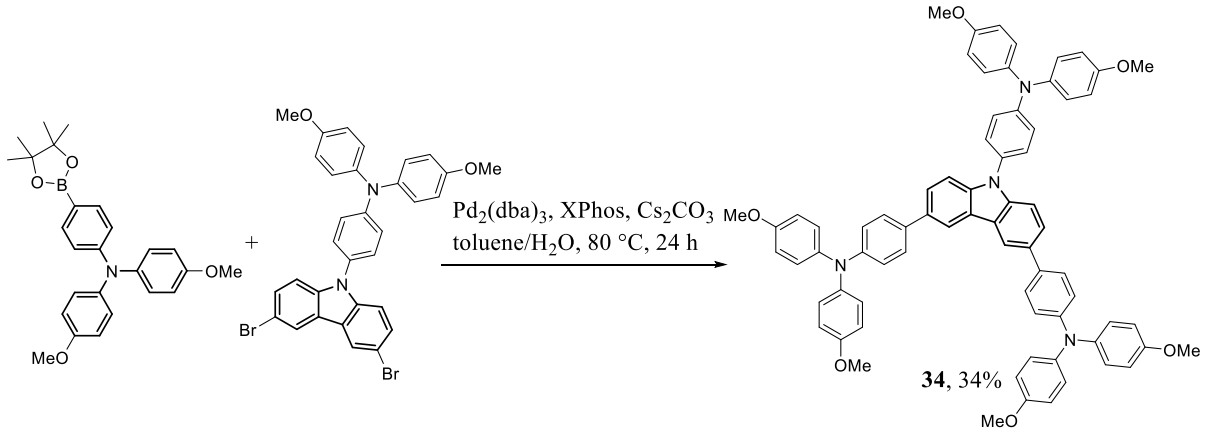

4-(3,6-Dibromo-9*H*-carbazol-9-yl)-*N,N*-bis(4-methoxyphenyl)aniline (600 mg, 955 µmol, 1.00 equiv.), *N,N*-bis(4-methoxyphenyl)-4-(4,4,5,5-tetramethyl-1,3,2-dioxaborolan-2-yl)aniline (515 mg, 1.19 mmol, 1.25 equiv.), tris(dibenzylidenaceton)dipalladium(0) (43.7 mg, 47.7 µmol, 0.0500 equiv.), XPhos (45.5 mg, 95.5 µmol, 0.100 equiv.) and dicesium carbonate (1.24 g, 3.82 mmol, 4.00 equiv.) were added together with 2 mL of water and 20 mL of toluene in a vial under argon. The mixture was purged with argon for 10 min. The mixture was stirred at 100 °C for 24 h. The obtained crude product

was purified *via* column chromatography on silica gel using cHex/EtOAc 10:1 as eluent to receive 4,4',4"-(9*H*-carbazole-3,6,9-triyl)tris(*N,N*-bis(4-methoxyphenyl)aniline) (354 mg, 329 µmol, 34% yield) as an orange solid.

R_f = 0.33 (cHex/EtOAc 5:1).

M.p.: 135 °C

^{1}H NMR (400 MHz, Dichloromethane-d_2 [5.32 ppm], ppm) δ = 8.24 (d, *J* = 1.8 Hz, 2H), 7.54 (dd, *J* = 8.6 Hz, *J* = 1.8 Hz, 2H), 7.48–7.42 (m, 4H), 7.36 (d, *J* = 8.5 Hz, 2H), 7.28–7.24 (m, 2H), 7.10–7.05 (m, 4H), 7.02–6.98 (m, 10H), 6.95–6.90 (m, 4H), 6.83–6.80 (m, 4H), 6.79–6.75 (m, 8H), 3.72 (s, 6H, OMe-CH_3), 3.70 (s, 12H, OMe-CH_3);

^{13}C NMR (100 MHz, Dichloromethane-d_2 [53.84 ppm], ppm) δ = 156.4 (C_q, 2C), 155.9 (C_q, 4C), 148.2 (C_q), 147.6 (C_q, 2C), 141.0 (C_q, 4C), 140.8 (C_q, 2C), 140.5 (C_q, 2C), 133.9 (C_q, 2C), 132.8 (C_q, 2C), 129.2 (C_q), 127.4 (+, CH, 4C), 127.4 (+, CH, 2C), 127.0 (+, CH, 4C), 126.4 (+, CH, 8C), 124.9 (+, CH, 2C), 123.7 (C_q, 2C), 121.1 (+, CH, 4C), 120.4 (+, CH, 2C), 117.8 (+, CH, 2C), 114.8 (+, CH, 4C), 114.6 (+, CH, 8C), 110.2 (+, CH, 2C), 55.5 (+, CH_3, 2C), 55.4 (+, CH_3, 4C);

MS (ESI), m/z (%): 1076 (1) $[M]^+$, 609 (43), 608 (100). HRMS (ESI): m/z = calcd for $C_{72}H_{60}N_4O_6$ $[M]^+$: 1076.4513; found 1076.7780;

IR (ATR, $\tilde{\nu}$) = 3036 (w), 2993 (w), 2946 (w), 2927 (w), 2904 (w), 2832 (w), 1604 (w), 1499 (vs), 1475 (vs), 1455 (vs), 1439 (s), 1315 (m), 1276 (s), 1232 (vs), 1176 (s), 1164 (s), 1103 (m), 1031 (vs), 945 (w), 911 (w), 881 (w), 824 (vs), 806 (vs), 779 (m), 751 (w), 724 (m), 697 (m), 643 (m), 601 (m), 572 (s), 520 (s), 486 (m), 453 (w), 416 (m), 397 (w), 385 (w), 378 (w) cm^{-1}.

Additional information on chemical synthesis is available *via* the Chemotion repository:

https://doi.org/10.14272/reaction/SA-FUHFF-UHFFFADPSC-VVWBQFVBYT-UHFFFADPSC-NUHFF-NUHFF-NUHFF-ZZZ

Additional information on the analysis of the target compound is available *via* the Chemotion repository:

https://doi.org/10.14272/VVWBQFVBYTVRCK-UHFFFAOYSA-N.1

4,16-(4,4',4'',4'''-bis(*9H*-carbazole-6,3,9-triyl))tetrakis(*N,N*-bis(4-methoxyphenyl)aniline) [2.2]paracyclophane (35)

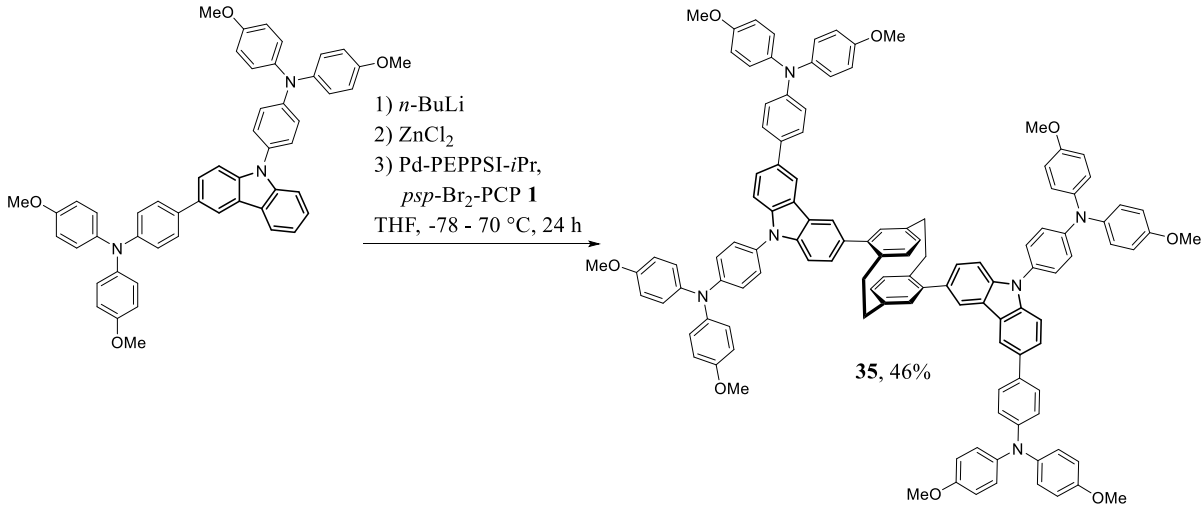

Preparation of Negishi reactant:

4,4'-(9*H*-Carbazole-3,9-diyl)bis(*N,N*-bis(4-methoxyphenyl)aniline) (69.8 mg, 90.1 µmol, 2.20 equiv.) was added to a crimp cap vial and flushed with Ar three times. 2 mL of dry THF were added and the mixture was cooled to -78 °C. *n*-Butyllithium solution (7.87 mg, 49.2 µL, 123 µmol, 2.50M in hexane, 3.00 equiv.) was added dropwise, and the reaction mixture was allowed to warm to 22 °C. After stirring for 30 min, the reaction mixture was cooled to 0 °C, and zinc chloride solution (22.3 mg, 164 µL, 164 µmol, 1.00M in THF, 4.00 equiv.) was added. The reaction was stirred for 15 min at 0 °C and then warmed to 22 °C.

Negishi coupling:

4,16-Dibromo[2.2]paracyclophane (15.0 mg, 41.0 µmol, 1.00 equiv.) and PEPPSI-IPr catalyst (2.79 mg, 4.10 µmol, 0.100 equiv.) were added to a crimp cap vial and flushed with Ar three times. 2 mL of dry THF were added and zinc chloride solution (16.8 mg, 123 µL, 123 µmol, 1.00M in THF, 3.00 equiv.) was added. After dissolving, the Negishi reactant was added via syringe, and the reaction mixture was heated to 70 °C. After three days, the reaction was allowed to cool to 22 °C, and the solvent was removed under reduced pressure. Column chromatography on silica using cHex/DCM 1:0 to 1:2 as eluent yielded 4,16-(4,4',4'',4'''-bis(9*H*-carbazole-6,3,9-triyl))tetrakis(*N,N*-bis(4-methoxyphenyl)aniline)[2.2]paracyclophane (33.0 mg, 18.8 µmol, 46% yield) as dark-red solid.

R_f = 0.42 (cHex/DCM 1:1).

^{1}H NMR (400 MHz, Dichloromethane-d_2 [5.32 ppm], ppm) δ = 8.27–8.19 (m, 2H), 8.07–8.02 (m, 2H), 7.57–6.66 (m, 55H), 6.61–6.00 (m, 7H), 3.77–3.59 (m, 24H), 2.94–2.68 (m, 8H);

MS (ESI), m/z (%):1752 (1) $[M+2H]^+$, 773 (40), 282 (81), 251 (28), 229 (100), 186 (73) HRMS (ESI): m/z = calcd for $C_{120}H_{98}N_6O_8$ $[M]^+$: 1750.7447; found 1750.7498;

IR (ATR, $\tilde{\nu}$) = 3037 (w), 2992 (w), 2948 (w), 2927 (w), 2871 (w), 2853 (w), 2833 (w), 1721 (w), 1601 (w), 1502 (vs), 1473 (s), 1455 (vs), 1439 (s), 1405 (w), 1366 (w), 1315 (m), 1276 (m), 1231 (vs), 1177 (s), 1132 (m), 1103 (m), 1075 (w), 1030 (vs), 993 (m), 952 (m), 911 (m), 891 (w), 868 (w), 826 (vs), 805 (vs), 783 (m), 768 (m), 745 (s), 724 (m), 710 (m), 670 (w), 639 (m), 623 (m), 599 (m), 572 (s), 521 (s), 490 (w), 482 (w), 477 (w), 469 (w), 462 (w), 450 (w), 418 (m), 399 (w), 377 (w) cm^{-1}.

4,15-(4,4',4'',4'''-bis(9*H*-carbazole-6,3,9-triyl))tetrakis(*N*,*N*-bis(4-methoxyphenyl)aniline) [2.2]paracyclophane (36)

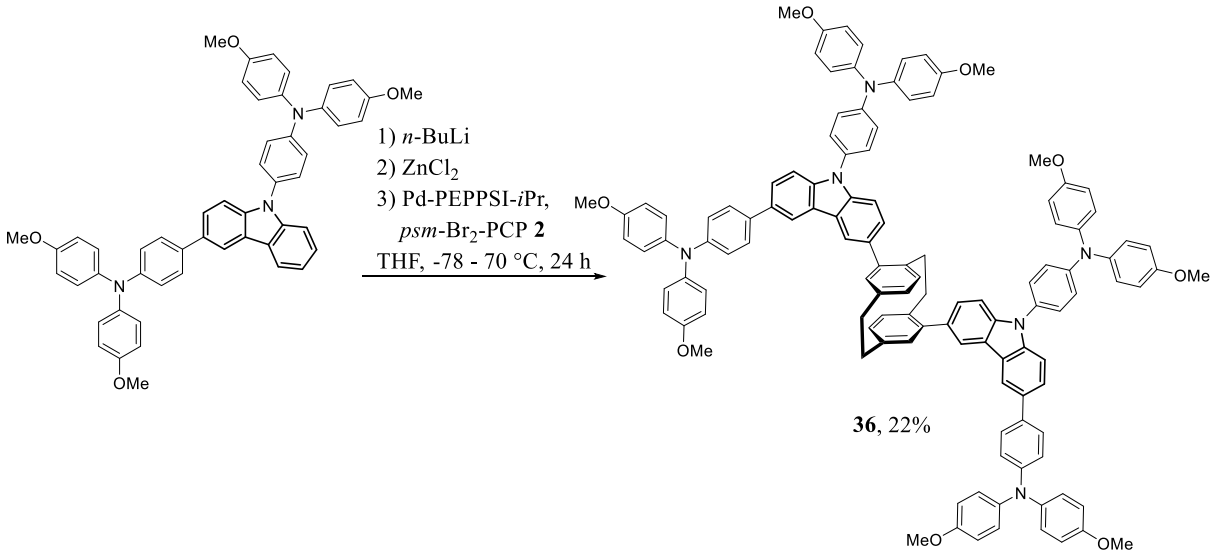

Preparation of Negishi reactant:

4,4'-(9*H*-Carbazole-3,9-diyl)bis(*N*,*N*-bis(4-methoxyphenyl)aniline) (69.8 mg, 90.1 µmol, 2.20 equiv.) was added to a crimp cap vial and flushed with Ar three times. 2 mL of dry THF were added and the mixture was cooled to -78 °C. *n*-Butyllithium solution (7.87 mg, 49.2 µL, 123 µmol, 2.50M in hexane, 3.00 equiv.) was added dropwise, and the reaction mixture was allowed to warm to 22 °C. After stirring for 30 min, the reaction mixture was cooled to 0 °C, and zinc chloride solution (22.3 mg, 164 µL, 164 µmol, 1.00M in THF, 4.00 equiv.) was added. The reaction was stirred for 15 min at 0 °C and then warmed to 22 °C.

Negishi coupling:

4,15-Dibromo[2.2]paracyclophane (15.0 mg, 41.0 µmol, 1.00 equiv.) and PEPPSI-IPr catalyst (2.79 mg, 4.10 µmol, 0.100 equiv.) were added to a crimp cap vial and flushed with Ar three times. 2 mL of dry THF were added and zinc chloride solution (16.8 mg, 123 µL, 123 µmol, 1.00M in THF,

3.00 equiv.) was added. After dissolving, the Negishi reactant was added via syringe, and the reaction mixture was heated to 70 °C. After three days, the reaction was allowed to cool to 22 °C, and the solvent was removed under reduced pressure. Column chromatography on silica using cHex/DCM 1:0 to 1:2 as eluent yielded 4,15-(4,4',4",4"'-bis(9*H*-carbazole-6,3,9-triyl))tetrakis(*N,N*-bis(4-methoxyphenyl)aniline)[2.2]paracyclophane (16.0 mg, 9.13 µmol, 22% yield) as dark-red solid.

R_f = 0.42 (cHex/DCM 1:1).

^{1}H NMR (400 MHz, Dichloromethane-d_2 [5.32 ppm], ppm) δ = 8.21–8.20 (m, 2H), 8.13–8.04 (m, 2H), 7.54–6.76 (m, 56H), 6.57–5.99 (m, 6H), 3.72–3.62 (m, 24H), 3.12–2.68 (m, 7H), 2.38 – 2.21 (m, 1H);

MS (ESI), m/z (%): 1752 (0.2) $[M+H]^+$, 774 (57), 773 (100), 608 (35), 324 (33). HRMS (ESI): m/z = calcd for $C_{120}H_{99}N_6O_8$ $[M+H]^+$: 1751.7525; found 1751.9880;

IR (ATR, ṽ) = 3037 (w), 2997 (w), 2951 (w), 2927 (w), 2904 (w), 2870 (w), 2851 (w), 2832 (w), 1602 (w), 1500 (vs), 1473 (s), 1455 (vs), 1439 (s), 1315 (m), 1278 (m), 1262 (m), 1232 (vs), 1177 (s), 1103 (m), 1030 (vs), 952 (w), 909 (w), 882 (w), 824 (vs), 803 (vs), 782 (m), 768 (m), 745 (s), 731 (m), 724 (m), 708 (s), 674 (w), 660 (w), 637 (m), 622 (m), 601 (m), 575 (s), 521 (s), 475 (m), 463 (m), 442 (w), 415 (m), 395 (m), 388 (m), 378 (m) cm^{-1}.

4,16-Divinyl[2.2]paracyclophane (**39**)

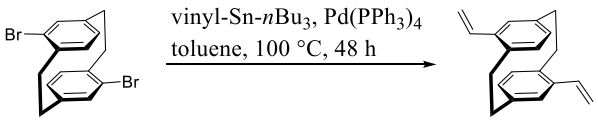

39, 80%

A mixture of 4,16-dibromo[2.2]paracyclophane (500 mg, 1.37 mmol, 1.00 equiv.) and tetrakis(triphenylphosphine)palladium(0) (158 mg, 137 µmol, 0.100 equiv.) was stirred in 75 mL of dry toluene under argon, then tri-*n*-butyl(vinyl)stannane (1.30 g, 1.20 mL, 4.10 mmol, 3.00 equiv.) was added to the reaction mixture. The reaction mixture was heated to 100 °C for 48 hours. Afterward, the solvent was evaporated, and 50 mL of DCM was added to the reaction mixture. The organic layer was washed with 3 x 100 mL of water, dried over Na_2SO_4, and the solvent removed in vacuo. The residue was purified by column chromatography on silica using pentane/DCM 100:1 as eluent to yield 4,16-divinyl[2.2]paracyclophane (284 mg, 1.09 mmol, 80% yield) as a colorless solid.

R_f = 0.20 (pentane/DCM 30:1).

M.p.: 176 °C

^{1}H NMR (400 MHz, Chloroform-d [7.26 ppm], ppm) δ = 6.81 (dd, *J* = 17.4 Hz, *J* = 10.9 Hz, 2H, vinyl-C*H*), 6.67 (dd, *J* = 7.7 Hz, *J* = 1.9 Hz, 2H, CH_{Ar}), 6.54 (d, *J* = 1.9 Hz, 2H, CH_{Ar}), 6.33 (d, *J* = 7.7 Hz, 2H, CH_{Ar}), 5.54 (dd, *J* = 17.4 Hz, *J* = 1.4 Hz, 2H, vinyl-CH_2), 5.28 (dd, *J* = 10.9 Hz, *J* = 1.4 Hz, 2H, vinyl-CH_2), 3.47 (ddd, *J* = 13.1 Hz, *J* = 10.0 Hz, *J* = 2.7 Hz, 2H, PCP-CH_2), 3.10–2.90 (m, 4H, PCP-CH_2), 2.83 (ddd, *J* = 13.5 Hz, *J* = 10.6 Hz, *J* = 5.7 Hz, 2H, PCP-CH_2);

^{13}C NMR (100 MHz, Chloroform-d [77.16 ppm], ppm) δ = 139.4 (C_q, 2C), 137.7 (C_q, 2C), 137.7 (C_q, 2C), 135.3 (+, *C*H, 2C, vinyl-*C*H), 133.4 (+, *C*H, 2C, *C*H$_{Ar}$), 130.1 (+, *C*H, 2C, *C*H$_{Ar}$), 129.3 (+, *C*H, 2C, *C*H$_{Ar}$), 114.3 (–, *C*H_2, 2C, vinyl-*C*H_2), 34.3 (–, *C*H_2, 2C, PCP-*C*H_2), 33.0 (–, *C*H_2, 2C, PCP-*C*H_2);

MS (EI, 70 eV, 60 °C), m/z (%): 260 (32) $[M]^+$, 131 (44), 130 (55), 129 (100), 128 (54), 127 (20), 115 (78). HRMS (EI): m/z = calcd for $C_{20}H_{20}$ $[M]^+$: 260.1560; found 260.1559;

IR (ATR, ṽ) = 3092 (vw), 3041 (vw), 3024 (w), 3010 (w), 2983 (vw), 2934 (m), 2919 (m), 2900 (m), 2870 (w), 2850 (m), 1895 (vw), 1884 (vw), 1816 (w), 1738 (vw), 1622 (w), 1588 (w), 1551 (w), 1479 (w), 1459 (w), 1436 (w), 1417 (w), 1375 (w), 1310 (w), 1279 (w), 1248 (w), 1222 (w), 1200 (w), 1157 (vw), 1142 (w), 1081 (vw), 1047 (w), 986 (s), 946 (w), 928 (w), 907 (vs), 877 (vs), 850 (m), 798 (w), 776 (m), 765 (s), 734 (w), 687 (w), 667 (vs), 603 (w), 548 (w), 509 (w), 465 (w), 459 (w), 428 (m), 390 (w) cm^{-1}.

Additional information on chemical synthesis is available *via* the Chemotion repository:

https://doi.org/10.14272/reaction/SA-FUHFF-UHFFFADPSC-TTXZIYBDKN-UHFFFADPSC-NUHFF-NUHFF-NUHFF-ZZZ

Additional information on the analysis of the target compound is available *via* the Chemotion repository:

https://doi.org/10.14272/TTXZIYBDKNEJBG-UHFFFAOYSA-N.1

4,15-Divinyl[2.2]paracyclophane (**40**)

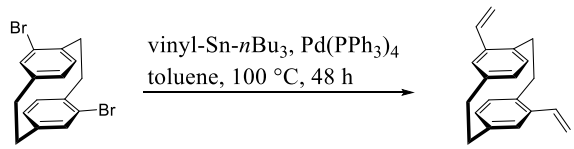

40, 52%

A mixture of 4,15-dibromo[2.2]paracyclophane (500 mg, 1.37 mmol, 1.00 equiv.) and tetrakis(triphenylphosphine)palladium(0) (158 mg, 137 µmol, 0.100 equiv.) in 100 mL of dry toluene was stirred under argon, then tri-*n*-butyl(vinyl)stannane (1.52 g, 1.40 mL, 4.78 mmol, 3.50 equiv.) was added to the reaction mixture. The reaction mixture was heated at 100 °C for 48 h. Afterward, the

solvent was evaporated, and 50 mL of DCM was added. The organic layer was washed with 3 x 100 mL of water, dried over Na_2SO_4, and the solvent removed in vacuo. The residue was purified by column chromatography on silica using pentane/DCM 100:1 as eluent to yield 4,15-divinyl[2.2]paracyclophane (185 mg, 711 µmol, 52% yield) as a colorless solid.

R_f = 0.22 (pentane/DCM 30:1).

M.p.: 105 °C

^{1}H NMR (400 MHz, Chloroform-d [7.26 ppm], ppm) δ = 6.79 (dd, *J* = 17.4 Hz, *J* = 10.9 Hz, 2H, vinyl-C*H*), 6.68 (d, *J* = 7.8 Hz, 2H, CH_{Ar}), 6.62 (d, *J* = 1.9 Hz, 2H, CH_{Ar}), 6.36 (dd, *J* = 7.8 Hz, *J* = 1.9 Hz, 2H, CH_{Ar}), 5.57 (dd, *J* = 17.4 Hz, *J* = 1.4 Hz, 2H, vinyl-CH_2), 5.29 (dd, *J* = 10.9 Hz, *J* = 1.4 Hz, 2H, vinyl-CH_2), 3.44–3.36 (m, 2H, PCP-CH_2), 3.15–3.05 (m, 2H, PCP-CH_2), 3.02–2.91 (m, 2H, PCP-CH_2), 2.85–2.73 (m, 2H, PCP-CH_2;

^{13}C NMR (100 MHz, Chloroform-d [77.16 ppm], ppm) δ = 139.6 (C_q, 2C, C_{Ar}), 138.2 (C_q, 2C, C_{Ar}), 137.7 (C_q, 2C, C_{Ar}), 135.0 (+, CH, 2C, vinyl *C*H), 131.1 (+, CH, 2C, *C*H$_{Ar}$), 130.8 (+, CH, 2C, *C*H$_{Ar}$), 129.6 (+, CH, 2C, *C*H$_{Ar}$), 114.1 (–, CH_2, 2C, vinyl CH_2), 35.0 (–, CH_2, 2C, PCP-*C*H_2), 32.8 (–, CH_2, 2C, PCP-*C*H_2);

MS (EI, 70 eV, 40 °C), m/z (%): 260 (41) $[M]^+$, 131 (36), 130 (41), 129 (100), 115 (35). HRMS (EI): m/z = calcd for $C_{20}H_{20}$ $[M]^+$: 260.1560; found 260.1561;

IR (ATR, $\tilde{\nu}$) = 3081 (w), 3040 (vw), 3006 (w), 2979 (w), 2949 (w), 2925 (m), 2904 (w), 2888 (w), 2851 (w), 1895 (vw), 1820 (w), 1618 (m), 1588 (w), 1553 (w), 1480 (m), 1456 (w), 1442 (w), 1432 (w), 1415 (m), 1307 (w), 1276 (w), 1222 (w), 1201 (w), 1187 (w), 1173 (w), 1157 (w), 1137 (w), 1047 (w), 986 (vs), 943 (w), 908 (vs), 890 (vs), 873 (s), 807 (m), 749 (vs), 676 (s), 663 (vs), 630 (w), 578 (w), 561 (m), 499 (m), 463 (w), 439 (m), 387 (w) cm^{-1}.

Additional information on chemical synthesis is available *via* the Chemotion repository:

https://doi.org/10.14272/reaction/SA-FUHFF-UHFFFADPSC-FURJPBBXDV-UHFFFADPSC-NUHFF-NUHFF-NUHFF-ZZZ

Additional information on the analysis of the target compound is available *via* the Chemotion repository:

https://doi.org/10.14272/FURJPBBXDVSGQT-UHFFFAOYSA-N.1

4-(5-Bromo-2-thienyl)phenyl-bis(4-methoxyphenyl)amine (41)

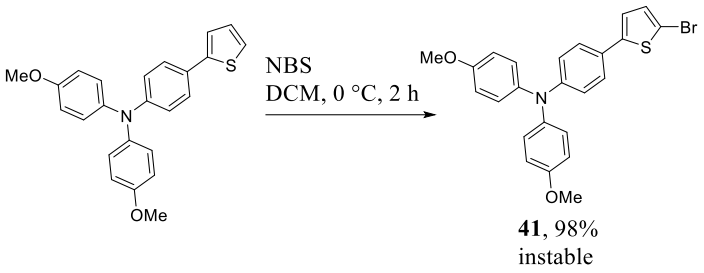

N,N-Bis(4-methoxyphenyl)-4-thiophen-2-ylaniline (120 mg, 310 µmol, 1.00 equiv.) was dissolved in 10 mL of DCM at 0 °C. *N*-Bromosuccinimide (60.6 mg, 341 µmol, 1.10 equiv.) was added portionwise, stirring the reaction mixture for 2 h. The organic phase was washed four times with 10 mL water, dried over Na_2SO_4, and concentrated in vacuo. Flash column chromatography on silica gel using pentane/DCM 2:1 as eluent afforded 4-(5-bromo-2-thienyl)phenyl-bis(4-methoxyphenyl)amine (142 mg, 305 µmol, 98% yield) as a colorless solid.

The product is instable and must be used immediately.

^{1}H NMR (400 MHz, THF-d_8 [3.58 ppm], ppm) δ = 7.34 – 7.28 (m, 2H), 7.05 – 7.01 (m, 4H), 7.01 (d, *J* = 2.7 Hz, 2H), 6.87 – 6.83 (m, 6H), 3.75 (s, 6H).

4,16-(Bis(ethenyl-thiophene-5,2-diyl-*N,N*-bis(4-methoxyphenyl)aniline)[2.2]paracyclophane (42)

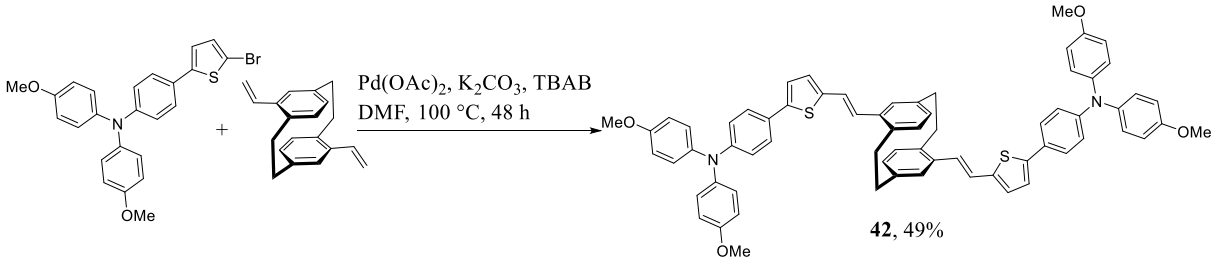

4,16-Divinyl[2.2]paracyclophane (30.0 mg, 115 µmol, 1.00 equiv.), 4-(5-bromothiophen-2-yl)-*N,N*-bis(4-methoxyphenyl)aniline (113 mg, 242 µmol, 2.10 equiv.), $Pd(OAc)_2$ (3.88 mg, 17.3 µmol, 0.150 equiv.), tetrabutylammonium bromide (37.1 mg, 115 µmol, 1.00 equiv.), and dipotassium carbonate (47.8 mg, 346 µmol, 3.00 equiv.) were dissolved in 4 mL of dry DMF. The solution was stirred at 100 °C for 48 h. 50 mL of water was added, and the solution was extracted with 3 x 10 mL of DCM. After drying over Na_2SO_4, the solvent was removed under vacuum. The residue was subjected to column chromatography on silica using pentane/DCM 1:1 as an eluent to yield 4,16-(bis(ethenyl-thiophene-5,2-diyl-*N,N*-bis(4-methoxyphenyl)aniline)[2.2]paracyclophane (58.1 mg, 92% purity 56.3 µmol, 49% yield) as yellow solid.

Because of the low purity, no ^{13}C or 2D NMR could be recorded.

R_f = 0.43 (pentane/DCM 1:1).

M.p.: 92 °C

^{1}H NMR (400 MHz, THF-d_8 [3.58 ppm], ppm) δ = 7.48–7.42 (m, 4H), 7.17 (d, *J* = 3.7 Hz, 2H), 7.12–6.96 (m, 14H), 6.93–6.80 (m, 12H), 6.69 (d, *J* = 1.8 Hz, 2H), 6.63 (dd, *J* = 7.8 Hz, *J* = 1.7 Hz, 2H), 6.38 (d, *J* = 7.8 Hz, 2H), 3.76 (s, 12H), 3.61–3.55 (m, 2H), 3.12–2.86 (m, 6H);

MS (ESI), m/z (%): 1030 (11) $[M]^+$, 516 (74), 515 (100), 322 (49), 221 (28). HRMS (ESI): m/z = calcd for $C_{68}H_{58}N_2O_4{}^{32}S_2$ $[M]^+$: 1030.3838; found 1030.3805;

IR (ATR, ṽ) = 3027 (w), 2997 (w), 2922 (m), 2850 (m), 2833 (w), 1599 (m), 1499 (vs), 1451 (s), 1439 (s), 1317 (m), 1283 (m), 1235 (vs), 1191 (s), 1177 (s), 1164 (s), 1103 (m), 1085 (m), 1031 (vs), 945 (m), 911 (w), 897 (w), 880 (w), 823 (vs), 793 (vs), 721 (m), 701 (m), 656 (w), 635 (w), 602 (w), 574 (vs), 554 (m), 511 (s), 469 (m), 445 (w), 432 (w), 421 (w), 408 (w), 391 (w), 382 (w) cm^{-1}.

4,15-(Bis(ethenyl-thiophene-5,2-diyl-*N,N*-bis(4-methoxyphenyl)aniline)[2.2]paracyclophane (43)

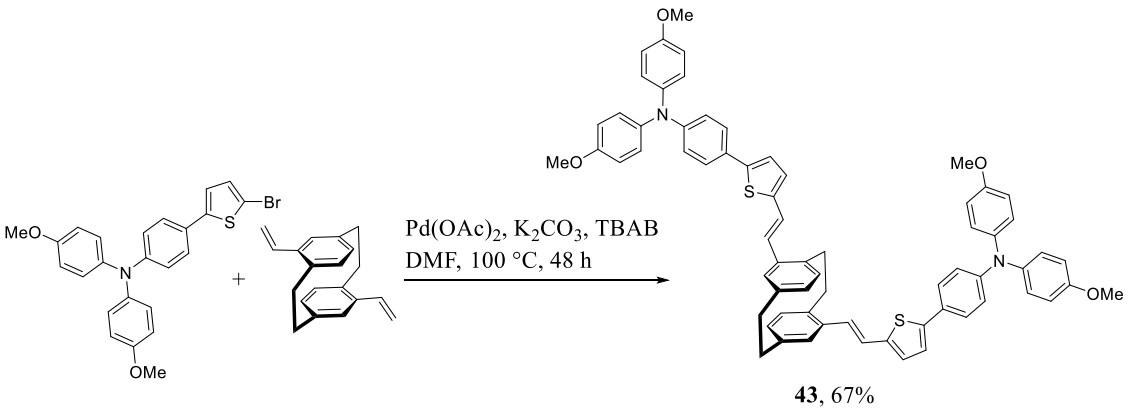

43, 67%

4,15-Divinyl[2.2]paracyclophane (30.0 mg, 115 µmol, 1.00 equiv.), 4-(5-bromothiophen-2-yl)-*N,N*-bis(4-methoxyphenyl)aniline (113 mg, 242 µmol, 2.10 equiv.), $Pd(OAc)_2$ (3.88 mg, 17.3 µmol, 0.150 equiv.), tetrabutylammonium bromide (37.1 mg, 115 µmol, 1.00 equiv.), and dipotassium carbonate (47.8 mg, 346 µmol, 3.00 equiv.) were dissolved in 4 mL of dry DMF. The solution was stirred at 100 °C for 48 h. 50 mL of water was added, and the solution was extracted with 3 x 10 mL of DCM. After drying over Na_2SO_4, the solvent was removed under vacuum. The residue was subjected to column chromatography on silica using pentan/DCM 1:1 as an eluent to yield 4,15-(bis(ethenyl-thiophene-5,2-diyl-*N,N*-bis(4-methoxyphenyl)aniline)[2.2]paracyclophane (79.1 mg, 80% purity, 76.7 µmol, 67% yield) as yellow solid.

Because of the low purity, no ^{13}C or 2D NMR could be recorded.

R_f = 0.42 (pentane/DCM 1:1).

M.p.: 82 °C

^{1}H NMR (400 MHz, THF-d_8 [3.58 ppm], ppm) δ = 7.48–7.42 (m, 4H), 7.18 (d, *J* = 3.7 Hz, 2H), 7.09–6.95 (m, 12H), 6.90–6.82 (m, 14H), 6.75 (d, *J* = 1.7 Hz, 2H), 6.67 (d, *J* = 7.8 Hz, 2H), 6.39 (dd, *J* = 7.8 Hz, *J* = 1.8 Hz, 2H), 3.76 (s, 12H, OMe-CH_3), 3.56–3.45 (m, 2H, PCP-CH_2), 3.10–2.81 (m, 6H, PCP-CH_2);

MS (ESI), m/z (%): 1030 (17) $[M]^+$, 773 (52), 772 (100), 516 (29), 515 (38). HRMS (ESI): m/z = calcd for $C_{68}H_{58}N_2O_4{}^{32}S_2$ $[M]^+$: 1030.3838; found 1030.3826;

IR (ATR, ṽ) = 3037 (w), 3002 (w), 2922 (m), 2847 (w), 2832 (w), 1599 (w), 1499 (vs), 1449 (s), 1439 (s), 1317 (m), 1283 (m), 1266 (m), 1235 (vs), 1191 (s), 1177 (s), 1164 (s), 1103 (m), 1031 (vs), 943 (m), 912 (w), 892 (w), 823 (vs), 792 (vs), 721 (s), 701 (m), 662 (w), 649 (w), 633 (w), 601 (w), 574 (vs), 520 (s), 514 (s), 490 (m), 470 (m), 449 (w), 421 (w), 408 (m), 390 (w), 381 (w) cm^{-1}.

4-(5-Bromothieno[3,2-b]thiophen-2-yl)-*N,N*-bis(4-methoxyphenyl)aniline (44)

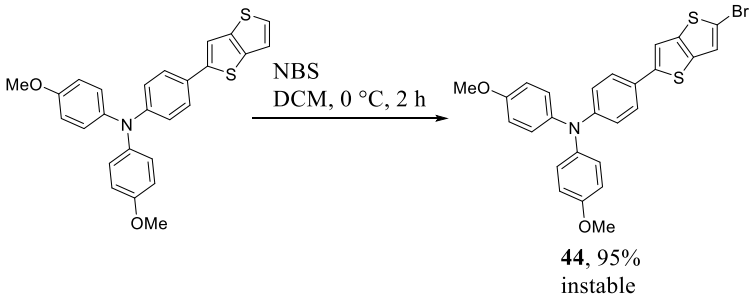

44, 95%
instable

4-Methoxy-*N*-(4-methoxyphenyl)-*N*-(4-(thieno[3,2-b]thiophen-2-yl)phenyl)aniline (700 mg, 1.58 mmol, 1.00 equiv.) was dissolved in 55 mL of DCM at 0 °C. *N*-Bromosuccinimide (351 mg, 1.97 mmol, 1.25 equiv.) was added portionwise, and the reaction mixture stirred for 2 h. The organic phase was washed four times with 50 mL water, dried over Na_2SO_4, and concentrated in vacuo. Flash column chromatography on silica gel using pentane/DCM 2:1 as eluent afforded 4-(5-bromothieno[3,2-b]thiophen-2-yl)-*N,N*-bis(4-methoxyphenyl)aniline (820 mg, 1.57 mmol, 99% yield) as a colorless solid.

The product is instable and must be used immediately.

^{1}H NMR (400 MHz, THF-d_8 [3.58 ppm], ppm) δ = 7.45 (s, 1H), 7.44–7.36 (m, 3H), 7.10–7.01 (m, 4H), 6.98–6.90 (m, 2H), 6.89–6.81 (m, 4H), 3.77 (s, 6H, OMe-CH_3);

4,15-(Bis(ethenyl-thieno[3,2-b]thiophene-5,2-diyl-*N,N*-bis(4-methoxyphenyl)aniline) [2.2]paracyclophane (46)

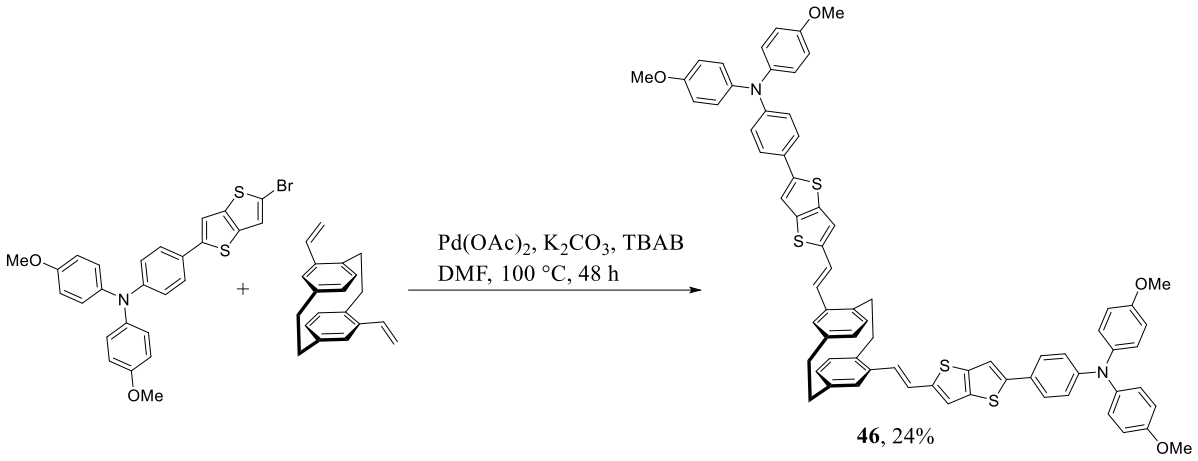

4,15-Divinyl[2.2]paracyclophane (30.0 mg, 115 µmol, 1.00 equiv.), 4-(5-bromothienothiophen-2-yl)-*N,N*-bis(4-methoxyphenyl)aniline (120 mg, 230 µmol, 2.00 equiv.), $Pd(OAc)_2$ (3.88 mg, 17.3 µmol, 0.150 equiv.), tetrabutylammonium bromide (37.1 mg, 115 µmol, 1.00 equiv.), and dipotassium carbonate (47.8 mg, 346 µmol, 3.00 equiv.) were dissolved in 4 mL of dry DMF. The solution was stirred at 100 °C for 48 h. 50 mL of water was added, and the solution was extracted with 3 x 10 mL of DCM. After drying over Na_2SO_4, the solvent was removed under vacuum. The residue was subjected to column chromatography on silica using pentane/DCM 1:1 as an eluent to yield 4,15-(bis(ethenyl-thieno[3,2-b]thiophene-5,2-diyl-*N,N*-bis(4-methoxyphenyl)aniline)[2.2]paracyclophane (31.0 mg, 75% purity, 27.1 µmol, 24% yield) as yellow solid.

Because of the low purity, no ^{13}C or 2D NMR could be recorded.

R_f = 0.42 (pentane/DCM 1:1).

M.p.: 115 °C

^1H NMR (400 MHz, Dichloromethane-d_2 [5.32 ppm], ppm) δ = 7.52–7.48 (m, 2H), 7.42–7.34 (m, 4H), 7.29 (d, *J* = 2.1 Hz, 2H), 7.15–7.04 (m, 12H), 6.92–6.82 (m, 16H), 6.77–6.65 (m, 2H), 6.50–6.37 (m, 2H), 3.80–3.76 (m, 13H, OMe-CH_3 +PCP-CH_2), 3.59–3.46 (m, 1H, PCP-CH_2), 3.22–2.81 (m, 4H, PCP-CH_2);

MS (ESI), m/z (%): 1142 (11) $[M]^+$, 964 (54), 962 (43), 885 (61), 884 (100), 571 (35), 482 (40), 481 (29), 443 (38), 442 (63), 413 (79). HRMS (ESI): m/z = calcd for $C_{72}H_{58}N_2O_4{}^{32}S_4$ $[M]^+$: 1142.3280; found 1142.3312;

IR (ATR, ṽ) = 3036 (w), 2993 (w), 2945 (w), 2921 (m), 2904 (m), 2868 (w), 2850 (w), 2830 (m), 2775 (w), 1598 (m), 1500 (vs), 1483 (vs), 1458 (s), 1438 (s), 1317 (m), 1283 (m), 1234 (vs), 1193 (s), 1174 (vs), 1163 (vs), 1103 (s), 1031 (vs), 941 (m), 911 (m), 823 (vs), 800 (vs), 781 (s), 756 (m), 720 (s), 700

(s), 676 (m), 650 (m), 633 (m), 574 (vs), 518 (vs), 486 (s), 466 (m), 452 (m), 419 (m), 407 (m), 394 (m), 380 (m) cm^{-1}.

4,16-(4,4'-((Bis(ethene-2,1-diyl))bis(dibenzo[b,d]thiophene-8,2-diyl))bis(*N,N*-bis(4-methoxyphenyl)aniline)[2.2]paracyclophane (**47**)

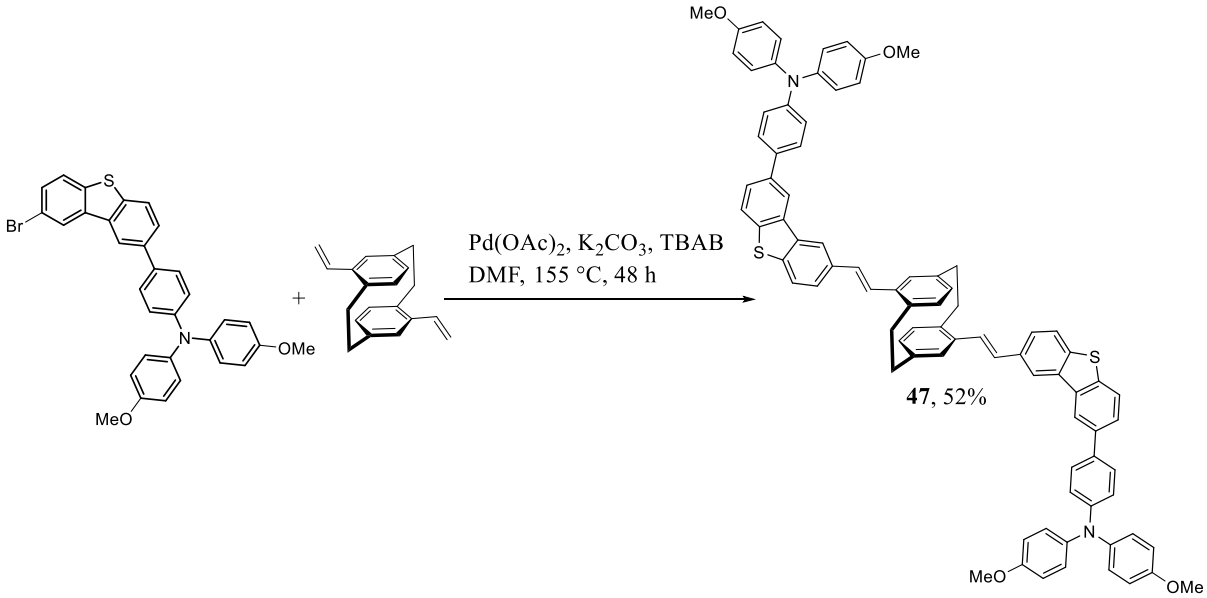

In a vial, 4,12-divinyl[2.2]paracyclophane (30.0 mg, 115 µmol, 1.00 equiv.), 4-(8-bromodibenzothiophen-2-yl)-*N,N*-bis(4-methoxyphenyl)aniline (137 mg, 242 µmol, 2.10 equiv.), $Pd(OAc)_2$ (3.88 mg, 17.3 µmol, 0.150 equiv.), tetrabutylammonium bromide (37.1 mg, 115 µmol, 1.00 equiv.), and dipotassium carbonate (47.8 mg, 346 µmol, 3.00 equiv) were dissolved in 2 mL of anhydrous DMF. The resulting mixture was stirred at 155 °C for 24 h. After cooling, 10 mL of DCM was added. The mixture was washed with 3 x 30 mL water and dried over Na_2SO_4. The organic solvent was removed under vacuum, and the crude product was purified by column chromatography on silica using cHex/DCM 4:1 to 1:2 as eluent to yield 4,16-(4,4'-((bis(ethene-2,1-diyl))bis(dibenzo[b,d]thiophene-8,2-diyl))bis(*N,N*-bis(4-methoxyphenyl)aniline)[2.2]paracyclophane (74.1 mg, 60.3 µmol, 52% yield) as yellow solid.

Because of the low solubility, no ^{13}C could be recorded.

R_f = 0.38 (cHex/DCM 1:1).

M.p.: 243 °C

^1H NMR (400 MHz, Dichloromethane-d_2 [5.32 ppm], ppm) δ = 8.43 (dd, *J* = 11.8 Hz, *J* = 1.8 Hz, 3H), 7.92 (dd, *J* = 8.3 Hz, *J* = 1.8 Hz, 3H), 7.78 (dd, *J* = 8.4 Hz, *J* = 1.7 Hz, 2H), 7.72 (dd, *J* = 8.3 Hz, *J* = 1.8 Hz, 2H), 7.62–7.60 (m, 4H), 7.40 (d, *J* = 16.2 Hz, 2H), 7.19–7.04 (m, 16H), 6.89–6.80 (m, 12H),

6.73 (dd, J = 7.3 Hz, J = 1.6 Hz, 2H), 6.50 (d, J = 7.8 Hz, 2H), 3.80 (s, 12H), 3.73–3.68 (m, 2H), 3.21–2.97 (m, 6H);

MS (ESI), m/z (%): 1248 (14) $[M+H+NH_4]^+$, 1230 (17) $[M+H]^+$, 616 (71), 615 (90), 501 (48), 431 (90), 320 (100), 319 (72). HRMS (ESI): m/z = calcd for $^{12}C_{85}{}^{13}CH_{69}O_4S_2$ $[M+H]^+$: 1230.4671; found 1230.4442;

IR (ATR, $\tilde{\nu}$) = 2946 (w), 2922 (w), 2850 (w), 2832 (w), 2791 (w), 1601 (w), 1500 (vs), 1460 (s), 1436 (s), 1380 (w), 1317 (w), 1278 (m), 1261 (m), 1235 (vs), 1194 (m), 1177 (m), 1164 (m), 1103 (m), 1084 (w), 1069 (w), 1031 (s), 953 (w), 911 (w), 877 (w), 824 (s), 803 (vs), 725 (w), 710 (w), 688 (w), 639 (w), 605 (w), 577 (w), 565 (w), 518 (w), 416 (w) cm^{-1}.

Additional information on chemical synthesis is available *via* the Chemotion repository:

https://doi.org/10.14272/reaction/SA-FUHFF-UHFFFADPSC-MAPYDYSIRU-UHFFFADPSC-NUHFF-NRTVQ-NUHFF-ZZZ

Additional information on the analysis of the target compound is available *via* the Chemotion repository:

https://doi.org/10.14272/MAPYDYSIRUOQRZ-BEQMOXJMSA-N.1

4,16-Bis[(trimethylsilyl)ethynyl][2.2]paracyclophane (48)

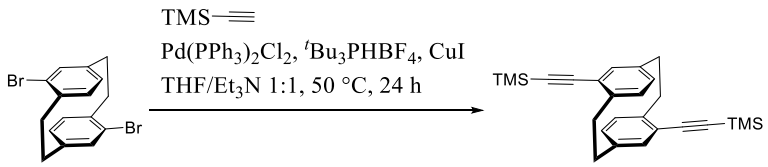

48, 81%

4,16-Dibromo[2.2]paracyclophane (1.50 g, 4.10 mmol, 1.00 equiv.), tri-*tert*-butylphosphonium tetrafluoroborate (333 mg, 1.15 mmol, 0.280 equiv.), bis(triphenylphosphine)palladium(II) dichloride (288 mg, 410 µmol, 0.100 equiv.), and copper(I) iodide (109 mg, 574 µmol, 0.140 equiv.) were dissolved in 60 mL of dry THF and 60 mL of dry triethylamine. A stream of argon degassed the mixture for 15 min. Trimethylsilylacetylene (2.41 g, 3.50 mL, 24.6 mmol, 6.00 equiv.) was added slowly, and the reaction mixture was stirred for 24 h at 50 °C. The solvent was removed under reduced pressure, and the crude solid was purified by flash column chromatography on silica using pentane/DCM 9:1 as eluent to obtain 4,16-bis[(trimethylsilyl)ethynyl][2.2]paracyclophane (1.34 g, 3.33 mmol, 81% yield) as an off-white solid.

R_f = 0.39 (pentane/DCM 10:1).

M.p.: 95-105 °C

^{1}H NMR (400 MHz, Chloroform-d [7.26 ppm], ppm) δ = 6.99 (dd, *J* = 7.9 Hz, *J* = 1.9 Hz, 2H, C*H*$_{Ar}$), 6.49 (d, *J* = 1.9 Hz, 2H, C*H*$_{Ar}$), 6.44 (d, *J* = 7.8 Hz, 2H, C*H*$_{Ar}$), 3.57 (ddd, *J* = 13.1 Hz, *J* = 10.4 Hz, *J* = 2.9 Hz, 2H, PCP-C*H*$_2$), 3.15 (ddd, *J* = 12.8 Hz, *J* = 10.4 Hz, *J* = 4.7 Hz, 2H, PCP-C*H*$_2$), 2.97 (ddd, *J* = 13.1 Hz, *J* = 10.5 Hz, *J* = 2.9 Hz, 2H, PCP-C*H*$_2$), 2.83 (ddd, *J* = 12.9 Hz, *J* = 10.6 Hz, *J* = 4.7 Hz, 2H, PCP-C*H*$_2$), 0.32 (s, 18H, TMS-C*H*$_3$);

^{13}C NMR (100 MHz, Chloroform-d [77.16 ppm], ppm) δ = 142.6 (C$_q$, 2C, *C*$_{Ar}$), 139.3 (C$_q$, 2C, *C*$_{Ar}$), 137.4 (+, CH, 2C, *C*H$_{Ar}$), 133.0 (+, CH, 2C, *C*H$_{Ar}$), 130.1 (+, CH, 2C, *C*H$_{Ar}$), 124.6 (C$_q$, 2C, *C*$_{Ar}$), 105.8 (C$_q$, 2C, *C*$_{alkyne}$), 97.5 (C$_q$, 2C, *C*$_{alkyne}$), 34.0 (–, CH$_2$, 2C, PCP-*C*H$_2$), 33.6 (–, CH$_2$, 2C, PCP-*C*H$_2$), 0.2 (+, CH$_3$, 6C, TMS-*C*H$_3$);

MS (FAB, 3-NBA), m/z (%): 400 (17) [M]$^+$, 155 (30), 154 (100), 138 (35), 137 (64), 136 (73). HRMS (FAB, matrix NBA): m/z = calcd for $C_{26}H_{32}{}^{28}Si_2$ [M]$^+$: 400.2037; found 400.2038;

IR (ATR, ṽ) = 2955 (w), 2929 (w), 2895 (w), 2850 (w), 2145 (m), 2108 (vw), 1588 (vw), 1476 (w), 1448 (vw), 1432 (w), 1405 (w), 1320 (vw), 1259 (w), 1244 (s), 1205 (vw), 1142 (vw), 1091 (w), 955 (w), 941 (w), 897 (w), 881 (w), 834 (vs), 781 (s), 754 (vs), 730 (s), 694 (m), 662 (w), 645 (s), 599 (w), 564 (vw), 555 (w), 544 (w), 520 (vw), 494 (s), 412 (w), 385 (w) cm^{-1}.

Additional information on chemical synthesis is available *via* the Chemotion repository:

https://doi.org/10.14272/reaction/SA-FUHFF-UHFFFADPSC-LDEBDNXBXN-UHFFFADPSC-NUHFF-NUHFF-NUHFF-ZZZ

Additional information on the analysis of the target compound is available *via* the Chemotion repository:

https://doi.org/10.14272/LDEBDNXBXNZBJK-UHFFFAOYSA-N.1

4,16-Diethynyl[2.2]paracyclophane (**49**)

49, 65%

4,16-Bis((trimethylsilyl)ethynyl)[2.2]paracyclophane (1.00 g, 2.50 mmol, 1.00 equiv.) and tetrabutylammonium fluoride hydrate (5.23 g, 18.7 mmol, 7.50 equiv.) were added together in 20 mL of DCM and stirred for 16 h at 21 °C. Afterward, the mixture was washed with 150 mL of water, dried over Na_2SO_4, and the solvent was evaporated. Column chromatography on silica using pentane/DCM

10:1 as eluent yielded 4,16-diethynyl[2.2]paracyclophane (413 mg, 1.61 mmol, 65% yield) as a colorless solid.

R_f = 0.63 (pentane/DCM 10:1).

M.p.: 205 °C

^{1}H NMR (400 MHz, Chloroform-d [7.26 ppm], ppm) δ = 7.00 (d, *J* = 7.9 Hz, 2H), 6.56 (s, 2H), 6.45 (d, *J* = 8.0 Hz, 2H), 3.62–3.54 (m, 2H), 3.27 (s, 2H), 3.23–3.15 (m, 2H), 3.01–2.94 (m, 2H), 2.91–2.83 (m, 2H);

^{13}C NMR (100 MHz, Chloroform-d [77.16 ppm], ppm) δ = 142.7 (C_q, 2C), 139.6 (C_q, 2C), 137.9 (+, CH, 2C), 133.3 (+, CH, 2C), 130.6 (+, CH, 2C), 123.6 (C_q, 2C), 83.9 (C_q, 2C, C_{alkyne}), 80.3 (+, CH, 2C, C_{alkyne}), 33.8 (–, CH_2, 4C, PCP-CH_2);

MS (EI, 70 eV, 140 °C), m/z (%): 256 (47) $[M]^+$, 128 (100). HRMS (EI): m/z = calcd for $C_{20}H_{16}$ $[M]^+$: 256.1247; found 256.1245;

IR (ATR, $\tilde{\nu}$) = 3291 (w), 3272 (m), 3043 (w), 2955 (w), 2927 (w), 2888 (w), 2850 (w), 2567 (vw), 2096 (vw), 1587 (w), 1548 (vw), 1479 (w), 1448 (vw), 1432 (w), 1402 (w), 1320 (vw), 1273 (vw), 1242 (w), 1204 (w), 1154 (w), 1139 (w), 1086 (vw), 946 (vw), 931 (w), 897 (m), 874 (m), 846 (w), 758 (w), 721 (m), 653 (vs), 625 (vs), 605 (vs), 560 (m), 538 (m), 513 (w), 494 (vs), 466 (s), 433 (w), 421 (w), 395 (w), 381 (w) cm^{-1}.

Additional information on chemical synthesis is available *via* the Chemotion repository:

https://doi.org/10.14272/reaction/SA-FUHFF-UHFFFADPSC-BMYMQUMNIX-UHFFFADPSC-NUHFF-NUHFF-NUHFF-ZZZ

Additional information on the analysis of the target compound is available *via* the Chemotion repository:

https://doi.org/10.14272/BMYMQUMNIXYUGD-UHFFFAOYSA-N.1

4,15-Bis[(trimethylsilyl)ethynyl][2.2]paracyclophane (50)

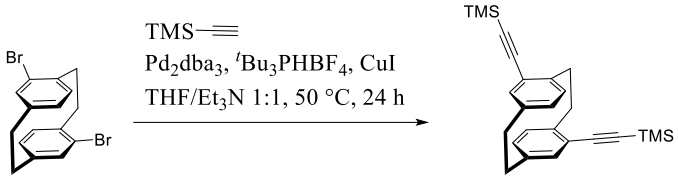

50, 85%

4,15-Dibromo[2.2]paracyclophane (1.50 g, 4.10 mmol, 1.00 equiv.), tri-*tert*-butylphosphonium tetrafluoroborate (333 mg, 1.15 mmol, 0.280 equiv.) tris(dibenzylidenaceton)dipalladium(0) (263 mg, 0.287 mmol, 0.0700 equiv.), and copper(I) iodide (109 mg, 574 µmol, 0.140 equiv.) were dissolved in 60 mL of dry THF and 60 mL of dry triethylamine. A stream of argon degassed the mixture for 15 min. Trimethylsilylacetylene (2.41 g, 3.50 mL, 24.6 mmol, 6.00 equiv.) was added slowly, and the reaction mixture was stirred for 24 h at 50 °C. The solvent was removed under reduced pressure, and the crude solid was purified by flash column chromatography on silica using pentane/DCM, 9:1 to obtain the title compound 4,15-bis[(trimethylsilyl)ethynyl][2.2]paracyclophane (1.39 g, 3.47 mmol, 85% yield) as an off-white solid.

R_f = 0.39 (pentane/DCM 10:1).

M.p.: 201 °C

^{1}H NMR (400 MHz, Chloroform-d [7.26 ppm], ppm) δ = 7.00 (d, *J* = 7.8 Hz, 2H, C*H*$_{Ar}$), 6.53 (d, *J* = 1.9 Hz, 2H, C*H*$_{Ar}$), 6.50 (dd, *J* = 7.9, 2.0 Hz, 2H, C*H*$_{Ar}$), 3.51–3.44 (m, 2H, PCP-CH_2), 3.10–2.99 (m, 4H, PCP-CH_2), 2.95–2.87 (m, 2H, PCP-CH_2), 0.31 (s, 18H, TMS-CH_3);

^{13}C NMR (100 MHz, Chloroform-d [77.16 ppm], ppm) δ = 143.0 (C_q, 2C, $C_{Ar,}$), 139.3 (C_q, 2C, $C_{Ar,}$), 136.7 (+, CH, 2C, $CH_{Ar,}$), 132.3 (+, CH, 2C, CH_{Ar}), 130.0 (+, CH, 2C, CH_{Ar}), 125.4 (C_q, 2C, C_{Ar}), 105.6 (C_q, 2C, alkyne-C), 97.8 (C_q, 2C, alkyne-C), 34.8 (–, CH_2, 2C, PCP-CH_2), 32.8 (–, CH_2, 2C, PCP-CH_2), 0.1 (+, CH_3, 6C, TMS-CH_3);

MS (FAB, 3-NBA), m/z (%): 401 (90) $[M+H]^+$, 400 (25) $[M]^+$, 201 (46), 200 (100), 185 (94), 155 (32), 154 (66), 137 (39), 136 (69). HRMS (FAB, matrix NBA): m/z = calcd for $C_{26}H_{33}{}^{28}Si_2$ $[M+H]^+$: 401.2115; found 401.2114;

IR (ATR, $\tilde{\nu}$) = 2958 (w), 2928 (w), 2897 (vw), 2853 (vw), 2142 (w), 1482 (vw), 1448 (vw), 1428 (vw), 1405 (w), 1247 (m), 1088 (vw), 953 (w), 897 (w), 837 (vs), 756 (vs), 724 (m), 698 (w), 671 (w), 646 (m), 618 (w), 602 (vw), 551 (w), 511 (w), 492 (m), 418 (vw), 381 (w) cm^{-1}.

Additional information on chemical synthesis is available *via* the Chemotion repository:

https://doi.org/10.14272/reaction/SA-FUHFF-UHFFFADPSC-XJXYEEJOVF-UHFFFADPSC-NUHFF-NUHFF-NUHFF-ZZZ

Additional information on the analysis of the target compound is available *via* the Chemotion repository:

https://doi.org/10.14272/XJXYEEJOVFDEHB-UHFFFAOYSA-N.1

4,15-Diethynyl[2.2]paracyclophane (51)

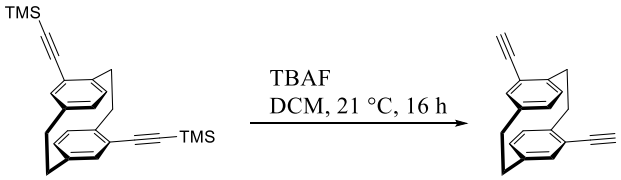

51, 68%

4,15-Bis((trimethylsilyl)ethynyl)[2.2]paracyclophane (1.40 g, 3.49 mmol, 1.00 equiv.) and tetrabutylammonium fluoride hydrate (7.32 g, 26.2 mmol, 7.50 equiv.) were added together in 30 mL of DCM and stirred 16 h at 21 °C. Afterward, the mixture was washed with 200 mL water, dried over Na_2SO_4, and the solvent was evaporated. Column chromatography on silica using pentane/DCM 10:1 as eluent yielded 4,15-diethynyl[2.2]paracyclophane (649 mg, 2.38 mmol, 68% yield) as a colorless solid.

R_f = 0.63 (pentane/DCM 10:1).

M.p.: 133 °C

^{1}H NMR (400 MHz, Chloroform-d [7.26 ppm], ppm) δ = 7.00 (d, *J* = 7.9 Hz, 2H), 6.60 (d, *J* = 2.0 Hz, 2H), 6.50 (dd, *J* = 7.9 Hz, *J* = 2.0 Hz, 2H), 3.54–3.46 (m, 2H), 3.28 (s, 2H), 3.15–3.03 (m, 4H), 2.98–2.90 (m, 2H);

^{13}C NMR (100 MHz, Chloroform-d [77.16 ppm], ppm) δ = 143.0 (C_q, 2C), 139.5 (C_q, 2C), 137.2 (+, CH, 2C), 132.8 (+, CH, 2C), 130.5 (+, CH, 2C), 124.3 (C_q, 2C), 83.8 (C_q, 2C, C_{alkyne}), 80.5 (+, CH, 2C, C_{alkyne}), 34.8 (–, CH_2, 2C, PCP-CH_2), 32.7 (–, CH_2, 2C, PCP-CH_2);

MS (EI, 70 eV, 40 °C), m/z (%): 256 (69) $[M]^+$, 255 (37), 241 (31), 128 (100). HRMS (EI): m/z = calcd for $C_{20}H_{16}$ $[M]^+$: 256.1247; found 256.1245;

IR (ATR, $\tilde{\nu}$) = 3278 (vs), 3037 (w), 3009 (w), 2952 (w), 2928 (m), 2890 (w), 2850 (w), 2091 (w), 1588 (w), 1479 (w), 1449 (w), 1432 (w), 1404 (w), 1248 (w), 1227 (w), 1203 (w), 1188 (w), 1180 (w), 1159 (w), 1136 (vw), 1084 (w), 960 (w), 942 (w), 891 (s), 878 (w), 867 (m), 834 (w), 816 (w), 795 (w), 722

(vs), 653 (vs), 619 (vs), 603 (vs), 560 (m), 543 (s), 510 (w), 487 (vs), 462 (w), 439 (w), 433 (w), 395 (m) cm^{-1}.

Additional information on the chemical synthesis is available *via* Chemotion repository:

https://doi.org/10.14272/reaction/SA-FUHFF-UHFFFADPSC-MXSVQOJVES-UHFFFADPSC-NUHFF-NUHFF-NUHFF-ZZZ

Additional information on the analysis of the target compound is available *via* Chemotion repository:

https://doi.org/10.14272/MXSVQOJVESTWLA-UHFFFAOYSA-N.1

4,16-(Bis(ethynyl-thiophene-5,2-diyl-*N,N*-bis(4-methoxyphenyl)aniline)[2.2]paracyclophane (52)

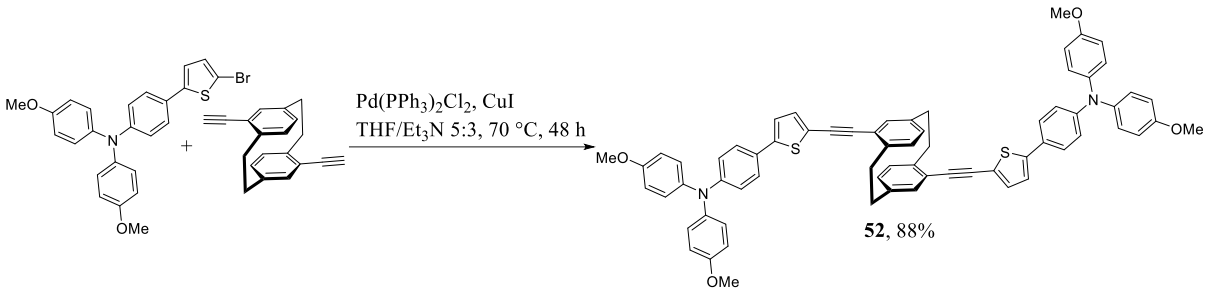

4,16-Diethynyl[2.2]paracyclophane (30.0 mg, 117 µmol, 1.00 equiv.), 4-(5-bromothiophen-2-yl)-*N,N*-bis(4-methoxyphenyl)aniline (120 mg, 257 µmol, 2.20 equiv.), bis(triphenylphosphine)palladium(II) dichloride (8.21 mg, 11.7 µmol, 0.100 equiv.) and copper(I) iodide (2.23 mg, 11.7 µmol, 0.100 equiv.) were dissolved in 15 mL of dry THF and 9 mL of dry Et_3N. The solution was stirred at 70 °C for 48 h. The solvent was evaporated under reduced pressure. Column chromatography on silica with pentane/DCM 1:1 as eluent yielded 4,16-(bis(ethynyl-thiophene-5,2-diyl-*N,N*-bis(4-methoxyphenyl)aniline)[2.2]paracyclophane (106 mg, 103 µmol, 88% yield) as a yellow-to-brown solid.

R_f = 0.15 (pentane/DCM 1:1).

M.p.: 115 °C

^{1}H NMR (400 MHz, Dichloromethane-d_2 [5.32 ppm], ppm) δ = 7.44–7.42 (m, 4H), 7.26 (d, *J* = 3.8 Hz, 2H), 7.15 (d, *J* = 3.8 Hz, 2H), 7.10–7.06 (m, 8H), 7.02 (dd, *J* = 7.9 Hz, *J* = 1.9 Hz, 2H), 6.91–6.86 (m, 12H), 6.57 (d, *J* = 2.0 Hz, 2H), 6.52 (d, *J* = 7.9 Hz, 2H), 3.80 (s, 12H), 3.61 (ddd, *J* = 13.2 Hz, *J* = 10.4 Hz, *J* = 2.9 Hz, 2H), 3.22 (ddd, *J* = 12.8 Hz, *J* = 10.4 Hz, *J* = 4.7 Hz, 2H), 3.06 (ddd, *J* = 12.8 Hz, *J* = 10.8 Hz, *J* = 2.9 Hz, 2H), 2.94 (ddd, *J* = 12.7 Hz, *J* = 10.6 Hz, *J* = 4.6 Hz, 2H);

^{13}C NMR (100 MHz, Dichloromethane-d_2 [53.84 ppm], ppm) δ = 175.4 (C_q, 2C), 156.4 (C_q, 4C), 150.8 (C_q, 2C), 146.2 (C_q, 2C), 142.1 (C_q, 2C), 140.3 (C_q, 2C), 140.3 (C_q, 2C), 139.7 (C_q, 4C), 138.9 (C_q, 2C),

136.8 (+, CH, 2C), 133.2 (+, CH, 2C), 132.7 (+, CH, 2C), 130.4 (+, CH, 2C), 127.0 (C_q, 2C), 127.0(+, CH, 8C), 126.4 (+, CH, 4C), 121.6 (+, CH, 2C), 119.8 (+, CH, 4C), 114.7 (+, CH, 8C), 86.4 (C_q, 2C), 55.4 (+, CH_3, 4C, OMe-CH_3), 34.0 (–, CH_2, 2C, PCP-CH_2), 29.7 (–, CH_2, 2C, PCP-CH_2);

MS (ESI), m/z (%): 1026 (29) $[M]^+$, 514 (66), 513 (100). HRMS (ESI): m/z = calcd for $C_{68}H_{54}N_2O_4{}^{32}S_2$ $[M]^+$: 1026.3525; found 1026.3518;

IR (ATR, $\tilde{\nu}$) = 3034 (w), 2997 (w), 2924 (m), 2849 (w), 2830 (w), 1599 (m), 1499 (vs), 1449 (s), 1439 (s), 1404 (m), 1317 (m), 1283 (m), 1235 (vs), 1191 (s), 1176 (s), 1163 (s), 1103 (s), 1031 (vs), 953 (m), 931 (w), 911 (w), 895 (w), 875 (w), 823 (vs), 795 (vs), 721 (s), 701 (m), 666 (m), 653 (m), 635 (m), 609 (m), 581 (s), 572 (vs), 543 (m), 520 (s), 487 (s), 452 (m), 436 (m), 421 (m), 407 (m), 388 (m) cm^{-1}.

Additional information on the chemical synthesis is available *via* Chemotion repository:

https://doi.org/10.14272/reaction/SA-FUHFF-UHFFFADPSC-DHAFZGFFAY-UHFFFADPSC-NUHFF-NUHFF-NUHFF-ZZZ

Additional information on the analysis of the target compound is available *via* Chemotion repository:

https://doi.org/10.14272/DHAFZGFFAYBPIL-UHFFFAOYSA-N.1

4,15-(Bis(ethynyl-thieno[3,2-b]thiophene-5,2-diyl-*N,N*-bis(4-methoxyphenyl)aniline) [2.2]paracyclophane (53)

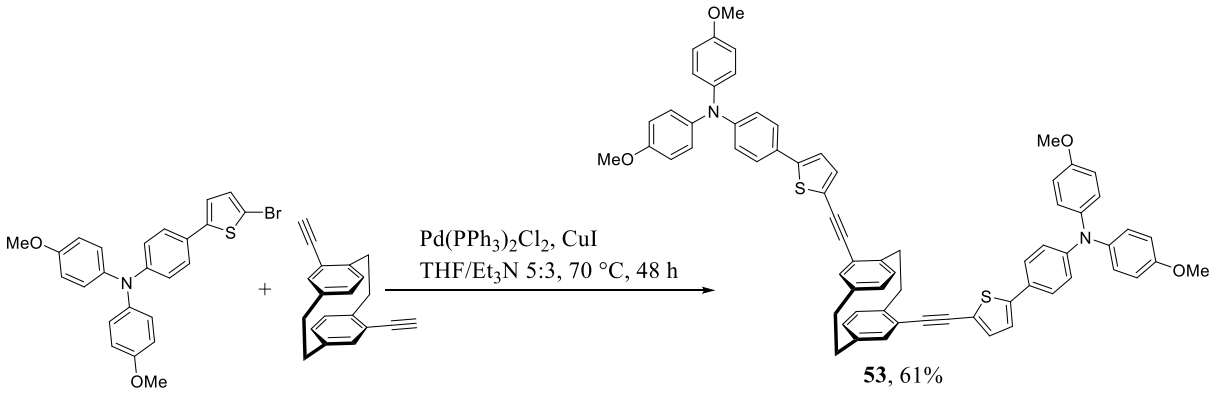

53, 61%

4,15-Diethynyl[2.2]paracyclophane (30.0 mg, 117 µmol, 1.00 equiv.), 4-(5-bromothiophen-2-yl)-*N,N*-bis(4-methoxyphenyl)aniline (120 mg, 257 µmol, 2.20 equiv.), bis(triphenylphosphine)palladium(II) dichloride (8.21 mg, 11.7 µmol, 0.100 equiv.) and copper(I) iodide (2.23 mg, 11.7 µmol, 0.100 equiv.) in 15 mL of dry THF and 9 mL of dry Et_3N. The solution was stirred at 70 °C for 48 h. The solvent was evaporated under reduced pressure. Column chromatography on silica with pentane/DCM 1:1 as eluent yielded 4,15-(bis(ethynyl-thieno[3,2-b]thiophene-5,2-diyl-*N,N*-bis(4-

methoxyphenyl)aniline)[2.2]paracyclophane (106 mg, 91% purity, 103 µmol, 88% yield) as yellow-to-brown solid.

Because of the low purity, no ^{13}C or 2D NMR could be recorded.

R_f = 0.15 (pentane/DCM 1:1).

M.p.: 104 °C

^1H NMR (400 MHz, Dichloromethane-d_2 [5.32 ppm], ppm) δ = 7.32–7.23 (m, 4H), 7.11–7.08 (m, 2H), 7.05–7.02 (m, 2H), 6.94–6.82 (m, 10H), 6.71–6.66 (m, 12H), 6.45–6.41 (m, 2H), 6.40–6.35 (m, 2H), 3.40 (s, 12H), 3.37–3.36 (m, 2H), 2.97–2.90 (m, 4H), 2.84–2.79 (m, 2H);

MS (ESI), m/z (%): 1026 (20) $[M]^+$, 514 (57), 513 (84), 282 (42), 269 (6), 221 (55), 124 (30), 122 (100), 120 (33). HRMS (ESI): m/z = calcd for $C_{68}H_{54}N_2O_4{}^{32}S_2$ $[M]^+$: 1026.3525; found 1026.3494;

IR (ATR, ṽ) = 2949 (w), 2921 (m), 2849 (w), 2832 (w), 1599 (w), 1500 (vs), 1449 (s), 1441 (m), 1405 (w), 1317 (m), 1283 (m), 1265 (m), 1237 (vs), 1191 (m), 1177 (s), 1164 (s), 1103 (m), 1033 (s), 824 (vs), 796 (vs), 721 (s), 701 (w), 609 (w), 582 (s), 572 (s), 518 (m), 486 (m), 408 (w) cm^{-1}.

4,16-(Bis(ethynyl-thieno[3,2-b]thiophene-5,2-diyl-*N,N*-bis(4-methoxyphenyl)aniline) [2.2]paracyclophane (54)

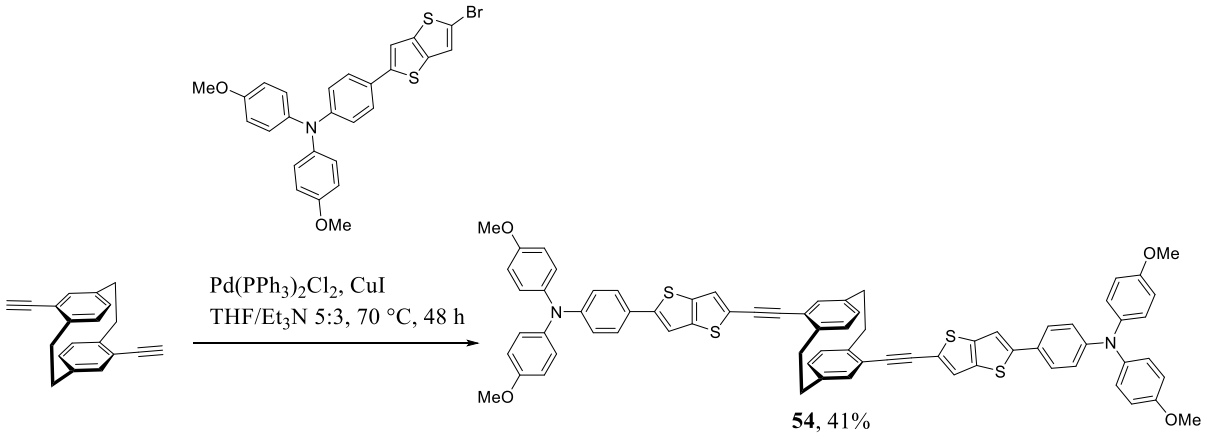

54, 41%

4,16-Diethynyl[2.2]paracyclophane (30.0 mg, 117 µmol, 1.00 equiv.), 4-(5-bromothiophen-2-yl)-*N,N*-bis(4-methoxyphenyl)aniline (122 mg, 234 µmol, 2.00 equiv.), bis(triphenylphosphine)palladium(II) dichloride (8.21 mg, 11.7 µmol, 0.100 equiv.), and copper(I) iodide (2.23 mg, 11.7 µmol, 0.100 equiv.)were dissolved in 15 mL of dry THF and 9 mL of dry Et_3N. The solution was stirred at 70 °C for 48 h. The solvent was evaporated under reduced pressure. Column chromatography on silica using pentane/DCM 1:1 as eluent yielded 4,16-(bis(ethynyl-thieno[3,2-b]thiophene-5,2-diyl-*N,N*-bis(4-

methoxyphenyl)aniline)[2.2]paracyclophane (54.4 mg, 92% purity, 47.7 µmol, 41% yield) as a yellow-to-brown solid.

Because of the low purity, no ^{13}C or 2D NMR could be recorded.

R_f = 0.41 (pentane/DCM 1:1).

M.p.: 168 °C

^1H NMR (400 MHz, Dichloromethane-d_2 [5.32 ppm], ppm) δ = 7.54–7.43 (m, 6H), 7.34 (s, 2H), 7.13–7.01 (m, 10H), 6.93–6.84 (m, 12H), 6.62–6.59 (m, 2H), 6.55–6.52 (m, 2H), 3.77 (s, 12H), 3.65–3.59 (m, 2H), 3.26–3.19 (m, 2H), 3.10–3.03 (m, 2H), 2.99–2.91 (m, 2H);

MS (ESI), m/z (%): 1138 (8) $[M]^+$, 570 (44), 569 (63), 282 (52), 221 (100). HRMS (ESI): m/z = calcd for $C_{72}H_{54}N_2O_4{}^{32}S_4$ $[M]^+$: 1138.2967; found 1138.2919;

IR (ATR, ṽ) = 3036 (w), 2995 (w), 2945 (w), 2927 (m), 2849 (w), 2830 (w), 1598 (m), 1500 (vs), 1480 (vs), 1462 (vs), 1438 (s), 1418 (m), 1317 (s), 1283 (s), 1235 (vs), 1193 (s), 1164 (vs), 1103 (s), 1068 (m), 1031 (vs), 969 (m), 949 (m), 932 (m), 911 (m), 895 (m), 871 (m), 822 (vs), 781 (s), 721 (s), 701 (s), 669 (s), 652 (s), 639 (m), 595 (s), 575 (vs), 564 (s), 524 (vs), 489 (vs), 470 (s), 460 (s), 452 (s), 442 (s), 435 (s), 412 (s), 405 (s), 390 (s), 381 (s), 377 (s) cm^{-1}.

4,15-(Bis(ethynyl-thieno[3,2-b]thiophene-5,2-diyl-*N,N*-bis(4-methoxyphenyl)aniline) [2.2]paracyclophane (**55**)

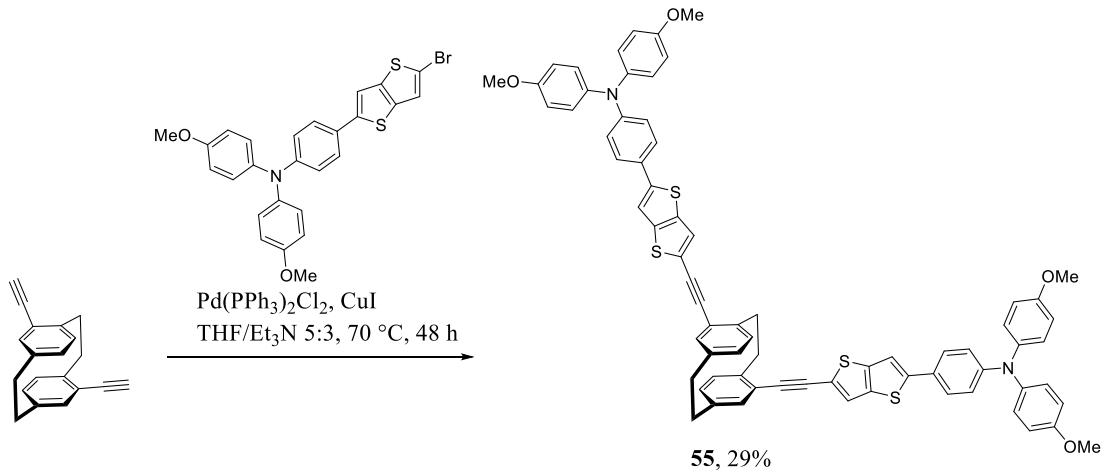

55, 29%

4,15-Diethynyl[2.2]paracyclophane (30.0 mg, 117 µmol, 1.00 equiv.), 4-(5-bromothiophen-2-yl)-*N,N*-bis(4-methoxyphenyl)aniline (122 mg, 234 µmol, 2.00 equiv.), bis(triphenylphosphine)palladium(II) dichloride (8.21 mg, 11.7 µmol, 0.100 equiv.), and copper(I) iodide (2.23 mg, 11.7 µmol, 0.100 equiv.) were dissolved in 15 mL of dry THF and 9 mL of dry Et_3N. The solution was stirred at 70 °C for 48 h. The solvent was evaporated under reduced pressure. Column chromatography on silica using

pentane/DCM 1:1 as an eluent yielded 4,15-(bis(ethynyl-thieno[3,2-b]thiophene-5,2-diyl-*N,N*-bis(4-methoxyphenyl)aniline)[2.2]paracyclophane (38.3 mg, 83% purity, 33.6 µmol, 29% yield) as a yellow-to-brown solid.

Because of the low purity, no ^{13}C or 2D NMR could be recorded.

R_f = 0.40 (pentane/DCM 1:1).

M.p.: 192 °C

^1H NMR (400 MHz, Dichloromethane-d_2 [5.32 ppm], ppm) δ = 7.44–7.40 (m, 2H), 7.37–7.33 (m, 4H), 7.23 (s, 2H), 7.03–6.94 (m, 10H), 6.83–6.71 (m, 12H), 6.56–6.44 (m, 4H), 3.67 (s, 12H, OMe-CH_3), 3.53–3.44 (m, 2H, PCP-CH_2), 3.16–2.99 (m, 4H, PCP-CH_2), 2.93–2.84 (m, 2H, PCP-CH_2);

MS (ESI), m/z (%): 1138 (8) $[M]^+$, 570 (45), 569 (66), 443 (50), 385 (26), 383 (28), 282 (61), 221 (100). HRMS (ESI): m/z = calcd for $C_{72}H_{54}N_2O_4{}^{32}S_4$ $[M]^+$: 1138.2967; found 1138.2927;

IR (ATR, $\tilde{\nu}$) = 3033 (w), 2924 (w), 2850 (w), 2830 (w), 1775 (w), 1598 (m), 1500 (vs), 1479 (vs), 1462 (s), 1436 (s), 1418 (m), 1317 (m), 1283 (m), 1235 (vs), 1191 (s), 1163 (vs), 1102 (s), 1068 (m), 1031 (vs), 976 (m), 949 (m), 891 (m), 822 (vs), 781 (s), 721 (vs), 701 (s), 690 (s), 674 (m), 652 (m), 640 (m), 632 (m), 611 (m), 596 (s), 572 (vs), 561 (s), 545 (s), 527 (vs), 507 (s), 486 (vs), 455 (s), 449 (s), 438 (s), 426 (m), 415 (s), 408 (s), 388 (s) cm^{-1}.

4,16-Bis(4-(trimethylsilyl)phenyl)[2.2]paracyclophane (56)

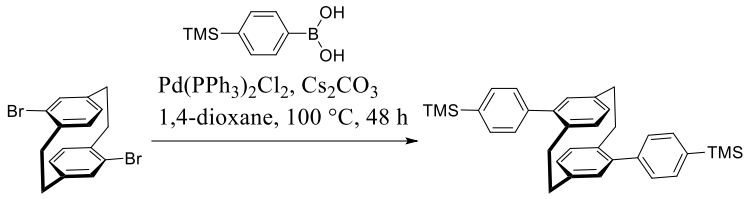

56, 63%

4,16-Dibromo[2.2]paracyclophane (750 mg, 2.05 mmol, 1.00 equiv.), (4-trimethylsilylphenyl)boronic acid (1.59 g, 8.19 mmol, 4.00 equiv.), bis(triphenylphosphine)palladium(II) dichloride (115 mg, 164 µmol, 0.0800 equiv.) and dicesium carbonate (2.00 g, 6.15 mmol, 3.00 equiv.) were added to a vial and purged with argon. Dry dioxane (75 mL) was added, and the reaction mixture was stirred under an atmosphere of argon at 100 °C for 2 d. The reaction mixture was cooled and filtered through a short pad of celite. The solvent was removed under reduced pressure. The crude solid was purified by flash column chromatography on silica using cHex/DCM 20:1 to 15:1 as eluent to yield the product 4,16--bis(4-(trimethylsilyl)phenyl)[2.2]paracyclophane (650 mg, 1.21 mmol, 59% yield) as a colorless solid.

R_f = 0.35 (cHex/DCM 10:1).

M.p.: 151 °C

^{1}H NMR (400 MHz, Chloroform-d [7.26 ppm], ppm) δ = 7.66–7.63 (m, 4H, CH_{Ar}), 7.54–7.51 (m, 4H, CH_{Ar}), 6.68–6.66 (m, 4H, CH_{Ar}), 6.61 (dd, *J* = 7.7 Hz, *J* = 1.8 Hz, 2H, CH_{Ar}), 3.46 (ddt, *J* = 13.4 Hz, *J* = 8.7 Hz, *J* = 4.5 Hz, *J* = 4.5 Hz, 2H, PCP-CH_2), 3.05 (ddd, *J* = 13.7 Hz, *J* = 9.3 Hz, *J* = 5.3 Hz, 2H, PCP-CH_2), 2.92–2.77 (m, 4H, PCP-CH_2), 0.35 (s, 18H, TMS-CH_3;

^{13}C NMR (100 MHz, Chloroform-d [77.16 ppm], ppm) δ = 142.1 (C_q, 2C), 141.7 (C_q, 2C), 140.0 (C_q, 2C), 138.6 (C_q, 2C), 136.9 (C_q, 2C), 134.9 (+, CH, 2C), 133.6 (+, CH, 4C), 132.4 (+, CH, 2C), 129.4 (+, CH, 2C), 129.2 (+, CH, 4C), 34.8 (–, CH_2, 2C, PCP-CH_2), 33.8 (–, CH_2, 2C, PCP-CH_2), -1.1 (+, CH_3, 6C, TMS-CH_3;

MS (FAB, 3-NBA), m/z (%): 504 (46) $[M]^+$, 357 (33), 356 (51),179 (42), 178 (38), 177 (50), 154 (100), 138 (33), 137 (57), 136 (84). HRMS (FAB, matrix NBA): m/z = calcd for $C_{34}H_{40}{}^{28}Si_2$ $[M]^+$: 504.2663; found 504.2661;

IR (ATR, ṽ) = 3009 (vw), 2951 (w), 2929 (w), 2894 (w), 2853 (w), 1588 (w), 1538 (vw), 1477 (w), 1453 (vw), 1434 (vw), 1411 (w), 1387 (w), 1313 (vw), 1247 (m), 1194 (vw), 1164 (vw), 1115 (w), 1033 (w), 908 (w), 834 (vs), 822 (vs), 754 (m), 737 (m), 727 (m), 708 (m), 690 (m), 664 (m), 652 (m), 635 (w), 618 (w), 592 (w), 561 (w), 528 (w), 516 (w), 487 (m), 475 (w), 452 (w), 424 (w), 401 (w) cm^{-1}.

Additional information on the chemical synthesis is available *via* Chemotion repository:

https://doi.org/10.14272/reaction/SA-FUHFF-UHFFFADPSC-UMKYUWSCNM-UHFFFADPSC-NUHFF-NUHFF-NUHFF-ZZZ.1

Additional information on the analysis of the target compound is available *via* Chemotion repository:

https://doi.org/10.14272/UMKYUWSCNMUWIY-UHFFFAOYSA-N.2

4,16-Bis(iodophenyl)[2.2]paracyclophane (57)

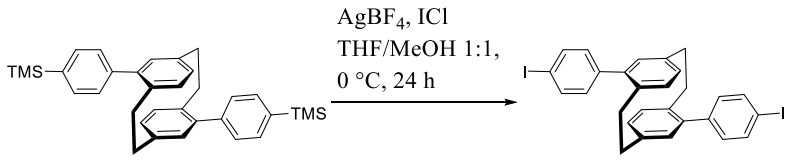

57, 65%

4,16-Bis(4-trimethylsilyl)phenyl[2.2]paracyclophane (650 mg, 1.29 mmol, 1.00 equiv.) and silver tetrafluoroborate (752 mg, 3.86 mmol, 3.00 equiv.) were added to a vial that had been purged with argon. Dry THF/MeOH (52 mL, v/v 1:1) was added and the reaction mixture was cooled to 0 °C. Iodine

monochloride (1.05 g, 6.44 mL, 6.44 mmol, 1.00M in DCM, 5.00 equiv.) was added dropwise under argon. The reaction mixture was stirred for 30 minutes at 0 °C and 24 h at 22 °C. The solvent was removed under reduced pressure. The crude solid was purified by a short flash column chromatography on silica using pentane/DCM 1:1 as eluent to yield 4,16-bis(iodophenyl)[2.2]paracyclophane (513 mg, 837 μmol, 65% yield) as an off-white solid.

R_f = 0.24 (pentane/DCM 10:1).

M.p.: 320 °C

^{1}H NMR (400 MHz, Dichloromethane-d_2 [5.32 ppm], ppm) δ = 7.85–7.82 (m, 4H, CH_{Ar}), 7.30–7.27 (m, 4H, CH_{Ar}), 6.65–6.62 (m, 4H, CH_{Ar}), 6.55 (dd, *J* = 7.7 Hz, *J* = 1.9 Hz, 2H, CH_{Ar}), 3.39 (ddd, *J* = 13.9 Hz, *J* = 10.0 Hz, *J* = 4.1 Hz, 2H, PCP-CH_2), 3.02 (ddd, *J* = 13.9 Hz, *J* = 10.1 Hz, *J* = 4.7 Hz, 2H, PCP-CH_2), 2.86 (ddd, *J* = 14.0 Hz, *J* = 10.1 Hz, *J* = 4.1 Hz, 2H, PCP-CH_2), 2.74 (ddd, *J* = 13.7 Hz, *J* = 10.0 Hz, *J* = 4.7 Hz, 2H, PCP-CH_2);

^{13}C NMR (100 MHz, Dichloromethane-d_2 [53.84 ppm], ppm) δ = 140.9 (C_q, 2C), 140.8 (C_q, 2C), 140.1 (C_q, 2C), 137.7 (+, CH, 4C), 136.9 (C_q, 2C), 134.9 (+, CH, 2C), 132.0 (+, CH, 2C), 131.7 (+, CH, 4C), 129.4 (+, CH, 2C), 92.5 (C_q, 2C), 34.5 (–, CH_2, 2C, PCP-CH_2), 33.6 (–, CH_2, 2C, PCP-CH_2);

MS (ESI), m/z (%): 613 (2) $[M+H]^+$, 564 (34), 282 (54), 221 (44), 202 (100). HRMS–ESI (m/z): $[M+H]^+$ calcd for $C_{28}H_{23}I_2$: 612.9889; found 612.9873;

IR (ATR, $\tilde{\nu}$) = 3017 (w), 2962 (w), 2932 (w), 2907 (m), 2884 (m), 2843 (m), 2800 (w), 2785 (w), 2771 (w), 2749 (w), 2740 (w), 1904 (w), 1653 (w), 1588 (w), 1541 (w), 1470 (s), 1448 (m), 1431 (w), 1411 (w), 1380 (m), 1356 (w), 1238 (w), 1205 (w), 1180 (w), 1166 (w), 1156 (w), 1098 (w), 1058 (m), 999 (vs), 949 (w), 936 (w), 911 (m), 873 (w), 836 (s), 820 (vs), 766 (m), 725 (vs), 686 (m), 654 (s), 625 (m), 562 (m), 554 (s), 524 (m), 482 (vs), 443 (m), 433 (s), 411 (w), 382 (m), 375 (w) cm^{-1}.

Additional information on the chemical synthesis is available *via* Chemotion repository:

https://doi.org/10.14272/reaction/SA-FUHFF-UHFFFADPSC-FNQCIKYPHC-UHFFFADPSC-NUHFF-NUHFF-NUHFF-ZZZ.1

Additional information on the analysis of the target compound is available *via* Chemotion repository:

https://doi.org/10.14272/FNQCIKYPHCWPGB-UHFFFAOYSA-N.2

4,15-Bis(4-trimethylsilyl)phenyl[2.2]paracyclophane (58)

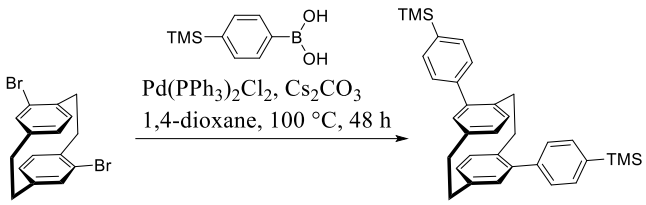

58, 74%

4,15-Dibromo[2.2]paracyclophane (750 mg, 2.05 mmol, 1.00 equiv.), (4-trimethylsilylphenyl)boronic acid (1.59 g, 8.19 mmol, 4.00 equiv.), bis(triphenylphosphine)palladium(II) dichloride (115 mg, 164 µmol, 0.0800 equiv.) and dicesium carbonate (2.00 g, 6.15 mmol, 3.00 equiv.) were added to a vial and purged with argon. Dry dioxane (75 mL) was added, and the reaction mixture was stirred under an atmosphere of argon at 100 °C for 2 d. The reaction mixture was cooled and filtered through a short pad of celite. The solvent was removed under reduced pressure. The crude solid was purified by flash column chromatography on silica using cHex/DCM 20:1 to 15:1 as eluent to yield the product 4,15-bis(4-trimethylsilyl)phenyl[2.2]paracyclophane (769 mg, 1.52 mmol, 74% yield) as a colorless solid.

R_f = 0.35 (pentane/DCM 10:1).

M.p.: 75 °C

^{1}H NMR (400 MHz, Chloroform-d [7.26 ppm], ppm) δ = 7.64–7.61 (m, 4H, CH_{Ar}), 7.49–7.47 (m, 4H, CH_{Ar}), 6.73 (d, J = 1.9 Hz, 2H, CH_{Ar}), 6.69 (d, J = 7.8 Hz, 2H, CH_{Ar}), 6.57 (dd, J = 7.7 Hz, J = 1.9 Hz, 2H, CH_{Ar}), 3.31–3.04 (m, 6H, PCP-CH_2), 2.60 (td, J = 9.7 Hz, J = 9.4 Hz, J = 3.6 Hz, 2H, PCP-CH_2), 0.35 (s, 18H, TMS-CH_3);

^{13}C NMR (100 MHz, Chloroform-d [77.16 ppm], ppm) δ = 142.5 (C_q, 2C), 141.6 (C_q, 2C), 139.5 (C_q, 2C), 138.6 (C_q, 2C), 137.5 (C_q, 2C), 133.6 (+, CH, 4C), 132.4 (+, CH, 2C), 131.9 (+, CH, 2C), 131.4 (+, CH, 2C), 129.0 (+, CH, 4C), 35.2 (–, CH_2, 2C, PCP-CH_2), 33.4 (–, CH_2, 2C, PCP-CH_2), -1.0 (+, CH_3, 6C, TMS-CH_3);

MS (FAB, 3-NBA), m/z (%): 504 (66) $[M]^+$, 417 (55), 237 (100), 226 (28), 193 (37), 191 (30), 179 (67), 178 (56), 165 (29), 154 (32), 136 (60). HRMS (FAB, matrix NBA): m/z = calcd for $C_{34}H_{40}{}^{28}Si_2$ $[M]^+$: 504.2663; found 504.2662;

IR (ATR, $\tilde{\nu}$) = 3058 (vw), 3009 (vw), 2952 (w), 2927 (w), 2891 (w), 2856 (vw), 1595 (w), 1538 (vw), 1477 (vw), 1451 (vw), 1434 (vw), 1408 (vw), 1381 (w), 1307 (vw), 1259 (w), 1247 (m), 1205 (vw), 1115 (w), 1033 (vw), 949 (vw), 916 (vw), 836 (vs), 822 (vs), 754 (m), 727 (s), 691 (w), 671 (w), 656 (w), 640 (w), 622 (w), 613 (w), 551 (w), 509 (w), 484 (w), 425 (w) cm^{-1}.

Additional information on the chemical synthesis is available *via* Chemotion repository:

https://doi.org/10.14272/reaction/SA-FUHFF-UHFFFADPSC-CMRRTDDLXL-UHFFFADPSC-NUHFF-NUHFF-NUHFF-ZZZ.1

Additional information on the analysis of the target compound is available *via* Chemotion repository:

https://doi.org/10.14272/CMRRTDDLXLZQJJ-UHFFFAOYSA-N.2

4,15-Bis(4-iodophenyl)[2.2]paracyclophane (59)

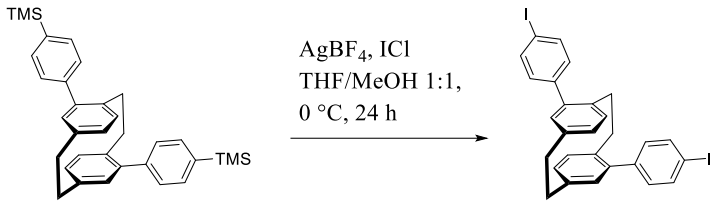

59, 54%

4,15-Bis(4-trimethylsilyl)phenyl[2.2]paracyclophane (750 mg, 1.49 mmol, 1.00 equiv.) and silver tetrafluoroborate (868 mg, 4.46 mmol, 3.00 equiv.) were added to a vial that had been purged with argon. Dry THF/MeOH (60 mL, v/v 1:1) was added and the reaction mixture was cooled to 0 °C. Iodine monochloride (1.21 g, 7.43 mL, 7.43 mmol, 1.00M in DCM, 5.00 equiv.) was added dropwise under argon. The reaction mixture was stirred for 30 minutes at 0 °C and 24 h at 22 °C. The solvent was removed under reduced pressure. The crude solid was purified by a short flash column chromatography on silica using pentane/DCM 1:1 as eluent to yield 4,15-bis(4-iodophenyl)[2.2]paracyclophane (492 mg, 804 µmol, 54% yield) as a colorless solid.

R_f = 0.24 (pentane/DCM 10:1).

M.p.: 239 °C

^{1}H NMR (400 MHz, Dichloromethane-d_2 [5.32 ppm], ppm) δ = 7.83–7.77 (m, 4H, CH_{Ar}), 7.27–7.21 (m, 4H, CH_{Ar}), 6.66–6.61 (m, 4H, CH_{Ar}), 6.55 (dd, *J* = 7.8 Hz, *J* = 1.9 Hz, 2H, CH_{Ar}), 3.24–3.01 (m, 6H, PCP-CH_2), 2.52–2.43 (m, 2H, PCP-CH_2);

^{13}C NMR (100 MHz, Dichloromethane-d_2 [53.84 ppm], ppm) δ = 141.3 (C_q, 2C), 140.6 (C_q, 2C), 140.0 (C_q, 2C), 137.7 (+, CH, 4C), 137.2 (C_q, 2C), 132.2 (+, CH, 2C), 131.6 (+, CH, 2C), 131.5 (+, CH, 4C), 131.5 (+, CH, 2C), 92.6 (C_q, 2C), 34.9 (–, CH_2, 2C, PCP-CH_2), 33.3 (–, CH_2, 2C, PCP-CH_2);

MS (ESI), m/z (%): 613 (8) $[M+H]^+$, 282 (55), 229 (43), 221 (100), 209 (76). HRMS–ESI (m/z): $[M+H]^+$ calcd for $C_{28}H_{23}I_2$: 612.9889; found 612.9869;

IR (ATR, ṽ) = 3014 (w), 3002 (w), 2945 (w), 2924 (w), 2887 (w), 2846 (w), 1591 (w), 1582 (w), 1547 (vw), 1472 (s), 1451 (w), 1434 (w), 1383 (w), 1302 (w), 1261 (w), 1235 (w), 1200 (w), 1180 (w), 1156

(w), 1098 (vw), 1057 (w), 1001 (vs), 955 (w), 914 (w), 849 (m), 840 (w), 822 (vs), 807 (m), 728 (s), 714 (m), 686 (w), 664 (m), 632 (m), 611 (w), 540 (m), 531 (w), 517 (w), 482 (vs), 449 (w), 439 (w), 388 (w) cm^{-1}.

Additional information on the chemical synthesis is available *via* Chemotion repository:

https://doi.org/10.14272/reaction/SA-FUHFF-UHFFFADPSC-YQTVOHOFVU-UHFFFADPSC-NUHFF-NUHFF-NUHFF-ZZZ.1

Additional information on the analysis of the target compound is available *via* Chemotion repository:

https://doi.org/10.14272/YQTVOHOFVUOTPI-UHFFFAOYSA-N.2

4,16-(Bis(4,1-phenylene-thiophene-5,2-diyl-*N*,*N*-bis(4-methoxyphenyl)aniline) [2.2]paracyclophane (60)

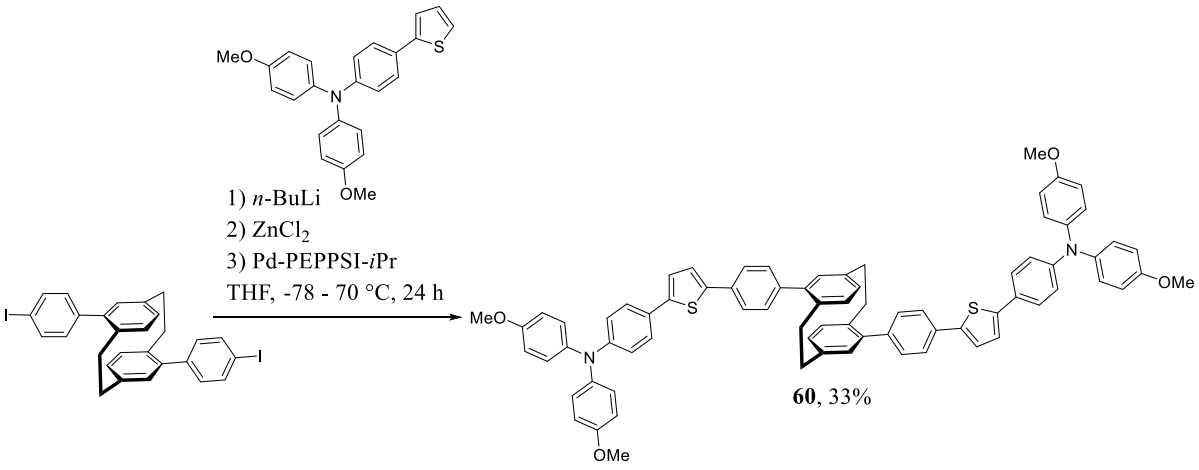

Preparation of Negishi reactant:

Bis(4-methoxyphenyl)-[4-(2-thienyl)phenyl]amine (104 mg, 269 µmol, 2.20 equiv.) was added to a crimp cap vial and flushed with Ar three times. 4.5 mL of dry THF were added and the mixture was cooled to -78 °C. *n*-Butyllithium solution (20.4 mg, 127 µL, 318 µmol, 2.50M in hexane, 2.60 equiv.) were added dropwise and the reaction mixture was allowed to warm to 22 °C. After stirring for 30 min, the reaction mixture was cooled to 0 °C and a zinc chloride solution (50.1 mg, 367 µL, 367 µmol, 1.00M in THF, 3.00 equiv.) was added. The reaction was stirred for 15 min at 0 °C and then warmed to 22 °C.

Negishi coupling:

4,16-Bis(iodo)phenyl[2.2]paracyclophane (75.0 mg, 122 µmol, 1.00 equiv.) and PEPPSI-IPr catalyst (8.35 mg, 12.2 µmol, 0.100 equiv.) were added to a crimp cap vial and flushed with Ar three times. 4.5 mL of dry THF were added and zinc chloride solution (50.1 mg, 367 µL, 367 µmol, 1.00M in THF,

3.00 equiv.) was added. After dissolving, the Negishi reactant was added *via* syringe and the reaction mixture was heated to 70 °C. After three days, the reaction was allowed to cool to 22 °C and the solvent was removed under reduced pressure. Column chromatography on silica using cHex/DCM 1:0 to 1:2 as eluent yielded 4,16-(bis(4,1-phenylene-thiophene-5,2-diyl-*N,N*-bis(4-methoxyphenyl)aniline)[2.2]paracyclophane (45.8 mg, 40.5 µmol, 33% yield) as yellow solid.

Extremly low solubility made NMR analysis impossible.

R_f = 0.27 (cHex/DCM 1:1).

M.p.: 120 °C

MS (ESI), m/z (%): 1130 (13) $[M]^+$, 773 (51), 772 (100), 690 (34), 566 (55), 565 (71), 457 (34). HRMS (ESI): m/z = calcd for $C_{76}H_{62}N_2O_4{}^{32}S_2$ $[M]^+$: 1130.4151; found 1130.4125;

IR (ATR, $\tilde{\nu}$) = 3029 (w), 2995 (w), 2922 (w), 2849 (w), 2832 (w), 1599 (w), 1494 (vs), 1452 (s), 1439 (s), 1397 (w), 1317 (m), 1278 (m), 1235 (vs), 1191 (m), 1177 (s), 1164 (s), 1103 (m), 1072 (w), 1033 (s), 972 (w), 950 (w), 939 (w), 912 (w), 824 (vs), 793 (vs), 748 (w), 728 (m), 721 (m), 701 (m), 670 (w), 652 (w), 635 (w), 596 (m), 574 (s), 523 (s), 489 (m), 452 (w), 441 (w), 431 (w), 418 (w), 408 (m), 390 (w), 382 (w) cm^{-1}.

4,15-Bis(4,1-phenylene-thiophene-5,2-diyl-*N,N*-bis(4-methoxyphenyl)aniline[2.2]paracyclophane (61)

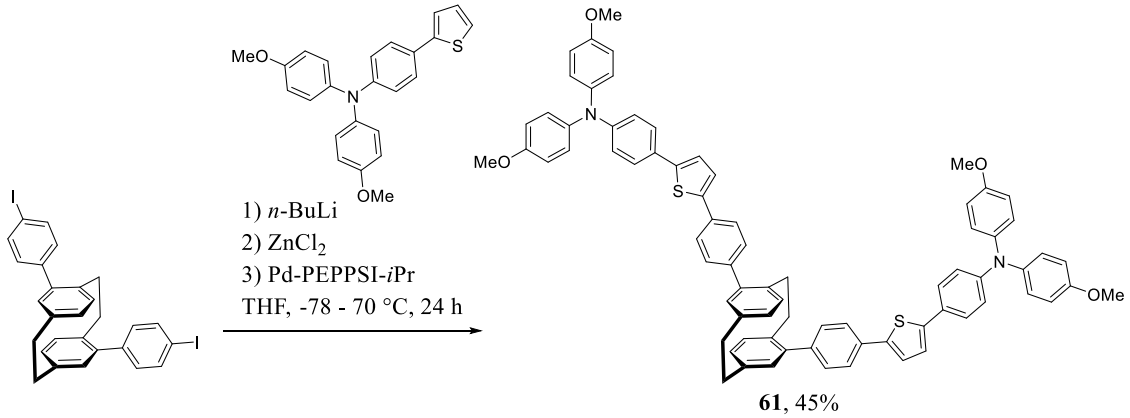

61, 45%

Preparation of Negishi reactant:

Bis(4-methoxyphenyl)-[4-(2-thienyl)phenyl]amine (104 mg, 269 µmol, 2.20 equiv.) was added to a crimp cap vial and flushed with Ar three times. 4.5 mL of dry THF was added, and the mixture was cooled to -78 °C. *n*-Butyllithium solution (20.4 mg, 127 µL, 318 µmol, 2.50M in hexane, 2.60 equiv.) was added dropwise, and the reaction mixture was allowed to warm to 22 °C. After stirring for 30 min,

the reaction mixture was cooled to 0 °C, and zinc chloride solution (50.1 mg, 367 µL, 367 µmol, 1.00M in THF, 3.00 equiv.) was added. The reaction was stirred for 15 min at 0 °C and then warmed to 22 °C.

Negishi coupling:

4,15-Bis(4-iodophenyl)[2.2]paracyclophane (75.0 mg, 122 µmol, 1.00 equiv.) and PEPPSI-IPr catalyst (8.35 mg, 12.2 µmol, 0.100 equiv.) were added to a crimp cap vial and flushed with Ar three times. 4.5 mL of dry THF and zinc chloride solution (50.1 mg, 367 µL, 367 µmol, 1.00M in THF, 3.00 equiv.) were added. After dissolving, the Negishi reactant was added *via* syringe, and the reaction mixture was heated to 70 °C. After three days, the reaction was allowed to cool to 22 °C, and the solvent was removed under reduced pressure. Column chromatography on silica using cHex/DCM 1:0 to 1:2 as eluent was performed to yield 4,15-bis(4,1-phenylene-thiophene-5,2-diyl-N,N-bis(4-methoxyphenyl)aniline[2.2]paracyclophane (62.3 mg, 55.1 µmol, 45% yield) as a yellow-to-brown solid.

R_f = 0.27 (cHex/DCM 1:1).

M.p.: 125 °C

^{1}H NMR (400 MHz, Dichloromethane-d_2 [5.32 ppm], ppm) δ = 7.76–7.72 (m, 4H), 7.52 (d, *J* = 8.2 Hz, 4H), 7.49–7.45 (m, 4H), 7.36 (d, *J* = 3.8 Hz, 2H), 7.22 (d, *J* = 3.8 Hz, 2H), 7.11–7.06 (m, 8H), 6.93–6.90 (m, 4H), 6.88–6.84 (m, 8H), 6.74 (d, *J* = 7.8 Hz, 4H), 6.63 (dd, *J* = 7.8 Hz, *J* = 1.8 Hz, 2H), 3.78 (s, 12H, OME-CH_3), 3.28–3.20 (m, 4H, PCP-CH_2), 3.15–3.08 (m, 2H, PCP-CH_2), 2.58–2.51 (m, 2H, PCP-CH_2);

^{13}C NMR (100 MHz, Dichloromethane-d_2 [53.84 ppm], ppm) δ = 156.3 (C_q, 4C), 148.5 (C_q, 2C), 143.9 (C_q, 2C), 141.8 (C_q, 2C), 141.7 (C_q, 2C), 140.5 (C_q, 4C), 140.2 (C_q, 2C), 139.9 (C_q, 2C), 137.5 (C_q, 2C), 132.9 (C_q, 2C), 132.4 (+, CH, 2C), 131.6 (+, CH, 2C), 131.3 (+, CH, 2C), 130.1 (+, CH, 4C), 126.8 (+, CH, 8C), 126.1 (+, CH, 4C), 126.1 (C_q, 2C), 125.4 (+, CH, 4C), 124.1 (+, CH, 2C), 122.7 (+, CH, 2C), 120.2 (+, CH, 4C), 114.7 (+, CH, 8C), 55.4 (+, CH_3, 4C, OMe-CH_3), 35.0 (–, CH_2, 2C, PCP-CH_2), 33.5 (–, CH_2, 2C, PCP-CH_2);

MS (ESI), m/z (%): 1130 (8) $[M]^+$, 773 (53), 772 (100), 566 (32), 565 (40). HRMS (ESI): m/z = calcd for $C_{76}H_{62}N_2O_4{}^{32}S_2[M]^+$: 1130.4151; found 1130.4126;

IR (ATR, $\tilde{\nu}$) = 3030 (w), 2997 (w), 2924 (w), 2849 (w), 2832 (w), 1599 (w), 1494 (vs), 1453 (s), 1439 (s), 1317 (m), 1279 (m), 1235 (vs), 1191 (s), 1177 (s), 1164 (s), 1103 (m), 1033 (vs), 972 (w), 949 (w), 939 (w), 912 (w), 824 (vs), 793 (vs), 728 (m), 721 (m), 701 (m), 676 (w), 656 (w), 636 (w), 612 (w), 596 (m), 575 (s), 521 (s), 484 (m), 456 (m), 441 (m), 408 (m), 395 (w), 387 (w), 378 (w) cm^{-1}.

Additional information on chemical synthesis is available *via* the Chemotion repository:

https://doi.org/10.14272/reaction/SA-FUHFF-UHFFFADPSC-KQANGQZHEB-UHFFFADPSC-NUHFF-NUHFF-NUHFF-ZZZ

Additional information on the analysis of the target compound is available *via* the Chemotion repository:

https://doi.org/10.14272/KQANGQZHEBOIGS-UHFFFAOYSA-N.1

4,16-(Bis(4,1-phenylene-thieno[3,2-b]thiophene-5,2-diyl-*N*,*N*-bis(4-methoxyphenyl)aniline) [2.2]paracyclophane (62)

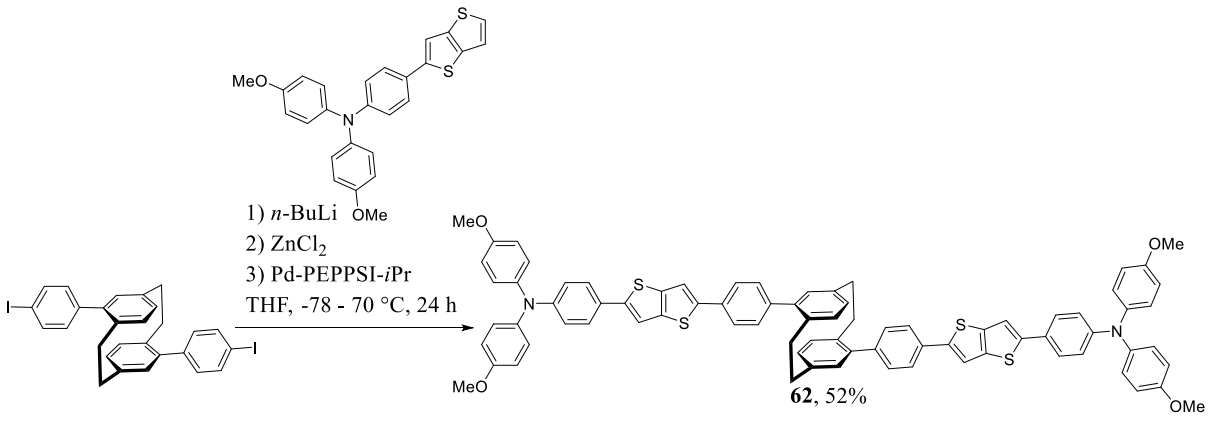

Preparation of Negishi reactant:

4-Methoxy-*N*-(4-methoxyphenyl)-*N*-(4-(thieno[3,2-b]thiophen-2-yl)phenyl)aniline (120 mg, 269 µmol, 2.20 equiv.) was added to a crimp cap vial and flushed with Ar three times. 4.5 mL of dry THF was added, and the mixture was cooled to -78 °C. *n*-Butyllithium solution (20.4 mg, 127 µL, 318 µmol, 2.50M in hexane, 2.60 equiv.) was added dropwise, and the reaction mixture was allowed to warm to 22 °C. After stirring for 30 min, the reaction mixture was cooled to 0 °C, and zinc chloride solution (50.1 mg, 367 µL, 367 µmol, 1.00M in THF, 3.00 equiv.) was added. The reaction was stirred for 15 min at 0 °C and then warmed to 22 °C.

Negishi coupling:

4,16-Bis-(iodophenyl)[2.2]paracyclophane (75.0 mg, 122 µmol, 1.00 equiv.) and PEPPSI-IPr catalyst (8.35 mg, 12.2 µmol, 0.100 equiv.) were added to a crimp cap vial and flushed with Ar three times. 4.5 mL of dry THF and zinc chloride solution (50.1 mg, 367 µL, 367 µmol, 1.00M in THF, 3.00 equiv.) were added. After dissolving, the Negishi reactant was added *via* syringe, and the reaction mixture was heated to 70 °C. After three days, the reaction was allowed to cool to 22 °C, and the solvent was removed under reduced pressure. Column chromatography on silica using cHex/DCM 1:0 to 1:2 as

eluent yielded 4,16-(bis(4,1-phenylene-thieno[3,2-b]thiophene-5,2-diyl-*N,N*-bis(4-methoxyphenyl)aniline)[2.2]paracyclophane (78.8 mg, 63.4 µmol, 52% yield) as yellow solid.

R_f = 0.28 (cHex/DCM 1:1).

M.p.: 305 °C

^{1}H NMR (400 MHz, Dichloromethane-d_2 [5.32 ppm], ppm) δ = 7.70 (d, *J* = 7.4 Hz, 4H), 7.51 (d, *J* = 7.1 Hz, 6H), 7.39–7.31 (m, 6H), 7.01 (d, *J* = 8.2 Hz, 8H), 6.81 (dd, *J* = 18.9 Hz, *J* = 8.0 Hz, 12H), 6.63–6.54 (m, 6H), 3.72 (s, 12H, OMe-CH_3), 3.43–3.43 (m, 2H, PCP-CH_2), 3.00–2.96 (m, 2H, PCP-CH_2), 2.82–2.72 (m, 4H, PCP-CH_2);

MS (ESI), m/z (%):1242 (3) $[M]^+$, 622 (45), 621 (54), 299 (25), 282 (90), 221 (100), 171 (32), 145 (55). HRMS (ESI): m/z = calcd for $C_{80}H_{62}N_2O_4{}^{32}S_4$ $[M]^+$: 1242.3593; found 1242.3541;

IR (ATR, $\tilde{\nu}$) = 3031 (w), 2999 (w), 2944 (w), 2922 (w), 2898 (w), 2850 (w), 2830 (w), 1601 (w), 1504 (vs), 1492 (s), 1470 (m), 1460 (m), 1439 (w), 1395 (w), 1316 (w), 1286 (m), 1265 (m), 1241 (vs), 1194 (m), 1177 (m), 1132 (w), 1105 (w), 1033 (s), 983 (w), 946 (w), 912 (w), 824 (s), 813 (vs), 782 (w), 749 (w), 721 (w), 701 (w), 677 (w), 654 (w), 632 (w), 619 (w), 594 (w), 577 (m), 561 (w), 548 (w), 518 (m), 484 (w), 458 (w), 450 (w), 431 (w), 409 (w), 395 (w), 378 (w) cm^{-1}.

Additional information on chemical synthesis is available *via* the Chemotion repository:

https://doi.org/10.14272/reaction/SA-FUHFF-UHFFFADPSC-WYYIOXHFIP-UHFFFADPSC-NUHFF-NUHFF-NUHFF-ZZZ

Additional information on the analysis of the target compound is available *via* the Chemotion repository:

https://doi.org/10.14272/WYYIOXHFIPAEBC-UHFFFAOYSA-N.1

4,15-(Bis(4,1-phenylene-thieno[3,2-b]thiophene-5,2-diyl-*N,N*-bis(4-methoxyphenyl)aniline)[2.2]paracyclophane (63)

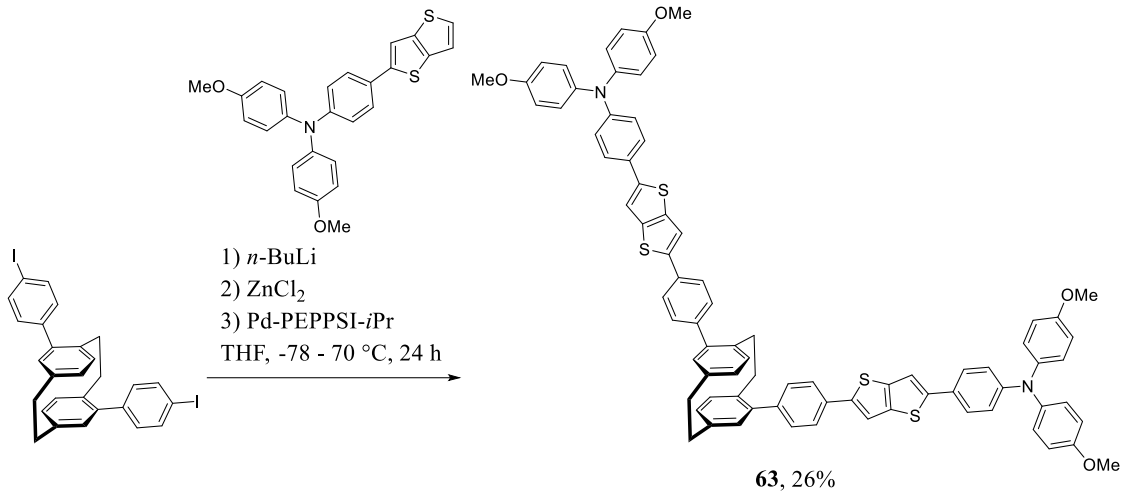

Preparation of Negishi reactant:

4-Methoxy-*N*-(4-methoxyphenyl)-*N*-(4-(thieno[3,2-b]thiophen-2-yl)phenyl)aniline (120 mg, 269 µmol, 2.20 equiv.) was added to a crimp cap vial and flushed with Ar three times. 4.5 mL of dry THF was added, and the mixture was cooled to -78 °C. *n*-Butyllithium solution (20.4 mg, 127 µL, 318 µmol, 2.50M in hexane, 2.60 equiv.) was added dropwise, and the reaction mixture was allowed to warm to 22 °C. After stirring for 30 min, the reaction mixture was cooled to 0 °C, and zinc chloride solution (50.1 mg, 367 µL, 367 µmol, 1.00M in THF, 3.00 equiv.) was added. The reaction was stirred for 15 min at 0 °C and then warmed to 22 °C.

Negishi coupling:

4,15-Bis(4-iodophenyl)[2.2]paracyclophane (75.0 mg, 122 µmol, 1.00 equiv.) and PEPPSI-IPr catalyst (8.35 mg, 12.2 µmol, 0.100 equiv.) were added to a crimp cap vial and flushed with Ar three times. 4.5 mL of dry THF and zinc chloride solution (50.1 mg, 367 µL, 367 µmol, 1.00M in THF, 3.00 equiv.) were added. After dissolving, the Negishi reactant was added *via* syringe, and the reaction mixture was heated to 70 °C. After three days, the reaction was allowed to cool to 22 °C, and the solvent was removed under reduced pressure. Column chromatography on silica using cHex/DCM 1:0 to 1:2 as eluent yielded 4,15-(bis(4,1-phenylene-thieno[3,2-b]thiophene-5,2-diyl-*N,N*-bis(4-methoxyphenyl)aniline)[2.2]paracyclophane (39.2 mg, 31.5 µmol, 26% yield) as a yellow-to-brown solid.

R_f = 0.28 (cHex/DCM 1:1).

M.p.: 147 °C

^{1}H NMR (400 MHz, Dichloromethane-d_2 [5.32 ppm], ppm) δ = 7.78–7.74 (m, 4H), 7.61–7.54 (m, 6H), 7.49–7.42 (m, 4H), 7.39 (s, 2H), 7.12–7.05 (m, 8H), 6.93–6.83 (m, 12H), 6.76–6.72 (m, 4H), 6.64 (dd, *J* = 7.7 Hz, *J* = 1.8 Hz, 2H), 3.79 (s, 12H, OMe-CH_3), 3.29–3.23 (m, 4H, PCP-CH_2), 3.16–3.08 (m, 2H, PCP-CH_2), 2.58–2.53 (m, 2H, PCP-CH_2);

^{13}C NMR (100 MHz, Dichloromethane-d_2 [53.84 ppm], ppm) δ = 156.3 (C_q, 4C), 146.4 (C_q, 2C), 144.7 (C_q, 2C), 141.7 (C_q, 4C), 140.6 (C_q, 4C), 140.3 (C_q, 2C), 139.9 (C_q, 2C), 139.5 (C_q, 2C), 138.4 (C_q, 2C), 137.5 (C_q, 4C), 133.2 (C_q, 2C), 132.4 (+, CH, 2C), 131.7 (+, CH, 2C), 131.3 (+, CH, 2C), 130.2 (+, CH, 4C), 126.9 (+, CH, 8C), 126.3 (+, CH, 4C), 125.7 (+, CH, 4C), 120.0 (+, CH, 4C), 115.5 (+, CH, 2C), 114.7 (+, CH, 8C), 113.9 (+, CH, 2C), 55.4 (+, CH_3, 4C, OMe-CH_3), 35.0 (–, CH_2, 2C, PCP-CH_2), 33.5 (–, CH_2, 2C, PCP-CH_2);

MS (ESI), m/z (%): 1242 (4) $[M]^+$, 622 (44), 621 (49), 514 (34), 513 (100), 375 (49). HRMS (ESI): m/z = calcd for $C_{80}H_{62}N_2O_4{}^{32}S_4$ $[M]^+$: 1242.3593; found 1242.3556;

IR (ATR, $\tilde{\nu}$) = 3029 (w), 2946 (w), 2921 (m), 2850 (w), 2830 (w), 1599 (w), 1502 (vs), 1470 (s), 1438 (s), 1317 (m), 1283 (m), 1235 (vs), 1191 (s), 1174 (s), 1103 (m), 1031 (vs), 982 (m), 949 (w), 912 (w), 823 (vs), 806 (vs), 781 (s), 728 (s), 721 (s), 701 (s), 653 (m), 636 (m), 619 (m), 591 (m), 575 (s), 514 (s), 484 (s), 466 (m), 448 (m), 439 (m), 431 (m), 418 (m), 407 (m), 381 (m) cm^{-1}.

Additional information on chemical synthesis is available *via* the Chemotion repository:

https://doi.org/10.14272/reaction/SA-FUHFF-UHFFFADPSC-FCILJFSEUA-UHFFFADPSC-NUHFF-NUHFF-NUHFF-ZZZ

Additional information on the analysis of the target compound is available *via* the Chemotion repository:

https://doi.org/10.14272/FCILJFSEUAWXKN-UHFFFAOYSA-N.1

6.2.2. Procedures Chapter 4.1 "Chiral PCP-Polymers and their Application in CP-TADF Emitters"

6.2.2.1. Procedures Monomers

10-[4-(4,6-Diphenyl-1,3,5-triazin-2-yl)phenyl]-9,9-dimethyl-acridine (DMAC-TRZ) (71)

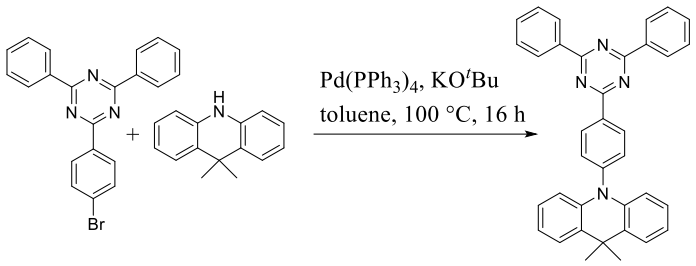

71, 70%

A vial was charged with 9,9-dimethyl-10*H*-acridine (750 mg, 3.58 mmol, 1.00 equiv.), 2-(4-bromophenyl)-4,6-diphenyl-1,3,5-triazine (1.53 g, 3.94 mmol, 1.10 equiv.), tetrakis(triphenylphosphine)palladium(0) (414 mg, 0.358 mmol, 0.100 equiv.) and potassium *tert*-butanolate (1.21 g, 10.8 mmol, 3.00 equiv.). It was evacuated and flushed with argon three times. Anhydrous toluene (50.0 mL) was added, then heated to 100 °C and stirred for 16 h. After cooling to 21 °C, the reaction mixture was washed with 3 x 50 mL brine. The organic layer was dried over Na_2SO_4, and the solvent was removed under reduced pressure. The obtained crude product was purified *via* column chromatography on silica gel using pentane/DCM 10:1 as eluent to yield 10-[4-(4,6-diphenyl-1,3,5-triazin-2-yl)phenyl]-9,9-dimethyl-acridine (1.30 g, 2.52 mmol, 70% yield) as a yellow solid.

R_f = 0.57 (pentane/DCM 4:1).

M.p.: 249 °C

^{1}H NMR (400 MHz, Chloroform-d [7.26 ppm], ppm) δ = 9.05–9.02 (m, 2H, CH_{Ar}), 8.84–8.82 (m, 4H, CH_{Ar}), 7.68–7.56 (m, 8H, CH_{Ar}), 7.52–7.49 (m, 2H, CH_{Ar}), 7.03–6.95 (m, 4H, CH_{Ar}), 6.40 (dt, *J* = 7.8 Hz, *J* = 1.3 Hz, 2H, CH_{Ar}), 1.74 (s, 6H, CH_3);

^{13}C NMR (100 MHz, Chloroform-d [77.16 ppm], ppm) δ = 171.9 (C_q, 2C), 171.1 (C_q), 145.4 (C_q), 140.6 (C_q, 2C), 136.1 (C_q), 136.1 (C_q, 2C), 132.7 (+, CH, 2C), 131.6 (+, CH, 2C), 131.5 (+, CH, 2C), 130.3 (C_q, 2C), 129.0 (+, CH, 4C), 128.7 (+, CH, 4C), 126.5 (+, CH, 2C), 125.4 (+, CH, 2C), 120.9 (+, CH, 2C), 114.2 (+, CH, 2C), 36.1 (C_q), 31.3 (+, CH_3, 2C);

MS (EI, 70 eV, 60 °C), m/z (%): 517 (28) $[M+H]^+$, 516 (16) $[M]^+$, 501 (34), 307 (30), 155 (27), 154 (100), 138 (32), 137 (60), 136 (63). HRMS (EI): m/z = calcd for $C_{36}H_{29}N_4$ $[M+H]^+$: 517.2387; found 517.2385;

IR (ATR, $\tilde{\nu}$) = 3070 (vw), 3031 (vw), 2962 (vw), 2955 (vw), 1588 (m), 1511 (vs), 1475 (vs), 1465 (s), 1445 (vs), 1408 (m), 1363 (vs), 1326 (vs), 1269 (vs), 1170 (m), 1159 (w), 1146 (w), 1126 (w), 1113 (w), 1098 (w), 1089 (w), 1067 (w), 1047 (w), 1024 (w), 1017 (w), 1001 (w), 989 (w), 975 (w), 926 (w), 836 (m), 769 (m), 739 (vs), 694 (s), 681 (vs), 666 (m), 645 (m), 636 (w), 622 (m), 605 (w), 578 (w), 551 (w), 518 (m), 477 (w), 450 (w), 409 (w) cm^{-1}.

Additional information on the chemical synthesis is available *via* the Chemotion repository: https://doi.org/10.14272/reaction/SA-FUHFF-UHFFFADPSC-IVXBGKPGZO-UHFFFADPSC-NUHFF-NUHFF-NUHFF-ZZZ.

Additional information on the analysis of the target compound is available *via* the Chemotion repository: https://doi.org/10.14272/IVXBGKPGZOETEW-UHFFFAOYSA-N.1.

2-Bromo-10-(4-(4,6-diphenyl-1,3,5-triazin-2-yl)phenyl)-9,9-dimethyl-9,10-dihydroacridine (72)

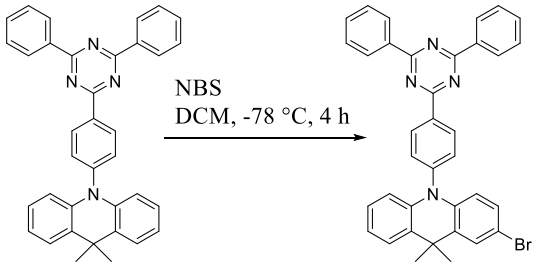

72, 93%

N-Bromosuccinimide (543 mg, 3.05 mmol, 1.05 equiv.) was added portionwise to a dry-ice cooled solution of 10-[4-(4,6-diphenyl-1,3,5-triazin-2-yl)phenyl]-9,9-dimethylacridine (1.50 g, 2.90 mmol, 1.00 equiv.) in 75 mL of DCM while stirring over 2 h. The solution was stirred for another hour and then warmed to 21 °C. It was then washed with water (3 x 100 mL), dried over Na_2SO_4 and subjected to column chromatography on silica using pentane/DCM 10:1 as eluent to yield the product 2-bromo-10-(4-(4,6-diphenyl-1,3,5-triazin-2-yl)phenyl)-9,9-dimethyl-9,10-dihydroacridine (1.61 g, 2.71 mmol, 93% yield) as a yellow solid.

R_f = 0.51 (pentane/DCM 4:1).

M.p.: 263 °C

^{1}H NMR (400 MHz, Chloroform-d [7.26 ppm], ppm) δ = 9.05–9.01 (m, 2H, CH_{Ar}), 8.85–8.79 (m, 4H, CH_{Ar}), 7.67–7.59 (m, 6H, CH_{Ar}), 7.56 (d, *J* = 2.3 Hz, 1H, CH_{Ar}), 7.56–7.52 (m, 2H, CH_{Ar}), 7.50–7.47 (m, 1H, CH_{Ar}), 7.08 (dd, *J* = 8.8 Hz, *J* = 2.3 Hz, 1H, CH_{Ar}), 7.03–6.96 (m, 2H, CH_{Ar}), 6.41–6.35 (m, 1H, CH_{Ar}), 6.24 (d, *J* = 8.8 Hz, 1H, CH_{Ar}), 1.70 (s, 6H, CH_3);

^{13}C NMR (100 MHz, Chloroform-d [77.16 ppm], ppm) δ = 171.9 (C_q, 2C), 171.0 (C_q), 144.8 (C_q), 140.2 (C_q), 139.8 (C_q), 136.4 (C_q), 136.0 (C_q, 2C), 132.8 (+, CH, 2C), 132.4 (C_q), 131.7 (+, CH, 2C), 131.4 (+, CH, 2C), 129.7 (C_q), 129.2 (+, CH), 129.0 (+, CH, 4C), 128.7 (+, CH, 4C), 128.2 (+, CH), 126.7 (+, CH), 125.3 (+, CH), 121.2 (+, CH), 115.8 (+, CH), 114.3 (+, CH), 113.2 (C_q), 36.2 (C_q), 31.2 (+, CH3, 2C);

MS (FAB, 3-NBA), m/z (%): 595/597 (6/6) $[M+H]^+$, 594/596 (5/4) [M]+, 307 (35), 155 (30), 154 (100), 138 (34), 137 (66), 136 (67). HRMS (FAB, matrix NBA): m/z = calcd for $C_{36}H_{28}N_4{}^{79}Br$ $[M+H]^+$: 595.1492; found 595.1491;

IR (ATR, $\tilde{\nu}$) = 3067 (w), 3034 (w), 2959 (w), 2918 (w), 2859 (w), 1588 (m), 1521 (vs), 1500 (s), 1476 (vs), 1460 (s), 1446 (s), 1408 (m), 1366 (vs), 1332 (s), 1316 (s), 1285 (m), 1269 (m), 1230 (w), 1215 (w), 1169 (w), 1146 (w), 1123 (w), 1096 (w), 1084 (w), 1067 (w), 1048 (w), 1026 (w), 1017 (w), 1001 (w), 932 (w), 878 (w), 839 (m), 802 (m), 771 (s), 742 (vs), 690 (vs), 680 (s), 670 (w), 656 (w), 646 (m), 635 (w), 606 (w), 565 (w), 551 (w), 533 (s), 517 (m), 484 (w), 470 (w), 446 (w), 415 (w), 402 (w), 394 (w), 377 (w) cm^{-1}.

Additional information on the chemical synthesis is available *via* the Chemotion repository: https://doi.org/10.14272/reaction/SA-FUHFF-UHFFFADPSC-QDIRQRCGOT-UHFFFADPSC-NUHFF-NUHFF-NUHFF-ZZZ.

Additional information on the analysis of the target compound is available *via* the Chemotion repository: https://doi.org/10.14272/QDIRQRCGOTXLOJ-UHFFFAOYSA-N.1.

10-(4-(4,6-Diphenyl-1,3,5-triazin-2-yl)phenyl)-9,9-dimethyl-2-vinyl-9,10-dihydroacridine (73)

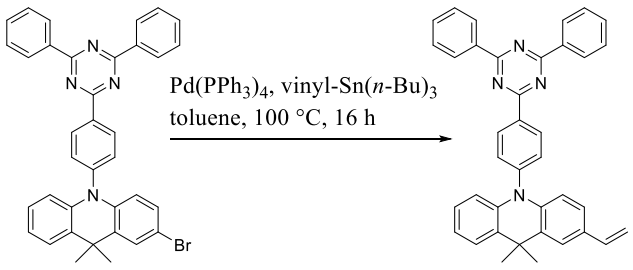

73, 52%

Tetrakis(triphenylphosphine)palladium(0) (291 mg, 252 µmol, 0.100 equiv.) and 2-bromo-10-(4-(4,6-diphenyl-1,3,5-triazin-2-yl)phenyl)-9,9-dimethyl-9,10-dihydroacridine (1.50 g, 2.52 mmol, 1.00 equiv.) were added together under argon and dissolved in 75 mL of dry toluene. After stirring for 15 min, tri-*n*-butyl(vinyl)stannane (1.20 g, 1.10 mL, 3.78 mmol, 1.50 equiv.) was added dropwise. The mixture was stirred for 12 h at 100 °C. The mixture was cooled to 21 °C, poured into 300 mL of

saturated $KF_{(aq.)}$ solution, and extracted with 3 x 50 mL of DCM. The organic extracts were washed with 2 x 100 mL of brine and then dried over Na_2SO_4. After evaporating the solvent, the residue was purified by column chromatography on silica using pentane/DCM 10:1 as eluent to yield 10-(4-(4,6-diphenyl-1,3,5-triazin-2-yl)phenyl)-9,9-dimethyl-2-vinyl-9,10-dihydroacridine (712 mg, 1.22 mmol, 48% yield) as a yellow solid.

R_f = 0.44 (pentane/DCM 4:1).

M.p.: 219 °C

^{1}H NMR (400 MHz, Chloroform-d [7.26 ppm], ppm) δ = 9.05–9.03 (m, 2H, C*H*$_{Ar}$), 8.83 (m, 4H, C*H*$_{Ar}$), 7.68–7.49 (m, 10H, C*H*$_{Ar}$), 7.08 (dd, *J* = 8.6 Hz, *J* = 2.0 Hz, 1H, C*H*$_{Ar}$), 7.03–6.95 (m, 2H, C*H*$_{Ar}$), 6.69 (dd, *J* = 17.5 Hz, *J* = 10.9 Hz, 1H, vinyl-*H*), 6.39 (m, 1H, C*H*$_{Ar}$), 6.35 (d, *J* = 8.5 Hz, 1H, C*H*$_{Ar}$), 5.62 (dd, *J* = 17.5 Hz, *J* = 1.0 Hz, 1H, vinyl-*H*), 5.12 (dd, *J* = 10.8 Hz, *J* = 1.0 Hz, 1H, vinyl-*H*), 1.77–1.74 (m, 6H, C*H*$_3$);

^{13}C NMR (100 MHz, Chloroform-d [77.16 ppm], ppm) δ = 171.9 (C_q, 2C), 171.0 (C_q), 145.2 (C_q), 140.3 (C_q), 140.3 (C_q), 136.6 (+, CH, vinyl-CH), 136.2 (C_q), 136.1 (C_q, 2C), 132.7 (+, CH, 2C), 131.6 (+, CH, 2C), 131.5 (+, CH, 2C), 130.4 (C_q), 130.1 (C_q), 130.1 (C_q), 129.0 (+, CH, 4C), 128.8 (+, CH, 4C), 126.5 (+, CH), 125.5 (+, CH), 124.3 (+, CH), 123.7 (+, CH), 121.0 (+, CH), 114.3 (+, CH), 114.2 (+, CH), 110.9 (–, CH_2, vinyl-CH_2), 36.1 (C_q), 31.6 (+, CH_3, 2C);

MS (FAB, 3-NBA), m/z (%): 543 (2) $[M+H]^+$, 307 (36), 155 (29), 154 (100),138 (34), 137 (66), 136 (64). HRMS (FAB, matrix NBA): m/z = calcd for $C_{38}H_{31}N_4$ $[M+H]^+$: 543.2543 ; found 543.2541;

IR (ATR, $\tilde{\nu}$) = 1588 (m), 1520 (vs), 1482 (vs), 1463 (m), 1445 (vs), 1408 (m), 1397 (w), 1366 (vs), 1333 (vs), 1293 (s), 1271 (s), 1232 (w), 1228 (w), 1197 (w), 1176 (m), 1169 (m), 1146 (m), 1125 (w), 1088 (w), 1067 (w), 1050 (w), 1024 (w), 1016 (m), 993 (w), 975 (w), 931 (w), 898 (m), 881 (w), 843 (m), 830 (w), 815 (w), 803 (w), 769 (s), 751 (vs), 741 (vs), 690 (vs), 680 (s), 663 (m), 646 (s), 635 (m), 608 (w), 596 (w), 586 (w), 564 (w), 526 (m), 517 (m), 472 (w), 453 (w), 429 (w), 401 (w) cm^{-1}.

Additional information on chemical synthesis is available *via* the Chemotion repository:

https://doi.org/10.14272/reaction/SA-FUHFF-UHFFFADPSC-PJYLHMAQYD-UHFFFADPSC-NUHFF-NUHFF-NUHFF-ZZZ

Additional information on the analysis of the target compound is available *via* the Chemotion repository:

https://doi.org/10.14272/PJYLHMAQYDQPAM-UHFFFAOYSA-N.1

6.2.2.2. General Procedures Polymers

General Procedures Homopolymerization Vinyl-PCP to Poly(vinyl[2.2]paracyclophane) (69)

Anionic Polymerization

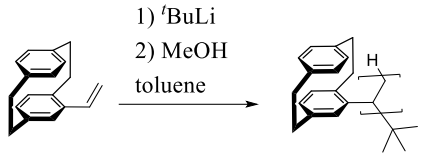

69

The polymerization reactor was immersed in a thermostated ^{i}PrOH bath to maintain the reaction temperature at 0 °C. Under argon atmosphere, the initiator *tert*-butyllithium (0.0100 – 0.100 equiv.) was added to 4-vinyl[2.2]paracyclophane (250 mg, 1.07 mmol, 1.00 equiv.) in toluene (0.2 mL) to start the reaction. After 24 h, the reaction was terminated by precipitating from 10 mL of MeOH, and the product was collected by centrifugation. The solid was redissolved in 1.5 mL of DCM and precipitated from 10 mL of MeOH to yield poly(vinyl[2.2]paracyclophane).

^{1}H NMR (400 MHz, Dichloromethane-d_2 [5.32 ppm], ppm) δ = 6.40–6.40 (m, 7H), 3.05–3.05 (m, 8H), 1.30–1.27 (m, 2H), 0.88–0.86 (m, 1H).

GPC S_p: M_n: 1.781E^{+3} g/mol; M_w: 2.036E^{+3} g/mol; D: 1.143E^{+0};

GPC R_p: M_n: 1.011E^{+3} g/mol; M_w: 3.245E^{+3} g/mol; D: 3.211E^{+0}.

Additional information on the chemical synthesis is available *via* the Chemotion repository: https://doi.org/10.14272/reaction/SA-FUHFF-UHFFFADPSC-UHFFFADPSC-UHFFFADPSC-NUHFF-NUHFF-NUHFF-ZAZ.10.

Additional information on the analysis of the target compound is available *via* the Chemotion repository: https://doi.org/0.14272/DUMMY.9.

Radical Polymerization

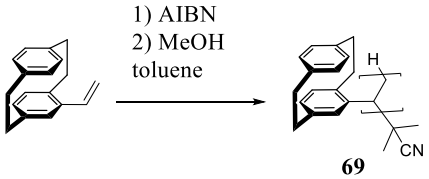

69

Under an argon atmosphere, the initiator AIBN (0.0100 – 0.200 equiv.) was added to R_p- or S_p-4-vinyl[2.2]paracyclophane (250 mg, 1.07 mmol, 1.00 equiv.) in dry toluene (1 mL) to start the reaction and heated to 60 °C for 24 h. The reaction was terminated by precipitating from 10 mL of

MeOH, and the product was collected by centrifugation. The solid was redissolved in 1.5 mL of DCM and precipitated from 10 mL of MeOH to yield poly(vinyl[2.2]paracyclophane).

^{1}H NMR (400 MHz, Dichloromethane-d_2 [5.32 ppm], ppm) δ = 6.47 (m, 7H), 3.51–3.00 (m, 8H), 1.27–0.87 (m, 3H).

GPC S_p: M_n: 1.665E^{+3} g/mol; M_w: 1.898E^{+3} g/mol; D: 1.140E^{+0};

GPC R_p: M_n: 7.784E^{+2} g/mol; M_w: 1.379E^{+3} g/mol; D: 1.772E^{+0};

GPC S_p, double run: M_n: 1.716E^{+3} g/mol; M_w: 2.744E^{+3} g/mol; D: 1.599E^{+0}.

Additional information on the chemical synthesis is available *via* the Chemotion repository: https://doi.org/10.14272/reaction/SA-FUHFF-UHFFFADPSC-MVZQZJZNEJ-UHFFFADPSC-NUHFF-NUHFF-NUHFF-ZZZ.

Additional information on the analysis of the target compound is available *via* the Chemotion repository: https://doi.org/10.14272/MVZQZJZNEJDERU-UHFFFAOYSA-N.1.

Cationic Polymerization

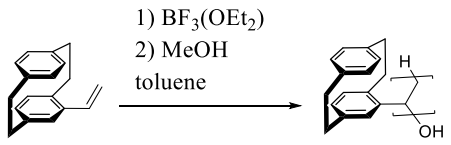

69

The polymerization reactor was immersed in a thermostated ^{i}PrOH bath to maintain the reaction temperature at 0 °C. Under argon atmosphere, the initiator $BF_3(OEt_2)$ (31.5 mg, 28.2 µL, 213 µmol, 0.100 equiv.) was added to S_p-4-vinyl[2.2]paracyclophane (500 mg, 2.13 mmol, 1.00 equiv.) in dry toluene (1 mL) to start the reaction. After 24 h, the reaction was terminated by precipitating from 10 mL of MeOH, and the product was collected by centrifugation. The solid was redissolved in 1.5 mL of DCM and precipitated from 10 mL of MeOH to yield S_p-poly(vinyl[2.2]paracyclophane).

^{1}H NMR (400 MHz, Chloroform-d [7.26 ppm], ppm) δ = 6.63–6.34 (m, 7H), 3.01–2.50 (m, 8H), 1.43–0.86 (m, 3H).

GPC: M_n: 5.820E^{+2} g/mol; M_w: 7.890E^{+2} g/mol; D: 1.356E^{+0}.

Additional information on the chemical synthesis is available *via* the Chemotion repository: https://doi.org/10.14272/reaction/SA-FUHFF-UHFFFADPSC-OJVMIRUKBR-UHFFFADPSC-NUHFF-NUHFF-NUHFF-ZZZ.

Additional information on the analysis of the target compound is available *via* the Chemotion repository: https://doi.org/10.14272/OJVMIRUKBRPGIQ-UHFFFAOYSA-N.1.

General Procedure Copolymerization Vinyl-PCP + Styrene to Poly(styrene-vinyl[2.2]paracyclophane) (70)

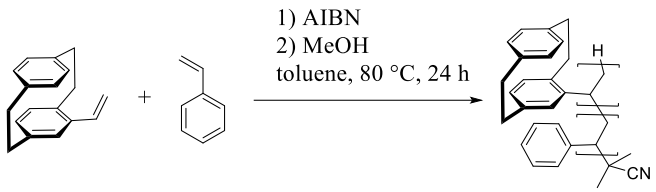

70

In a Schlenck tube, 0.02 eq/monomer of the initiator AIBN was added to styrene (1.00–50.0 equiv.), and S_p-4-vinyl[2.2]paracyclophane (25.0 mg, 107 µmol, 1.00 equiv.) in 0.25 mL of dry degassed toluene and the reaction heated to 80 °C to start the reaction. The reaction was cooled and terminated by precipitation by adding 5 mL of MeOH after 24 h. The product was collected by centrifugation and redissolved in 0.25 mL of DCM. Afterward, it was precipitated by adding 5 mL of MeOH, collected by centrifugation, and dried in a vacuum to yield S_p-poly(styrene-vinyl[2.2]paracyclophane).

Vinyl-PCP:styrene 1:1

^{1}H NMR (400 MHz, Dichloromethane-d_2 [5.32 ppm], ppm) δ = 7.75-6.82 (m, 4H, CH_{Ar}), 6.81–6.37 (m, 9H, CH_{Ar}), 3.49–2.83 (m, 8H, PCP-CH_2), 2.33–1.73 (m, 6H, alkyl-H);

GPC: M_n: 4.790E^{+3} g/mol; M_w: 1.046E^{+4} g/mol; D: 2.183E^{+0};

IR (ATR, ṽ) = 3478 (w), 3441 (w), 3429 (w), 3421 (w), 3393 (w), 3381 (w), 3371 (w), 3364 (w), 3350 (w), 3342 (w), 3332 (w), 3323 (w), 3308 (w), 3291 (w), 3286 (w), 3228 (w), 3218 (w), 3024 (w), 2924 (m), 2893 (w), 2851 (w), 1592 (w), 1492 (w), 1452 (m), 1438 (w), 1411 (w), 1366 (w), 1344 (w), 1320 (w), 1293 (w), 1261 (w), 1234 (w), 1184 (w), 1118 (w), 1061 (vs), 1034 (s), 956 (s), 933 (s), 898 (s), 849 (m), 795 (m), 759 (s), 730 (s), 715 (s), 700 (vs), 649 (m), 603 (m), 585 (m), 545 (s), 510 (vs), 475 (m), 459 (m), 442 (m), 429 (m), 412 (m), 387 (m), 375 (m) cm^{-1}.

Additional information on the chemical synthesis is available *via* the Chemotion repository: https://doi.org/10.14272/reaction/SA-FUHFF-UHFFFADPSC-IXIVTXOHXV-UHFFFADPSC-NUHFF-NUHFF-NUHFF-ZZZ.1.

Additional information on the analysis of the target compound is available *via* the Chemotion repository: https://doi.org/10.14272/IXIVTXOHXVVPAC-UHFFFAOYSA-N.2.

Vinyl-PCP:styrene 1:10

^{1}H NMR (400 MHz, Dichloromethane-d_2 [5.32 ppm], ppm) δ = 7.31–6.84 (m, 32H, CH_{Ar}), 6.83–6.37 (m, 19H, CH_{Ar}), 6.36–5.95 (m, 4H, CH_{Ar}), 3.14–2.76 (m, 8H, PCP-CH_2), 2.13–1.55 (m, 18H, alkyl backbone), 1.51–1.28 (m, 12H, alkyl backbone)

GPC: M_n: 2.561E^{+3} g/mol; M_w: 1.394E^{+4} g/mol; D: 5.443E^{+0};

IR (ATR, ṽ) = 3391 (vw), 3376 (vw), 3353 (vw), 3306 (vw), 3084 (vw), 3058 (vw), 3026 (w), 2922 (w), 2851 (w), 1601 (w), 1582 (vw), 1492 (w), 1452 (m), 1412 (vw), 1367 (w), 1346 (w), 1317 (vw), 1183 (w), 1156 (vw), 1115 (w), 1065 (m), 1030 (w), 982 (w), 962 (w), 935 (w), 904 (w), 863 (w), 844 (w), 796 (w), 756 (m), 697 (vs), 625 (w), 608 (w), 594 (w), 540 (m), 511 (w), 472 (w), 459 (w), 449 (w), 432 (w), 425 (w), 414 (w), 408 (w), 395 (w), 387 (w), 378 (w) cm^{-1}.

Additional information on the chemical synthesis is available *via* the Chemotion repository: https://doi.org/10.14272/reaction/SA-FUHFF-UHFFFADPSC-IXIVTXOHXV-UHFFFADPSC-NUHFF-NUHFF-NUHFF-ZZZ.2.

Additional information on the analysis of the target compound is available *via* the Chemotion repository: https://doi.org/10.14272/IXIVTXOHXVVPAC-UHFFFAOYSA-N.3.

Vinyl-PCP:styrene 1:25

^{1}H NMR (400 MHz, Dichloromethane-d_2 [5.32 ppm], ppm) δ = 7.29–6.96 (m, 94H, CH_{Ar}), 6.78–6.39 (m, 46H, CH_{Ar}), 3.16–2.64 (m, 8H, PCP-CH_2), 2.20–1.52 (m, 46H, alkyl backbone), 1.50–0.90 (s, 31H, alkyl backbone);

GPC: M_n: 4.682E^{+3} g/mol; M_w: 1.064E^{+4} g/mol; D: 2.272E^{+0};

IR (ATR, ṽ) = 3429 (vw), 3364 (vw), 3303 (vw), 3058 (vw), 3024 (w), 2999 (vw), 2922 (w), 2850 (w), 1601 (w), 1492 (w), 1452 (w), 1412 (vw), 1367 (w), 1344 (vw), 1330 (vw), 1320 (vw), 1293 (vw), 1183 (w), 1154 (vw), 1118 (vw), 1065 (w), 1030 (w), 1001 (w), 963 (w), 935 (w), 922 (w), 908 (w), 844 (w), 756 (m), 697 (vs), 622 (w), 594 (w), 538 (m), 513 (w), 466 (w), 456 (w), 449 (w), 419 (w), 412 (w), 405 (w), 391 (vw), 384 (vw) cm^{-1}.

Additional information on the chemical synthesis is available *via* the Chemotion repository: https://doi.org/10.14272/reaction/SA-FUHFF-UHFFFADPSC-IXIVTXOHXV-UHFFFADPSC-NUHFF-NUHFF-NUHFF-ZZZ.3.

Additional information on the analysis of the target compound is available *via* the Chemotion repository: https://doi.org/10.14272/IXIVTXOHXVVPAC-UHFFFAOYSA-N.4.

Vinyl-PCP:styrene 1:50

^{1}H NMR (400 MHz, Dichloromethane-d_2 [5.32 ppm], ppm) δ = 7.44–6.86 (m, 147H, CH_{Ar}), 6.83–6.14 (m, 85H, CH_{Ar}), 3.15–2.63 (m, 8H, PCP-CH_2), 2.23–1.53 (m, 72H, alkyl backbone), 1.45–0.89 (m, 52H, alkyl backbone);

GPC: M_n: 6.015E^{+3} g/mol; M_w: 1.369E^{+4} g/mol; D: 2.276E^{+0};

IR (ATR, $\tilde{\nu}$) = 3427 (vw), 3350 (vw), 3301 (vw), 3087 (vw), 3061 (vw), 3026 (w), 2922 (w), 2851 (w), 1601 (w), 1493 (w), 1452 (w), 1367 (w), 1346 (vw), 1183 (w), 1153 (vw), 1065 (w), 1030 (w), 1003 (w), 962 (w), 935 (w), 922 (w), 908 (w), 844 (w), 755 (m), 697 (vs), 626 (w), 619 (w), 608 (w), 594 (w), 538 (m), 514 (w), 494 (w), 477 (w), 469 (w), 463 (w), 453 (w), 446 (w), 432 (w), 419 (w), 408 (w), 399 (w), 387 (w) cm^{-1}.

Additional information on the chemical synthesis is available *via* the Chemotion repository: https://doi.org/10.14272/reaction/SA-FUHFF-UHFFFADPSC-IXIVTXOHXV-UHFFFADPSC-NUHFF-NUHFF-NUHFF-ZZZ.

Additional information on the analysis of the target compound is available *via* the Chemotion repository: https://doi.org/10.14272/IXIVTXOHXVVPAC-UHFFFAOYSA-N.1.

General Procedure Copolymerization of Vinyl-PCP and Vinyl-DMAC-TRZ to Poly(vinyl[2.2]paracyclophane-co-2-vinyl-DMAC-TRZ (74)

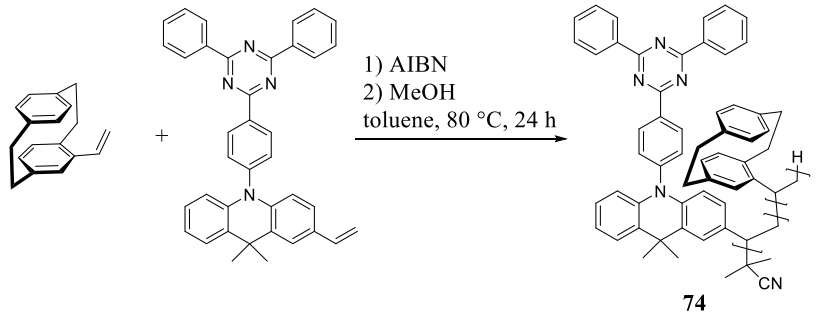

74

In a Schlenk tube, 0.02 eq/monomer of the initiator AIBN was added to 10-(4-(4,6-diphenyl-1,3,5-triazin-2-yl)phenyl)-9,9-dimethyl-2-vinyl-9,10-dihydroacridine (1.00 equiv.) and 4-vinyl[2.2]paracyclophane (10.0 – 100 equiv.) in 0.1 mL of dry degassed toluene and the reaction heated to 80 °C to start the reaction. The reaction was cooled to 21 °C and terminated by precipitation by adding 5 mL of MeOH after 24 h. The product was collected by centrifugation and redissolved in 0.25 mL of DCM. Afterward, it was precipitated by adding 5 mL of MeOH, collected by centrifugation, and dried in a vacuum to yield poly(vinyl[2.2]paracyclophane-co-2-vinyl-DMAC-TRZ) as a yellow solid.

***R_p*-Vinyl-PCP:Vinyl-DMAC-TRZ 10:1**

^{1}H NMR (400 MHz, Dichloromethane-d_2 [5.32 ppm], ppm) δ = 9.06–8.82 (m, 6H, DMAC-TRZ-CH_{Ar}), 7.67–6.34 (m, 38H, CH_{Ar}), 3.14–2.76 (m, 30H, PCP-CH_2), 2.23–0.84 (m, 40H, alkyl backbone);

GPC: M_n: 1.166E^{+3} g/mol; M_w: 6.567E^{+3} g/mol; D: 5.633E^{+0};

IR (ATR, ṽ) = 3422 (w), 3405 (w), 3394 (w), 3388 (w), 3381 (w), 3361 (w), 3340 (w), 3332 (w), 2924 (m), 2853 (w), 1771 (w), 1721 (w), 1667 (w), 1588 (w), 1516 (s), 1476 (w), 1446 (m), 1411 (w), 1366 (s), 1323 (m), 1261 (m), 1241 (w), 1180 (s), 1057 (vs), 1033 (vs), 987 (vs), 921 (vs), 860 (s), 843 (s), 798 (vs), 772 (s), 745 (vs), 717 (s), 696 (s), 683 (s), 663 (s), 646 (s), 635 (s), 601 (s), 591 (s), 581 (s), 572 (s), 557 (s), 535 (s), 511 (s), 476 (s), 463 (s), 456 (s), 441 (s), 431 (m), 422 (m), 401 (s), 392 (s), 384 (s) cm^{-1}.

Additional information on the chemical synthesis is available *via* the Chemotion repository: https://doi.org/10.14272/reaction/SA-FUHFF-UHFFFADPSC-JIWMTSMBOD-UHFFFADPSC-NUHFF-NUHFF-NUHFF-ZZZ.3.

Additional information on the analysis of the target compound is available *via* the Chemotion repository: https://doi.org/10.14272/JIWMTSMBODORIT-UHFFFAOYSA-N.

***R_p*-Vinyl-PCP:Vinyl-DMAC-TRZ 20:1**

^{1}H NMR (400 MHz, Dichloromethane-d_2 [5.32 ppm], ppm) δ = 9.07–8.81 (m, 6H, DMAC-TRZ-CH_{Ar}), 7.69–6.36 (m, 64H, CH_{Ar}), 3.50–2.50 (m, 53H, PCP-CH_2), 2.19–0.85 (m, 37H, alkyl backbone);

GPC: M_n: 2.428E^{+3} g/mol; M_w: 1.568E^{+4} g/mol; D: 6.458E^{+0};

IR (ATR, ṽ) = 3509 (vw), 3495 (w), 3397 (w), 3353 (w), 3337 (w), 3330 (w), 3320 (w), 3312 (w), 3281 (w), 3250 (w), 2955 (w), 2925 (w), 2893 (w), 2853 (w), 1721 (w), 1639 (w), 1588 (w), 1554 (vw), 1517 (m), 1476 (w), 1445 (m), 1411 (m), 1366 (s), 1344 (m), 1322 (m), 1261 (m), 1188 (m), 1118 (m), 1058 (vs), 1034 (vs), 960 (vs), 925 (vs), 899 (s), 843 (s), 798 (vs), 772 (s), 745 (s), 730 (s), 717 (s), 696 (s), 684 (s), 663 (s), 646 (s), 636 (s), 603 (s), 557 (s), 534 (s), 511 (vs), 484 (s), 452 (s), 438 (s), 426 (s), 411 (s), 392 (s), 384 (s), 377 (s) cm^{-1}.

Additional information on the chemical synthesis is available *via* the Chemotion repository: https://doi.org/10.14272/reaction/SA-FUHFF-UHFFFADPSC-JIWMTSMBOD-UHFFFADPSC-NUHFF-NUHFF-NUHFF-ZZZ.

Additional information on the analysis of the target compound is available *via* the Chemotion repository: https://doi.org/10.14272/JIWMTSMBODORIT-UHFFFAOYSA-N.1.

R_p-Vinyl-PCP:Vinyl-DMAC-TRZ 50:1

^{1}H NMR (400 MHz, Dichloromethane-d_2 [5.32 ppm], ppm) δ = 9.07–8.82 (m, 6H, DMAC-TRZ-CH_{Ar}), 7.67–6.34 (m, 92H, CH_{Ar}), 3.50–2.76 (m, 82H, PCP-CH_2), 2.01–0.82 (m, 246H, alkyl backbone);

GPC: M_n: 8.888E^{+2} g/mol; M_w: 3.977E^{+3} g/mol; D: 4.474E^{+0};

IR (ATR, $\tilde{\nu}$) = 3401 (w), 3384 (w), 3377 (w), 3370 (w), 3359 (w), 3346 (w), 3329 (w), 3284 (w), 3269 (w), 3257 (w), 2925 (m), 2893 (w), 2853 (w), 1771 (w), 1721 (w), 1664 (w), 1656 (w), 1647 (w), 1642 (w), 1619 (w), 1589 (w), 1517 (w), 1482 (w), 1445 (m), 1411 (m), 1366 (m), 1343 (m), 1322 (m), 1289 (w), 1261 (m), 1239 (w), 1181 (s), 1057 (vs), 1034 (vs), 986 (vs), 958 (vs), 922 (vs), 899 (vs), 858 (s), 850 (s), 846 (s), 798 (vs), 773 (s), 745 (s), 730 (s), 717 (s), 697 (s), 684 (s), 646 (s), 637 (s), 603 (s), 596 (s), 589 (s), 584 (s), 574 (s), 558 (s), 538 (s), 530 (s), 511 (vs), 477 (s), 469 (s), 452 (s), 443 (s), 428 (m), 419 (m), 405 (s), 395 (m), 387 (s), 375 (m) cm^{-1}.

Additional information on the chemical synthesis is available *via* the Chemotion repository: https://doi.org/10.14272/reaction/SA-FUHFF-UHFFFADPSC-JIWMTSMBOD-UHFFFADPSC-NUHFF-NUHFF-NUHFF-ZZZ.2.

Additional information on the analysis of the target compound is available *via* the Chemotion repository: https://doi.org/10.14272/JIWMTSMBODORIT-UHFFFAOYSA-N.3.

R_p-Vinyl-PCP:Vinyl-DMAC-TRZ 100:1

^{1}H NMR (400 MHz, Dichloromethane-d_2 [5.32 ppm], ppm) δ = 9.05–8.83 (m, 6H, DMAC-TRZ-CH_{Ar}), 7.67–5.64 (m, 144H, CH_{Ar}), 3.50–2.73 (m, 139H, PCP-CH_2), 2.18–0.84 (m, 158H, alkyl backbone);

GPC: M_n: 5.073E^{+2} g/mol; M_w: 1.955E^{+3} g/mol; D: 3.854E^{+0};

IR (ATR, $\tilde{\nu}$) = 3442 (w), 3431 (w), 3410 (w), 3394 (w), 3377 (w), 3359 (w), 3347 (w), 3332 (w), 3299 (w), 3264 (w), 3208 (w), 2956 (m), 2922 (m), 2851 (w), 1744 (vw), 1720 (w), 1710 (w), 1656 (w), 1639 (w), 1626 (w), 1589 (w), 1553 (w), 1541 (w), 1517 (m), 1446 (m), 1411 (m), 1366 (m), 1344 (m), 1322 (m), 1286 (w), 1259 (s), 1188 (m), 1061 (vs), 1034 (vs), 963 (vs), 925 (vs), 899 (s), 860 (s), 843 (s), 796 (vs), 745 (s), 731 (s), 717 (s), 697 (s), 684 (s), 662 (s), 646 (m), 606 (s), 586 (m), 561 (s), 554 (s), 511 (s), 482 (m), 448 (m), 436 (m), 431 (m), 395 (s) cm^{-1}.

Additional information on the chemical synthesis is available *via* the Chemotion repository: https://doi.org/10.14272/reaction/SA-FUHFF-UHFFFADPSC-JIWMTSMBOD-UHFFFADPSC-NUHFF-NUHFF-NUHFF-ZZZ.1.

Additional information on the analysis of the target compound is available *via* the Chemotion repository: https://doi.org/10.14272/JIWMTSMBODORIT-UHFFFAOYSA-N.2.

S_p-Vinyl-PCP:Vinyl-DMAC-TRZ 20:1

^{1}H NMR (400 MHz, Dichloromethane-d_2 [5.32 ppm], ppm) δ = 9.10–8.82 (m, 6H, DMAC-TRZ-CH_{Ar}), 7.69–6.01 (m, 76H, CH_{Ar}), 3.28–2.60 (m, 63H, PCP-CH_2), 1.91–0.84 (m, 64H, alkyl backbone).

GPC: M_n: 7.335E^{+2} g/mol; M_w: 2.190E^{+3} g/mol; D: 2.986E^{+0}.

IR (ATR, $\tilde{\nu}$) = 3031 (w), 3004 (w), 2921 (vs), 2894 (s), 2850 (s), 2772 (w), 1720 (w), 1684 (w), 1679 (w), 1588 (m), 1514 (vs), 1480 (m), 1446 (s), 1411 (m), 1366 (vs), 1322 (m), 1268 (m), 1230 (w), 1201 (w), 1176 (m), 1157 (m), 1096 (w), 1085 (w), 1067 (w), 1050 (w), 1024 (m), 1017 (m), 1000 (w), 936 (w), 897 (s), 863 (m), 843 (m), 795 (vs), 771 (s), 744 (vs), 730 (s), 715 (vs), 696 (s), 684 (m), 663 (w), 646 (s), 636 (m), 606 (m), 586 (w), 509 (vs) cm^{-1}.

Additional information on the chemical synthesis is available *via* the Chemotion repository: https://doi.org/10.14272/reaction/SA-FUHFF-UHFFFADPSC-JIWMTSMBOD-UHFFFADPSC-NUHFF-NUHFF-NUHFF-ZZZ.4.

Additional information on the analysis of the target compound is available *via* the Chemotion repository: https://doi.org/10.14272/JIWMTSMBODORIT-UHFFFAOYSA-N.5.

S_p-Vinyl-PCP:Vinyl-DMAC-TRZ 50:1

^{1}H NMR (400 MHz, Dichloromethane-d_2 [5.32 ppm], ppm) δ = 9.12–8.82 (m, 6H, DMAC-TRZ-CH_{Ar}), 7.80–6.00 (m, 160H, CH_{Ar}), 3.31–2.74 (m, 140H, PCP-CH_2), 1.77–0.90 (m, 206H, alkyl backbone).

GPC: M_n: 7.566E^{+2} g/mol; M_w: 2.272E^{+3} g/mol; D: 3.003E^{+0};

IR (ATR, $\tilde{\nu}$) = 3469 (w), 3429 (w), 3401 (w), 3384 (w), 3377 (w), 3370 (w), 3359 (w), 3346 (w), 3329 (w), 3284 (w), 3269 (w), 3257 (w), 2955 (m), 2925 (m), 2893 (w), 2853 (w), 1771 (w), 1721 (w), 1664 (w), 1656 (w), 1647 (w), 1642 (w), 1619 (w), 1589 (w), 1517 (w), 1482 (w), 1445 (m), 1411 (m), 1366 (m), 1343 (m), 1322 (m), 1289 (w), 1261 (m), 1239 (w), 1181 (s), 1057 (vs), 1034 (vs), 986 (vs), 958 (vs), 922 (vs), 899 (vs), 858 (s), 850 (s), 846 (s), 798 (vs), 773 (s), 745 (s), 730 (s), 717 (s), 697 (s), 684 (s), 646 (s), 637 (s), 603 (s), 596 (s), 589 (s), 584 (s), 574 (s), 558 (s), 538 (s), 530 (s), 511 (vs), 477 (s), 469 (s), 452 (s), 443 (s), 428 (m), 419 (m), 405 (s), 395 (m), 387 (s), 375 (m) cm^{-1}.

Additional information on the chemical synthesis is available *via* the Chemotion repository: https://doi.org/10.14272/reaction/SA-FUHFF-UHFFFADPSC-JIWMTSMBOD-UHFFFADPSC-NUHFF-NUHFF-NUHFF-ZZZ.5.

Additional information on the analysis of the target compound is available *via* the Chemotion repository: https://doi.org/10.14272/JIWMTSMBODORIT-UHFFFAOYSA-N.6.

Polymerization Procedure Poly(Vinyl-DMAC-TRZ) (75)

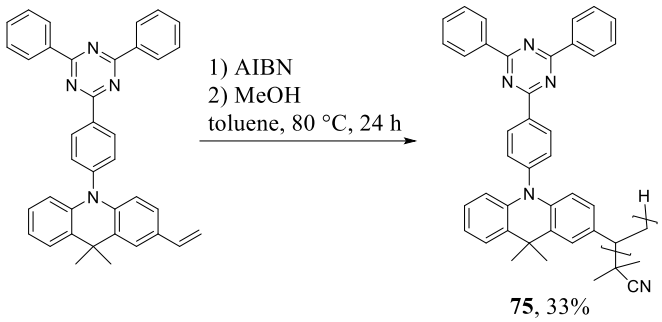

75, 33%

In a Schlenck tube, AIBN (1.13 mg, 6.91 µmol, 0.0500 equiv.) was added to 2-vinyl-DMAC-TRZ (75.0 mg, 138 µmol, 1.00 equiv.) in 0.2 mL of dry degassed toluene and the reaction heated to 80 °C to start the reaction. After 24 h, the reaction was cooled to 21 °C and terminated by injecting 5 mL of MeOH. The product was collected by centrifugation and redissolved in 0.25 mL of DCM. Afterwards, it was precipitated again by adding 5 mL of MeOH to yield poly(vinyl-DMAC-TRZ) (25.1 mg, 33% yield).

^{1}H NMR (400 MHz, Dichloromethane-d_2 [5.32 ppm], ppm) δ = 9.10–8.69 (m, 5H, CH_{Ar}), 8.07–7.87 (m, 1H, CH_{Ar}), 7.69–7.30 (m, 10H, CH_{Ar}), 7.10–6.86 (m, 3H, CH_{Ar}), 6.47–6.25 (m, 2H, CH_{Ar}), 1.78–0.84 (m, 9H, DMAC-CH_3 + alkyl backbone).

GPC: M_n: 1.456E^{+3} g/mol; M_w: 2.711E^{+3} g/mol; D: 1.862E^{+0}.

IR (ATR, $\tilde{\nu}$) = 3064 (w), 3057 (w), 3040 (w), 3031 (w), 2961 (w), 2917 (w), 2854 (w), 1718 (w), 1599 (w), 1587 (w), 1510 (vs), 1475 (s), 1445 (vs), 1408 (w), 1363 (vs), 1320 (s), 1264 (vs), 1193 (w), 1173 (m), 1146 (w), 1106 (m), 1096 (m), 1068 (m), 1050 (w), 1024 (m), 1017 (m), 1001 (w), 989 (w), 973 (w), 929 (w), 901 (w), 887 (w), 874 (w), 841 (m), 830 (w), 813 (m), 769 (s), 742 (vs), 710 (s), 691 (vs), 683 (vs), 663 (m), 646 (s), 636 (m), 618 (w), 603 (w), 571 (w), 557 (w), 517 (m), 489 (w), 466 (w), 450 (w), 439 (w), 428 (w), 416 (w), 409 (w), 404 (w), 390 (w), 375 (w) cm^{-1}.

Additional information on the chemical synthesis is available *via* the Chemotion repository: https://doi.org/10.14272/reaction/SA-FUHFF-UHFFFADPSC-UHFFFADPSC-UHFFFADPSC-NUHFF-NUHFF-NUHFF-ZAZ.9.

Additional information on the analysis of the target compound is available *via* the Chemotion repository: https://doi.org/10.14272/10.14272/DUMMY.8.

6.2.3. Procedures Chapter 4.2 “PCP-Polymers as Semiconductors”

N,N-Bis(4-bromophenyl)-4-methoxyaniline (76)

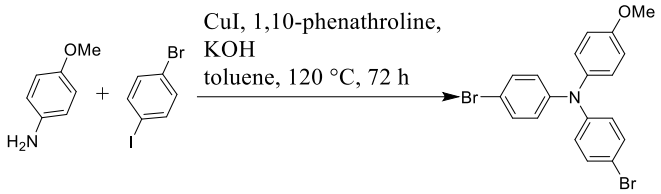

76, 64%

To 40 mL toluene in a round-bottom flask fitted with Dean-Stark trap and reflux condenser were added *p*-anisidine (1.00 g, 8.12 mmol, 1.00 equiv.), 1-bromo-4-iodo-benzene (6.89 g, 6.76 mL, 24.4mmol, 3.00 equiv.), copper(I) iodide (309 mg, 1.62 mmol, 0.200 equiv.), 1,10-phenanthroline (293 mg, 1.62 mmol, 0.200 equiv.), and potassium hydroxide (3.64 g, 65.0 mmol, 8.00 equiv.). The resulting solution was stirred at 120 °C for 3 d. The solvent was evaporated and the residue purified by column chromatography on silica using cHex/EtOAc 30:1 as eluent to yield *N*,*N*-bis(4-bromophenyl)-4-methoxyaniline (2.24 g, 5.17 mmol, 64% yield) as a yellow oil.

R_f = 0.73 (cHex/EtOAc 10:1).

^{1}H NMR (400 MHz, Chloroform-d [7.26 ppm], ppm) δ = 7.32–7.28 (m, 4H), 7.08–6.99 (m, 2H), 6.92–6.88 (m, 4H), 6.86–6.83 (m, 2H), 3.79 (s, 3H, OMe-CH_3);

^{13}C NMR (100 MHz, Chloroform-d [77.16 ppm], ppm) δ = 156.7 (C_q), 146.8 (C_q, 2C), 139.7 (C_q), 132.2 (+, CH, 4C), 127.4 (+, CH, 2C), 124.3 (+, CH, 4C), 115.0 (+, CH, 2C), 114.5 (C_q, 2C), 55.5 (+, CH_3);

MS (FAB, 3-NBA), m/z (%): 433/431/435 (100/53/52) $[M]^+$. HRMS (FAB, matrix NBA): m/z = calcd for $C_{19}H_{15}ON^{79}Br^{81}Br[M]^+$: 432.9494; found 432.9494;

IR (ATR, $\tilde{\nu}$) = 3060 (vw), 3034 (vw), 2997 (w), 2979 (vw), 2951 (w), 2929 (w), 2904 (w), 2873 (vw), 2859 (vw), 2854 (vw), 2833 (w), 1884 (vw), 1738 (vw), 1608 (vw), 1578 (m), 1506 (vs), 1480 (vs), 1439 (s), 1398 (w), 1378 (vw), 1310 (s), 1298 (m), 1281 (vs), 1256 (s), 1238 (vs), 1176 (s), 1164 (s), 1102 (m), 1069 (s), 1033 (s), 1003 (s), 953 (w), 938 (w), 916 (w), 816 (vs), 724 (m), 701 (s), 666 (w), 637 (w), 628 (w), 585 (s), 534 (s), 506 (vs), 480 (s), 450 (m), 409 (m), 385 (w), 380 (w) cm^{-1}.

Additional information on chemical synthesis is available *via* the Chemotion repository:

https://doi.org/10.14272/reaction/SA-FUHFF-UHFFFADPSC-ZOISYEZQRC-UHFFFADPSC-NUHFF-NUHFF-NUHFF-ZZZ

Additional information on analysis of the target compound is available *via* the Chemotion repository:

https://doi.org/10.14272/ZOISYEZQRCIVDZ-UHFFFAOYSA-N.1

4-Methoxy-*N,N*-bis(4-(thiophen-2-yl)phenyl)aniline (77)

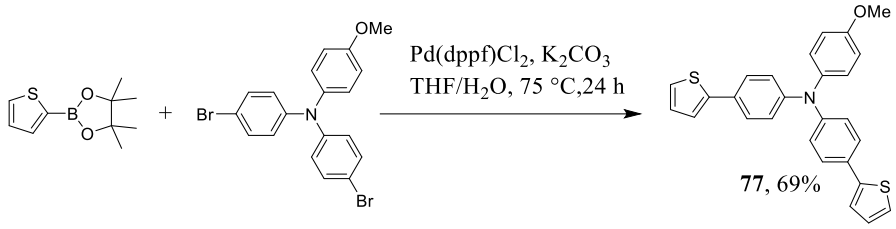

4,4,5,5-Tetramethyl-2-thiophen-2-yl-1,3,2-dioxaborolane (910 mg, 4.33 mmol, 2.50 equiv.), *N,N*-bis(4-bromophenyl)-4-methoxyaniline (750 mg, 1.73 mmol, 1.00 equiv.), $Pd(dppf)Cl_2$ (253 mg, 346 µmol, 0.200 equiv.), dipotassium carbonate (957 mg, 6.93 mmol, 4.00 equiv.) were added together with 3 mL of water and 37 mL of THF under argon. The solution was purged with argon for 10 min. Afterwards, the mixture was stirred at 75 °C for 24 h. The solvent was evaporated under reduced pressure and the obtained crude product was purified *via* column chromatography on silica gel using pentane/DCM 3:1 as eluent to yield 4-methoxy-*N,N*-bis(4-(thiophen-2-yl)phenyl)aniline (521 mg, 1.15 mmol, 66% yield) as a yellow solid.

R_f = 0.27 (pentane/DCM 3:1).

M.p.: 56 °C

^{1}H NMR (400 MHz, Chloroform-d [7.26 ppm], ppm) δ = 7.52–7.43 (m, 4H), 7.24–7.20 (m, 4H), 7.13–7.11 (m, 2H), 7.08–7.05 (m, 6H), 6.90–6.85 (m, 2H), 3.83 (s, 3H, OMe-CH_3);

^{13}C NMR (100 MHz, Chloroform-d [77.16 ppm], ppm) δ = 156.6 (C_q), 147.2 (C_q, 2C), 144.3 (C_q, 2C), 140.1 (C_q), 128.3 (C_q, 2C), 128.0 (+, CH, 2C), 127.5 (+, CH, 2C), 126.7 (+, CH, 4C), 124.0 (+, CH, 2C), 123.0 (+, CH, 4C), 122.2 (+, CH, 2C), 115.0 (+, CH, 2C), 55.5 (+, CH_3, OMe-CH_3);

MS (ESI), m/z (%): 439 (100) $[M]^+$. HRMS (ESI): m/z = calcd for $C_{27}H_{21}NO^{32}S_2$ $[M]^+$: 439.1064; found 439.1058;

IR (ATR, ṽ) = 3104 (w), 3068 (w), 3033 (w), 3024 (w), 2997 (w), 2949 (w), 2925 (w), 2904 (w), 2873 (w), 2851 (w), 2832 (w), 1596 (m), 1531 (w), 1494 (vs), 1462 (s), 1431 (s), 1317 (vs), 1283 (vs), 1262 (vs), 1238 (vs), 1210 (s), 1196 (s), 1180 (vs), 1164 (s), 1106 (s), 1078 (m), 1031 (vs), 958 (m), 914 (w), 847 (m), 813 (vs), 728 (m), 715 (m), 688 (vs), 642 (m), 630 (m), 615 (m), 588 (vs), 530 (vs), 490 (s), 477 (s), 455 (m), 407 (s), 387 (m), 377 (m) cm^{-1}.

Additional information on chemical synthesis is available *via* the Chemotion repository:

https://doi.org/10.14272/reaction/SA-FUHFF-UHFFFADPSC-MXMNPLMVKQ-UHFFFADPSC-NUHFF-NUHFF-NUHFF-ZZZ

Additional information on analysis of the target compound is available *via* the Chemotion repository:

https://doi.org/10.14272/MXMNPLMVKQOFRH-UHFFFAOYSA-N.1

4-(5-Bromothiophen-2-yl)-*N*-(4-(5-bromothiophen-2-yl)phenyl)-*N*-(4-methoxyphenyl)aniline (78)

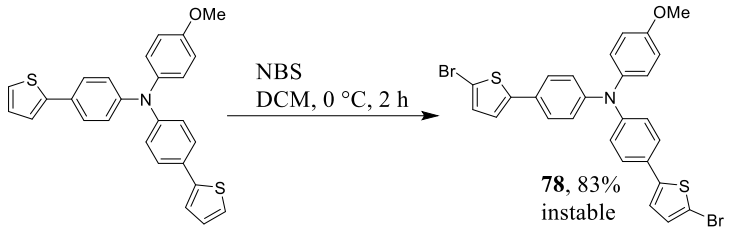

4-Methoxy-*N,N*-bis(4-(thiophen-2-yl)phenyl)aniline (160 mg, 364 µmol, 1.00 equiv.) was dissolved in 15 mL of DCM at 0 °C. *N*-Bromosuccinimide (143 mg, 801 µmol, 2.20 equiv.) was added portionwise and the reaction mixture stirred for 2 h. The organic phase was washed four times with 20 mL water, dried over Na_2SO_4 and concentrated in vacuo. Flash column chromatography on silica gel using pentane/DCM 2:1 as eluent afforded 4-(5-bromothiophen-2-yl)-*N*-(4-(5-bromothiophen-2-yl)phenyl)-*N*-(4-methoxyphenyl)aniline (180 mg, 301 µmol, 83% yield) as a colorless solid.

The product is instable and must be used immediately.

^{1}H NMR (400 MHz, Chloroform-d [7.26 ppm], ppm) δ = 7.49 – 7.32 (m, 4H), 7.18 – 6.83 (m, 12H), 3.82 (s, 3H, OMe-CH_3).

(4-Methoxyphenyl)-bis(4-thieno[3,2-b]thiophen-5-ylphenyl)amine (79)

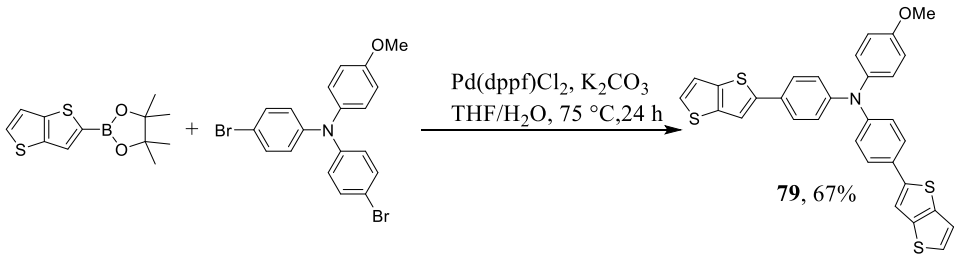

4,4,5,5-Tetramethyl-2-thieno[3,2-b]thiophen-5-yl-1,3,2-dioxaborolane (1.38 g, 5.19 mmol, 2.50 equiv.), *N,N*-bis(4-bromophenyl)-4-methoxyaniline (900 mg, 2.08 mmol, 1.00 equiv.), $Pd(dppf)Cl_2$ (304 mg, 416 µmol, 0.200 equiv.), dipotassium carbonate (1.15 g, 8.31 mmol, 4.00 equiv.) were added together with 3 mL of water and 37 mL of THF under argon. The solution was purged with argon for 10 min. Afterwards, the mixture was stirred at 75 °C for 24 h. After evaporating the solvent under reduced pressure, the obtained crude product was purified *via* column chromatography on silica gel using pentane/DCM 3:1 as eluent to yield (4-methoxyphenyl)-bis(4-thieno[3,2-b]thiophen-5-ylphenyl)amine (763 mg, 1.38 mmol, 67% yield) as a yellow solid.

R_f = 0.39 (pentane/DCM 3:1).

M.p.: 199 °C

^{1}H NMR (400 MHz, Chloroform-d [7.26 ppm], ppm) δ = 7.52–7.47 (m, 4H), 7.38 (d, *J* = 0.7 Hz, 2H), 7.32 (d, *J* = 5.2 Hz, 2H), 7.23 (dd, *J* = 5.3 Hz, *J* = 0.7 Hz, 2H), 7.15–7.13 (m, 2H), 7.10–7.08 (m, 4H), 6.93–6.87 (m, 2H), 3.83 (s, 3H);

^{13}C NMR (100 MHz, Chloroform-d [77.16 ppm], ppm) δ = 156.7 (C_q), 147.4 (C_q, 2C), 146.3 (C_q, 2C), 140.1 (C_q, 2C), 140.0 (C_q), 137.9 (C_q, 2C), 128.6 (C_q, 2C), 127.7 (CH, 2C), 126.6 (+, CH, 4C), 126.4 (+, CH, 2C), 123.0 (+, CH, 4C), 119.6 (+, CH, 2C), 115.0 (+, CH, 2C), 114.3 (+, CH, 2C), 55.5 (+, CH_3, OMe-CH_3);

MS (ESI), m/z (%): 551 (100). HRMS (ESI): m/z = calcd for $C_{31}H_{21}NO^{32}S_4$ $[M]^+$: 551.0506; found 551.0499;

IR (ATR, ṽ) = 1595 (m), 1520 (w), 1504 (vs), 1487 (vs), 1455 (s), 1439 (m), 1426 (w), 1322 (s), 1288 (s), 1262 (s), 1238 (vs), 1200 (m), 1194 (m), 1183 (s), 1169 (m), 1112 (m), 1082 (w), 1030 (s), 967 (m), 894 (m), 832 (vs), 807 (vs), 764 (m), 734 (m), 727 (w), 703 (vs), 693 (vs), 630 (s), 601 (m), 582 (s), 561 (w), 528 (s), 510 (vs), 482 (w), 407 (m) cm^{-1}.

Additional information on chemical synthesis is available *via* the Chemotion repository:

https://doi.org/10.14272/reaction/SA-FUHFF-UHFFFADPSC-AQCBNUCXBU-UHFFFADPSC-NUHFF-NUHFF-NUHFF-ZZZ

Additional information on analysis of the target compound is available *via* the Chemotion repository:

https://doi.org/10.14272/AQCBNUCXBUCINR-UHFFFAOYSA-N.1

4-(5-Bromothieno[3,2-b]thiophen-2-yl)-*N*-(4-(5-bromothieno[3,2-b]thiophen-2-yl)phenyl)-*N*-(4-methoxyphenyl)aniline (**80**)

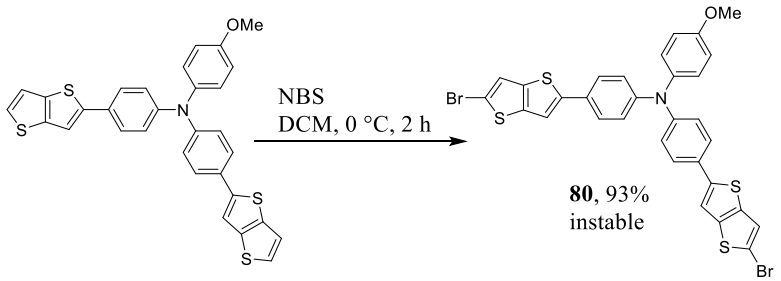

(4-Methoxyphenyl)-bis(4-thieno[3,2-b]thiophen-5-ylphenyl)amine (550 mg, 997 µmol, 1.00 equiv.) was dissolved in 30 mL of DCM at 0 °C. *N*-Bromosuccinimide (408 mg, 2.29 mmol, 2.30 equiv.) was

added portion-wise and the reaction mixture stirred for 2 h. The organic phase was washed four times with 30 mL water, dried over Na_2SO_4 and concentrated in vacuo. Flash column chromatography on silica gel using pentane/DCM 4:1 as eluent afforded 4-(5-bromothieno[3,2-b]thiophen-2-yl)-*N*-(4-(5-bromothieno[3,2-b]thiophen-2-yl)phenyl)-*N*-(4-methoxyphenyl)aniline (656 mg, 925 µmol, 93% yield) as a colorless solid.

The product is instable and must be used immediately.

^{1}H NMR (400 MHz, Chloroform-d [7.26 ppm], ppm) δ = 7.55–7.30 (m, 6H), 7.23–7.08 (m, 8H), 6.92–6.85 (m, 2H), 3.85 (s, 3H, OMe-CH_3).

Poly(4-methoxy-*N*,*N*-diphenylaniline-co-thieno[3,2-b]thiophen) (81)

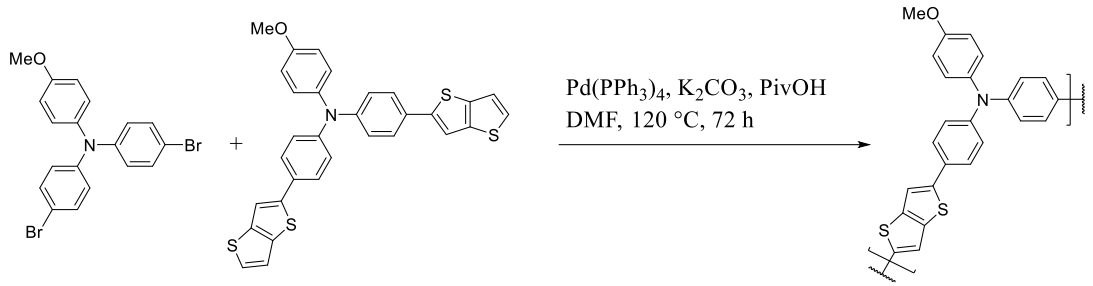

81, 32%

N-(4-Methoxyphenyl)-4-thieno[3,2-b]thiophen-5-yl-*N*-(4-thieno[3,2-b]thiophen-5-ylphenyl)aniline (127 mg, 231 µmol, 1.00 equiv.), *N,N*-bis(4-bromophenyl)-4-methoxyaniline (100 mg, 231 µmol, 1.00 equiv.), tetrakis(triphenylphosphine)palladium(0) (26.7 mg, 23.1 µmol, 0.100 equiv.), dipotassium carbonate (95.7 mg, 693 µmol, 3.00 equiv.) and pivalic acid (14.1 mg, 139 µmol, 0.600 equiv.) were added into a crimp cap vial, evacuated and refilled with argon three times. Then, 1.5 mL of dry DMF were added and the reaction mixture was heated to 120 °C for 72 h. The crude product was precipitated by adding 40 mL of MeOH and collected by centrifugation. The solid was dissolved in 1 mL of DCM and again precipitated from 20 mL of MeOH. The solid was collected by centrifugation and dried in vacuo to give poly(4-methoxy-*N,N*-diphenylaniline-co-thieno[3,2-b]thiophen) (30.4 mg, 13% yield) as an orange-to-brown solid.

^{1}H NMR (400 MHz, Dichloromethane-d_2 [5.32 ppm], ppm) δ = 7.75–6.70 (m, 15H), 3.82–3.79 (m, 3H);

GPC: M_n: 1.420E^{+3} g/mol; M_w: 5.149E^{+3} g/mol; D: 3.625E^{+0};

IR (ATR, $\tilde{\nu}$) = 2949 (w), 2918 (w), 2849 (w), 2833 (w), 1592 (m), 1584 (m), 1504 (vs), 1483 (vs), 1460 (s), 1438 (m), 1316 (s), 1283 (s), 1264 (s), 1239 (vs), 1198 (m), 1177 (s), 1164 (s), 1103 (s), 1071 (m), 1031 (s), 969 (w), 950 (w), 914 (w), 892 (w), 874 (w), 866 (w), 809 (vs), 752 (m), 745 (m), 696 (s),

630 (m), 619 (m), 585 (s), 561 (m), 528 (vs), 511 (s), 480 (m), 473 (m), 456 (m), 452 (m), 439 (m), 431 (m), 422 (m), 407 (m), 390 (m), 380 (m), 375 (m) cm^{-1}.

Additional information on chemical synthesis is available *via* the Chemotion repository:

https://doi.org/10.14272/reaction/SA-FUHFF-UHFFFADPSC-HTYXKPNPUN-UHFFFADPSC-NUHFF-NUHFF-NUHFF-ZZZ

Additional information on analysis of the target compound is available *via* the Chemotion repository:

https://doi.org/10.14272/HTYXKPNPUNORDY-UHFFFAOYSA-N.1

Poly(4,16-diethenyl[2.2]paracyclophane-co-4-methoxy-*N,N*-bis(4-(thieno[3,2-b]thiophen-2-yl)phenyl)aniline) (82)

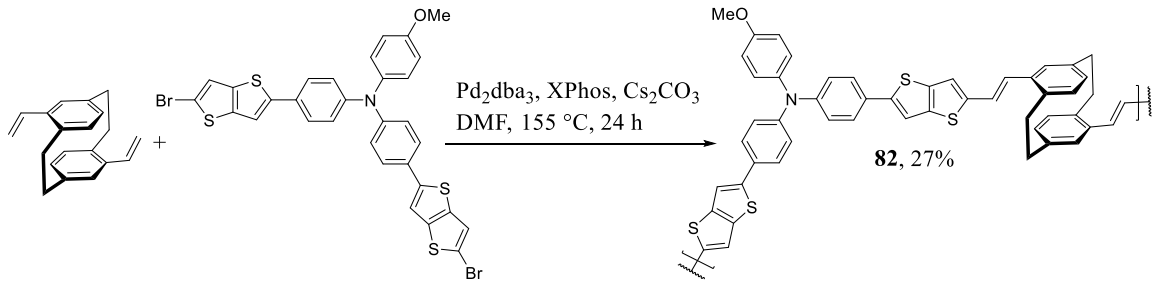

4,16-Divinyl[2.2]paracyclophane (35.0 mg, 134 µmol, 1.00 equiv.), 4-(5-bromothieno[3,2-b]thiophen-2-yl)-*N*-(4-(5-bromothieno[3,2-b]thiophen-2-yl)phenyl)-*N*-(4-methoxyphenyl)aniline (95.4 mg, 134 µmol, 1.00 equiv.), tris(dibenzylidenaceton)dipalladium(0) (6.15 mg, 6.72 µmol, 0.0500 equiv.), XPhos (6.41 mg, 13.4 µmol, 0.100 equiv.), and dicesium carbonate (175 mg, 538 µmol, 4.00 equiv.) were dissolved in 4 mL of dry DMF. The solution was stirred at 155 °C for 24 h. The crude product was precipitated by adding 40 mL of MeOH and collected by centrifugation. The solid was dissolved in 1 mL of DCM and again precipitated from 20 mL of MeOH. The solid was collected by centrifugation and dried in vacuo to give poly(4,16-diethenyl[2.2]paracyclophane-co-4-methoxy-*N,N*-bis(4-(thieno[3,2-b]thiophen-2-yl)phenyl)aniline) (35.7 mg, 27% yield) as an orange-to-brown solid.

^{1}H NMR (400 MHz, Dichloromethane-d_2 [5.32 ppm], ppm) δ = 7.53–6.32 (m, 26H), 3.81–3.78 (m, 3H), 3.56–3.42 (m, 1H), 3.19–2.80 (m, 7H);

GPC: M_n: 1.843E^{+3} g/mo;l M_w: 4.051E^{+3} g/mol; D: 2.625E^{+0};

IR (ATR, ṽ) = 2918 (w), 2856 (w), 2836 (w), 2184 (w), 2159 (w), 2138 (w), 2071 (w), 2009 (w), 1986 (w), 1977 (w), 1945 (w), 1673 (w), 1653 (w), 1594 (m), 1521 (w), 1504 (s), 1486 (s), 1458 (m), 1417 (m), 1315 (s), 1285 (s), 1241 (vs), 1180 (s), 1162 (s), 1101 (m), 1074 (m), 1054 (m), 1030 (s), 966 (m),

946 (m), 890 (m), 873 (m), 815 (vs), 803 (vs), 765 (s), 727 (s), 715 (s), 694 (vs), 669 (s), 633 (s), 609 (s), 581 (vs), 575 (s), 551 (s), 517 (vs), 504 (vs), 487 (vs), 476 (vs), 466 (vs), 449 (vs), 429 (vs), 408 (vs), 385 (vs) cm^{-1}.

Additional information on chemical synthesis is available *via* the Chemotion repository:

https://doi.org/10.14272/reaction/SA-FUHFF-UHFFFADPSC-NBURKRWKHC-UHFFFADPSC-NUHFF-NHFLS-NUHFF-ZZZ

Additional information on analysis of the target compound is available *via* the Chemotion repository:

https://doi.org/10.14272/NBURKRWKHCTQFT-PCLIKHOPSA-N.1

Poly(4,15-diethenyl[2.2]paracyclophane-co-4-methoxy-*N,N*-bis(4-(thieno[3,2-b]thiophen-2-yl)phenyl)aniline) (83)

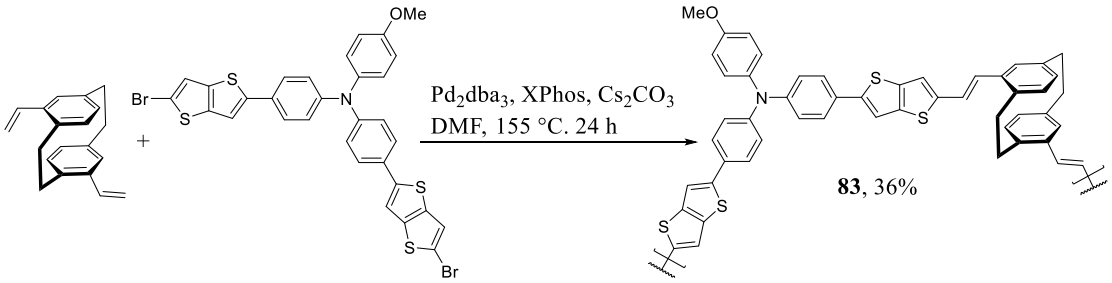

4,15-Divinyl[2.2]paracyclophane (35.0 mg, 134 µmol, 1.00 equiv.), 4-(5-bromothieno[3,2-b]thiophen-2-yl)-*N*-(4-(5-bromothieno[3,2-b]thiophen-2-yl)phenyl)-*N*-(4-methoxyphenyl)aniline (95.4 mg, 134 µmol, 1.00 equiv.), tris(dibenzylidenaceton)dipalladium(0) (6.15 mg, 6.72 µmol, 0.0500 equiv.), XPhos (6.41 mg, 13.4 µmol, 0.100 equiv.), and dicesium carbonate (175 mg, 538 µmol, 4.00 equiv.) were dissolved in 4 mL of dry DMF. The solution was stirred at 155 °C for 24 h. The crude product was precipitated by adding 40 mL of MeOH and collected by centrifugation. The solid was dissolved in 1 mL of DCM and again precipitated from 20 mL of MeOH. The solid was collected by centrifugation and dried in vacuo to give poly(4,15-diethenyl[2.2]paracyclophane-co-4-methoxy-*N,N*-bis(4-(thieno[3,2-b]thiophen-2-yl)phenyl)aniline) (38.6 mg, 30% yield) as an orange-to-brown solid.

^{1}H NMR (400 MHz, Dichloromethane-d_2 [5.32 ppm], ppm) δ = 7.54–6.35 (m, 26H), 3.82–3.78 (m, 3H), 3.51–3.37 (m, 1H), 3.13–2.76 (m, 7H);

GPC: M_n: 1.652E^{+3} g/mol; M_w: 3.831E^{+3} g/mol; D: 2.319E^{+0};

IR (ATR, ṽ) = 2915 (w), 2856 (w), 2830 (w), 1670 (w), 1594 (m), 1519 (w), 1503 (vs), 1486 (vs), 1458 (s), 1439 (m), 1422 (m), 1316 (s), 1283 (s), 1264 (s), 1238 (vs), 1196 (s), 1176 (vs), 1163 (vs), 1103 (s), 1082 (m), 1031 (s), 967 (m), 942 (m), 891 (m), 823 (vs), 803 (vs), 762 (s), 714 (s), 697 (vs), 670 (s),

660 (s), 649 (s), 629 (s), 582 (vs), 560 (s), 510 (vs), 480 (vs), 469 (vs), 445 (vs), 436 (s), 424 (s), 405 (vs), 392 (vs), 381 (vs) cm^{-1}.

Additional information on chemical synthesis is available *via* the Chemotion repository:

https://doi.org/10.14272/reaction/SA-FUHFF-UHFFFADPSC-XZJBSPOOLA-UHFFFADPSC-NUHFF-NHFLS-NUHFF-ZZZ

Additional information on the analysis of the target compound is available *via* the Chemotion repository:

https://doi.org/10.14272/XZJBSPOOLAXLAB-PCLIKHOPSA-N.1

Poly(4,16-diethynyl[2.2]paracyclophane-co-4-methoxy-*N,N*-bis(4-(thieno[3,2-b]thiophen-2-yl)phenyl)aniline) (84)

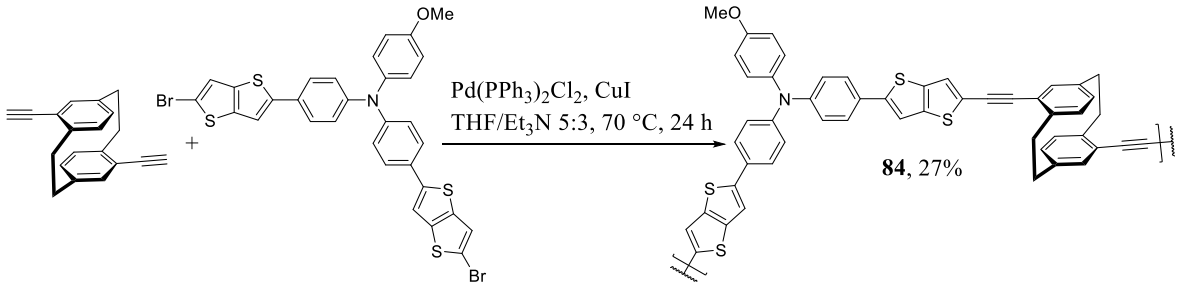

4,16-Diethynyl[2.2]paracyclophane (30.0 mg, 117 µmol, 1.00 equiv.), 4-(5-bromothieno[3,2-b]thiophen-2-yl)-*N*-(4-(5-bromothieno[3,2-b]thiophen-2-yl)phenyl)-*N*-(4-methoxyphenyl)aniline (83.0 mg, 117 µmol, 1.00 equiv.), bis(triphenylphosphine)palladium(II) dichloride (8.21 mg, 11.7 µmol, 0.100 equiv.), and copper(I) iodide (2.23 mg, 11.7 µmol, 0.100 equiv.) were dissolved under argon in 14 mL of dry THF and 9 mL of dry Et_3N. The mixture was purged with argon for 10 min and stirred at 70 °C for 24 h. The solvent was reduced to 5 mL under reduced pressure. The crude product was precipitated by adding 40 mL MeOH and collected by centrifugation. The solid was dissolved in 1 mL of DCM and precipitated from 20 mL MeOH again. The solid was collected by centrifugation and dried in vacuo to give poly(4,16-diethynyl[2.2]paracyclophane-co-4-methoxy-*N,N*-bis(4-(thieno[3,2-b]thiophen-2-yl)phenyl)aniline) (30.7 mg, 27% yield) as orange-to-brown solid.

^{1}H NMR (400 MHz, Dichloromethane-d_2 [5.32 ppm], ppm) δ = 7.54–6.54 (m, 22H), 3.82 (s, 3H), 3.63 (s, 2H), 3.23–2.96 (m, 6H), 1.85 (s, 8H);

GPC: M_n: 5.673E^{+3} g/mol; M_w: 2.425E^{+4} g/mol; D: 4.275E^{+0};

IR (ATR, $\tilde{\nu}$) = 2946 (w), 2924 (m), 2856 (w), 1723 (w), 1594 (m), 1519 (w), 1503 (vs), 1480 (vs), 1460 (s), 1438 (m), 1317 (s), 1285 (s), 1265 (s), 1239 (vs), 1163 (vs), 1103 (s), 1055 (vs), 1031 (vs), 980 (s),

967 (s), 942 (s), 935 (s), 928 (s), 914 (s), 898 (s), 892 (s), 868 (s), 807 (vs), 759 (s), 751 (s), 727 (vs), 693 (vs), 670 (vs), 654 (s), 632 (vs), 585 (vs), 562 (vs), 528 (vs), 520 (vs), 510 (vs), 489 (vs), 479 (vs), 463 (vs), 452 (vs), 432 (vs), 422 (vs), 414 (vs), 405 (vs), 395 (vs), 388 (vs), 377 (vs) cm^{-1}.

Additional information on chemical synthesis is available *via* the Chemotion repository:

https://doi.org/10.14272/reaction/SA-FUHFF-UHFFFADPSC-GGOKFXUBOM-UHFFFADPSC-NUHFF-NUHFF-NUHFF-ZZZ

Additional information on the analysis of the target compound is available *via* the Chemotion repository:

https://doi.org/10.14272/GGOKFXUBOMUCAL-UHFFFAOYSA-N.1

Poly(4,15-diethynyl[2.2]paracyclophane-co-4-methoxy-*N,N*-bis(4-(thieno[3,2-b]thiophen-2-yl)phenyl)aniline) (85)

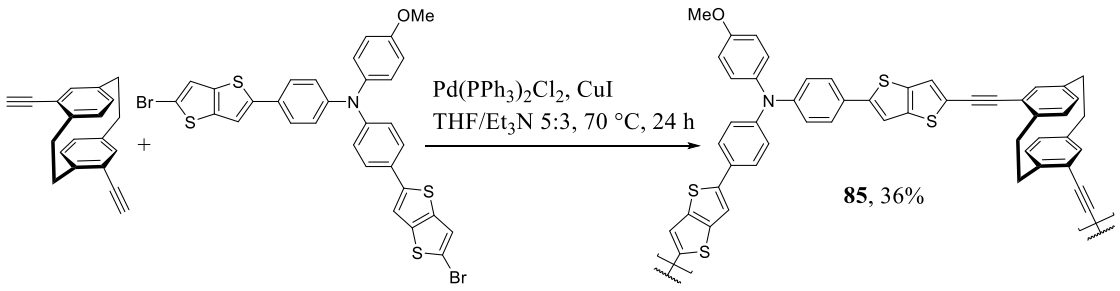

4,15-Diethynyl[2.2]paracyclophane (30.0 mg, 117 µmol, 1.00 equiv.), 4-(5-bromothieno[3,2-b]thiophen-2-yl)-*N*-(4-(5-bromothieno[3,2-b]thiophen-2-yl)phenyl)-*N*-(4-methoxyphenyl)aniline (83.0 mg, 117 µmol, 1.00 equiv.), bis(triphenylphosphine)palladium(II) dichloride (8.21 mg, 11.7 µmol, 0.100 equiv.), and copper(I) iodide (2.23 mg, 11.7 µmol, 0.100 equiv.) were dissolved under argon in 14 mL of dry THF and 9 mL of dry Et_3N. The mixture was purged with argon for 10 min and stirred at 70 °C for 24 h. The solvent was reduced to 5 mL under reduced pressure. The crude product was precipitated by adding 40 mL of MeOH and collected by centrifugation. The solid was dissolved in 1 mL of DCM and precipitated from 20 mL of MeOH. The solid was collected by centrifugation and dried in vacuo to give poly(4,15-diethynyl[2.2]paracyclophane-co-4-methoxy-*N,N*-bis(4-(thieno[3,2-b]thiophen-2-yl)phenyl)aniline) (40.9 mg, 36% yield) as an orange-to-brown solid.

^{1}H NMR (400 MHz, Dichloromethane-d_2 [5.32 ppm], ppm) δ = 7.62–7.22 (m, 9H), 7.18–6.89 (m, 10H), 6.73–6.53 (m, 3H), 3.83–3.80 (m, 3H), 3.59–3.58 (m, 2H), 3.19–3.14 (m, 6H), 1.67–1.56 (m, 6H);

GPC: M_n: 3.631E$^+$ g/mol; M_w: 8.066E^{+3} g/mol; D: 2.222E^{+0};

IR (ATR, $\tilde{\nu}$) = 2927 (w), 2853 (w), 1725 (vw), 1595 (m), 1520 (w), 1504 (vs), 1482 (vs), 1438 (w), 1317 (s), 1286 (s), 1266 (s), 1241 (vs), 1167 (s), 1105 (w), 1034 (m), 894 (w), 810 (vs), 722 (s), 697 (w), 633 (w), 588 (m), 562 (w), 530 (vs), 510 (m), 486 (m), 456 (w), 408 (w) cm^{-1}.

Additional information on the chemical synthesis is available *via* the Chemotion repository:

https://doi.org/10.14272/reaction/SA-FUHFF-UHFFFADPSC-CPWLYTQJHP-UHFFFADPSC-NUHFF-NUHFF-NUHFF-ZZZ

Additional information on the analysis of the target compound is available *via* the Chemotion repository:

https://doi.org/10.14272/CPWLYTQJHPSSFQ-UHFFFAOYSA-N.1

Poly(4,15-diethenyl[2.2]paracyclophane-co-4-methoxy-*N,N*-bis(4-(thiophene-2-yl)phenyl)aniline) (86)

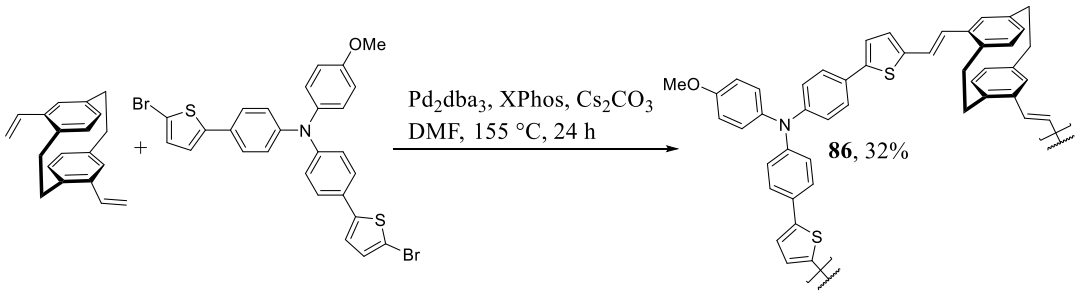

4,15-Divinyl[2.2]paracyclophane (43.6 mg, 167 µmol, 1.00 equiv.), 4-(5-bromothiophen-2-yl)-*N*-(4-(5-bromothiophen-2-yl)phenyl)-*N*-(4-methoxyphenyl)aniline (100 mg, 167 µmol, 1.00 equiv.), tris(dibenzylidenaceton)dipalladium(0) (7.66 mg, 8.37 µmol, 0.0500 equiv.), XPhos (7.98 mg, 16.7 µmol, 0.100 equiv.) and dicesium carbonate (218 mg, 670 µmol, 4.00 equiv.) were dissolved in 5 mL of dry DMF. The solution was stirred at 155 °C for 24 h. The crude product was precipitated by adding 40 mL of MeOH and collected by centrifugation. The solid was dissolved in 1 mL of DCM and precipitated from 20 mL of MeOH. The solid was collected by centrifugation and dried in vacuo to give poly(4,15-diethenyl[2.2]paracyclophane-co-4-methoxy-*N,N*-bis(4-(thiophene-2-yl)phenyl)aniline) (45.3 mg, 31% yield) as an orange-to-brown solid.

^{1}H NMR (400 MHz, Dichloromethane-d_2 [5.32 ppm], ppm) δ = 7.47–6.36 (m, 26H), 3.81–3.62 (m, 5H), 2.93–2.82 (m, 6H);

GPC: M_n: 3.757E^{+3} g/mol; M_w: 1.581E^{+4} g/mol; D: 4.208E^{+0};

IR (ATR, $\tilde{\nu}$) = 2962 (w), 2922 (vw), 2850 (vw), 1595 (vw), 1499 (w), 1459 (vw), 1451 (vw), 1441 (vw), 1412 (vw), 1378 (vw), 1319 (vw), 1259 (vs), 1179 (w), 1160 (w), 1084 (vs), 1018 (vs), 864 (w), 793

(vs), 700 (m), 660 (w), 615 (w), 603 (w), 588 (w), 562 (w), 531 (w), 517 (w), 504 (w), 469 (w), 459 (w), 449 (w), 438 (w), 385 (s) cm^{-1}.

Additional information on chemical synthesis is available *via* the Chemotion repository:

https://doi.org/10.14272/reaction/SA-FUHFF-UHFFFADPSC-AQKXDUXCIM-UHFFFADPSC-NUHFF-NHFLS-NUHFF-ZZZ

Additional information on the analysis of the target compound is available *via* the Chemotion repository:

https://doi.org/10.14272/AQKXDUXCIMJXEK-PCLIKHOPSA-N.1

Poly(4,15-diethynyl[2.2]paracyclophane-co-4-methoxy-*N,N*-bis(4-(thiophene-2-yl)phenyl)aniline) (87)

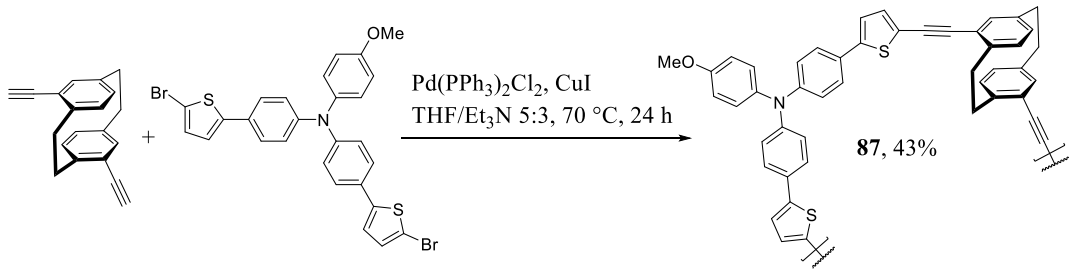

4,15-Diethynyl[2.2]paracyclophane (32.2 mg, 126 µmol, 1.00 equiv.), 4-(5-bromothiophen-2-yl)-*N*-(4-(5-bromothiophen-2-yl)phenyl)-*N*-(4-methoxyphenyl)aniline (75.0 mg, 126 µmol, 1.00 equiv.), bis(triphenylphosphine)palladium(II) dichloride (8.81 mg, 12.6 µmol, 0.100 equiv.), and copper(I) iodide (2.39 mg, 12.6 µmol, 0.100 equiv.) were dissolved under argon in 15 mL of dry THF and 9 mL of dry Et_3N. The mixture was purged with argon for 10 min and stirred at 70 °C for 24 h. The solvent was reduced to 5 mL under reduced pressure. The crude product was precipitated by adding 40 mL of MeOH and collected by centrifugation. The solid was dissolved in 1 mL of DCM and precipitated from 20 mL of MeOH. The solid was collected by centrifugation and dried in vacuo to give poly(4,15-diethynyl[2.2]paracyclophane-co-4-methoxy-*N,N*-bis(4-(thiophene-2-yl)phenyl)aniline) (46.4 mg, 44% yield) as an orange-to-brown solid.

^{1}H NMR (400 MHz, Dichloromethane-d_2 [5.32 ppm], ppm) δ = 7.61–6.47 (m, 22H), 3.81–3.77 (m, 3H), 3.68–3.54 (m, 2H), 3.26–3.08 (m, 4H), 3.04–2.91 (m, 2H);

GPC: M_n: 3.932E^{+3} g/mol; M_w: 1.274E^{+4} g/mol; D: 3.240E^{+0};

IR (ATR, ṽ) = 3339 (vw), 3320 (vw), 3303 (vw), 3293 (vw), 3286 (vw), 3027 (vw), 2959 (w), 2924 (w), 2850 (w), 2769 (vw), 1595 (w), 1502 (vs), 1451 (m), 1404 (w), 1377 (w), 1317 (m), 1286 (m),

1259 (vs), 1239 (s), 1181 (m), 1163 (m), 1065 (s), 1030 (vs), 956 (m), 935 (w), 890 (w), 864 (m), 796 (vs), 721 (s), 697 (s), 657 (m), 611 (m), 582 (m), 531 (s), 486 (s), 448 (m), 404 (s), 391 (s), 381 (s) cm^{-1}.

Additional information on chemical synthesis is available *via* the Chemotion repository:

https://doi.org/10.14272/reaction/SA-FUHFF-UHFFFADPSC-QJGQMKUIBK-UHFFFADPSC-NUHFF-NUHFF-NUHFF-ZZZ

Additional information on the analysis of the target compound is available *via* the Chemotion repository:

https://doi.org/10.14272/QJGQMKUIBKTNLC-UHFFFAOYSA-N.1

7. Table of Abbreviations

3-NBA	3-Nitrobenzyl alcohol
AIBN	Azobisisobutyronitrile
ATR	Attenuated total reflection
BPhen	Bathophenanthroline
BuLi	Buthyllithium
CB	Conduction band
CD	Circular dichroism
CIGS	Copper-indium-gallium-diselenide
CIP	Cahn-Ingold-Prelog
CP	Circularly polarized
CPL	Circularly polarized luminescence
ΔE_{opt}	Optical band gap
D	Dispersity
DCM	Dichloromethane
dd	Doublet of a doublet
DEPT	Distortionless enhancement by polarization transfer
DMAC-TRZ	9,10-Dihydro-9,9-dimethyl-10-(4-(4,6-diphenyl-1,3,5-triazin-2-yl)phenyl)acridine
DMF	Dimethylformamide
DPEPO	Bis[2-(diphenylphosphino) phenyl] ether oxide
DSSC	Dye-sensitized solar cells
dt	Doublet of a triplet
ECD	Electronic circular dichroism
EI	Electron ionization
ESI MS	Electrospray ionization mass spectrometry
ETL	Electron transport layer
ETM	Electron transport material
FAB	Fast atom bombardment
FF	Fill factor
GPC	Gel permeation chromatography
HOMO	Highest occupied molecular orbital
HSQC	Heteronuclear single quantum coherence
HTL	Hole transport layer
HTM	Hole transport material
I_{MMP}	Maximum power point current
IP	Ionization potential
I_{SC}	Short circuit current
ITO	Indium tin oxide
I-V curve	Current-voltage curve
J	Coupling constant in Hz
KIT	Karlsruhe Institut für Technologie

λ_{max}	Absorption maximum
LED	Light-emitting diode
LUMO	Lowest unoccupied molecular orbital
m	Multiplet
M.p.	Melting point
MAPbI	Methylammonium lead iodide
mcP	1,3-Bis(*N*-carbazolyl) benzene
M_n	Number average molecular weight
MPP	Maximum power point
M_w	Weight average molecular weight
NBS	*N-B*romosuccinimide
NIS	*N*-Iodosuccinimide
NMR	Nuclear magnetic resonance spectroscopy
n-type	Negative type
OFET	Organic field-effect transistors
OLED	Organic light-emitting diodes
OMe-TPA	4-Methoxy-triphenylamine
OPV	Organic photovoltaics
OSC	Organic solar cell
P3HT	Poly(3-hexylthiophene)
PCE	Power conversion efficiency
PCBM	Phenyl-C61-butyric acid methyl ester
PCP	[2.2]Paracyclophane
PESA	Photoemission spectroscopy in air
PEDOT	Poly(3,4-ethylene-dioxythiophene)
P_{in}	Applied power
PL	Photo luminescence
PLQY	Photo luminescence quantum yield
P_{out}	Output power
ppm	Parts per million
PPV	Poly(*para*-phenylene vinylene)
PSC	Perovskite solar cell
Psg	Pseudo *geminal*
Psm	Pseudo *meta*
Pso	Pseudo *ortho*
Psp	Pseudo *para*
PSS	Polystyrene sulfonate
PTAA	Poly(bis-(4-phenyl)-(2,4,6-trimethylphenyl)-amine)
p-type	Positive type
ROMP	Ring-opening metathesis polymerization

s	Singlet
Spiro-OMeTAD	2,2',7,7'-Tetrakis(*N,N*-di-*p*-methoxyphenylamine)-9,9'-spirobifluorene
t	Triplet
T	Thiophene
TADF	Thermally activated delayed fluorescence
TBAB	*Tert*-butyl ammonium bromide
TBAF	*Tert*-butyl ammonium fluoride
TCSPC	Time-correlated single photon counting
THF	Tetrahydrofuran
TLC	Thin layer chromatography
TMS	Trimethylsilyl
TPA	Triphenylamine
TT	Thienothiophene
TTF	Tetrathiafulvalene
VB	Valence band
V_{MMP}	Maximum power point voltage
V_{OC}	Open circuit voltage
XRD	X-ray diffraction

8. Bibliography

[1] Energy Outlook 2024, BP, https://www.bp.com/en/global/corporate/energy-economics/energy-outlook.html, last accessed: 10.10.2024.

[2] C. J. Brown, A. C. Farthing, *Nature* **1949**, *164*, 915-916.

[3] D. J. Cram, H. Steinberg, *Journal of the American Chemical Society* **2002**, *73*, 5691-5704.

[4] Z. Hassan, E. Spuling, D. M. Knoll, S. Brase, *Angew Chem Int Ed Engl* **2020**, *59*, 2156-2170.

[5] J. Paradies, *Synthesis* **2011**, *2011*, 3749-3766.

[6] O. R. P. David, *Tetrahedron* **2012**, *68*, 8977-8993.

[7] H. E. Winberg, F. S. Fawcett, W. E. Mochel, C. W. Theobald, *Journal of the American Chemical Society* **2002**, *82*, 1428-1435.

[8] M. Montanari, A. Bugana, A. K. Sharma, D. Pasini, *Org Biomol Chem* **2011**, *9*, 5018-5020.

[9] Z. Hassan, E. Spuling, D. M. Knoll, J. Lahann, S. Brase, *Chem Soc Rev* **2018**, *47*, 6947-6963.

[10] H. Hope, J. Bernstein, K. N. Trueblood, *Acta Crystallographica Section B Structural Crystallography and Crystal Chemistry* **1972**, *28*, 1733-1743.

[11] F. Rozpłoch, J. Patyk, J. Stankowski, *Acta Physica Polonica A* **2007**, *112*, 557-562.

[12] S. Wu, S. Felder, J. Brom, F. Pointillart, O. Maury, L. Micouin, E. Benedetti, *Advanced Optical Materials* **2024**, *12*.

[13] A. Marrocchi, I. Tomasi , L. Vaccaro, *Israel Journal of Chemistry* **2012**, *52*, 41-52.

[14] C. Zippel, *Synthesis and Application of [2.2]Paracyclophane Derivatives in Catalysis and Material Science*, Logos, Berlin, **2021**.

[15] D. J. Cram, N. L. Allinger, H. Steinberg, *Journal of the American Chemical Society* **2002**, *76*, 6132-6141.

[16] V. Boekelheide, in *Cyclophanes I* (Ed.: F. Vögtle), Springer Berlin Heidelberg, Berlin, Heidelberg, **1983**, pp. 87-143.

[17] R. S. Cahn, C. Ingold, V. Prelog, *Angewandte Chemie International Edition in English* **2003**, *5*, 385-415.

[18] G. J. Rowlands, *Israel Journal of Chemistry* **2012**, *52*, 60-75.

[19] S. Felder, S. Wu, J. Brom, L. Micouin, E. Benedetti, *Chirality* **2021**, *33*, 506-527.

[20] Y. Morisaki, Y. Chujo, *Bulletin of the Chemical Society of Japan* **2019**, *92*, 265-274.

[21] Z. Zhou, Y. Zhang, H. Ji, Y. Jin, S. Chen, P. Duan, Y. Liu, *Angew Chem Int Ed Engl* **2023**, *62*, e202301085.

[22] W. Liu, H. Li, Y. Huo, Q. Yao, W. Duan, *Molecules* **2023**, *28*.

[23] Z. Hassan, E. Zysman-Colman, J. Lahann, S. Bräse, *Advanced Functional Materials* **2024**, *34*, 2403365.

[24] N. Sharma, E. Spuling, C. M. Mattern, W. Li, O. Fuhr, Y. Tsuchiya, C. Adachi, S. Bräse, I. D. W. Samuel, E. Zysman-Colman, *Chem Sci* **2019**, *10*, 6689-6696.

[25] H. Hopf, *Angew Chem Int Ed Engl* **2008**, *47*, 9808-9812.

[26] Y. Morisaki, Y. Chujo, *Polymer Chemistry* **2011**, *2*.

[27] S. Morab, M. M. Sundaram, A. Pivrikas, *Coatings* **2023**, *13*.

[28] B. Zhu, L. Fan, N. Mushtaq, R. Raza, M. Sajid, Y. Wu, W. Lin, J.-S. Kim, P. D. Lund, S. Yun, *Electrochemical Energy Reviews* **2021**, *4*, 757-792.

[29] M. A. Rahman, *American Scientific Research Journal for Engineering, Technology, and Sciences* **2014**, *7*, 50-70.

[30] V. Gopalakrishnan, D. Balaji, M. S. Dangate, *ECS Journal of Solid State Science and Technology* **2022**, *11*.

[31] L. Łukasiak, A. Jakubowski, *Journal of Telecommunications and Information Technology* **2010**, 3-9.

[32] *Springer Handbook of Semiconductor Devices*, Springer Cham, **2023**.

[33] J. A. Luceno-Sanchez, A. M. Diez-Pascual, R. Pena Capilla, *Int J Mol Sci* **2019**, *20*.

[34] A. F. Hepp, S. G. Bailey, R. P. Raffaelle, **2013**.

[35] S. Jaiswal, in *Smart Technologies for Energy and Environmental Sustainability* (Eds.: P. Agarwal, M. Mittal, J. Ahmed, S. M. Idrees), Springer International Publishing, Cham, **2022**, pp. 1-19.

[36] J. D. Myers, J. Xue, *Polymer Reviews* **2012**, *52*, 1-37.

[37] J. L. Bredas, J. P. Calbert, D. A. da Silva Filho, J. Cornil, *Proc Natl Acad Sci U S A* **2002**, *99*, 5804-5809.

[38] C. K. Chiang, C. R. Fincher, Y. W. Park, A. J. Heeger, H. Shirakawa, E. J. Louis, S. C. Gau, A. G. MacDiarmid, *Physical Review Letters* **1977**, *39*, 1098-1101.

[39] P. Meredith, C. J. Bettinger, M. Irimia-Vladu, A. B. Mostert, P. E. Schwenn, *Rep Prog Phys* **2013**, *76*, 034501.

[40] K. Walzer, B. Maennig, M. Pfeiffer, K. Leo, *Chemical Reviews* **2007**, *107*, 1233-1271.

[41] P. W. Atkins, J. De Paula, *Atkins' Physical chemistry*, 8th ed., Oxford University Press, Oxford, **2006**.

[42] J.-L. Bredas, *Mater. Horiz.* **2014**, *1*, 17-19.

[43] D. Gupta, Y. Hong, *Organic Electronics* **2010**, *11*, 127-136.

[44] P. Kowalczewski, L. C. Andreani, *Solar Energy Materials and Solar Cells* **2015**, *143*, 260-268.

[45] P. Hu, X. He, H. Jiang, *InfoMat* **2021**, *3*, 613-630.

[46] S. Revuelta, E. Cánovas, *Physical Review B* **2023**, *107*.

[47] S. E. Root, S. Savagatrup, A. D. Printz, D. Rodriquez, D. J. Lipomi, *Chem Rev* **2017**, *117*, 6467-6499.

[48] L. Yen-Yi, D. I. Gundlach, S. F. Nelson, T. N. Jackson, *IEEE Transactions on Electron Devices* **1997**, *44*, 1325-1331.

[49] Y. Yunus, N. A. Mahadzir, M. N. Mohamed Ansari, T. H. Tg Abd Aziz, A. Mohd Afdzaluddin, H. Anwar, M. Wang, A. G. Ismail, *Polymers (Basel)* **2022**, *14*.

[50] M. T. Dang, L. Hirsch, G. Wantz, *Adv Mater* **2011**, *23*, 3597-3602.

[51] E. M. Speller, *Materials Science and Technology* **2017**, *33*, 924-933.

[52] N. Martin, *Chem Commun (Camb)* **2013**, *49*, 7025-7027.

[53] R. Pfattner, S. T. Bromley, C. Rovira, M. Mas-Torrent, *Advanced Functional Materials* **2015**, *26*, 2256-2275.

[54] W. Hu, B. Gompf, J. Pflaum, D. Schweitzer, M. Dressel, *Applied Physics Letters* **2004**, *84*, 4720-4722.

[55] G. C. Bazan, *J Org Chem* **2007**, *72*, 8615-8635.

[56] Y. Yang, G. Zhang, C. Yu, C. He, J. Wang, X. Chen, J. Yao, Z. Liu, D. Zhang, *Chem Commun (Camb)* **2014**, *50*, 9939-9942.

[57] A. Marrocchi, D. Lanari, A. Facchetti, L. Vaccaro, *Energy & Environmental Science* **2012**, *5*.

[58] J. Zaumseil, in *P3HT Revisited – From Molecular Scale to Solar Cell Devices*, **2014**, pp. 107-137.

[59] J. H. Burroughes, D. D. C. Bradley, A. R. Brown, R. N. Marks, K. Mackay, R. H. Friend, P. L. Burns, A. B. Holmes, *Nature* **1990**, *347*, 539-541.

[60] G. Gustafsson, Y. Cao, G. M. Treacy, F. Klavetter, N. Colaneri, A. J. Heeger, *Nature* **1992**, *357*, 477-479.

[61] N. Armaroli, V. Balzani, *Chemistry* **2016**, *22*, 32-57.

[62] K. S. Ahmad, S. N. Naqvi, S. B. Jaffri, *Reviews in Inorganic Chemistry* **2021**, *41*, 21-39.

[63] A. E. Becquerel, *Comptes Rendus de l'Academie des Sciences* **1839**, *9*, 561 - 567.

[64] W. van Roosbroeck, W. Shockley, *Physical Review* **1954**, *94*, 1558-1560.

[65] W. P. Dumke, *Physical Review* **1957**, *105*, 139-144.

[66] R. N. Hall, *Physical Review* **1952**, *87*, 387-387.

[67] P. Auger, *Comptes rendus de l'Académie des sciences* **1923**, *177*, 169.

[68] *Proceedings of the Royal Society of London* **1997**, *25*, 113-117.

[69] D. M. Chapin, C. S. Fuller, G. L. Pearson, *Journal of Applied Physics* **1954**, *25*, 676-677.

[70] A. W. Blakers, A. Wang, A. M. Milne, J. Zhao, M. A. Green, *Applied Physics Letters* **1989**, *55*, 1363-1365.

[71] W. Long, S. Yin, F. Peng, M. Yang, L. Fang, X. Ru, M. Qu, H. Lin, X. Xu, *Solar Energy Materials and Solar Cells* **2021**, *231*.

[72] W. Shockley, H. J. Queisser, *Journal of Applied Physics* **1961**, *32*, 510-519.

[73] Suman, P. Sharma, P. Goyal, *Materials Today: Proceedings* **2020**, *28*, 1593-1597.

[74] D. A. Cusano, *Solid-State Electronics* **1963**, *6*, 217-232.

[75] S. Wagner, J. L. Shay, P. Migliorato, H. M. Kasper, *Applied Physics Letters* **1974**, *25*, 434-435.
[76] J. Pastuszak, P. Wegierek, *Materials (Basel)* **2022**, *15*.
[77] H. Hoppe, N. S. Sariciftci, *Journal of Materials Research* **2011**, *19*, 1924-1945.
[78] M. Grätzel, *Journal of Photochemistry and Photobiology C: Photochemistry Reviews* **2003**, *4*, 145-153.
[79] J.-P. Correa-Baena, A. Abate, M. Saliba, W. Tress, T. Jesper Jacobsson, M. Grätzel, A. Hagfeldt, *Energy & Environmental Science* **2017**, *10*, 710-727.
[80] S. Ruhle, M. Shalom, A. Zaban, *Chemphyschem* **2010**, *11*, 2290-2304.
[81] M. Yamaguchi, F. Dimroth, J. F. Geisz, N. J. Ekins-Daukes, *Journal of Applied Physics* **2021**, *129*.
[82] C. W. Tang, *Applied Physics Letters* **1986**, *48*, 183-185.
[83] B. Mohamed El Amine, Y. Zhou, H. Li, Q. Wang, J. Xi, C. Zhao, *Energies* **2023**, *16*.
[84] A. Kojima, K. Teshima, Y. Shirai, T. Miyasaka, *J Am Chem Soc* **2009**, *131*, 6050-6051.
[85] Z. Pan, H. Rao, I. Mora-Sero, J. Bisquert, X. Zhong, *Chem Soc Rev* **2018**, *47*, 7659-7702.
[86] J. F. Geisz, R. M. France, K. L. Schulte, M. A. Steiner, A. G. Norman, H. L. Guthrey, M. R. Young, T. Song, T. Moriarty, *Nature Energy* **2020**, *5*, 326-335.
[87] T. Salim, S. Sun, Y. Abe, A. Krishna, A. C. Grimsdale, Y. M. Lam, *Journal of Materials Chemistry A* **2015**, *3*, 8943-8969.
[88] T. Webb, S. J. Sweeney, W. Zhang, *Advanced Functional Materials* **2021**, *31*.
[89] P. Peumans, A. Yakimov, S. R. Forrest, *Journal of Applied Physics* **2003**, *93*, 3693-3723.
[90] L. V. Mercaldo, P. Delli Veneri, in *Solar Cells and Light Management*, **2020**, pp. 35-57.
[91] Y. Kawano, J. Chantana, T. Negami, T. Nishimura, A. Mavlonov, T. Minemoto, *Solar Energy* **2022**, *231*, 684-693.
[92] H. S. Jung, N. G. Park, *Small* **2015**, *11*, 10-25.
[93] J. Lee, J. Kim, C. S. Kim, S. Jo, *Nanomaterials (Basel)* **2022**, *12*.
[94] G. Yin, J. Ma, H. Jiang, J. Li, D. Yang, F. Gao, J. Zeng, Z. Liu, S. F. Liu, *ACS Appl Mater Interfaces* **2017**, *9*, 10752-10758.
[95] X. Liu, Z. Liu, B. Sun, X. Tan, H. Ye, Y. Tu, T. Shi, Z. Tang, G. Liao, *Nano Energy* **2018**, *50*, 201-211.
[96] Y. Tang, R. Roy, Z. Zhang, Y. Hu, F. Yang, C. Qin, L. Jiang, H. Liu, *Solar Energy* **2022**, *231*, 440-446.
[97] I. S. Yang, J. S. You, S. D. Sung, C. W. Chung, J. Kim, W. I. Lee, *Nano Energy* **2016**, *20*, 272-282.
[98] K.-P. Wang, H. Teng, *Applied Physics Letters* **2007**, *91*.
[99] Q. Jiang, X. Zhang, J. You, *Small* **2018**, e1801154.
[100] J. You, L. Meng, T. B. Song, T. F. Guo, Y. M. Yang, W. H. Chang, Z. Hong, H. Chen, H. Zhou, Q. Chen, Y. Liu, N. De Marco, Y. Yang, *Nat Nanotechnol* **2016**, *11*, 75-81.

[101] P. Zhang, J. Wu, T. Zhang, Y. Wang, D. Liu, H. Chen, L. Ji, C. Liu, W. Ahmad, Z. D. Chen, S. Li, *Adv Mater* **2018**, *30*.

[102] S. Naka, H. Okada, H. Onnagawa, T. Tsutsui, *Applied Physics Letters* **2000**, *76*, 197-199.

[103] T. Earmme, S. A. Jenekhe, *Journal of Materials Chemistry* **2012**, *22*.

[104] C. Fu, H. Lin, *Solid State Communications* **2024**, *378*.

[105] Y.-J. Li, H. Sasabe, S.-J. Su, D. Tanaka, T. Takeda, Y.-J. Pu, J. Kido, *Chemistry Letters* **2009**, *38*, 712-713.

[106] Z. Bin, D. Shi, R. Su, W. Han, D. Zhang, L. Duan, *Sci Bull (Beijing)* **2020**, *65*, 153-160.

[107] K. Wojciechowski, T. Leijtens, S. Siprova, C. Schlueter, M. T. Horantner, J. T. Wang, C. Z. Li, A. K. Jen, T. L. Lee, H. J. Snaith, *J Phys Chem Lett* **2015**, *6*, 2399-2405.

[108] N. Cho, C.-Z. Li, H.-L. Yip, A. K. Y. Jen, *Energy Environ. Sci.* **2014**, *7*, 638-643.

[109] R. Sandoval-Torrientes, J. Pascual, I. Garcia-Benito, S. Collavini, I. Kosta, R. Tena-Zaera, N. Martin, J. L. Delgado, *ChemSusChem* **2017**, *10*, 2023-2029.

[110] J. Zhen, Q. Liu, X. Chen, D. Li, Q. Qiao, Y. Lu, S. Yang, *Journal of Materials Chemistry A* **2016**, *4*, 8072-8079.

[111] L. L. Deng, S. Y. Xie, F. Gao, *Advanced Electronic Materials* **2017**, *4*.

[112] Y. Bai, H. Yu, Z. Zhu, K. Jiang, T. Zhang, N. Zhao, S. Yang, H. Yan, *Journal of Materials Chemistry A* **2015**, *3*, 9098-9102.

[113] X. Zeng, T. Zhou, C. Leng, Z. Zang, M. Wang, W. Hu, X. Tang, S. Lu, L. Fang, M. Zhou, *Journal of Materials Chemistry A* **2017**, *5*, 17499-17505.

[114] D. Yang, X. Zhang, K. Wang, C. Wu, R. Yang, Y. Hou, Y. Jiang, S. Liu, S. Priya, *Nano Lett* **2019**, *19*, 3313-3320.

[115] D. Di Girolamo, F. Di Giacomo, F. Matteocci, A. G. Marrani, D. Dini, A. Abate, *Chem Sci* **2020**, *11*, 7746-7759.

[116] X. Yin, Y. Guo, H. Xie, W. Que, L. B. Kong, *Solar RRL* **2019**, *3*.

[117] P. Nandi, H. Park, S. Shin, J. W. Lee, J. Y. Kim, M. J. Ko, H. S. Jung, N. G. Park, H. Shin, *Advanced Materials Interfaces* **2024**, *11*.

[118] X. Hu, L. Chen, Y. Chen, *The Journal of Physical Chemistry C* **2014**, *118*, 9930-9938.

[119] Y. Zhao, J. Chen, W. Chen, D. Ma, *Journal of Applied Physics* **2012**, *111*.

[120] M. Kröger, S. Hamwi, J. Meyer, T. Riedl, W. Kowalsky, A. Kahn, *Applied Physics Letters* **2009**, *95*.

[121] Y. Peng, N. Yaacobi-Gross, A. K. Perumal, H. A. Faber, G. Vourlias, P. A. Patsalas, D. D. C. Bradley, Z. He, T. D. Anthopoulos, *Applied Physics Letters* **2015**, *106*.

[122] S. Uthayaraj, D. Karunarathne, G. R. A. Kumara, T. Murugathas, S. Rasalingam, R. M. G. Rajapakse, P. Ravirajan, D. Velauthapillai, *Materials (Basel)* **2019**, *12*.

[123] W. Sun, S. Ye, H. Rao, Y. Li, Z. Liu, L. Xiao, Z. Chen, Z. Bian, C. Huang, *Nanoscale* **2016**, *8*, 15954-15960.

[124] A. M. Abdulwahab, E. A. Al-Mahdi, A. Al-Osta, A. A. Qaid, *Chinese Journal of Physics* **2021**, *73*, 479-492.

[125] A. Perumal, H. Faber, N. Yaacobi-Gross, P. Pattanasattayavong, C. Burgess, S. Jha, M. A. McLachlan, P. N. Stavrinou, T. D. Anthopoulos, D. D. Bradley, *Adv Mater* **2015**, *27*, 93-100.

[126] N. Chaudhary, R. Chaudhary, J. P. Kesari, A. Patra, S. Chand, *Journal of Materials Chemistry C* **2015**, *3*, 11886-11892.

[127] H. Lei, G. Yang, X. Zheng, Z.-G. Zhang, C. Chen, J. Ma, Y. Guo, Z. Chen, P. Qin, Y. Li, G. Fang, *Solar RRL* **2017**, *1*.

[128] H. Rao, W. Sun, S. Ye, W. Yan, Y. Li, H. Peng, Z. Liu, Z. Bian, C. Huang, *ACS Appl Mater Interfaces* **2016**, *8*, 7800-7805.

[129] M. A. Adedeji, M. S. G. Hamed, G. T. Mola, *Solar Energy* **2020**, *203*, 83-90.

[130] T. P. Kaloni, P. K. Giesbrecht, G. Schreckenbach, M. S. Freund, *Chemistry of Materials* **2017**, *29*, 10248-10283.

[131] H. Salleh, N. a. Ali, C. C. Yap, A. M. Sinin, N. Ishak, N. H. Kamarulzaman, S. M. Ghazali, N. A. Nik Ali, *Solid State Phenomena* **2020**, *307*, 207-216.

[132] W. Zhang, R. Zhu, F. Li, Q. Wang, B. Liu, *The Journal of Physical Chemistry C* **2011**, *115*, 7038-7043.

[133] Q. Liao, Y. Wang, X. Yao, M. Su, B. Li, H. Sun, J. Huang, X. Guo, *ACS Appl Mater Interfaces* **2021**, *13*, 16744-16753.

[134] D. B. Khadka, Y. Shirai, M. Yanagida, J. W. Ryan, K. Miyano, *Journal of Materials Chemistry C* **2017**, *5*, 8819-8827.

[135] L. Groenendaal, F. Jonas, D. Freitag, H. Pielartzik, J. R. Reynolds, *Advanced Materials* **2000**, *12*, 481-494.

[136] M. N. Gueye, A. Carella, J. Faure-Vincent, R. Demadrille, J.-P. Simonato, *Progress in Materials Science* **2020**, *108*.

[137] K. M. Reza, A. Gurung, B. Bahrami, S. Mabrouk, H. Elbohy, R. Pathak, K. Chen, A. H. Chowdhury, M. T. Rahman, S. Letourneau, H.-C. Yang, G. Saianand, J. W. Elam, S. B. Darling, Q. Qiao, *Journal of Energy Chemistry* **2020**, *44*, 41-50.

[138] Y. Li, N. Hong, *Journal of Materials Chemistry A* **2015**, *3*, 21537-21544.

[139] E. B. Çelebi, J. Cameron, P. J. Skabara, F. Hacıvelioğlu, *Journal of Materials Chemistry C* **2024**, *12*, 4261-4266.

[140] W. Cai, C. Musumeci, F. N. Ajjan, Q. Bao, Z. Ma, Z. Tang, O. Inganäs, *Journal of Materials Chemistry A* **2016**, *4*, 15670-15675.

[141] X. Jiang, Z. Yu, Y. Zhang, J. Lai, J. Li, G. G. Gurzadyan, X. Yang, L. Sun, *Sci Rep* **2017**, *7*, 42564.

[142] K. Chowdhury, S. K. Behura, M. Rahimi, M. Heydari Gharahcheshmeh, *ACS Applied Energy Materials* **2024**.

[143] M. Heydari Gharahcheshmeh, M. M. Tavakoli, E. F. Gleason, M. T. Robinson, J. Kong, K. K. Gleason, *Sci Adv* **2019**, *5*, eaay0414.

[144] Y. Wang, L. Duan, M. Zhang, Z. Hameiri, X. Liu, Y. Bai, X. Hao, *Solar RRL* **2022**, *6*.

[145] Y. Ko, Y. Kim, C. Lee, Y. Kim, Y. Jun, *ACS Appl Mater Interfaces* **2018**, *10*, 11633-11641.

[146] P. Cias, C. Slugovc, G. Gescheidt, *J Phys Chem A* **2011**, *115*, 14519-14525.

[147] L. Nakka, Y. Cheng, A. G. Aberle, F. Lin, *Advanced Energy and Sustainability Research* **2022**, *3*.

[148] Z. Hawash, L. K. Ono, Y. Qi, *Advanced Materials Interfaces* **2017**, *5*.

[149] G. Shao, D. Wang, Z. K. Zhou, H. J. Yu, T. Kang, W. H. Zhu, J. Xiao, Z. L. Yu, L. Peng, J. Chen, Q. U. Ain, Y. Chen, H. Yang, Z. Qiu, R. Hu, A. A. Khan, K. A. Alamry, Y. Zhang, J. Xia, M. K. K. Nazeeruddin, *Angew Chem Int Ed Engl* **2024**, e202411217.

[150] S. Wang, T. Wu, J. Guo, R. Zhao, Y. Hua, Y. Zhao, *ACS Cent Sci* **2024**, *10*, 1383-1395.

[151] J. Xu, P. Shi, K. Zhao, L. Yao, C. Deger, S. Wang, X. Zhang, S. Zhang, Y. Tian, X. Wang, J. Shen, C. Zhang, I. Yavuz, J. Xue, R. Wang, *ACS Energy Letters* **2024**, *9*, 1073-1081.

[152] B. Pashaei, S. Bellani, H. Shahroosvand, F. Bonaccorso, *Chem Sci* **2020**, *11*, 2429-2439.

[153] L. Hajikhanmirzaei, H. Shahroosvand, B. Pashaei, G. D. Monache, M. K. Nazeeruddin, M. Pilkington, *Journal of Materials Chemistry C* **2020**, *8*, 6221-6227.

[154] I. M. Abdellah, T. H. Chowdhury, J.-J. Lee, A. Islam, M. K. Nazeeruddin, M. Gräetzel, A. El-Shafei, *Sustainable Energy & Fuels* **2021**, *5*, 199-211.

[155] S. Gangala, R. Misra, *Journal of Materials Chemistry A* **2018**, *6*, 18750-18765.

[156] L. Vaghi, F. Rizzo, *Solar RRL* **2023**, *7*.

[157] Z. Zhang, W. Hu, J. Cui, R. He, W. Shen, M. Li, *Phys Chem Chem Phys* **2017**, *19*, 24574-24582.

[158] W. J. Chi, P. P. Sun, Z. S. Li, *Nanoscale* **2016**, *8*, 17752-17756.

[159] J. Zhang, Y. Hua, B. Xu, L. Yang, P. Liu, M. B. Johansson, N. Vlachopoulos, L. Kloo, G. Boschloo, E. M. J. Johansson, L. Sun, A. Hagfeldt, *Advanced Energy Materials* **2016**, *6*.

[160] S. Park, J. H. Heo, C. H. Cheon, H. Kim, S. H. Im, H. J. Son, *Journal of Materials Chemistry A* **2015**, *3*, 24215-24220.

[161] S. Park, J. H. Heo, J. H. Yun, T. S. Jung, K. Kwak, M. J. Ko, C. H. Cheon, J. Y. Kim, S. H. Im, H. J. Son, *Chem Sci* **2016**, *7*, 5517-5522.

[162] S. A. Otterbach, D. Elsing, A. D. Schulz, H. Tappert, W. Wenzel, M. Kozlowska, H. Röhm, S. Bräse, *Advanced Functional Materials* **2023**, 2309226.

[163] A. D. Schulz, S. A. Otterbach, H. Tappert, D. Elsing, W. Wenzel, M. Kozlowska, S. Bräse, A. Colsmann, H. Röhm, *Advanced Functional Materials* **2024**, 2402110.

[164] S. A. Otterbach, *Organic semiconductors based on [2.2]paracyclophanes and porphyrins as hole transport materials in perevoskite solar cells, Vol. 102*, Logos, Berlin, **2023**.

[165] V. Kumar, S. Chatterjee, P. Sharma, S. Chakrabarty, C. V. Avadhani, S. Sivaram, *Journal of Polymer Science Part A: Polymer Chemistry* **2018**, *56*, 1046-1057.

[166] Y. Wu, Z. Wang, M. Liang, H. Cheng, M. Li, L. Liu, B. Wang, J. Wu, R. Prasad Ghimire, X. Wang, Z. Sun, S. Xue, Q. Qiao, *ACS Appl Mater Interfaces* **2018**, *10*, 17883-17895.

[167] Y. Dienes, S. Durben, T. Karpati, T. Neumann, U. Englert, L. Nyulaszi, T. Baumgartner, *Chemistry* **2007**, *13*, 7487-7500.

[168] Y. Guo, G. Han, Z. Tu, Y. Yi, *Journal of Materials Chemistry A* **2019**, *7*, 12532-12537.

[169] X. Wang, Y. Sun, S. Chen, X. Guo, M. Zhang, X. Li, Y. Li, H. Wang, *Macromolecules* **2012**, *45*, 1208-1216.

[170] Y. Ou, A. Sun, H. Li, T. Wu, D. Zhang, P. Xu, R. Zhao, L. Zhu, R. Wang, B. Xu, Y. Hua, L. Ding, *Materials Chemistry Frontiers* **2021**, *5*, 876-884.

[171] Y. Zhou, C. Liu, F. Meng, C. Zhang, G. Wei, L. Gao, T. Ma, *Solar RRL* **2021**, *5*.

[172] C. Y. Liu, H. Zhao, H. H. Yu, *Org Lett* **2011**, *13*, 4068-4071.

[173] T. M. Ha Vuong, D. Villemin, H. H. Nguyen, T. T. Le, T. T. Dang, H. Nguyen, *Chem Asian J* **2017**, *12*, 2819-2826.

[174] H. Huang, L. Yang, A. Facchetti, T. J. Marks, *Chem Rev* **2017**, *117*, 10291-10318.

[175] K. Do, C. Kim, K. Song, S. J. Yun, J. K. Lee, J. Ko, *Solar Energy Materials and Solar Cells* **2013**, *115*, 52-57.

[176] P. Pahlavanlu, P. R. Christensen, J. A. Therrien, M. O. Wolf, *The Journal of Physical Chemistry C* **2015**, *120*, 70-77.

[177] M. Jakobi, C. Sparr, *Organic Process Research & Development* **2022**, *26*, 2756-2760.

[178] D. Mi, J.-H. Kim, S. C. Yoon, C. Lee, J.-K. Lee, D.-H. Hwang, *Synthetic Metals* **2011**, *161*, 1330-1335.

[179] A. A. Najmi, R. Bischoff, H. P. Permentier, *Molecules* **2022**, *27*.

[180] U. Shoukat, E. Baumeister, D. D. D. Pinto, H. K. Knuutila, *Journal of Natural Gas Science and Engineering* **2019**, *62*, 26-37.

[181] Y. Li, P. J. Lohr, A. Segapeli, J. Baltram, D. Werner, A. Allred, K. Muralidharan, A. D. Printz, *ACS Appl Mater Interfaces* **2023**, *15*, 24387-24398.

[182] P. R. Varadwaj, A. Varadwaj, H. M. Marques, K. Yamashita, *Int J Mol Sci* **2023**, *24*.

[183] T. Zhou, C. Liu, S. Gong, Y. Xiang, G. Xie, C. Yang, *Journal of Materials Chemistry C* **2018**, *6*, 6305-6311.

[184] G. Yang, F. Wang, C. Zhou, Y. Sun, T. Wang, Q. Li, Y. Li, X. Liang, X. Zhou, Q. Zhu, H. Lin, H. Hu, *Chemical Engineering Journal* **2024**, *493*.

[185] X. Tang, Q. Zhong, J. Hua, Y. Song, Y. Ma, H. Cheng, B. Wei, R. Yuan, *Inorganica Chimica Acta* **2016**, *439*, 77-81.

[186] M. Hasegawa, Y. Ishida, H. Sasaki, S. Ishioka, K. Usui, N. Hara, M. Kitahara, Y. Imai, Y. Mazaki, *Chemistry* **2021**, *27*, 16225-16231.

[187] M. Wielopolski, A. Molina-Ontoria, C. Schubert, J. T. Margraf, E. Krokos, J. Kirschner, A. Gouloumis, T. Clark, D. M. Guldi, N. Martin, *J Am Chem Soc* **2013**, *135*, 10372-10381.

[188] N. Miki, H. Maeda, R. Inoue, Y. Morisaki, *ChemistrySelect* **2021**, *6*, 12970-12974.

[189] Y. C. Chang, K. M. Lee, C. H. Lai, C. Y. Liu, *Chemistry – An Asian Journal* **2018**, *13*, 1510-1515.

[190] T. Koopmans, *Physica* **1934**, *1*, 104-113.

[191] J. Lahann, M. Balcells, T. Rodon, J. Lee, I. S. Choi, K. F. Jensen, R. Langer, *Langmuir* **2002**, *18*, 3632-3638.

[192] C. Y. Yu, M. L. Turner, *Angew Chem Int Ed Engl* **2006**, *45*, 7797-7800.

[193] Y. Morisaki, Y. Chujo, *Bulletin of the Chemical Society of Japan* **2009**, *82*, 1070-1082.

[194] Y. Morisaki, R. Hifumi, L. Lin, K. Inoshita, Y. Chujo, *Polymer Chemistry* **2012**, *3*.

[195] H. Tappert, Z. Li, J. Seibert, C. Zippel, Z. Hassan, S. Bräse, *ChemRxiv* **2021**.

[196] C. Zippel, Z. Hassan, A. Q. Parsa, J. Hohmann, S. Bräse, *Advanced Synthesis & Catalysis* **2021**, *363*, 2861-2865.

[197] S. Iwatsuki, T. Itoh, M. Kubo, H. Okuno, *Polymer Bulletin* **1994**, *32*, 27-34.

[198] N. Wada, Y. Morisaki, Y. Chujo, *Macromolecules* **2009**, *42*, 1439-1442.

[199] D. Li, C. Weng, Y. Ruan, K. Li, G. Cai, C. Song, Q. Lin, *Sensors (Basel)* **2021**, *21*, 1003.

[200] R. W. Lancaster, P. G. Karamertzanis, A. T. Hulme, D. A. Tocher, T. C. Lewis, S. L. Price, *J Pharm Sci* **2007**, *96*, 3419-3431.

[201] H. E. Stavely, W. Bergmann, *Journal of Organic Chemistry* **1937**, *1*, 575-579.

[202] Y. Imai, Y. Nakano, T. Kawai, J. Yuasa, *Angew Chem Int Ed Engl* **2018**, *57*, 8973-8978.

[203] T. Chatterjee, K. T. Wong, *Advanced Optical Materials* **2018**, *7*, 1800565.

[204] G. Zhang, Y. Bao, H. Ma, N. Wang, X. Cheng, Z. He, X. Wang, T. Miao, W. Zhang, *Angewandte Chemie International Edition* **2024**, *63*.

[205] P. Puneet, M. Fujiki, B. Nandan, in *Reactive and Functional Polymers Volume Three*, **2021**, pp. 117-139.

[206] S. Fratini, M. Nikolka, A. Salleo, G. Schweicher, H. Sirringhaus, *Nat Mater* **2020**, *19*, 491-502.

[207] C. S. Marques, E. P. Carreiro, A. J. Burke, *ISySyCat 2023: International Symposium on Synthesis and Catalysis : Évora, September 5-8 : Book of Abstracts*, **2023**.

Appendix

I. Publications

Open-access Preprint:

H. Tappert; Z. Li; J. Seibert; C. Zippel; Z. Hassan; S. Bräse, "Molecular Structuring of Novel Chiral Polymers via Cyclophane-based Monomer Design Strategies", *ChemRxiv* **2021**.

Peer-reviewed:

S. A. Otterbach, D. Elsing, A. D. Schulz, **H. Tappert**, W. Wenzel, M. Kozlowska, H. Röhm, S. Bräse, "Pseudo-Para-Substituted [2.2]Paracyclophanes for Hole Transport in Perovskite Solar Cells", *Advanced Functional Materials* **2023**, 2309226.

A. D. Schulz, S. A. Otterbach, **H. Tappert**, D. Elsing, W. Wenzel, M. Kozlowska, S. Bräse, A. Colsmann, H. Röhm, "Doping Strategies for Tetrasubstituted Paracyclophane Hole Transport Layers in Perovskite Solar Cells", *Advanced Functional Materials* **2024**, 2402110.

P. Kern, **H. Tappert**, S. Bräse, "A New Class of Chiral Polyethers and Polyesters Based on the [2.2]Paracyclophane Scaffold", *Polymers* **2024**, 16.

H. Tappert, E. V. Puttock, J. S. Oviedo Ortiz, E. Zysman-Colman, J. Crassous, S. Bräse, "Chiral Polymers based on Vinyl[2.2]paracyclophane and their Application as CPL Emitters", *Polymers* **2025**, 2500145.

H. Tappert, S. Bräse, "[2.2]Paracyclophane-Materials – Status and Perspectives", *Macromolecular Rapid Communications* **2025**, 17 (8), 1070.

Conference poster presentations:

S. Otterbach, **H. Tappert**, S. Bräse, "Design and Synthesis of Novel Hole Transport Materials for Emerging Active Layers", 08.05.2022 – 13.05.2022, Honolulu, Hawai'i, USA, 2022 MRS Spring Meeting & Exhibit

H. Tappert, S. Otterbach, S. Bräse, "Design and Synthesis of a Library of Novel Hole Transport Materials based on [2.2]Paracyclophane", 05.09.2023 – 08.09.2023, Évora, Portugal, International Symposium on Synthesis and Catalysis 2023[207]

II. Acknowledgements

First and foremost, I would like to express my deepest gratitude to Prof. Dr. Stefan Bräse for his invaluable supervision, guidance, and for giving me the opportunity to pursue this PhD. His support and encouragement have been instrumental for my academic journey.

I am also sincerely thankful to the KeraSolar project for their generous funding, which made this research possible.

I want to thank all the people, that helped me run the many experiments and all those difficult purifications. Lisa Wanner as lab technician, Mike Schäfer as HiWi and bachelor student, and Daniel Seiler as HiWi student.

A special thanks goes to my colleagues who have provided assistance with measurements and experiments: Alex Schulz, Holger Röhm, Tilmann Bohnert, Emma Puttock, Sebastian Ortiz, the Meier group, and the IOC Analytics team. I am grateful for your technical expertise and willingness to help.

I would also like to acknowledge Steffen Otterbach for his collaboration on the KeraSolar project, which greatly enriched the scope of my research.

Heartfelt thanks go to Patrick Kern, Steffen Otterbach, and Jasmin Seibert for their thorough review and insightful feedback on this thesis. Your comments and suggestions have greatly improved the quality of my work.

I am particularly thankful to Caroline Röttger, Aleksandra Vranić, Sophia Abou El Mirate for making the current 303 a lab where I could work with fun. I also want to thank their 303 predecessors Xuemin Gan, Alena Winter, and Clara Adam for their companionship and support throughout my PhD journey.

To the entire Bräse group, thank you for creating such a wonderful working atmosphere. I truly appreciated your help, camaraderie, and the memorable experiences we shared along the way.

Finally, I want to extend my deepest appreciation to David Frick, Maike Koch, and my family. Your unwavering support, and encouragement outside the university have been essential in keeping me motivated and sane throughout this process. Thank you for always being there.

This thesis would not be half as good, if not for all your support, and for that, I am deeply grateful.